

**UC Davis**

**UC Davis Electronic Theses and Dissertations**

**Title**

Characterization and Quantitation of Human Milk Oligosaccharides using LC-MS based methods- Impacts on Fetal Development and Infant Health

**Permalink**

<https://escholarship.org/uc/item/2b59447g>

**Author**

Vinjamuri, Anita

**Publication Date**

2022

Peer reviewed|Thesis/dissertation

Characterization and Quantitation of Human Milk Oligosaccharides  
using LC-MS based methods- Impacts on Fetal Development and Infant  
Health

By

ANITA VINJAMURI  
DISSERTATION

Submitted in partial satisfaction of the requirements for the degree of

DOCTOR OF PHILOSOPHY

in

CHEMISTRY

in the

OFFICE OF GRADUATE STUDIES

of the

UNIVERSITY OF CALIFORNIA

DAVIS

Approved:

---

Carlito B. Lebrilla, Chair

---

Gang-Yu Liu

---

Carolyn Slupsky

Committee in Charge

2022

# DEDICATION

*To my mom, my husband, my many pets, and my family and friends  
for their love and support*

# ACKNOWLEDGEMENTS

I'd like to first thank my mom who raised me to never give up on my dreams and always keep going. Without your sacrifice of moving to the United States I would not be where I am today. I know that my life changed completely in just a couple of years, but I will always be your little girl. Thank you for teaching me to take life a little less seriously and reminding me that there is so much more to look forward to. Your enthusiasm, passion and lighthearted energy has helped me overcome a lot of obstacles. Because of you: the way you raised me, supported me, and nurtured me; I have accomplished what I have to this day.

Marques, thank you for being the best husband, best friend, and teammate a women could ask for. I know that this journey has not been easy, but you have always believed in me even when I didn't and that means so much to me. I know my experiments often made little sense to you but thank you for caring, for listening, and for being my number one cheerleader. Thank you for calming me down when things didn't go my way in the lab and for always making me see things in a different perspective. I value your opinion so much and you always find the right words to put me at ease. You make light of every situation and can make me laugh through the toughest times. Thank you for staying by my side through the tears, late nights in lab, weekends away, and exhaustion. While this accomplishment was not easy, it would have been impossible without you.

I would also like to extend my gratitude to some of my close friends that have stood by my side through the countless cancelations, missed calls, unresponded text messages while I was perusing my dream in graduate school. Thank you for understanding, supporting, and sticking by my side through it all. A huge thank you to my childhood friends Amanda, Noor and Brandon (rest in peace BFF). You guys have molded me into the person I am today, and I couldn't be more grateful for all our adventures and memories we had together. I can't wait for the many more to come now that I will hopefully have a good income. Thank you to my new friends and relationships I have built along this journey. My dearest Diane, thank you for teaching me the fundamentals and being not only a good partner in crime through the most challenging years of grad school but also an amazing friend. I would not be here without your help, mentorship and support and I will forever be in your debt. Steph, thank you for being so kind and supportive though one of the toughest times in my life. Your positivity and presence always put me at ease and although we only met in my last year of graduate school, I feel like I have known you my whole life.

Dr. Mike and Dr. Schweikert, thank you for sparking a flame in my little undergraduate heart. If it was not for doing research in your lab I would not have been here today, literally. Mike, before I joined the lab, I had no idea what a PhD even was. I had never heard of one and more so never thought I was even capable of pursuing an even higher education. Thank you for believing in me when I did not. Thank you for your guidance in the process of applying for the program. And for the repeated "Anita, you can do it" pep talks I needed almost every day just to build up my confidence enough to even apply. You were always so patient, kind, encouraging and listened to

all my ideas (even if they weren't the best). If it wasn't for you, I would not have found my passion in science, and I most definitely would not have gotten my PhD.

Thank you to my cohort, Garret, Nikko and Cathy. We have gone through the ringer together and you guys have been so encouraging and kind. You guys are amazing people, and I would not have wanted to go through graduate school with anyone else. Thank you to all the Lebrilla league groupies for all the ideas that were bounced, papers that were edited, and encouraging words that were said.

I would like to acknowledge all of my mentors and collaborators along the way. Professor Gang-Yu, Professor Slupsky, Professor Zivkovic, Professor Bernstein, Dr. Kjersti, thank you for being strong women and role models in the field of science. I look up to every single one of you and cannot thank you enough for your mentorship and guidance. Professor Casey and Brad, you both specifically made me feel so welcomed my first year at UC Davis. Thank you for always having your door open to talk and for all the lighthearted conversations and pointers that kept me on the right track.

Lastly, I would like to thank my advisor Carlito Lebrilla. Thank you for taking a chance on me. You have been one of my strongest supporters and never wavered. You are one of my biggest inspirations, and I will forever be in your debt for all that you have taught me, both scientifically and personally. Because of you, I developed a stronger passion and appreciation for science that I did not know I had. You taught me how to be a better scientist, professional, communicator, and mentor. Thank you for taking the time to get to know me, understand how I operate, and coach me based on that. Your ability to understand that people learn, communicate, and work differently is one of the many reasons why I think you are such an amazing leader. Thank you also for always setting time apart from research for fun: for all the trips, birthday celebrations, dinners, coffees, and outings. Those memories and time away from the lab mean a lot to us graduate students. And lastly thank you for the opportunities you have given me during my time here at Davis and the doors you have opened for me and my future.

To everyone else that helped me through this journey, even if it was just a simple smile in the hallway or a wave across the building. Thank you for taking part in my journey. 😊

# Characterization and Quantitation of Human Milk Oligosaccharides using LC-MS based methods- impacts on fetal development and infant health

## Abstract

Human Milk Oligosaccharides (HMOs) are the third most abundant solid component in human breast milk, consisting of hundreds of unique structures. HMOs are indigestible by the infant but have shown to be very beneficial to the infant's development, making them an intriguing constituent. However, due to the lack of standards, reliable methods for quantitation, and complexity of performing large scale analysis, there are limits to our general knowledge of their abundances and functions. This dissertation focuses on the development and implication of mass spectrometry-based methods to characterize and quantitate HMOs to address unanswered questions in the field.

Chapter 1 provides an overview of HMO structures and the functions they collectively play in infant development. Chapter 2 details the development of a comprehensive library and a high-throughput method that allowed for accurate quantitation of HMOs using high resolution mass spectrometry. Optimized methods were applied to breast milk samples collected from over 2000 mothers from 19 geographically diverse sites to investigate how HMO profiles vary across the globe. The results revealed significant phenotypic variations in the mother's milk and secretor status globally. Chapter 3 reports discovery of several oligosaccharides, inclusive of 8 HMOs, found in amniotic fluid. This chapter detailed the methodologies from sample preparation to data analysis and was applied to a cohort of over 500 mothers, making it the most comprehensive

study of amniotic fluid to date. Analysis revealed compositional changes in HMO profiles across gestation. Chapter 4 studies demonstrated that select HMOs, including linkage-specific sialylated structures, can act as decoys to prevent SARS-Cov2 infection. This study also investigated the mechanism of binding between the spike protein and the ACE2 receptor on the cell surface. The results detailed here exemplify the important role that cell surface glycosylation plays in host-pathogen interactions.

## Glossary of Abbreviations

ACN – acetonitrile

CID – collision induced dissociation

FA – Formic Acid

Fuc – Fucose

EIC – extracted ion chromatogram

FUT2 –  $\alpha(1-2)$ -fucosyltransferase

Gal – Galactose

Glc – Glucose

GlcNAc – N-acetylglucosamine

Hex – Hexose

HexNAc – N-acetylhexosamine

HMO – Human Milk Oligosaccharide

LC – liquid chromatography

MS – mass spectrometry

Neu5Ac – N-acetylneuraminic acid

PGC – Porous Graphitized Carbon

Ppm – Parts per million

Q-TOF – quadrupole orthogonal time-of-flight

RT – Retention time

SD – Standard deviation

SPE – Solid phase extraction

TOF – time-of-flight

TFA – Trifluoroacetic acid

## Table of Contents

|  |            |
|--|------------|
| <b>Chapter One – INTRODUCTION.....</b>   | <b>1</b>   |
| <br>   |            |
| <b>Chapter Two – Human Milk Oligosaccharide Compositions Illustrate Global Variations in Early Nutrition.....</b>                                      | <b>33</b>  |
| Abstract.....  | 34         |
| Introduction.....  | 35         |
| Methods.....   | 37         |
| Results.....   | 45         |
| Discussion.....  | 65         |
| <br>   |            |
| <b>Chapter Three – Fetus Receives Breast Milk Carbohydrates in Utero: A High Throughput LC-MS based method for HMO analysis in Amniotic Fluid.....</b> | <b>78</b>  |
| Abstract.....  | 79         |
| Introduction.....  | 80         |
| Methods.....   | 81         |
| Results.....   | 82         |
| Discussion.....  | 105        |
| Conclusion.....  | 107        |
| <br>   |            |
| <b>Chapter Four – Host Cell Glycocalyx Remodeling Reveals SARS-Cov-2 Spike Protein Glycomic Binding Sites.....</b>                                     | <b>112</b> |
| Abstract.....  | 113        |
| Introduction.....  | 114        |
| Methods.....   | 116        |
| Results.....   | 122        |
| Discussion.....  | 143        |
| Conclusion.....  | 146        |
| Supplementary.....   | 147        |

## CHAPTER ONE

### INTRODUCTION

Human breast milk is recognized by the World Health Organization as the ideal source of nutrition for infants in at least the first six months of life.<sup>1</sup> Mother's milk contains all the components essential for the healthy development of a growing infant. Among food and diet, human milk is unique in that it is tailored to the nutritional needs of the baby, constantly adapting in compositions to the infant's developmental requirements.

The composition of human milk is complicated but well-regulated and consists of macronutrients from three major groups: fats, proteins, and carbohydrates. The most abundant component are the carbohydrates, which are predominantly composed of lactose corresponding to approximately 70 g/L of the constituents in milk.<sup>2</sup> A unique subset of the carbohydrates is comprised of longer oligomers based on a lactose core known collectively as human milk oligosaccharides (HMOs). While HMOs are significantly lower in abundance than lactose, they still comprise a large fraction of the dry mass of mother's milk and can even be more abundant than proteins particularly during early lactation. Although lactose is composed of a galactose bound to a reducing glucose through an  $\beta(1,4)$  linkage, human milk oligosaccharides (HMOs) are built by adding further to the lactose core with the addition of galactoses and glucose as well as terminal decorations of fucose and sialic acids. Endogenous human enzymes in the gut readily break down lactose to provide fuel and mass for the growth of the infant. However, there are no human enzymes in the gut in appreciable amounts that break down HMOs. Thus, the mystery since

the characterization of the first HMO structure in 1930<sup>3</sup> was – why do mothers produce these compounds in large amounts when they provide no direct nutritional value to the infant?

The answer to this question has been debated since the discovery of HMOs. However, new analytical and rapid genome sequencing tools have provided definitive answers that are even more remarkable, namely that mothers use HMOs to recruit bacteria by feeding them so that they can provide benefits to the infant. While the advancements in genome sequencing are discussed in detail elsewhere, less is known regarding the major advances in analytical techniques for macromolecular analysis, in particular liquid chromatography – mass spectrometry (LC-MS). LC-MS based methods have revealed many unknown HMO structures, and additionally provided rapid profiling with quantitation. These methods have provided HMO abundances in human milk as well as other bodily fluids and tissues including blood<sup>4</sup> and urine.<sup>5</sup> This contribution attempts to summarize a general view of HMOs through their structural analyses, compositions, and functions.

This work has been published in the Encyclopedia of Cellular Biology and is included with permission in this thesis.

## **Structures of HMO**

HMOs are composed of five monosaccharides: L-fucose, D-glucose, D-galactose, N-acetylglucosamine and N-acetylneuraminic (sialic) acid (**Figure 1.1**). The foundation of every HMO consists of lactose core (a disaccharide comprised of glucose and galactose) at the reducing end, which is then further elongated with additional monosaccharides to provide linear and branched structures with the branching occurring at the galactose of the lactose core. Despite the decades of studies on HMOs, their biosynthesis is still not fully resolved. As glycans, HMOs are most similar in structure to O-glycans on proteins and some glycolipids (some having a lactose

core) than to N-glycans, therefore it is commonly acknowledged that the syntheses of HMOs is likely to proceed through similar pathways. Genomic studies have also been performed to examine the variations in genes that code the same or similar transferases.<sup>6</sup> Further studies have attempted to correlate the gene and corresponding glycosyl transferase to HMO structures, identifying perhaps the sets of glycosyl transferases responsible for the structural diversity of these compounds.<sup>7</sup>

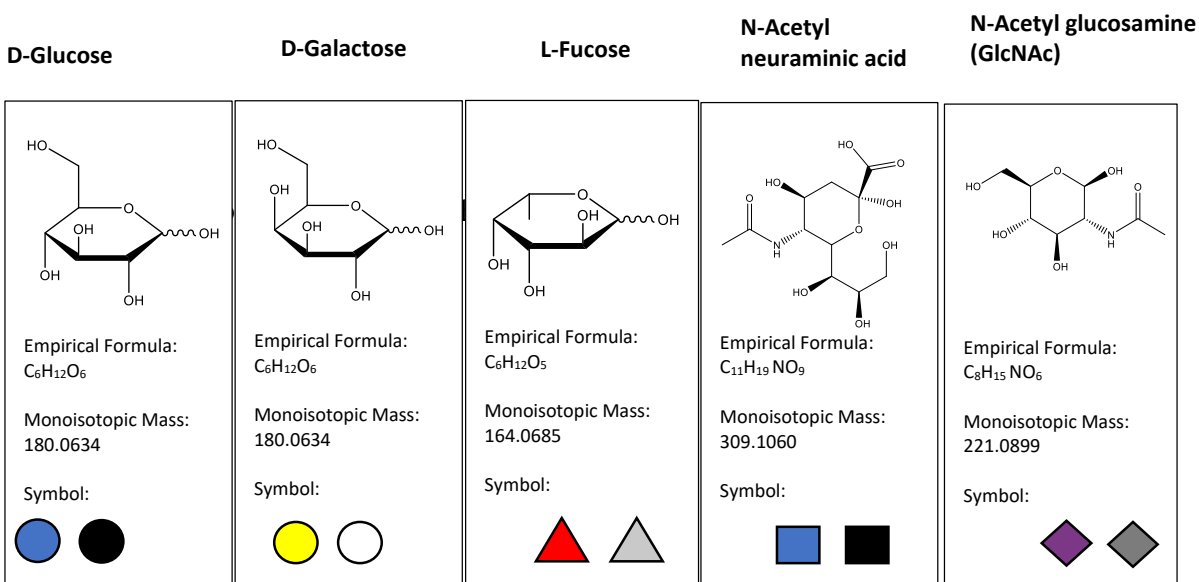


**Figure 1.1** Five building blocks of human milk oligosaccharides.

The addition of even a single monosaccharide residue readily differentiates the trisaccharide structure from the lactose core in several important ways. For example, the addition of a fucose to lactose produces fucosyllactose, while the addition of a sialic acid to lactose yields sialyllactose. Although lactose is readily digestible by human enzymes, adding a monosaccharide with no corresponding enzymes makes it indigestible to the infant. Most glycosyl hydrolases are exoglycosidase, which means they start at the nonreducing end or away from the lactose core. The

addition of either a sialic acid or fucose significantly alters the chemical characteristics and the biological functions of resulting compounds from each other and from lactose. Sialylated species contain a carboxylic acid group, making sialylated oligosaccharides acidic or anionic. Fucosylated and undecorated oligosaccharides are considered electronically neutral. The addition of even one monosaccharide can add significant variability in the resulting structures particularly with how it connects to the lactose core. The addition of fucose can occur on the 2, 3, 4, and 6 positions of the galactose. Additionally, the orientation of the linkage ( $\alpha$  or  $\beta$ ) at these positions results in even greater variability. However, the large number of possible structures are limited by the small number of glycosyl transferases. Thus, for example, although the addition of fucose may occur in 14 possible combinations, in reality only two of those are found in HMOs. The addition of fucose to lactose can occur either to the 2-position of the galactose to produce 2'-fucosyllactose (2'FL) or on the 3-position of the glucose to yield 3-fucosyllactose (3-FL).

HMOs may contain from 3 to more than 20 monosaccharides, however the most abundant structures have degree of polymerization between three and seven.<sup>8</sup> The potential structural diversity represented by all these variables were previously extrapolated to predict a large number of potential structures, with some estimates suggesting that as many as  $10^9$  structures were possible. However, LC-MS eventually resolved this issue by showing that in a single mother, there are only about 100 structures over the five orders of magnitude in dynamic range of the analytical method. When the milk from five mothers were combined, less than 300 structures were obtained.<sup>9</sup> The glycans that make up the ABO blood type are also shown in **Figure 1.2** for comparison illustrating the shared similarities between HMOs and glycans on glycolipids that define the blood type. With the analogy to the blood type, HMOs stratify individuals so that we should also develop a method for typing milk.

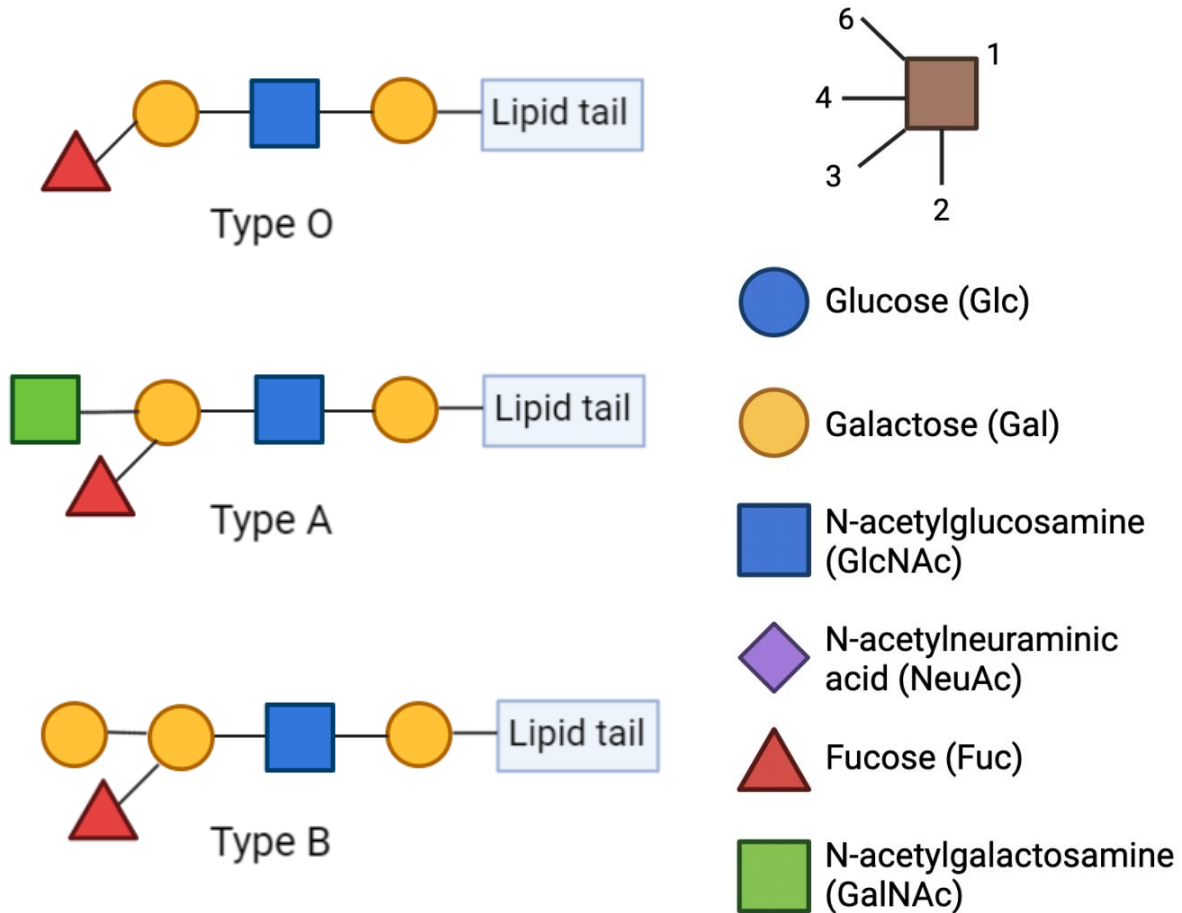


**Figure 1.2** Glycan composition on red blood cell distinguishes A, B, AB, and O blood groups.

HMOs can be classified into four structural subgroups based on their compositions: fucosylated, sialylated, sialofucosylated, and undecorated. Oligosaccharides with at least one fucose are fucosylated. Likewise, oligosaccharides with at least one sialic acid (N-acetylneuraminic acid) unit are sialylated, and structures with both are sialofucosylated. Undecorated structures contain neither a fucose nor a sialic acid and are only composed of glucose, galactose, and GlcNAc (N-acetylglucosamine). In general, mothers will have 35-60% fucosylated HMOs, 12-14% sialylated HMOs, 40-50% undecorated HMOs and 0-15% sialofucosylated.<sup>10</sup> As

discussed below, various factors such as geographical origin, genetic, and infant's age contribute to the variations in absolute and relative abundances of HMOs. However, the fraction of these distinct group of components varies greatly among mammalian species.

### **Structural Analysis of HMOs yields large numbers of structures**

Structural analysis of individual structures and quantitative profiling methods were key to elucidating the functions of HMOs. While there are general functional activities associated with the entire collections of structures, individual structures or group of structures are found to have unique and specific biological function. Thus, despite the complexity and heterogeneity of the structures, systematic structural analysis was important in elucidating the roles of individual HMOs. There have been individual efforts in determining specific structures, however there was no consistent earlier effort to analyze oligosaccharide structures comprehensively.<sup>11, 12</sup> Even now there remains no universal method for HMO analysis, however there are currently more systematic methods that provide good representation of the collection.

Isolation of HMOs from milk was complicated by the large abundances of lactose impeding the analysis of HMOs. However, solid phase extraction methods have made this more routine. A method for extensive profiling of HMOs structures now involves separation with liquid chromatography using a mass spectrometry detector. Preparation of HMOs using this method require four major steps: defatting, protein precipitation, reduction of HMOs, and solid phase extraction. The result is the production of chemically reduced structures or alditols that removes the anomeric reducing end to produce a single peak in the chromatogram.

A method developed for the comprehensive structural elucidation of many structures includes the use of liquid chromatography – mass spectrometry (LC-MS), tandem MS (MS/MS), and enzymatic digestion. In this approach, LC is used to isolate the individual compounds and MS to determine mass. LC-MS/MS in combination with exoglycosidases were used to determine the monosaccharide components and their linkages. Exoglycosidases are glycan cleaving enzymes that selectively cleave terminal residues and are highly specific to linkage, stereochemistry, and configuration of the anomeric carbon at the linkage. By systematically probing each HMO, the monosaccharides that make up the oligosaccharide and the specific linkages between each saccharide were deduced.<sup>13</sup> This LC-MS method provided a more systematic analysis by allowing the monitoring of hundreds of structures simultaneously with quantitative information making large clinical trials feasible with comprehensive HMO analyses (**Figure 1.3**).<sup>14</sup>

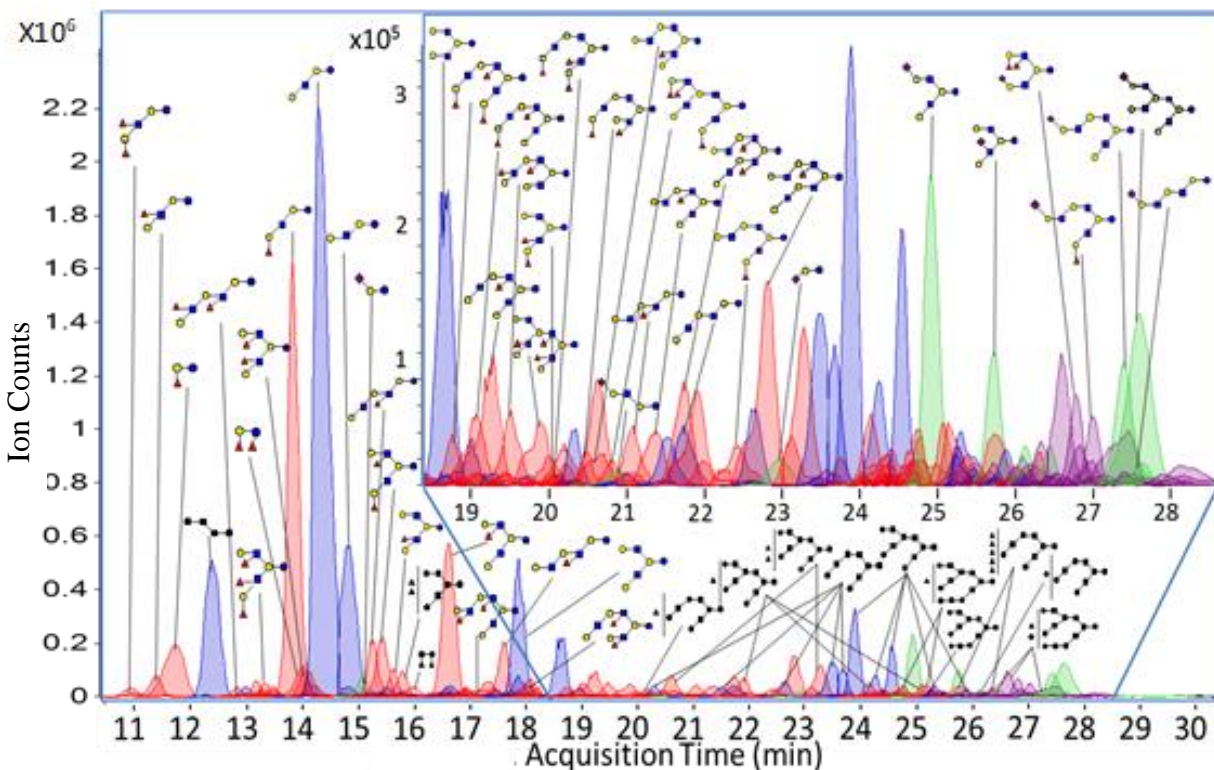


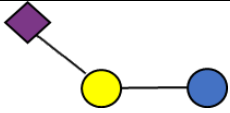
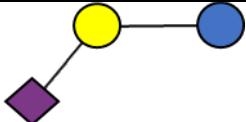
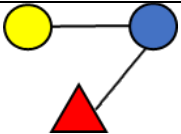
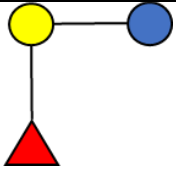
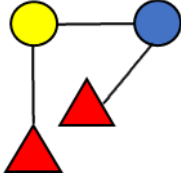
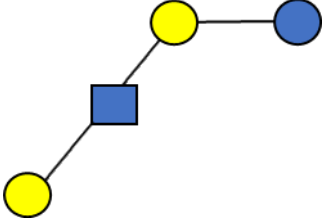
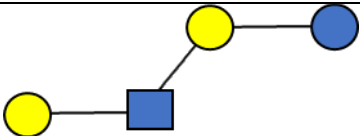
**Figure 1.3** LC-MS chromatogram of human milk oligosaccharides.

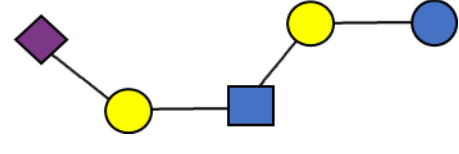
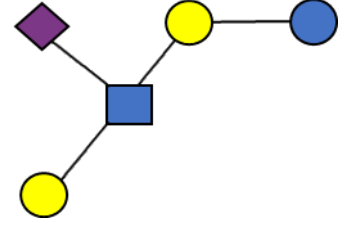
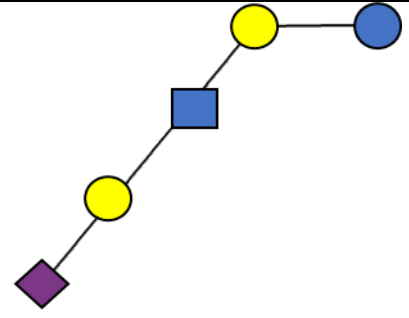
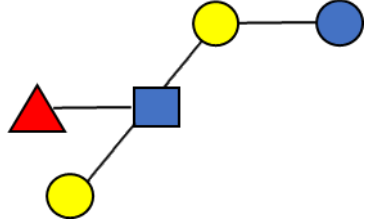
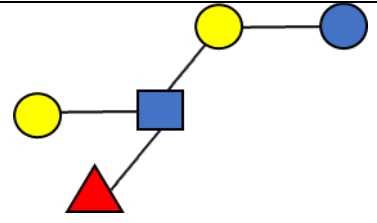
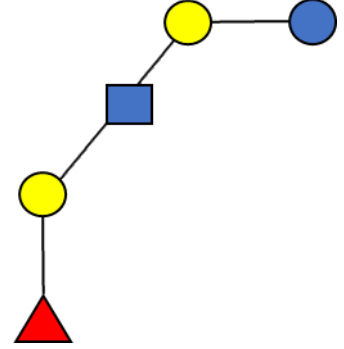
While semi-quantification (relative abundances) of HMOs more readily achieved, absolute quantitation of each structure remains problematic. There are very few HMO standards of sufficient quantity and purity for producing standard solutions. While LC-MS profiling provides relative quantitation, there are differences in ionization and detection efficiencies with LC-MS. Methods that employ spectrometric detection such as fluorescence and ultraviolet-visible are used for HMO analysis and are attractive because they are generally cheaper and provide similar detection efficiencies for each structure. These methods are however structurally non-specific, thus a shift in LC retention time or coeluting structures can complicate the identification of the compounds. Additionally, they require the addition of a label. While the detection efficiency is similar for the different labeled compounds facilitating quantitation, the reactivity of the HMOs toward the label can vary slightly. The labeling method also must be highly efficient. Even with 99% efficiency, this would still render the much less abundant species unidentifiable and more difficult to quantitate further decreasing the dynamic range to two as opposed to four or five for LC-MS. HMO methods for analysis are still constantly being refined. New methods that require no extensive enrichment, derivatization, with high quantitation have become available.<sup>8</sup> LC-MS, using a triple quadrupole detector, was employed with multiple reaction monitoring (MRM) to identify specific structures with quantitation. This method is fast and provides absolute quantitation and will likely play a greater role in the future HMO analysis.

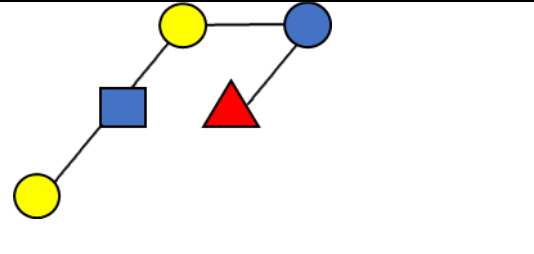
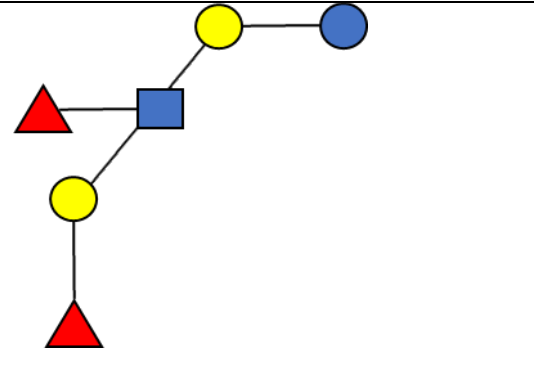
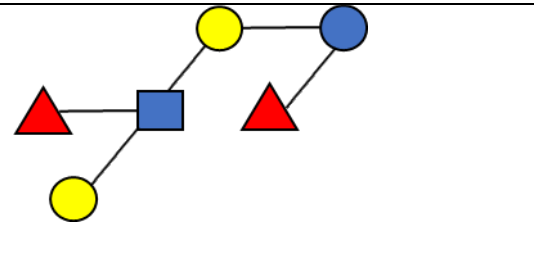
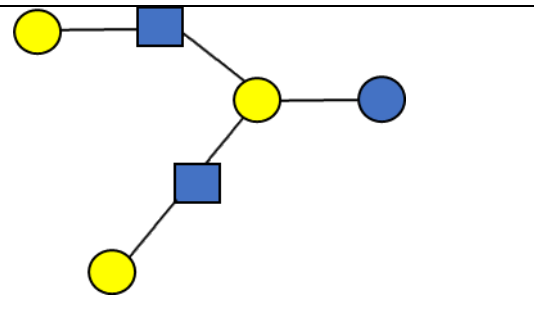
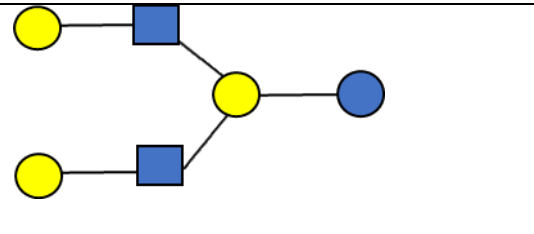
A systematic analysis of the structures and their abundances showed that a small number of structures dominate the abundances.<sup>15</sup> **Table 1.1** provides a schematic representation of the 30 most common HMO structures representing 80% of the abundances in mother's milk. Each mother has approximately 100 structures, with about 110 representing 100% of the HMO abundances.<sup>15</sup> About 50 structures represent 90% of the abundances, while 18 structures represent 70% of the

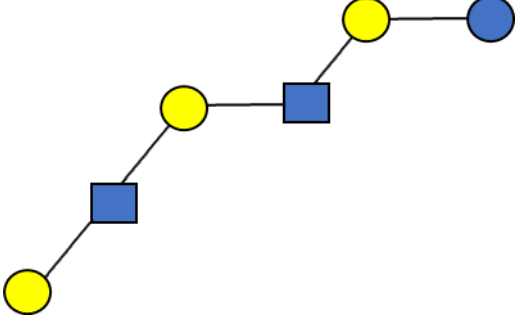
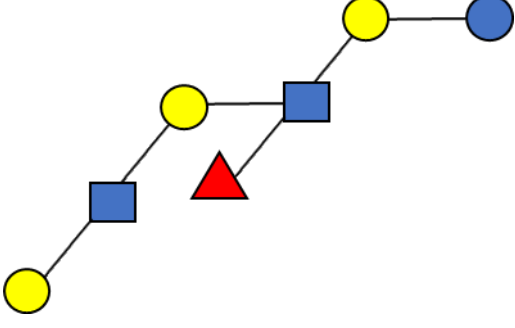
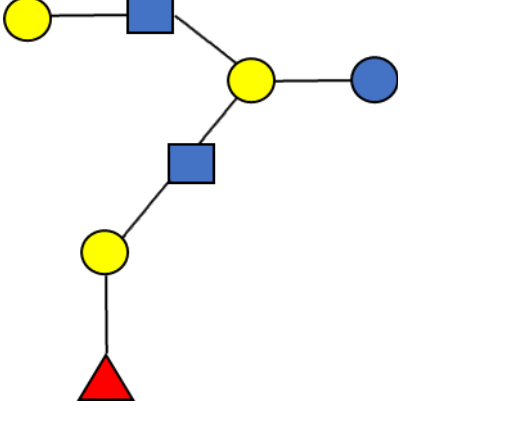
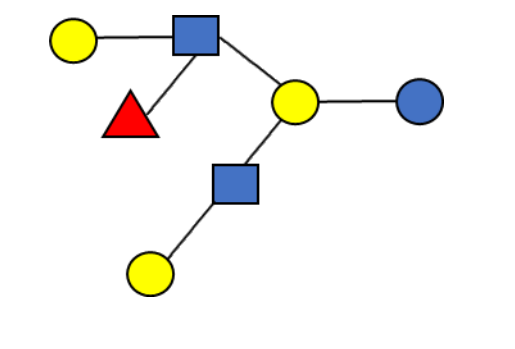
abundances. The accumulation of milk from five mothers may produce more than 300 unique structures. The smaller structures contain mono-fucosylation or sialylation with unique antigens such as Lewis b and Lewis x, while the larger ones can contain multi-fucosylation and sialylation with multiple antigens present in the same structure.

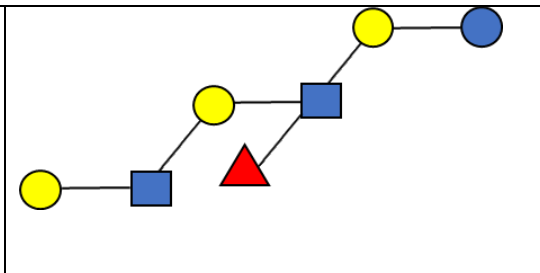
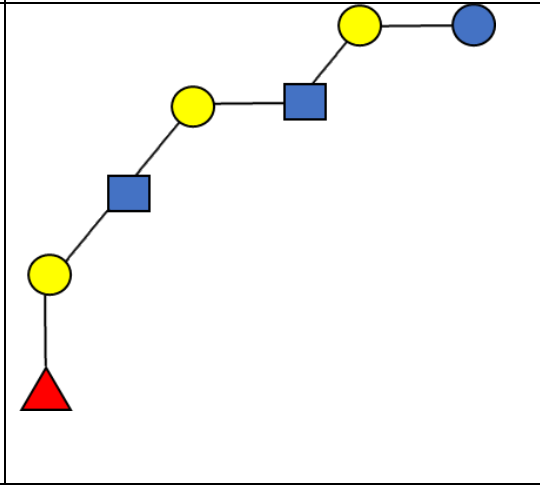
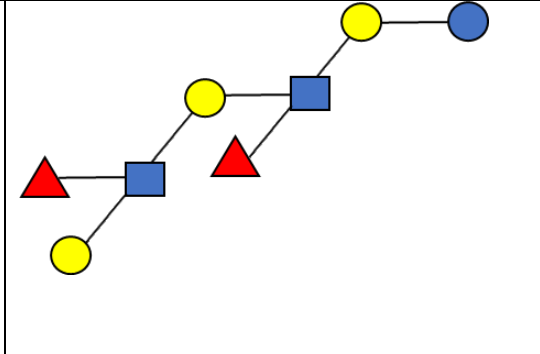
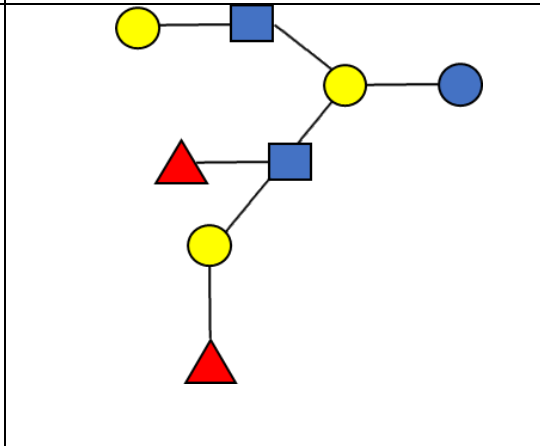
**Table 1.1** The 30 most abundant oligosaccharides found in human breast milk. Monosaccharide composition of structures are given as Hex\_HexNAc\_Fuc\_Neu5Ac and represented as glucose (●), galactose (●), N-acetylglucosamine (■), and fucose(▲).

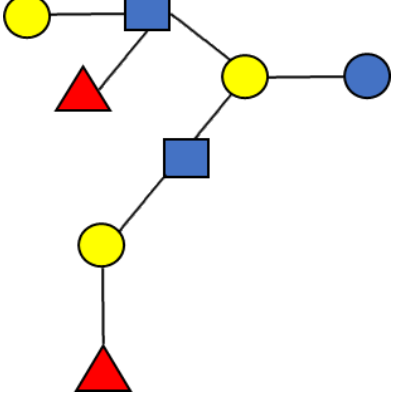
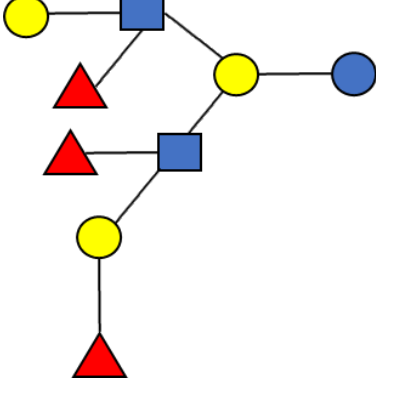
| HMO  | Structure   | Mass     | Composition |        |     |       |
|------|---|----------|-------------|--------|-----|-------|
|      |   |          | Hex         | HexNAc | Fuc | NeuAc |
| 6'SL |    | 635.2272 | 2           | 0      | 0   | 1     |
| 3'SL |    | 635.2272 | 2           | 0      | 0   | 1     |
| 3'FL |   | 490.190  | 2           | 0      | 1   | 0     |
| 2'FL |  | 490.190  | 2           | 0      | 1   | 0     |
| LDFT |  | 363.248  | 2           | 0      | 2   | 0     |
| LNT  |  | 709.264  | 3           | 1      | 0   | 0     |
| LNnT |  | 709.264  | 3           | 1      | 0   | 0     |

|          |   |          |   |   |   |   |
|----------|---|----------|---|---|---|---|
| LST c    |    | 1000.359 | 3 | 0 | 1 | 1 |
| LST b    |    | 1000.359 | 3 | 0 | 1 | 1 |
| LST a    |    | 1000.359 | 3 | 0 | 1 | 1 |
| LNFP II  |   | 855.322  | 3 | 1 | 1 | 0 |
| LNFP III |  | 855.322  | 3 | 1 | 1 | 0 |
| LNFP I   |  | 855.322  | 3 | 1 | 1 | 0 |

|          |   |          |   |   |   |   |
|----------|---|----------|---|---|---|---|
| LNFP V   |    | 855.322  | 3 | 1 | 1 | 0 |
| LNDFH I  |    | 1001.380 | 3 | 1 | 2 | 0 |
| LNDFH II |   | 1001.380 | 3 | 1 | 2 | 0 |
| LNH      |  | 1074.396 | 4 | 2 | 0 | 0 |
| LNnH     |  | 1074.396 | 4 | 2 | 0 | 0 |

|           |   |          |   |   |   |   |
|-----------|---|----------|---|---|---|---|
| P-LNH     |    | 1074.396 | 4 | 2 | 0 | 0 |
| MFpLNH IV |    | 1220.454 | 4 | 2 | 1 | 0 |
| MFLNH I   |   | 1220.454 | 4 | 2 | 1 | 0 |
| MFLNH III |  | 1220.454 | 4 | 2 | 1 | 0 |

|           |   |          |   |   |   |   |
|-----------|---|----------|---|---|---|---|
| IFLNH III |    | 1220.454 | 4 | 2 | 1 | 0 |
| IFLNH I   |    | 1220.454 | 4 | 2 | 1 | 0 |
| DFpLNH II |   | 1366.512 | 4 | 2 | 2 | 0 |
| DFLNHb    |  | 1366.512 | 4 | 2 | 2 | 0 |

|        |  |          |   |   |   |   |
|--------|--|----------|---|---|---|---|
| DFLNHa |   | 1366.512 | 4 | 2 | 2 | 0 |
| TFLNH  |  | 1512.570 | 4 | 2 | 3 | 0 |

### Compositions of HMOs and their abundances in mothers' milk

The abundances of the components of milk are dynamic during lactation with several factors that directly affect the total and relative abundances of the structures. The first few days after birth the mother's milk is the richest, containing the highest amounts of proteins, fats, and HMOs. This nutrient rich milk is known as colostrum. The colostrum contains on average 22g/L protein, 29 g/L fat and 20-23 g/L HMOs.<sup>16</sup> The most significant factor in the total abundances of HMOs is the month post-partum. The concentration of HMOs decreases monthly and reaches a stable concentration at 6 months postpartum corresponding to 7-12 g/L.<sup>17</sup> The standard recommendation of exclusive breast feeding for at least the first 6 months matches with the

moment where HMOs reach a stable concentration. Beyond month six, the abundances of HMO remain stable even for children who are nursed for up to two years. It is debatable whether the infant gets more HMO earlier and less later. In the later period as the infant grows bigger, the mother is also producing more milk while the infant is also consuming more milk.

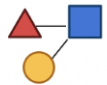
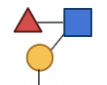
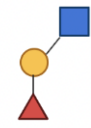
Although total abundances of HMOs in the mother's milk decrease in the first six months of lactation, the abundances of individual components vary little relative to each other throughout lactation. There is an increase in the relative abundances of fucosylated structures during the first six months but this trend is observed for all fucosylated structures and is not readily observed with individual structures.<sup>8</sup> The direct effect of this increased fucosylation on the infant health is unknown, however it has been observed that high concentrations of fucose containing structures in the mother's milk correlates to higher levels of *Bifidobacterium* and *Bacteroides*.<sup>18</sup> Sialylated structures appear to be constant and generally remain low during the first six months.

Exceptions to the above general behavior are milk for infants born preterm. Preterm or "premature" infants are born before the 37th week of pregnancy. The prevalence of preterm births is relatively high in the United States with nearly 1 in every 10 infants being born prematurely. The HMOs from the milk of mothers with preterm infant may not fit the common profile and may themselves be immature.<sup>19</sup> While some of the milks have normal HMO profiles, those that are born weeks early have milk that are lower in some structures such as *lacto N tetraose* with total fucosylation considerably reduced by as much as 75%. In general, preterm milk does not follow general trends of term births regarding total concentrations. Interestingly, even when the putative birth date is reached, the HMO concentrations remain in the same deficient state. Most premature infants receive processed breast milk, which contain HMO, and are further supplemented by

formula milk, which currently contain little or no HMO. However, this situation is being remedied as manufacturers are rapidly adding one or two structures in limited amounts.

Variations in HMO structures between individuals are due primarily to the specific genotype of the mother. Variations in HMO abundances from different mothers depends highly on the Secretor (Se) and Lewis blood group (Le) loci. The relationships between the genes and the structures they produce are shown in **Table 1.2**.

**Table 1.2** Secretor (Se) and Lewis blood group (Le) loci affect HMO abundances and structures in mothers milk.

| Secretor Genotype (FUT2) | Lewis Genotype (FUT3) | Phenotype      | Glycan Epitope, Fucose Linkage  |
|--------------------------|-----------------------|----------------|---|
| se/se non-sec            | le/le                 | Le (a-b-), Se- | <br>Type 1 chain                  |
| se/se non-sec            | Le/Le or Le/le        | Le (a+b-), Se- | <br>Le <sup>a</sup> Fuc α1-4      |
| Se/Se secretor           | Le/Le or Le/le        | Le (a-b+), Se+ | <br>Le <sup>b</sup> Fuc α1-4 α1-2 |
| Se/Se secretor           | le/le                 | Le (a-b-), Se+ | <br>H(O) Fuc α1-2                 |

There are several genotypes that affect the phenotypic HMO abundances. Between these various possibilities, the secretor genotype provides the greatest differentiation among HMO structures. A functional FUT2 allele produces an  $\alpha(1,2)$ -fucosyltransferase enzyme that adds a fucose in the  $\alpha(1,2)$  position of the nascent oligosaccharide. When this gene is active (secretor mother), it produces HMOs containing  $\alpha(1,2)$ -fucose in large abundances. Non-Secretors have an inactive FUT2 gene and subsequently produce little to no  $\alpha(1,2)$ -fucosylated structures. Among the fucosylated structures,  $\alpha(1,2)$ -fucosyllactose or 2'fucosyllactose (2'FL) is structurally the simplest and one of the more abundant oligosaccharides found in the milk of secretor mothers. LC-MS chromatograms highlight the differences in breast milk composition between secretor and non-secretor mothers for a few selected structures (**Figure 1.4**).

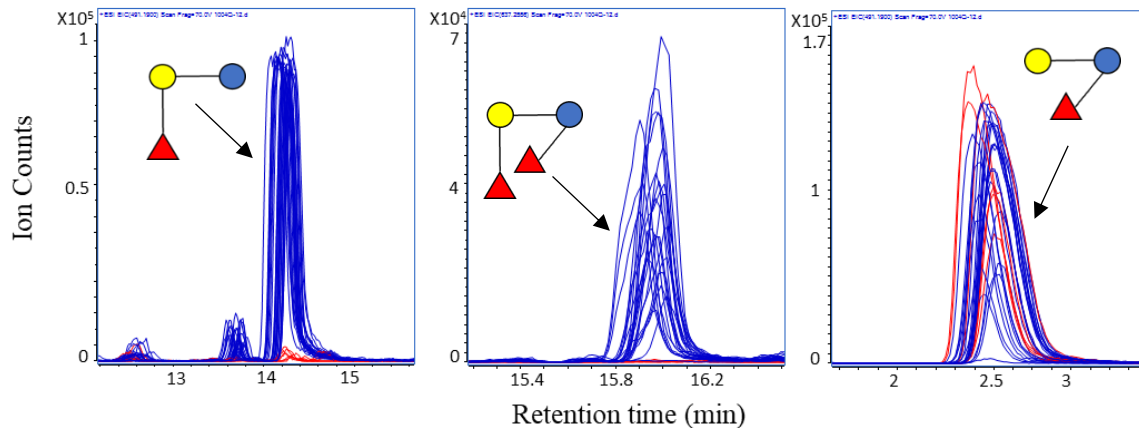


**Figure 1.4.** Extracted ion chromatograms (EICs) displaying differences in abundances of HMO markers (a) 2'FL (b) LDFT (c) 3'FL between mothers who are secretors (–) and Non-secretors (—) from a select group of mothers. Monosaccharide composition of structures are given as Hex\_HexNAc\_Fuc\_Neu5Ac and represented as glucose (●), galactose (●), and fucose (▲).

Milk from secretor mothers contain significantly more 2'FL, LNFP I, LDFT and other  $\alpha(1,2)$ -fucosylated structures in their milk compared to non-secretors. Nonsecretor mothers produce nearly no  $\alpha(1,2)$ -fucosylated structures, although in some cases there are small amounts of 2'FL

produced. In general, the LC-MS chromatograms yield very different profiles between secretors and nonsecretors. If measured precisely and reproducibly, HMOs can be used to phenotype the milk and determine the mother's phenotypic secretor status.<sup>20</sup> It is possible to phenotype the mother based on the abundance of  $\alpha(1,2)$ -fucosylated species with nearly 100% accuracy.

Non-secretor mothers have an inactivated FUT2 gene, with the nature of the inactivation differing between different populations.<sup>21</sup> Interestingly, the inactivation of a major fucosyl transferase gene should decrease the amount of fucosylation in nonsecretor mothers; however, fucose is such an important monosaccharide that other fucosyl transferases make up for the absence of the specific enzyme by producing other fucose linked structures such as  $\alpha(1,3)$ ,  $\alpha(1,4)$  (FUT3 gene) and  $\alpha(1,6)$ , which indeed are in greater abundance in nonsecretor mothers. The representation of the general abundances and structures that distinguish between secretors and nonsecretors are provided in **Figure 1.5** Although fucosylated structures do correlate with secretors and nonsecretor mothers, there are non-fucosylated structures that also differ consistently in abundances between the phenotypes.

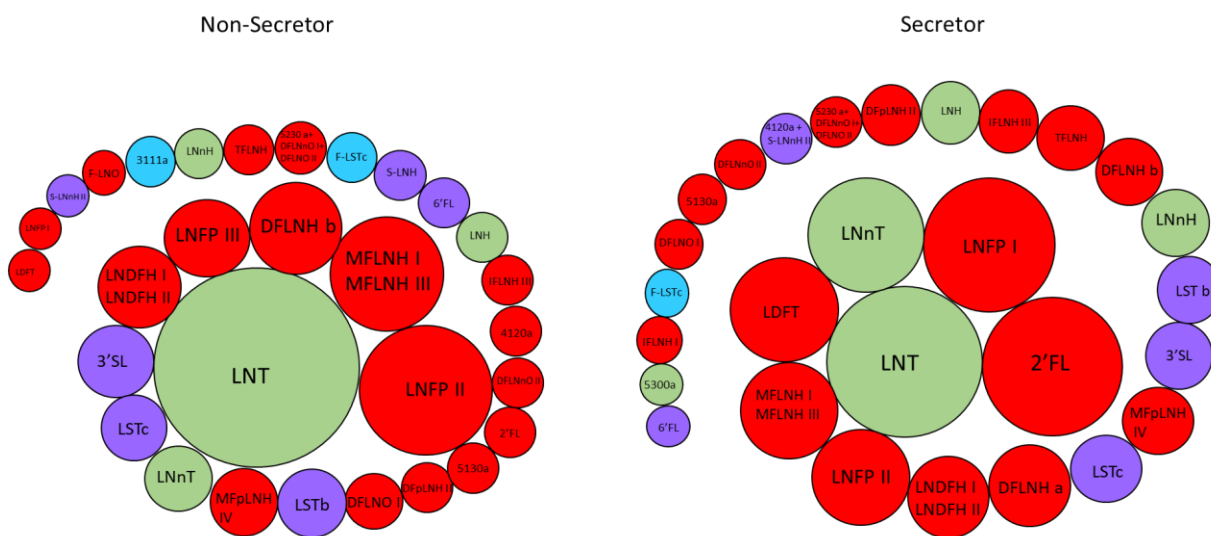


**Figure 1.5** Differences in oligosaccharide abundances in human milk between secretor (right) and non-secretors (non-secretors). Size of bubble represents the relative abundance of the oligosaccharide in the mother's milk.

The total fraction of nonsecretor mothers is smaller compared to secretor mothers. A value of 20% nonsecretors is often cited in literature, however this value varies with different populations and is not broadly maintained. In Europe and much of North America with a large population of European descendants, the fraction of non-secretors generally remains within the 20% range. HMO analysis of milk from mothers in West Africa show a considerably greater fraction of nonsecretors corresponding to nearly 40% nonsecretors, perhaps representing the upper limit for the fraction of non-secretors. Broader genomic studies, not related to human milk, have examined genotypic variations throughout various populations and found that the fraction of nonsecretors can reach near zero particularly among indigenous peoples.<sup>22</sup>

There is currently little evidence that indicates that one phenotype is generally more advantageous than the other. However, from the evolutionary standpoint there must have been local pressures that selected one phenotype over the other. While there have been several studies that compare the microbiota of an infant fed with secretor vs non-secretor milk, there is still a lack of understanding how these differences directly correlate to the health of the infant in the developmental stages and later in life. However, there has been some research that suggests that there are advantages and disadvantages that associate with each when comparing rates and severity of some diseases. For example, secretors are more likely to get stomach ulcers but are less likely to get yeast infections. Non secretors on the other hand have been shown to have a greater chance of developing type I diabetes and Ulcerative colitis but are less likely to get Crohn's disease.

There are other factors that affect HMO abundances but much less strongly than the mother's secretor status or period of lactation. Studies on the mode of delivery, the diet of the mother, the sex of the infant, the age of the mothers show they are all important considerations and have been found to affect the total concentrations of HMOs.<sup>23</sup> Diet is the natural potential source

for HMO variations. Indeed, mothers who go through seasonal changes in weight due to periods of under-nutrition produce lower abundances of HMOs with under-nutrition.<sup>24</sup> The variations have been further correlated to their impact on the gut microbiome of the infants. However, many of these studies are on limited cohorts with overlapping confounding factors that make it difficult to parse out small changes in abundances. Larger cohorts and more systematic studies are needed but are difficult to perform due to the sensitive nature of the subjects.

### **HMOs provide health benefits in its interactions with the gut microbiome**

The unique structures of HMOs and their abundances in human milk have provided early indications as to their roles in the infant. The structures resemble other glycan structures such as those on the cell membrane or the glycocalyx, which are known to interact with viruses and bacteria. For this reason, studies of HMO-microbe interactions have focused on the potential role primarily as decoys, binding to bacteria and virus to prevent pathogens from colonizing the gut. However, both commensal and pathogens bind HMOs so selectivity may be difficult to achieve. Furthermore, free oligosaccharides do not bind as strongly as conjugated ones. Thus, glycoproteins such as IgA and lactoferrin, which are highly glycosylated with similar Lewis epitopes as those found in HMOs and with similarly large abundances, are better suited for this role as they can coordinate more extensively to the surface of pathogens.<sup>25</sup> Additionally, many of the correlative studies regarding protection through HMO behavior as decoys can be better attributed to the enhancement of specific bacteria that are favored by their consumption of HMOs allowing them to better compete.

HMOs transit through the upper gastrointestinal tract (GIT) intact to reach the lower intestine where they interact with millions of bacteria. The distal gut is where HMOs provide the greatest benefit to the infant. A recent study reported high levels of HMOs, and in particular those

that are sialylated, promoted growth in mice suffering from under-nutrition.<sup>26</sup> There is a large number of different bacteria that colonize the infant's gut, but few have the enzymes that bind, transport and simultaneously catabolize HMOs. *Bifidobacterium longum* subsp. *infantis* (*B. infantis*) are gram-positive prokaryotes that are found in the distal gut of healthy infants and contain the gene *cassette* that have evolved to interact specifically with HMOs. These bacteria have the complement of solute binding proteins that bring in HMOs intact to be digested by glycosyl hydrolases in the bacteria with specificities that correspond to the linkages and monosaccharide compositions of HMOs. Indeed, monitoring the feces of infants in early lactation shows that much of the HMOs provided in milk are lost in feces.<sup>27</sup> However, when the bifidobacterial population increases in the gut and becomes established, much of the HMOs in feces are no longer there suggesting consumption of HMOs by the bacterial population. Other *Bifidobacterium* species consume HMOs but not to the extent of *B. infantis*. With the aid of HMOs, *B. infantis* can become the dominant bacterium and become the master colonizer of the gut.<sup>28</sup> The mother's secretor status also plays a role in the establishment of the gut microbiota. Secretor mothers producing the corresponding milk tend to establish bifidobacteria earlier than nonsecretor mothers.<sup>29</sup>

The broad benefits of *B. infantis* is still an evolving subject, but the bacteria's contribution to the infant's health already appears to be significant. *B. infantis* can lower pathogen concentrations in the gut by decreasing pH through the production of short chain fatty acids (SFCAs). *B. infantis* secretes acidic metabolites such as acetate, butyrate, and lactate that lower the pH of the gut making it inhospitable to various bacterial pathogens.<sup>30</sup> The presence of *B. infantis* in the gut has been shown to significantly decrease the amount of antimicrobial resistant genes belonging primarily to *Escherichia*, *Clostridium*, and *Staphylococcus* in the infant gut.<sup>31</sup>

Additionally, SCFA further aid the development of the gut by increasing intestinal barrier function thereby promoting immune maturation.

Aside from its interaction with the gut microbiome, there are other roles attributed to HMOs. The brain is highly sialylated, and thus sialic acid in HMOs have been proposed to play a role in the development of the infant brain. Sialic acids are a major component of brain tissues and are integral in influencing the brain development in the early stages of life, affecting neuronal transmissions, synaptogenesis, and memory formation.<sup>32</sup> In the first 6 months of life, the infant undergoes a critical period of growth where the brain has great plasticity to account for rapid physical and cognitive brain development. In the first 90 days alone, the infant brain grows approximately 1% per day, reaching 64% of an adult's brain volume by the end of 3 months.<sup>33</sup> This rapid expansion requires a continuous supply of nutrients. As several of the structures are sialylated, HMOs are one of the richest sources of sialic acid containing molecules.<sup>34</sup> The most abundant sialic acid containing structures are 6'-siallactose and 3'-siallactose; however larger structures with multiple sialic acids are also present. While HMOs themselves have not been reported intact in the brain, studies have shown that there is an increase in sialic acid containing molecules such as gangliosides in breastfed infants compared to formula fed further indicating the link between breastfeeding and neurological development. Compared to other mammals, the human brain has more sialic acid-containing molecules. In fact, humans have roughly 2-4 times the amount of sialylated glycoconjugates compared to other mammals such as our closest relatives, the chimpanzees.<sup>35</sup> Furthermore, the concentration of sialylated molecules increase with age confirming the association that these structures have with maturation and evolutionary development.<sup>35</sup>

Immune development occurs in the first few weeks of life when immune cells peak in circulation. HMOs have been proposed to play a key role in developing and modulating the immune system.<sup>36</sup> Selected HMO structures have the ability to promote epithelial barrier maturation and the production of mucins. The benefits that HMOs impart to the infant may also be found on the mother who produces them. Indeed, several in vitro studies do point to additional benefits of HMO alone. For example, the addition of 6'SL to intestinal cells increased secretions of cytokines such as IL-9 and CCL20.<sup>36</sup> Other observations included increased production of TNF $\alpha$  with cells subjected to the same compounds. Similarly, villi formation in intestinal cells were increased with the supplementation of 2'FL.

There are other attributes often associated with HMO supplementation, but many are difficult to separate from the symbiotic relationship of HMO and *B. infantis*. Clinical studies on the effects of HMO supplementation are observed with similar supplementation of *B. infantis*. For example, the supplementation of HMO has been suggested to decrease necrotizing enterocolitis; however, similar observations were observed with supplementation with *B. infantis* alone. Because of the key role that HMOs play in the colonization of the infant gut, the effects of HMOs alone are often clinically difficult to separate from the effects of *B. infantis* or other microbes.

### **Milk Oligosaccharides from other mammals**

A comparison of HMOs with other mammalian milk oligosaccharides provides further insight into the unique structures found in human milk and the potential evolutionary path of HMOs. While this topic can be significantly larger, the discussion here is brief highlighting the broad differences between HMO and other mammalian MOs. Many of the structures in other mammals are also found in humans. The structures found in most mammalian milks are typically

less abundant and smaller in numbers than human milk, with the exception of some primates. For example, bovine milk has only 1 g/L of oligosaccharides in colostrum, and this drops to 100 mg/L in mature milk.

A major structural difference between mammals is in the lactose core itself. In bovine milk (BMO), a fraction of the lactose core is modified with glucose replaced by an N-acetylglucosamine.<sup>37</sup> The milk oligosaccharides can also be elongated from the modified core. A broader difference between mammals is in the distribution of fucosylated, sialylated, and undecorated structures. For example, bovine milk has the highest level of sialylation and very low fucosylation in their milk oligosaccharides, in contrast to human milk which has very high levels of fucosylation and low levels of sialylation (**Figure 1.6**).<sup>38</sup> The most abundant BMOs are the isomers of sialyl lactose, namely 6'-siallactose and 3'-siallactose with the ratio of the two inverting between breeds.<sup>39</sup> An additional oligosaccharide structure of sialic acid found in bovine milk is not found in human milk, namely N-glycolylneuraminic acid (NeuGc).<sup>40</sup> Although this structure is found in bovine milk, its abundance is considerably lower than in bovine tissue. In general, fucosylated structures are in very low abundance in bovine milk and may not be detectable by modern analytical tools unless sufficiently enriched. In general, BMO abundances are significantly lower than other mammals, perhaps due to selective breeding.<sup>41</sup> The value of bovine milk is generally based on the protein content and not BMO. Selection of high protein yields may have decreased the abundances of BMO. Oligosaccharides in porcine milk have a somewhat greater amount of fucosylation, making it more similar to human milk.<sup>42</sup> Other mammalian milks, such as murine milk, have similar structures to bovine milk with little to no fucosylated structures.

The milk oligosaccharides of selected primates have been systematically studied and were found to have a greater overall similarity with the structures found in humans.<sup>15</sup> The numbers vary between species, with humans and chimpanzees having similar numbers (approximately 100) and gorilla having the least (approximately 50). Stratification of the oligosaccharides did not necessarily follow the phylogenetic tree. Rhesus and humans had much greater similarities compared to humans and gorillas. It was concluded that the milk oligosaccharides separated according to social structures, with those that had the more complicated social structures sharing more similar compounds, while more solitary animals, such as the gorilla, having different milk oligosaccharides.

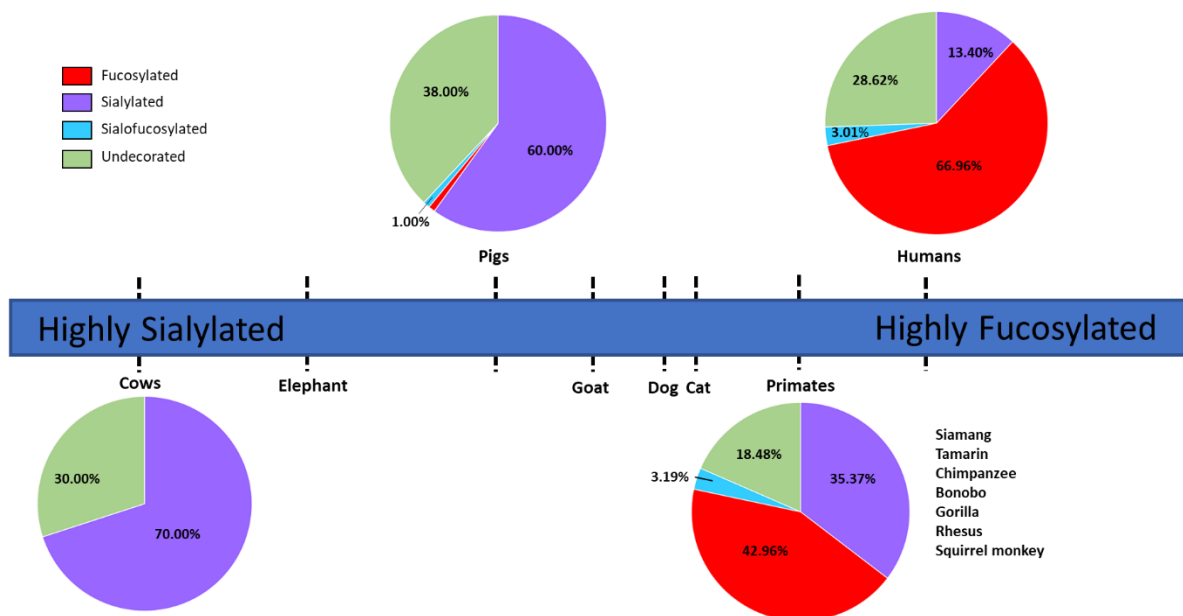


**Figure 1.6** Comparison of breast milk composition of different mammalian species from highly sialylated (left) to highly fucosylated (right).

The milk oligosaccharides of dogs and cats have levels of fucosylation and sialylation that are intriguingly closer to primates.<sup>43</sup> Indeed, canines and felines share many structures found in humans consistent with shared microbiomes between the species. Canines have milk oligosaccharides that are dominated with 3'SL, 6'SL and 2'FL representing over 90% of the

abundances. Felines have several more structures dominated by DFLNHb and 3'SL and others with very little 2'FL in the milk. Interestingly, dogs and cats appear to be similar to different secretor phenotypes. Dogs appear more like secretors, while cats seem to be more similar to nonsecretors.

### **HMO in Infant formula**

Infant formula has traditionally been produced from cow's milk, with the abundances of milk oligosaccharide extremely low as those observed in BMOs. Trace amount of sialyllactose and other trisaccharides are typically found in commercial products. However, with the significant interest in HMO, infant formula has now been enriched with HMOs, although generally not in abundances and complexity that would replicate breast milk. Supplementation has focused on simple structures that are easier to synthesize, specifically 2'FL and 6'SL. Mother's milk contains relatively large concentrations of lacto-*N*-tetraose (LNT), Lacto-*N*-fucopentaose (LNFP) and 6-Siallactose (6'SL), however these oligosaccharides are not yet commonly supplemented in infant formula because they have yet to be adapted for large scale production <sup>44</sup>, although this situation is rapidly changing.

### **CONCLUSION**

Human breast milk contains a unique blend of milk oligosaccharides. These oligosaccharides assist in the growth of a healthy infant throughout the most important developmental stages of life. Their main function in the infant is to establish the gut microbiome by feeding and enriching the proper gut bacteria. HMOs play critical roles not just in establishing a healthy gut microbiome, but also in protection by inhibiting pathogenic infections and in aiding

the development of the brain. These actions, while important to the infant, also have direct consequences on the child's well-being later in later life by decreasing the chances of childhood obesity, diabetes, and gastrointestinal diseases. Human milk oligosaccharides are therefore an important class of compounds that play critical roles in the development of the infant and their health trajectory throughout life.

The studies of HMOs further reveal the role of food. Human milk is the perfect food for a human infant, refined by millions of years of evolution. Human milk also serves as a model of the ideal food for adults. The ideal food therefore contains more than just fuel and material for building body mass. It contains nondigestible fiber that works with the gut microbiome to provide important compounds not produced by the person or the food alone. A more thorough understanding of HMOs have been enabled by new sequencing and analytical tools. These tools will similarly reveal the role of fiber in later life.

## **ACKNOWLEDGMENTS**

Funding provided by the National Institutes of Health are greatly appreciated. The author also acknowledges the help of Yu Wang in preparing the manuscript.

## REFERENCES

1. Organization, W. H., *Global strategy for infant and young child feeding*, *The optimal duration of exclusive breastfeeding*. Organization, W. H., Ed. 2001.
2. Lönnerdal, B.; Forsum, E.; Gebre-Medhin, M.; Hambraeus, L., Breast milk composition in Ethiopian and Swedish mothers. II. Lactose, nitrogen, and protein contents. *The American Journal of Clinical Nutrition* **1976**, *29* (10), 1134-1141.
3. Kunz, C., Historical aspects of human milk oligosaccharides. *Adv Nutr* **2012**, *3* (3), 430S-9S.
4. Ruhaak, L. R.; Stroble, C.; Underwood, M. A.; Lebrilla, C. B., Detection of milk oligosaccharides in plasma of infants. *Analytical and Bioanalytical Chemistry* **2014**, *406*, 5775-5784.
5. Rudloff, S.; Pohlentz, G.; Diekmann, L.; Egge, H.; Kunz, C., Urinary excretion of lactose and oligosaccharides in preterm infants fed human milk or infant formula. *Acta Paediatrica* **1996**, *85* (5), 598-603.
6. Kellman, B. P.; Richelle, A.; Yang, J.-Y.; Chapla, D.; Chiang, A. W. T.; Najera, J.; Bao, B.; Koga, N.; Mohammad, M. A.; Bruntse, A. B.; Haymond, M. W.; Moremen, K. W.; Bode, L.; Lewis, N. E., Elucidating Human Milk Oligosaccharide biosynthetic genes through network-based multiomics integration. *bioRxiv* **2020**, 2020.09.02.278663.
7. Zeuner, B.; Teze, D.; Muschiol, J.; Meyer, A. S., Synthesis of Human Milk Oligosaccharides: Protein Engineering Strategies for Improved Enzymatic Transglycosylation. *Molecules* **2019**, *24* (11), 2033.
8. Xu, G.; Davis, J. C. C.; Goonatileke, E.; Smilowitz, J. T.; German, J. B.; Lebrilla, C. B., Absolute Quantitation of Human Milk Oligosaccharides Reveals Phenotypic Variations during Lactation. *The Journal of Nutrition* **2016**, *147* (1), 117-124.
9. Ninonuevo, M. R.; Park, Y.; Yin, H.; Zhang, J.; Ward, R. E.; Clowers, B. H.; German, J. B.; Freeman, S. L.; Killeen, K.; Grimm, R.; Lebrilla, C. B., A Strategy for Annotating the Human Milk Glycome. *Journal of Agricultural and Food Chemistry* **2006**, *54*, 7471-7480.
10. Totten, S. M.; Zivkovic, A. M.; Wu, S.; Ngyuen, U.; Freeman, S. L.; Ruhaak, L. R.; Darboe, M. K.; German, J. B.; Prentice, A. M.; Lebrilla, C. B., Comprehensive Profiles of Human Milk Oligosaccharides Yield Highly Sensitive and Specific Markers for Determining Secretor Status in Lactating Mothers. *Journal of Proteome Research* **2012**, *11* (12), 6124-6133.
11. Bao, Y.; Zhu, L.; Newburg, D. S., Simultaneous quantification of sialyloligosaccharides from human milk by capillary electrophoresis. *Analytical Biochemistry* **2007**, *370* (2), 206-214.
12. van Leeuwen, S. S., Challenges and Pitfalls in Human Milk Oligosaccharide Analysis. *Nutrients* **2019**, *11* (11).
13. Wu, S.; Grimm, R.; German, J. B.; Lebrilla, C. B., Annotation and Structural Analysis of Sialylated Human Milk Oligosaccharides. *Journal of Proteome Research* **2011**, *10*, 856-868.
14. Totten, S. M.; Wu, L. D.; Parker, E. A.; Davis, J. C. C.; Hua, S.; Stroble, C.; Ruhaak, L. R.; Smilowitz, J. T.; German, J. B.; Lebrilla, C. B., Rapid-throughput glycomics applied to human milk oligosaccharide profiling for large human studies. *Analytical and Bioanalytical Chemistry* **2014**, *406*, 7925-7935.

15. Tao, N.; Wu, S.; Kim, J.; An, H. J.; Hinde, K.; Power, M. L.; Gagneux, P.; German, J. B.; Lebrilla, C. B., Evolutionary glycomics: characterization of milk oligosaccharides in primates. *J Proteome Res* **2011**, *10* (4), 1548-57.
16. Langer, P., Differences in the Composition of Colostrum and Milk in Eutherians Reflect Differences in Immunoglobulin Transfer. *Journal of Mammalogy* **2009**, *90* (2), 332-339.
17. Xu, G.; Davis, J. C. C.; Goonatilleke, E.; Smilowitz, J. T.; German, J. B.; Lebrilla, C. B., Absolute Quantitation of Human Milk Oligosaccharides Reveals Phenotypic Variations during Lactation. *The Journal of Nutrition* **2017**, *147* (1), 117-124.
18. Cabrera-Rubio, R.; Kunz, C.; Rudloff, S.; García-Mantrana, I.; Crehuá-Gaudiza, E.; Martínez-Costa, C.; Collado, M. C., Association of Maternal Secretor Status and Human Milk Oligosaccharides With Milk Microbiota: An Observational Pilot Study. *J Pediatr Gastroenterol Nutr* **2019**, *68* (2), 256-263.
19. De Leoz, M. L.; Gaerlan, S. C.; Strum, J. S.; Dimapasoc, L. M.; Mirmiran, M.; Tancredi, D. J.; Smilowitz, J. T.; Kalanetra, K. M.; Mills, D. A.; German, J. B.; Lebrilla, C. B.; Underwood, M. A., Lacto-N-tetraose, fucosylation, and secretor status are highly variable in human milk oligosaccharides from women delivering preterm. *J Proteome Res* **2012**, *11* (9), 4662-72.
20. Totten, S. M.; Zivkovic, A. M.; Wu, S.; Ngyuen, U.; Freeman, S. L.; Ruhaak, R. L.; Darboe, M. K.; German, J. B.; Prentice, A. M.; Lebrilla, C. B., Comprehensive Profiles of Human Milk Oligosaccharides Yield Highly Sensitive and Specific Markers for Determining Secretor Status in Lactating Mothers. *Journal of Proteome Research* **2012**, *11* (12), 6124-6133.
21. van Leeuwen, S. S.; Stoutjesdijk, E.; ten Kate, G. A.; Schaafsma, A.; Dijck-Brouwer, J.; Muskiet, F. A. J.; Dijkhuizen, L., Regional variations in human milk oligosaccharides in Vietnam suggest FucTx activity besides FucT2 and FucT3. *Scientific Reports* **2018**, *8* (1), 16790.
22. Lindén, S.; Mahdavi, J.; Semino-Mora, C.; Olsen, C.; Carlstedt, I.; Borén, T.; Dubois, A., Role of ABO Secretor Status in Mucosal Innate Immunity and *H. pylori* Infection. *PLOS Pathogens* **2008**, *4* (1), e2.
23. Samuel, T. M.; Binia, A.; de Castro, C. A.; Thakkar, S. K.; Billeaud, C.; Agosti, M.; Al-Jashi, I.; Costeira, M. J.; Marchini, G.; Martínez-Costa, C.; Picaud, J.-C.; Stiris, T.; Stoicescu, S.-M.; Vanpeé, M.; Domellöf, M.; Austin, S.; Sprenger, N., Impact of maternal characteristics on human milk oligosaccharide composition over the first 4 months of lactation in a cohort of healthy European mothers. *Scientific Reports* **2019**, *9* (1), 11767.
24. Davis, J. C. C.; Lewis, Z. T.; Krishnan, S.; Bernstein, R. M.; Moore, S. E.; Prentice, A. M.; Mills, D. A.; Lebrilla, C. B.; Zivkovic, A. M., Growth and Morbidity of Gambian Infants are Influenced by Maternal Milk Oligosaccharides and Infant Gut Microbiota. *Scientific Reports* **2017**, *7* (1), 40466.
25. Barboza, M.; Pinzon, J.; Wickramasinghe, S.; Froehlich, J. W.; Moeller, I.; Smilowitz, J. T.; Ruhaak, L. R.; Huang, J.; Lönnerdal, B.; German, J. B.; Medrano, J. F.; Weimer, B. C.; Lebrilla, C. B., Glycosylation of human milk lactoferrin exhibits dynamic changes during early lactation enhancing its role in pathogenic bacteria-host interactions. *Mol Cell Proteomics* **2012**, *11* (6), M111.015248.
26. Charbonneau, M. R.; O'Donnell, D.; Blanton, L. V.; Totten, S. M.; Davis, J. C.; Barratt, M. J.; Cheng, J.; Guruge, J.; Talcott, M.; Bain, J. R.; Muehlbauer, M. J.; Ilkayeva, O.; Wu, C.; Struckmeyer, T.; Barile, D.; Mangani, C.; Jorgensen, J.; Fan, Y. M.; Maleta, K.; Dewey, K. G.; Ashorn, P.; Newgard, C. B.; Lebrilla, C.; Mills, D. A.; Gordon, J. I., Sialylated Milk

- Oligosaccharides Promote Microbiota-Dependent Growth in Models of Infant Undernutrition. *Cell* **2016**, *164* (5), 859-71.
27. De Leoz, M. L.; Kalanetra, K. M.; Bokulich, N. A.; Strum, J. S.; Underwood, M. A.; German, J. B.; Mills, D. A.; Lebrilla, C. B., Human milk glycomics and gut microbial genomics in infant feces show a correlation between human milk oligosaccharides and gut microbiota: a proof-of-concept study. *J Proteome Res* **2015**, *14* (1), 491-502.
28. Zivkovic, A. M.; German, J. B.; Lebrilla, C. B.; Mills, D. A., Human milk glycobiome and its impact on the infant gastrointestinal microbiota. *Proceedings of the National Academy of Sciences* **2011**, *108* (Supplement 1), 4653.
29. Lewis, Z. T.; Totten, S. M.; Smilowitz, J. T.; Popovic, M.; Parker, E.; Lemay, D. G.; Van Tassell, M. L.; Miller, M. J.; Jin, Y. S.; German, J. B.; Lebrilla, C. B.; Mills, D. A., Maternal fucosyltransferase 2 status affects the gut bifidobacterial communities of breastfed infants. *Microbiome* **2015**, *3*, 13.
30. Tan, J.; McKenzie, C.; Potamitis, M.; Thorburn, A. N.; Mackay, C. R.; Macia, L., The role of short-chain fatty acids in health and disease. *Adv Immunol* **2014**, *121*, 91-119.
31. Casaburi, G.; Duar, R. M.; Vance, D. P.; Mitchell, R.; Contreras, L.; Frese, S. A.; Smilowitz, J. T.; Underwood, M. A., Early-life gut microbiome modulation reduces the abundance of antibiotic-resistant bacteria. *Antimicrobial Resistance & Infection Control* **2019**, *8* (1), 131.
32. Jacobi, S. K.; Yatsunenkov, T.; Li, D.; Dasgupta, S.; Yu, R. K.; Berg, B. M.; Chichlowski, M.; Odle, J., Dietary Isomers of Sialyllactose Increase Ganglioside Sialic Acid Concentrations in the Corpus Callosum and Cerebellum and Modulate the Colonic Microbiota of Formula-Fed Piglets. *J Nutr* **2016**, *146* (2), 200-8.
33. Holland, D.; Chang, L.; Ernst, T. M.; Curran, M.; Buchthal, S. D.; Alicata, D.; Skranes, J.; Johansen, H.; Hernandez, A.; Yamakawa, R.; Kuperman, J. M.; Dale, A. M., Structural growth trajectories and rates of change in the first 3 months of infant brain development. *JAMA Neurol* **2014**, *71* (10), 1266-74.
34. Wang, B.; Brand-Miller, J., The role and potential of sialic acid in human nutrition. *European Journal of Clinical Nutrition* **2003**, *57* (11), 1351-1369.
35. Wang, B.; Miller, J. B.; McNeil, Y.; McVeagh, P., Sialic acid concentration of brain gangliosides: variation among eight mammalian species. *Comp Biochem Physiol A Mol Integr Physiol* **1998**, *119* (1), 435-9.
36. Zuurveld, M.; van Witzenburg, N. P.; Garssen, J.; Folkerts, G.; Stahl, B.; Van't Land, B.; Willemsen, L. E. M., Immunomodulation by Human Milk Oligosaccharides: The Potential Role in Prevention of Allergic Diseases. *Front Immunol* **2020**, *11*, 801.
37. Tao, N.; DePeters, E. J.; German, J. B.; Grimm, R.; Lebrilla, C. B., Variations in bovine milk oligosaccharides during early and middle lactation stages analyzed by high-performance liquid chromatography-chip/mass spectrometry. *J Dairy Sci* **2009**, *92* (7), 2991-3001.
38. Tao, N.; DePeters, E. J.; Freeman, S.; German, J. B.; Grimm, R.; Lebrilla, C. B., Bovine milk glycome. *J Dairy Sci* **2008**, *91* (10), 3768-78.
39. Urashima, T.; Saito, T.; Nakamura, T.; Messer, M., Oligosaccharides of milk and colostrum in non-human mammals. *Glycoconjugate Journal* **2001**, *18* (5), 357-371.
40. Kooner, A. S.; Yu, H.; Chen, X., Synthesis of N-Glycolylneuraminic Acid (Neu5Gc) and Its Glycosides. *Frontiers in Immunology* **2019**, *10*.

41. Robinson, R. C., Structures and Metabolic Properties of Bovine Milk Oligosaccharides and Their Potential in the Development of Novel Therapeutics. *Frontiers in Nutrition* **2019**, *6*.
42. Salcedo, J.; Frese, S. A.; Mills, D. A.; Barile, D., Characterization of porcine milk oligosaccharides during early lactation and their relation to the fecal microbiome. *J Dairy Sci* **2016**, *99* (10), 7733-7743.
43. Wrigglesworth, D. J.; Goonatileke, E.; Haydock, R.; Hughes, K. R.; Lebrilla, C. B.; Swanson, K. S.; Jones, P.; Watson, P., High-throughput glycomic analyses reveal unique oligosaccharide profiles of canine and feline milk samples. *PLOS ONE* **2020**, *15* (12), e0243323.
44. Hong, Q.; Ruhaak, L. R.; Totten, S. M.; Smilowitz, J. T.; German, J. B.; Lebrilla, C. B., Label-Free Absolute Quantitation of Oligosaccharides Using Multiple Reaction Monitoring. *Analytical Chemistry* **2014**, *86* (5), 2640-2647.

## **CHAPTER TWO**

### **Human Milk Oligosaccharide Compositions Illustrate Global Variations in Early Nutrition**

## ABSTRACT

Human milk oligosaccharides (HMOs) are an abundant class of compounds found in human milk and have been linked to the development of the infant and specifically the brain, immune system, and gut microbiome. Liquid chromatography mass spectrometry-based analytical methods that profile these structures with broad structural coverage and quantitative information reveal their structural heterogeneity and potentially their biological roles. These methods were used to obtain relative quantitation of specific structures in over 2000 samples from over 1000 mothers in urban, semi-rural and rural sites across geographically diverse countries. A common behavior found among all sites was a decrease in HMO abundances during lactation until approximately month six postnatal, where they remained relatively constant. The greatest variations in structural abundances were associated with the presence of  $\alpha(1,2)$ -fucosylated species. Because genomic analyses of the mothers were not performed, milk was phenotyped according to the abundances of  $\alpha(1,2)$ -fucosylated structures. Those with high abundances were termed S+ milk, while those with low abundances were S- milk. However, previous studies have shown that the  $\alpha(1,2)$ -fucosylated structures correlated with the genetic secretor status. The fraction of mothers S- milk differed among various sites. Geographic variations in the representation of  $\alpha(1,2)$ -fucosylated as well as other fucosylated and sialylated carbohydrate HMO structures within and between sites and as a function of time of lactation were similarly observed. This study represents the largest structural HMO study to date and reveals the general behavior of HMOs during lactation among different populations.

## INTRODUCTION

Human milk for infants is a manifestation of a highly adapted, dynamic and personalized process of human postnatal development. Human milk is ‘dynamic’ in the sense that time-dependent changes occur in the presence and concentration of milk bioactives within and across mothers and ‘personalized’ in the sense that maternal genotype, health status, and environmental exposures, including diet, can impact milk compositions.<sup>1-5</sup>

Human milk oligosaccharides (HMOs) are among the most abundant and diverse components of breast milk, with hundreds of unique structures identified to date.<sup>6-9</sup> HMOs serve as nutrients for highly-adapted early bacterial colonizers of the infant gut, including specific strains of bifidobacteria endowed with suites of gene encoded proteins dedicated to the import and utilization of HMOs.<sup>10-14</sup> While the prebiotic effect is believed to be a major function, a small fraction of HMOs are absorbed in the small intestine and detectable in plasma<sup>15</sup> and urine<sup>16</sup> suggesting the potential for direct effects on host physiology including immunomodulation<sup>17-19</sup> and brain development.<sup>20</sup>

HMOs are assembled by glycosyltransferases to form either branched or linear structures. HMOs generally consist of a lactose [glucose (Glc) and galactose (Gal)] core, with variable combinations of N-acetylglucosamine (GlcNAc) and can be further bound to monosaccharides including sialic acids (N-acetylneuraminic acid or Neu5Ac) and fucose (Fuc).<sup>21</sup> The process yields an extensive number of oligosaccharides that in many cases are unique to human milk.<sup>22</sup>

Variations in HMOs are greatest among secretor genotypes. Secretors are individuals with a functioning FUT2 gene encoding  $\alpha(1,2)$ -fucosyltransferase that attaches fucose via an  $\alpha(1,2)$ -linkage to terminal Gal residues thereby producing blood antigens into secreted fluids (e.g., sweat, tears, semen, and milk).<sup>21, 23-25</sup> Non-secretors have diminished ability to produce

ABH or Lewis b antigens (Le<sup>b</sup>; Fuc $\alpha$ 1,2Gal $\beta$ 1,3[Fuc $\alpha$ 1,4]GlcNAc $\beta$ ) due to mutations in the *FUT2* gene.<sup>21, 23-25</sup> Genetic studies have documented variations in the prevalence of the wild-type and mutant *FUT2* alleles around the world.<sup>26-28</sup> The prevailing existence of different genotypes in populations show that there are unique advantages to individuals. This notion is consistent with evidence suggesting a protective effect against, for example, otitis media<sup>29</sup> and autoimmune diseases<sup>30, 31</sup> for secretors and against viral diarrhea for non-secretors.<sup>32</sup> While different alterations in the *FUT2* gene among various populations determine the secretor status of the mother, the milk and its function is guided by the abundances of HMO structures. Thus, classifying the milk phenotype, for example the amount of sialylation and fucosylation, is a more direct approach in surveying the differences between mothers' milks and correlating infant health outcomes. Advanced analytical methods now make it possible to accurately determine the phenotypic secretor status by directly quantitating the abundances of  $\alpha$ (1,2)-fucosylated structures present in the breast milk.<sup>23</sup> For the purpose of this study, we refer to milk that corresponds to high amounts of  $\alpha$ (1,2)-fucosylated structures as S+ milk, and milk corresponding to low abundances as S- milk. HMOs can therefore be used to type the milk according to the presence or absence of  $\alpha$ (1,2)-fucosylated structures regardless of the genotype.<sup>8, 23</sup>

Mass spectrometry-based analytical methods have enabled more rapid and precise characterization of human milk, including the capability to simultaneously determine the abundances of hundreds of distinct carbohydrate structures. However, determination of HMOs are largely limited to studies of cohorts living in a small number of sites or geographic locales.<sup>33-</sup>  
<sup>35</sup> In this report, we describe the results of a cross-sectional analysis that quantified the abundances of HMOs to determine the natural variations during lactation among various sites involving mothers from different ethnic groups. Milk samples were obtained and analyzed from

over 1000 mothers living in 15 countries encompassing six continents and representing a diverse set of ecological and cultural backgrounds.

This work has been published in the Journal of Nutrition and is included with permission in this thesis.

## **MATERIALS AND METHODS**

### **Sources of breast milk samples**

Breast milk samples (N=2234) were collected from mothers (N=1090) in 16 global sites, including urban, rural and semi-rural communities in 15 sites spanning Africa, Eurasia, the Americas, and Australia. Samples and resulting data were collected from different studies as detailed in the **Table 2.1**. However, the quality controls and analytical methods for each sample remained the same. A detailed summary of sample information including country, population, collection procedures, sample size, and infant age is provided in **Table 2.1** and **Table 2.2**.

**Table 2.1** Summary of successful milk collections as a function of location and lactation month.

| Location     | Lactation Month |            |            |            |            |            |            |            |           |           |           |           |           |           |           |          |          |          |          |          |          |          |          |          | Total       |     |
|--------------|-----------------|------------|------------|------------|------------|------------|------------|------------|-----------|-----------|-----------|-----------|-----------|-----------|-----------|----------|----------|----------|----------|----------|----------|----------|----------|----------|-------------|-----|
|              | -1              | 0          | 1          | 2          | 3          | 4          | 5          | 6          | 7         | 8         | 9         | 10        | 11        | 12        | 13        | 14       | 15       | 16       | 17       | 18       | 19       | 21       | 24       | 26       |             |     |
| Argentina    |                 |            | 1          | 1          |            | 2          | 1          | 3          | 2         |           | 3         | 3         | 2         | 2         |           |          |          |          |          |          |          |          |          |          |             | 20  |
| Bangladesh   |                 | 15         | 15         | 14         | 12         | 12         | 12         | 12         |           |           |           |           |           |           |           |          |          |          |          |          |          |          |          |          |             | 92  |
| Bolivia      |                 | 1          | 1          | 3          | 7          | 4          | 1          | 6          | 4         | 2         | 5         | 3         | 2         | 1         | 7         | 2        | 3        | 2        | 3        | 1        | 2        |          |          | 1        |             | 61  |
| Boston       |                 |            |            | 2          | 1          | 4          | 2          | 2          | 2         | 1         | 1         |           | 4         | 1         |           |          |          |          |          |          |          |          |          |          |             | 20  |
| Brazil       |                 |            | 22         | 18         | 14         | 20         | 18         | 17         |           |           |           |           |           |           |           |          |          |          |          |          |          |          |          |          |             | 109 |
| Davis        | 8               | 59         | 40         | 31         | 37         | 38         |            | 30         |           |           |           |           | 1         | 11        |           |          |          |          |          |          |          |          |          |          |             | 255 |
| Gambia       |                 |            | 33         |            |            | 33         | 33         |            |           |           |           |           |           |           |           |          |          |          |          |          |          |          |          |          |             | 99  |
| India        |                 |            | 42         | 42         | 42         | 42         | 40         | 39         |           |           |           |           |           |           |           |          |          |          |          |          |          |          |          |          |             | 247 |
| Malawi       |                 |            | 73         |            | 84         |            |            | 652        |           |           |           |           |           |           |           |          |          |          |          |          |          |          |          |          |             | 809 |
| Namibia      |                 |            | 3          | 2          |            | 1          |            |            | 1         | 2         |           |           |           |           | 1         | 1        |          |          |          | 1        |          |          |          |          |             | 12  |
| Nepal        |                 |            | 1          | 3          |            | 3          | 2          | 4          | 4         | 2         | 3         | 2         |           |           | 1         |          |          |          |          |          |          |          | 1        | 2        |             | 28  |
| Perth        |                 | 28         | 29         |            |            |            |            |            |           |           |           |           |           |           |           |          |          |          |          |          |          |          |          |          |             | 57  |
| Peru         |                 | 35         | 36         | 33         | 34         | 32         | 31         | 32         |           |           |           |           |           |           |           |          |          |          |          |          |          |          |          |          |             | 233 |
| Philippines  |                 | 5          | 1          | 1          | 2          | 2          | 2          | 1          | 2         | 2         | 1         | 1         | 2         | 1         |           |          |          |          |          |          |          |          |          |          |             | 18  |
| Poland       |                 |            | 1          | 2          | 1          | 4          | 2          | 2          | 4         | 1         |           | 3         |           | 2         | 1         |          |          |          |          |          |          |          |          |          |             | 23  |
| South Africa |                 |            | 26         | 26         | 27         | 26         | 25         | 26         |           |           |           |           |           |           |           |          |          |          |          |          |          |          |          |          |             | 151 |
| <b>Total</b> | <b>8</b>        | <b>143</b> | <b>324</b> | <b>178</b> | <b>261</b> | <b>223</b> | <b>169</b> | <b>816</b> | <b>19</b> | <b>10</b> | <b>13</b> | <b>12</b> | <b>11</b> | <b>18</b> | <b>10</b> | <b>3</b> | <b>3</b> | <b>2</b> | <b>3</b> | <b>2</b> | <b>2</b> | <b>1</b> | <b>2</b> | <b>1</b> | <b>2234</b> |     |

**Table 2.2 Summary** of all study sites and variations in milk types.

| <b>Country</b>       | <b>Site Location</b>          | <b>Setting</b> | <b>No. of mothers</b> | <b>No. of samples</b> | <b>S+ milk producers</b> | <b>S- milk producers</b> | <b>% S+ milk producers</b> |
|----------------------|-------------------------------|----------------|-----------------------|-----------------------|--------------------------|--------------------------|----------------------------|
| <b>Argentina</b>     | Namqom                        | Rural          | 20                    |                       | 17                       | 3                        | 85                         |
| <b>Bolivia</b>       | Amazonian Lowlands            | Rural          | 52                    |                       | 52                       | 0                        | 100                        |
| <b>Brazil</b>        | Fortaleza, Ceará              | Urban          | 23                    | 109                   | 21                       | 2                        | 91.3                       |
| <b>Peru</b>          | Loreto                        | Rural          | 37                    | 236                   | 36                       | 1                        | 97.3                       |
| <b>Australia</b>     | Perth                         |                | 26                    |                       | 20                       | 6                        | 76.9                       |
| <b>Bangladesh</b>    | Mirpur, Dhaka                 | Urban          | 15                    | 92                    | 12                       | 3                        | 80                         |
| <b>India</b>         | Vellore, Tamil Nadu           | Urban          | 43                    | 247                   | 29                       | 14                       | 67.4                       |
| <b>Nepal</b>         | Nubri Valley                  | Rural          | 28                    |                       | 20                       | 8                        | 71.4                       |
| <b>Philippines</b>   | Cebu                          | Rural & Urban  | 18                    |                       | 13                       | 5                        | 72.2                       |
| <b>Gambia</b>        |                               | Rural          | 33                    | 99                    | 21                       | 12                       | 63.6                       |
| <b>Malawi</b>        | Mangochi district             | Rural          | 658                   | 809                   | 491                      | 165                      | 74.9                       |
| <b>Namibia</b>       | Omuhonga Basin                | Rural          | 12                    |                       | 10                       | 2                        | 83.3                       |
| <b>South Africa</b>  | Thohoyandou, Limpopo Province | Rural          | 27                    | 151                   | 17                       | 10                       | 63                         |
| <b>Poland</b>        | Beskid Wyspowy Mtns           | Rural          | 23                    |                       | 18                       | 5                        | 78.3                       |
| <b>United States</b> | Boston, Massachusetts         | Urban          | 20                    |                       | 15                       | 5                        | 75                         |
| <b>United States</b> | Davis, California             | Urban          | 55                    | 252                   | 40                       | 14                       | 74.1                       |

<sup>1</sup>Values presented correspond to the number of samples collected

All infants were delivered full term. Written informed consent was obtained from all parents/guardians prior to study enrollment. Samples were collected using standardized protocols for all populations. The samples from the Gambia were analyzed from a sub-study embedded within a randomized trial to investigate the effects of pre-natal and infancy nutritional supplementation on infant immune development, The Early Nutrition and Immune Development (ENID) Trial, ISRCTN49285450, <http://www.isrctn.com/ISRCTN49285450>)64, registered on December 11, 2009. Ethical approval for the ENID Trial and the 'ENID-Bioactives' sub-study was obtained from the joint Gambian Government/MRC Unit. The Gambia Ethics Committee and the George Washington University Institutional Research Board (#13-0441). Full informed consent was obtained from each participant, prior to inclusion in the study.

There were 20 mothers from Argentina (approval provided by the University of Pennsylvania Institutional Review Board #811200), 52 from Bolivia (approval provided by the University of California, Santa Barbara, two study periods: 2009: IRB ANTH-GU-MI-010-3U #09-312 and ANTH-GU-MI-010-10R #10-290; 2012-2013: ANTH-GU-MI-010 #19-13-0206 and #3-15-067), 20 from Boston, USA (approval provided by the Harvard Committee on the Use of Human Subjects, File Number 23868), 12 from Namibia (approval provided by the Harvard Committee on the Use of Human Subjects, IRB13-0900 and the University of California, Los Angeles Institutional Review Board, IRB#13-000881), 28 from Nepal (approval provided by the Washington University in St. Louis, IRB 201302059 and the Nepal Health Research Council, IRB 1329), 18 from the Philippines (approval provided by Northwestern University and the University of San Carlos, Philippines, IRB STU00001299), and 23 from Poland (approval provided by the Harvard Committee on the Use of Human Subjects IRB21979) who provided breast milk samples (N=182). Informed consent was provided by all subjects. Samples were collected using a

standardized protocol for all populations. Premature births, multiple births, and those infants being exclusively bottle fed were excluded from the sample set. Participants were asked to nurse from the sample breast approximately two hours prior to sampling (except for the 2009 sampling period in Bolivia, in which case mothers were asked to not feed from either breast for one hour prior to sampling) and refrain from nursing from the sampled breast again until collection. At the time of sample collection, participants nursed their infants for approximately two to two and a half minutes before hand-expressing a small, mid-feed sample. Those from Bolivia evacuated the whole breast with a manual breast pump instead of hand expression from the 2009 study. Consent for data collection was secured at multiple levels. The Tsimane Health and Life History Project maintains formal agreements with the local municipal government of San Borja and the Tsimane governing body to conduct research in Tsimane territories. Researchers held community meetings to explain study aims and obtain community-wide consent to stay in and work with members of participating villages. Individual informed consent was obtained verbally from participants at recruitment and again before providing milk samples. Meetings, participant interviews, and explanation of study aims and procedures were conducted in the language preferred by the participant. An informational sheet with the main elements of the informed consent process was left with the prospective participants and sample collection was conducted by a team that included a local field assistant who could translate any questions and answers.

The Malnutrition and Enteric Disease (MAL-ED) Study (ClinicalTrials.gov Identifier: NCT02441426) was an observational birth cohort study conducted at multiple sites from November 2009 to February 2014, to investigate the linkages between malnutrition and intestinal infections and their effects on children in the developing world. Each of the sites, which included Bangladesh (Dhaka), India (Vellore), Brazil (Fortaleza), Peru (Loreto) and South Africa (Venda),

obtained ethical approval from their respective institutions and written informed consent from participants. iLiNS-DYAD-M (ClinicalTrials.gov Identifier: NCT01239693) was a randomized, controlled, single-blind, parallel group clinical trial of micronutrient fortified lipid-based nutrient supplements conducted in southern Malawi. The study was performed between February 2011 and April 2015 and approved by institutional review boards of the University of Malawi and Pirkanmaa Hospital (Finland); informed consent was provided by all participants. Breast milk samples from these studies that were included in the analysis presented here were collected under Bill & Melinda Gates Foundation Grant OPP1033518 with approval from the institutional review board at Washington University School of Medicine in St. Louis.

### **HMO extraction and mass spectrometric analysis**

HMOs were extracted from breast milk samples using previously reported methods.<sup>7, 8, 36, 37</sup> Briefly, whole milk samples were aliquoted into 96-well plates, diluted, and then defatted via centrifugation. Proteins were precipitated with ethanol, and the resulting glycans were reduced with sodium borohydride (Sigma-Aldrich, St. Louis, MO). Solid phase extraction was performed on graphitized carbon cartridges (Glygen, Columbia, MD) to remove lactose and salts. After the solvent was evaporated, purified HMOs were reconstituted and diluted prior to analysis. Standard solutions were made of HMO in water, with concentrations ranging from 0.05 mg/mL-0.2 mg/mL.

Extracted HMOs were analyzed on a nano-HPOC-TOF-MS The HPLC unit (Model series 1200, Agilent Technologies, Santa Clara, CA) that utilizes a capillary pump for sample loading (4  $\mu$ L/min) and a nano pump for analyte separation (0.3  $\mu$ L/min). Loading and separation were performed on a microfluidic chip packed with porous graphitized carbon via enrichment and analytical columns, respectively, using a binary gradient of solvent A [3% acetonitrile (ACN) in 0.1% formic acid] and solvent B (90% ACN in 0.1% formic acid). This system was coupled to an

Agilent 6220 series TOF mass spectrometer. Detection was performed in the positive mode, and calibration was achieved with a dual nebulizer electrospray source with calibrant ions ranging from mass-to-charge ( $m/z$ ) 118.086 to 2721.895.

### **Structural annotation of HMOs**

Data were collected using Agilent MassHunter Workstation Data Acquisition software (B.02.01) and analyzed using Agilent MassHunter Qualitative Analysis software B.03.01 and B.06.00. The 'Find Compound by Molecular Feature' function was used to extract ion abundances to within 20 ppm of theoretical HMO masses. Individual HMOs were identified by accurate mass, retention time, and elution order defined previously developed HMO libraries.<sup>7, 8</sup> An in-house software program was used to align peaks due to minor retention time shift.<sup>37</sup> HMOs were grouped into classes as follows: fucosylated HMOs (any structure with Fuc), sialylated HMOs (any structure with Neu5Ac), undecorated HMOs (neither Fuc nor Neu5Ac present), and fucosylated plus sialylated HMOs (both Fuc and Neu5Ac present). Relative abundances (%) were calculated by normalizing class and individual compound abundances to total HMO abundance in each breast milk sample. Compounds that were not identified in individual samples but were present in at least 50% of all samples were given a LOD/2 abundance.

### **Classification of milk secretor phenotype as S+ and S- based on HMO abundances**

Phenotypic secretor status was determined following our previously published method.<sup>23</sup> Structures with known  $\alpha(1,2)$ -Fuc linkages were identified by matching exact masses and retention times to previously developed annotated HMO libraries.<sup>7, 8</sup> The abundances of the most abundant  $\alpha(1,2)$ -fucosylated structures, namely 2'-fucosyllactose(2'FL), lactodifucotetraose(LDFT), difucosyllacto-N-hexaose a(DFLNH<sub>a</sub>) and trifucosyllacto-N-hexaose (TFLNH) were summed and normalized to the total HMO abundances in a given sample, so that a relative  $\alpha(1,2)$ -fucosylation

value could be determined. Secretor status was assigned based on a previously established and validated threshold of 6%.<sup>23</sup> If this value exceeded the threshold, the mother was deemed a secretor (S+), conversely if the value fell below this threshold the mother was deemed a non-secretor (S-). The number of mothers producing S+ and S- milk in each location was determined and the proportion of S- mothers was calculated for each location. If a mother provided multiple samples from different postpartum time points, her secretor status was determined based on the secretor status determination in the majority of her samples. If there was no 'majority milk type', she was excluded from the statistical analysis (one mother from Davis, USA, two mothers from Malawi, and three mothers from Perth, Australia).

### **Statistical analyses**

Mann-Whitney tests were used to determine the differences between absolute and relative abundances of the HMO classes. Furthermore, the data was grouped to show how secretor status, geographical location, age, sex, and lactation month affected the HMO profiles. An alpha correction of  $\alpha=0.05$  was used for the statistical analysis. Differences were determined when all samples from all time points were combined (S+  $N=1709$ , S-  $N=524$ ), and when samples were split by location including all time points (Argentina: S+  $N=17$ , S-  $N=3$ ; Boliva: S+  $N=52$ , S-  $N=0$ ; Bangladesh: S+  $N=72$ , S-  $N=20$ ; USA[Boston]: S+  $N=15$ , S-  $N=5$ ; Brazil: S+  $N=97$ , S-  $N=12$ ; USA[Davis]: S+  $N=194$ , S-  $N=58$ ; Gambia: S+  $N=63$ , S-  $N=36$ ; India: S+  $N=166$ , S-  $N=81$ ; Malawi: S+  $N=601$ , S-  $N=208$ ; Namibia: S+  $N=10$ , S-  $N=2$ ; Nepal: S+  $N=20$ , S-  $N=8$ ; Australia: S+  $N=42$ , S-  $N=15$ ; Peru: S+  $N=227$ , S-  $N=8$ ; Philippines: S+  $N=13$ , S-  $N=5$ ; Poland: S+  $N=18$ , S-  $N=5$ ; South Africa: S+  $N=93$ , S-  $N=58$ ). Due to the vast changes in milk composition throughout lactation, samples were binned based on lactation month, therefore milk collected from a single mother at different time points were treated as independent samples.

## **Data Availability**

Data that support the findings of this study are available upon request from the corresponding author (C.B.L.).

## **RESULTS**

### ***HMO-based classification of milk into S+ and S- phenotypes***

Over 2000 breast milk samples were collected from 1,090 mothers in 15 geographical sites. The samples obtained from six continents were analyzed under one protocol allowing direct comparison of abundances by classes and individual structures (**Table 2.2**). Using nano-HPLC-qTOF-MS, we identified 60 structures that were common to most samples. However, the total number of unique structures varied for each mother, with the average count of nearly 100 structures in a single mother. The abundances for these structures varied widely, spanning four orders of magnitude.

**Table 2.2** The 60 most common HMO structures in S+ and S- milks across all study sites.

| Neutral Mass (Da) | Composition (Hex_HexNAc_Fuc_Neu5Ac) | HMO                       | S- type milk mean | S+ type milk mean | P-value |
|-------------------|-------------------------------------|---------------------------|-------------------|-------------------|---------|
| 490.19            | 2010                                | 2'FL                      | 0.002 ± 0.005     | 0.07 ± 0.04       | <0.0001 |
| 636.24            | 2020                                | LDFT                      | 0.001 ± 0.003     | 0.04 ± 0.03       | <0.0001 |
| 709.26            | 3100                                | LNT + LNnT                | 0.2 ± 0.09        | 0.1 ± 0.06        | <0.0001 |
| 855.32            | 3110                                | LNFP II                   | 0.04 ± 0.03       | 0.02 ± 0.02       | <0.0001 |
| 855.32            | 3110                                | LNFP I + LNFP III         | 0.02 ± 0.02       | 0.06 ± 0.04       | <0.0001 |
| 1074.39           | 4200                                | LNH                       | 0.009 ± 0.01      | 0.009 ± 0.007     | 0.06    |
| 1074.39           | 4200                                | LNnH                      | 0.009 ± 0.01      | 0.01 ± 0.01       | <0.0001 |
| 1074.39           | 4200                                | p-LNH                     | 0.004 ± 0.007     | 0.004 ± 0.005     | <0.0001 |
| 1220.45           | 4210                                | MFpLNH IV                 | 0.02 ± 0.01       | 0.02 ± 0.009      | 0.1     |
| 1220.45           | 4210                                | 412Oa                     | 0.007 ± 0.01      | 0.003 ± 0.006     | <0.0001 |
| 1220.45           | 4210                                | MFLNH III + MFLNH I       | 0.03 ± 0.02       | 0.02 ± 0.01       | 0.02    |
| 1220.45           | 4210                                | IFLNH III                 | 0.008 ± 0.006     | 0.01 ± 0.006      | <0.0001 |
| 1220.45           | 4210                                | IFLNH I                   | 0.001 ± 0.003     | 0.004 ± 0.004     | <0.0001 |
| 1366.51           | 4220                                | DFpLNH II                 | 0.01 ± 0.007      | 0.01 ± 0.006      | <0.0001 |
| 1366.51           | 4220                                | DFLNH b                   | 0.02 ± 0.01       | 0.01 ± 0.007      | <0.0001 |
| 1366.51           | 4220                                | DFLNHa                    | 0.001 ± 0.002     | 0.01 ± 0.01       | <0.0001 |
| 1512.57           | 4230                                | TFLNH                     | 0.004 ± 0.004     | 0.006 ± 0.005     | <0.0001 |
| 1585.58           | 5310                                | 5130a                     | 0.006 ± 0.006     | 0.004 ± 0.003     | <0.0001 |
| 1585.58           | 5310                                | F-LNO                     | 0.004 ± 0.003     | 0.003 ± 0.002     | 0.002   |
| 1731.64           | 5320                                | DFLNO I                   | 0.007 ± 0.005     | 0.003 ± 0.003     | <0.0001 |
| 1731.64           | 5320                                | DFLNnO II                 | 0.004 ± 0.005     | 0.003 ± 0.003     | 0.9     |
| 1731.64           | 5320                                | 5230a + DFLNnO I/DFLNO II | 0.004 ± 0.003     | 0.006 ± 0.004     | <0.0001 |
| 635.22            | 2001                                | 6'SL                      | 0.003 ± 0.003     | 0.002 ± 0.003     | <0.0001 |
| 635.22            | 2001                                | 3'SL                      | 0.01 ± 0.008      | 0.01 ± 0.007      | 0.4     |
| 1000.36           | 3101                                | LSTc + LSTb               | 0.03 ± 0.02       | 0.03 ± 0.01       | <0.0001 |
| 1000.36           | 3101                                | LSTa                      | 0.003 ± 0.002     | 0.002 ± 0.002     | <0.0001 |
| 1365.49           | 4201                                | S-LNH                     | 0.003 ± 0.004     | 0.002 ± 0.002     | <0.0001 |
| 1365.49           | 4201                                | 4021a + S-LNnH II         | 0.004 ± 0.005     | 0.006 ± 0.005     | <0.0001 |
| 490.19            | 2010                                | %2'FL                     | 0.4 ± 0.9         | 11.1 ± 4.6        | <0.0001 |
| 636.24            | 2020                                | %LDFT                     | 0.2 ± 0.5         | 5.8 ± 5.1         | <0.0001 |
| 709.26            | 3100                                | %LNT + LNnT               | 30.3 ± 10         | 21.7 ± 5.9        | <0.0001 |
| 855.32            | 3110                                | %LNFP II                  | 6.1 ± 5           | 2.9 ± 2.6         | <0.0001 |
| 855.32            | 3110                                | %LNFP I + LNFP III        | 3.8 ± 2.5         | 8.2 ± 5           | <0.0001 |
| 1074.39           | 4200                                | %LNH                      | 1.5 ± 1.6         | 1.2 ± 0.9         | 0.5     |
| 1074.39           | 4200                                | %LNnH                     | 1.4 ± 1.8         | 1.7 ± 1.4         | <0.0001 |
| 1074.39           | 4200                                | %p-LNH                    | 0.7 ± 1.2         | 0.6 ± 0.7         | <0.0001 |
| 1220.45           | 4210                                | %MFpLNH IV                | 2.8 ± 1.5         | 2.3 ± 1.2         | <0.0001 |
| 1220.45           | 4210                                | %412Oa                    | 1.1 ± 1.7         | 0.6 ± 1           | <0.0001 |

|                |      |                            |           |           |         |
|----------------|------|----------------------------|-----------|-----------|---------|
| <b>1220.45</b> | 4210 | %MFLNH III + MFLNH I       | 4.3 ± 2.6 | 3.3 ± 1.8 | <0.0001 |
| <b>1220.45</b> | 4210 | %IFLNH III                 | 1.3 ± 0.9 | 1.4 ± 0.9 | 0.007   |
| <b>1220.45</b> | 4210 | %IFLNH I                   | 0.2 ± 0.5 | 0.5 ± 0.6 | <0.0001 |
| <b>1366.51</b> | 4220 | %DFpLNH II                 | 2.2 ± 1.3 | 1.5 ± 0.8 | <0.0001 |
| <b>1366.51</b> | 4220 | %DFLNH b                   | 3.3 ± 2.6 | 1.6 ± 1.2 | <0.0001 |
| <b>1366.51</b> | 4220 | %DFLNHa                    | 0.2 ± 0.3 | 2 ± 1.8   | <0.0001 |
| <b>1512.57</b> | 4230 | %TFLNH                     | 0.7 ± 0.6 | 0.9 ± 0.7 | <0.0001 |
| <b>1585.58</b> | 5310 | %5130a                     | 0.9 ± 0.8 | 0.5 ± 0.4 | <0.0001 |
| <b>1585.58</b> | 5310 | %F-LNO                     | 0.6 ± 0.4 | 0.4 ± 0.3 | <0.0001 |
| <b>1731.64</b> | 5320 | %DFLNO I                   | 1.1 ± 0.7 | 0.5 ± 0.4 | <0.0001 |
| <b>1731.64</b> | 5320 | %DFLNnO II                 | 0.7 ± 0.7 | 0.5 ± 0.4 | 0.0007  |
| <b>1731.64</b> | 5320 | %5230a + DFLNnO I/DFLNO II | 0.7 ± 0.5 | 0.8 ± 0.4 | <0.0001 |
| <b>635.22</b>  | 2001 | %6'SL                      | 0.5 ± 0.5 | 0.3 ± 0.4 | <0.0001 |
| <b>635.22</b>  | 2001 | %3'SL                      | 2.6 ± 1.7 | 2.2 ± 1.4 | <0.0001 |
| <b>1000.36</b> | 3101 | %LSTc + LSTb               | 5.2 ± 2   | 3.8 ± 1.6 | <0.0001 |
| <b>1000.36</b> | 3101 | %LSTa                      | 0.5 ± 0.3 | 0.3 ± 0.3 | <0.0001 |
| <b>1365.49</b> | 4201 | %S-LNH                     | 0.5 ± 0.5 | 0.3 ± 0.3 | <0.0001 |
| <b>1365.49</b> | 4201 | %4021a + S-LNnH II         | 0.6 ± 0.7 | 0.8 ± 0.6 | <0.0001 |

<sup>1</sup>Values are presented as Mean Abundance ± SD. All data collected was used for this analysis including data from the same mother at different time points of lactation. Monosaccharide composition represented by four-digit code (Hex\_HexNAc\_Fuc\_Neu5Ac). Common HMO abbreviations were used to name oligosaccharides. Oligosaccharides with two compound names are isomers that were difficult to resolve chromatographically, the data presented are the sum of their combined abundances. Oligosaccharide names preceding a percentage indicates that the values presented are mean relative abundances. P values were obtained using Mann-Whitney tests.

HMOs containing Lewis b structures ( $\alpha(1,2)$ -fucose), a feature of the secretor genotype (homozygous or heterozygous for the functional *FUT2* allele)<sup>23,38,25</sup>, were most variable between mothers. We defined milk rich in Lewis b structures [2'-fucosyllactose(2'FL), lactodifucotetraose(LDFT), difucosyllacto-*N*-hexaose a(DFLNHa) and trifucosyllacto-*N*-hexaose (TFLNH)] that were consistently represented in samples collected within and across the different geographic sites S+ milk, belonging to a secretor mother. Milk containing a total relative abundance of <6% of these four Lewis b structures was defined as S+ milk, thus belonging to a non-secretor mother. This criterion was developed previously and has been validated with genomic data.<sup>23</sup> Phenotyping the milk addresses what the infant receives, while genotyping the mother does not necessarily translate to HMO abundances.

**Figure 2.1** shows extracted ion chromatograms (EICs) of the most abundant  $\alpha(1,2)$ -fucosylated compounds in human milk, namely 2'-fucosyllactose (2'FL) and lactodifucotetraose (LDFT) (**Figure 2.1a, b**). These compounds were consistently higher in S+ milk (blue) compared to S- (red, near baseline) across all sites ( $P < 0.05$ ). Five other  $\alpha(1,2)$ -Fuc-containing structures, namely lacto-*N*-fucopentaose I (LNFP I), lacto-*N*-difucohexaose I (LNDFH I), monofucosyllacto-*N*-hexaose I (MFLNH I), isomer I fucosyl-paralacto-*N*-hexaose (IFLNH I), and difucosyllacto-*N*-hexaose c (DFLNH c), were much less ubiquitous, and when detected, were present at much lower abundances than the four structures used for determination of secretor status (**Table 2.2**). Conversely, there were structures, particularly  $\alpha(1,3)$ - and  $\alpha(1,4)$ -fucosylated HMOs, that were significantly higher in S- milk (**Figure 2.1c-f, Table 2.2**). Three isomers with composition 3Hex:1HexNAc:1Fuc and having  $\alpha(1,3/4)$ -Fuc linkages were produced in higher abundances in mothers with S- milk (**Figure 2.1e**).

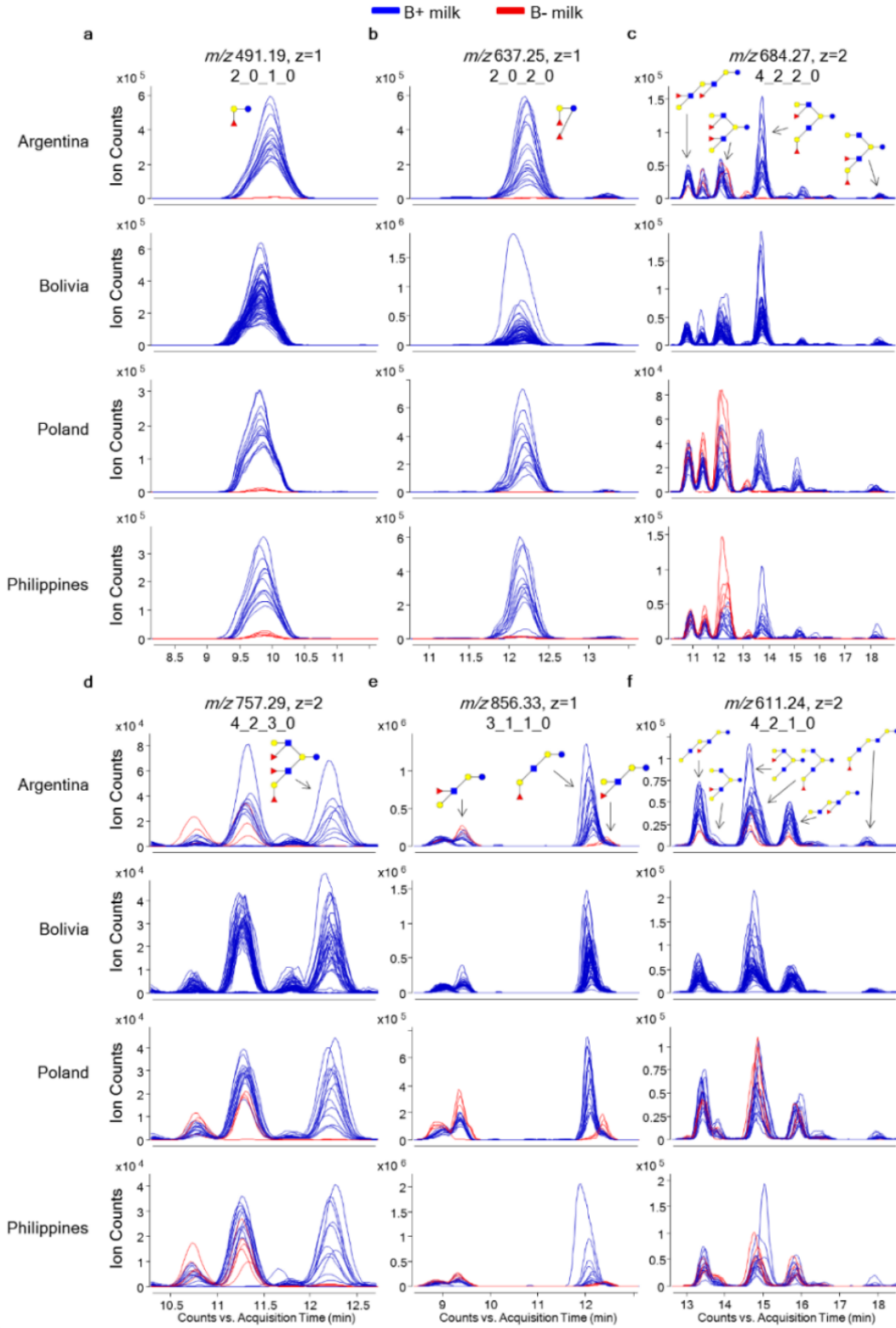


**Figure 2.1** Extracted ion chromatograms (EICs) displaying differences in abundances of HMO markers with  $\alpha(1-2)$ -linked Fuc between mothers with S+ (–) and S- (–) milk from different locations around the world. Locations were chosen to represent different areas with both S+ and

S- milk producers. Bolivia was also chosen to display EICs of 100% S+ milk producers. Monosaccharide composition of structures are given as Hex\_HexNAc\_Fuc\_Neu5Ac and represented as glucose (●), galactose (●), N-acetylglucosamine (■), and fucose (▲). (a) EIC of 2'-fucosyllactose (2'FL) with  $m/z$  491.19. (b) EIC of lactodifucotetraose (LDFT) with  $m/z$  637.25. (c) EIC of isomers difucosyl-*para*-lacto-*N*-hexaose (DFpLNH II), difucosyllacto-*N*-hexaose (b) (DFLNH b), difucosyllacto-*N*-hexaose (a) (DFLNHa), and difucosyllacto-*N*-hexaose (c) (DFLNHc) with  $m/z$  684.27. (d) EIC of trifucosyllacto-*N*-hexaose (TFLNH) with  $m/z$  757.29. (e) EIC of isomers lacto-*N*-fucopentaose II (LNFP II), lacto-*N*-fucopentaose I (LNFP I), and lacto-*N*-fucopentaose III (LNFP III) with  $m/z$  856.33. (f) EIC of isomers fucosyl-*para*-lacto-*N*-hexaose (MFpLNH IV), 4120a, monofucosyllacto-*N*-hexaose III (MFLNH III), monofucosyllacto-*N*-hexaose I (MFLNH I), isomer III fucosyl-*para*-lacto-*N*-hexaose (IFLNH III), and isomer I fucosyl-*para*-lacto-*N*-hexaose (IFLNH I) with  $m/z$  611.24.

The relative abundances of the 60 most common structures were shown for S+ milk and S- in **Figure 2.2** (see **Table 2.2**).

The abundance of each HMO was normalized to the total abundances of the selected group, which made up approximately 97% of all abundances. For mothers that produce S+ milk, the most abundant HMOs were Lacto-*N*-Tetraose/Lacto-*N*-Neotetraose (LNT/LNnT). These two compounds are isomers and were difficult to resolve chromatographically, and the data presented are the sum of their combined abundances. At all sites, mothers with S- milk had higher abundances of LNFP II, suggesting this HMO is a potential marker of S- milk ( $P < 0.0001$ ; Mann-Whitney). Other HMOs, including MFLNH I, MFLNH III and DFpLNH II were also higher in S- milk achieving statistical significance ( $P < 0.05$ ; Mann-Whitney) at all sites except Brazil ( $P < 0.38$ ; Mann-Whitney).

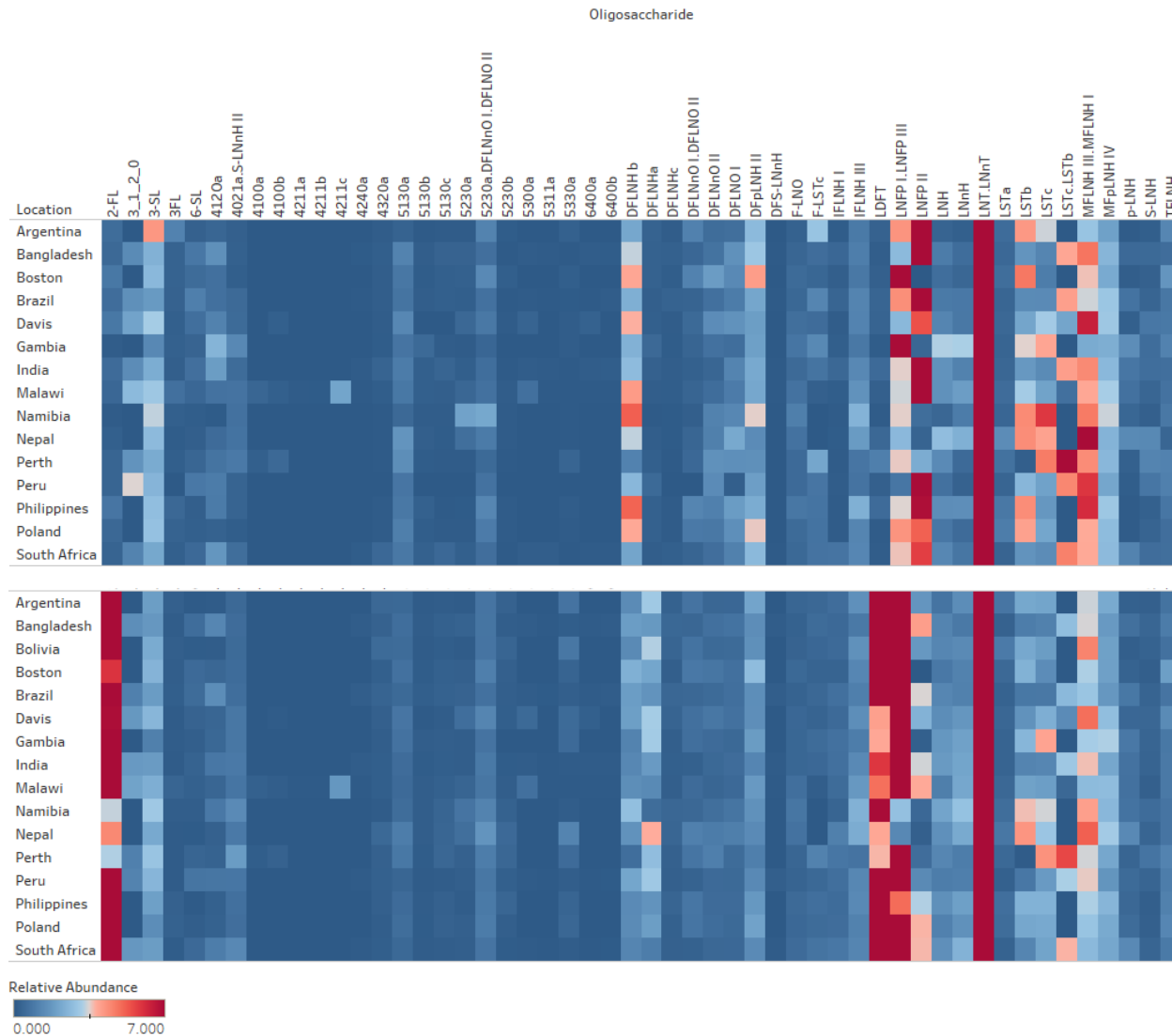


**Figure 2.2** Heatmap of relative abundances of the most common (60) HMOs across 15 geographically diverse sites. Comparison of abundances from mothers who are (top) S-producers and (bottom) S+ producers. HMO abundance values correspond to HPLC-qTOF MS spectral abundance normalized to the mean of the total abundance of counts from each sample. HMOs that were not baseline separated (resolution >1.5) were grouped together and labeled accordingly.

### *Total HMO abundances between sites and during lactation*

The total abundances of HMOs between mothers from various sites were compared as a function of months postpartum. **Figure 2.3** compared total HMOs from mothers living in Brazil, Bangladesh, Davis-USA, Peru, India and South Africa sampled between postpartum months 1-6.

These sites were selected because they provided the most extensive longitudinal sampling. The highest abundances were observed at month 1 and decreased uniformly thereafter. Each site showed similar behavior and similar decreases in total abundances with some variations in months 3 and 4. For example, in both the Peru and India sites total abundances decreased at month 3 and remained nearly constant thereafter, while in the other sites HMO abundances dropped uniformly between month 1 and 6. When comparing total absolute abundance in secretors between month 1 and 6 statistical significance was achieved across all selected sites, were higher significance was achieved in sites with more sampling (**Figure 2.3b**). Similarly, statistical significance was similarly achieved when comparing abundances in non-secretors between month 1 and 6 where there were sufficient number of samples. HMO abundances were also comparing between S+ and S- milk across these sites by averaging the means of all time points within one site. In all counties except Brazil, S+ milk possessed higher abundances of HMOs ( $P < 0.0001$ , Mann-Whitney).

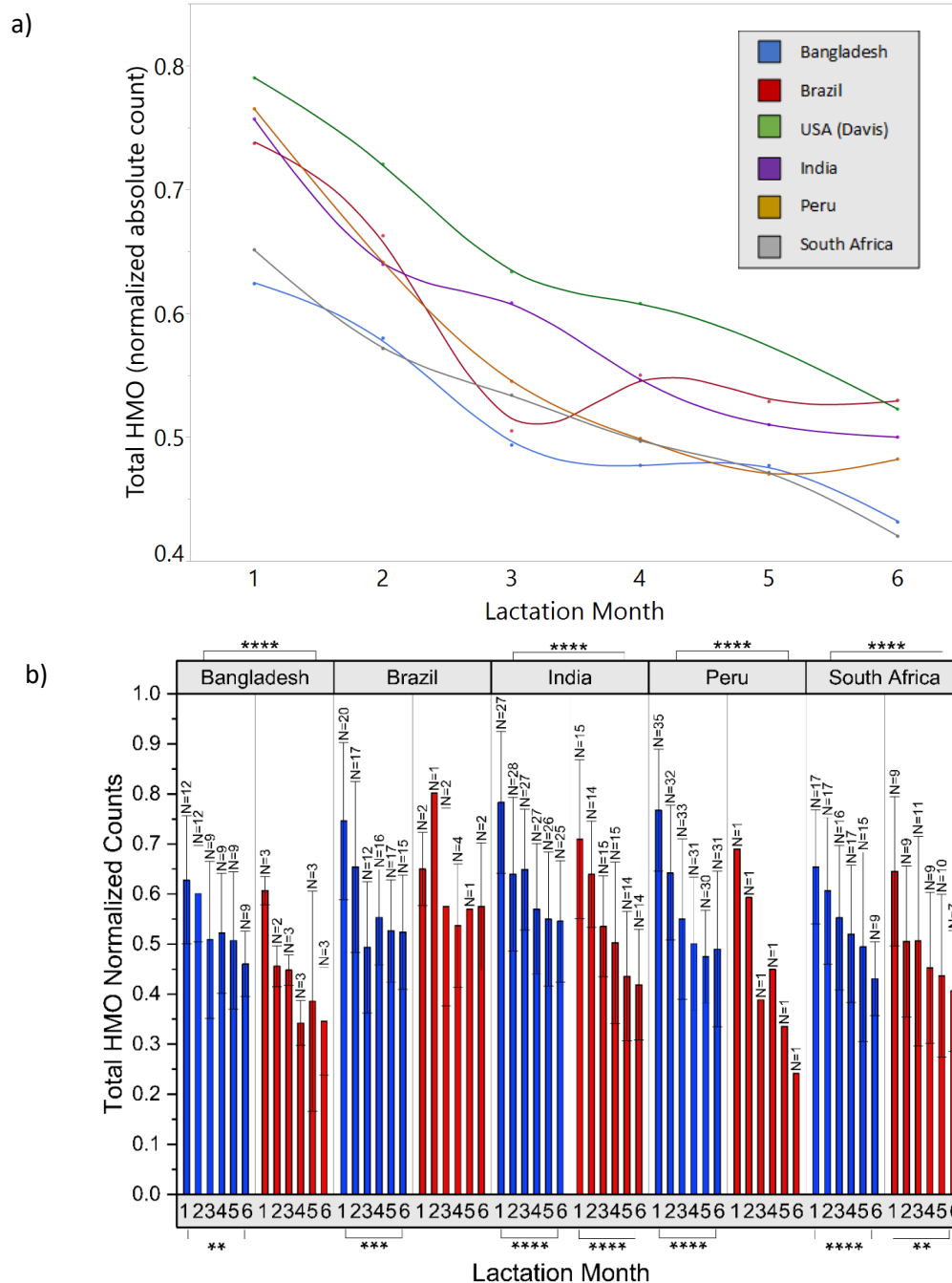


**Figure 2.3** (A) Mean changes in HMO concentrations in breastmilk samples collected monthly during the first 6 months postpartum at sites with extensive longitudinal sampling. (B) Total HMO abundances as a function of location, lactation month, and secretor status. HMO abundance values correspond to HPLC-qTOF MS spectral abundance normalized to the mean of the total abundance of ion counts from each sample. N values correspond to the number of samples. Error bars represent standard deviation. P values were obtained using Mann-Whitney tests with an  $\alpha$  correction of  $\alpha=0.05$ .

### ***Total HMO abundances and maternal age***

Variations in HMOs by maternal age were examined at sites with large numbers of samples [Malawi, Davis-USA, India, Peru]. The milk samples were binned into age groups <20, 21-30, 31- 40 and 41-50 years. Total absolute abundances of HMOs were not different between the age groups (**Figure 2.4**) or between S+ and S- milk (Data not shown). There were also no maternal age-related differences in total fucosylation, total sialylation or levels of 2'FL (the latter among S+ mothers).

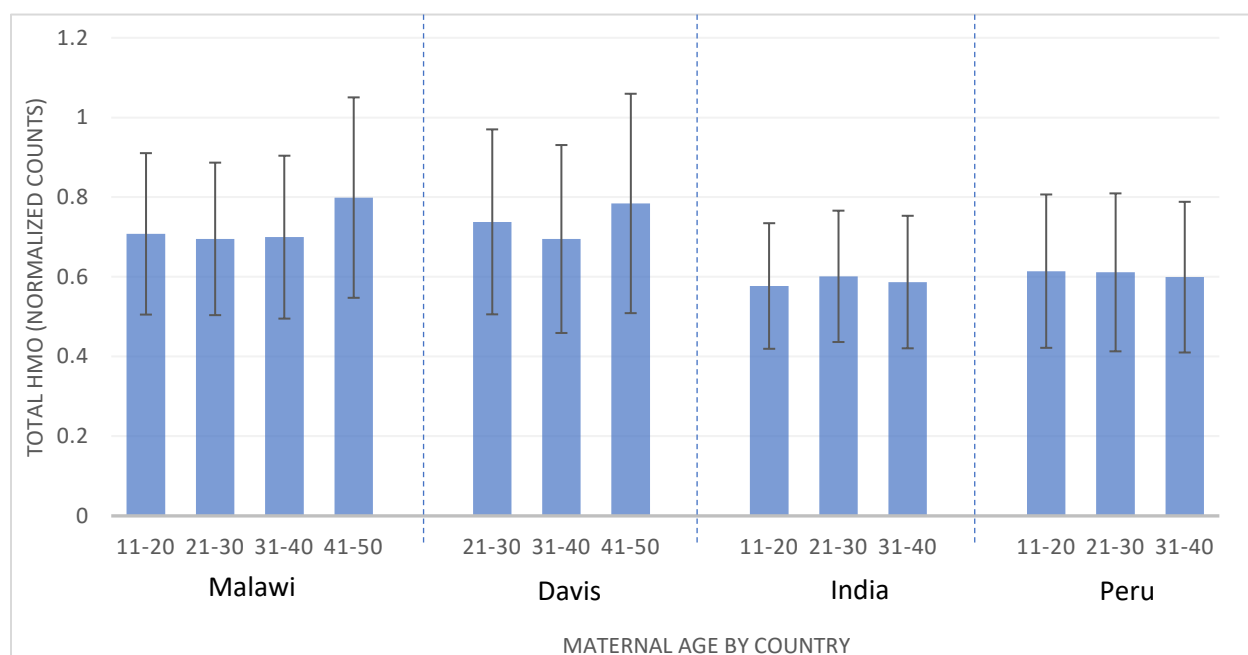


**Figure 2.4** Total abundance of HMOs categorized by maternal age groups and countries. HMO abundance values correspond to HPLC-qTOF MS spectral abundance normalized to the mean of the total abundance of ion counts from each sample. Error bars represent standard error.

### Total HMO abundances and infant sex

HMOs were compared to determine whether the sex of the infant affected total HMO abundances. Comparisons were made within sites (**Figure 2.5**). We found no statistically significant differences in absolute HMO abundances in milk from mothers of male compared to mothers of female infants. Similarly, total fucosylation and total sialylation yielded no differences based on sex of the offspring (not shown).

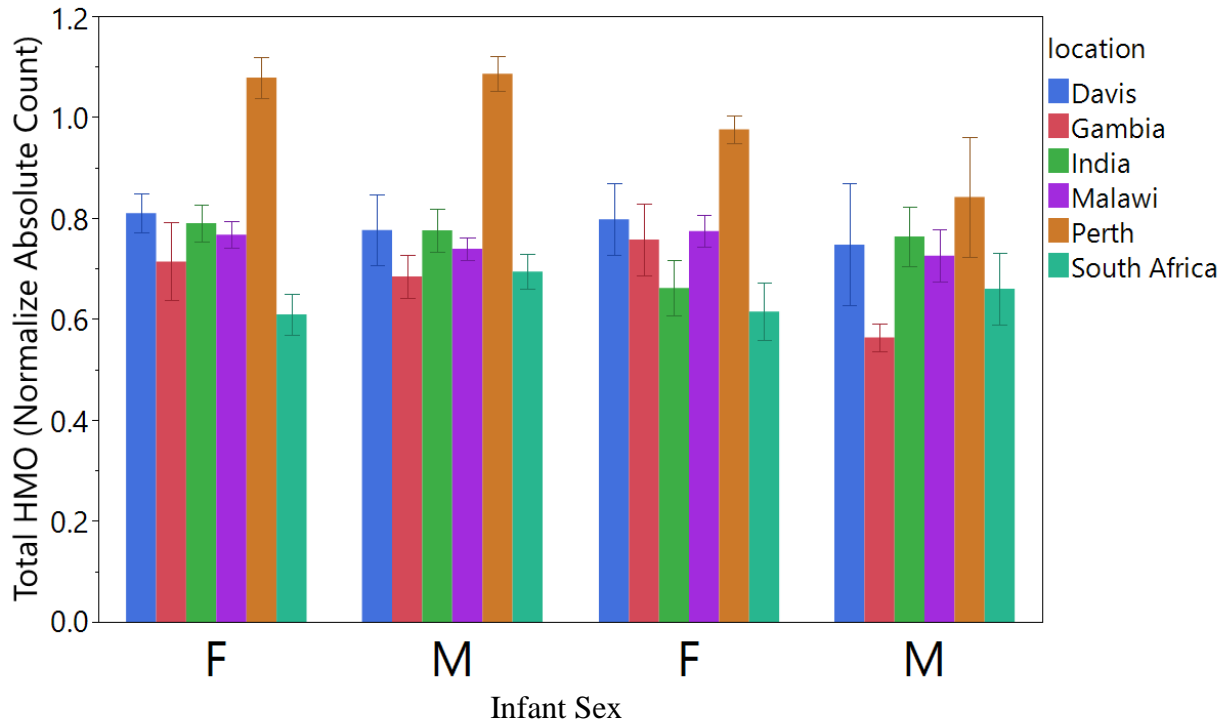


**Figure 2.5** Total Abundances of HMOs based on infant gender from regions with the most complete longitudinal samples, where F corresponds to Female infants and M corresponds to male infants. Error bars represent standard error.

*Variations in HMO subtypes across study sites and secretor status*

**Fucosylated HMOs.** Fucosylated oligosaccharides comprised the largest and most abundant groups of HMO structures. We first compared the total abundances of  $\alpha(1-2)$ -fucosylated HMOs in milk collected monthly during the first 6 months from mothers at study sites with longitudinal sampling, namely Bangladesh, Bolivia, India, Peru, and South Africa (**Figure 2.6a and Table 2.3**).

**Table 2.3** Mean levels of total HMO,  $\alpha(1,2)$ -fucosylated HMOs, total fucosylation, total sialylation and total undecorated HMOs by study site and secretor status.

| Country             | Site Location                 | GDP per capita | Total HMO (Normalized Counts) |             | Total Fucosylation (%) |               | Total Sialylation (%) |              | Total Undecorated (%) |               | $\alpha(1,2)$ -Fucosylated (%) |             |
|---------------------|-------------------------------|----------------|-------------------------------|-------------|------------------------|---------------|-----------------------|--------------|-----------------------|---------------|--------------------------------|-------------|
|                     |                               |                | B+                            | B-          | B+                     | B-            | B+                    | B-           | B+                    | B-            | B+                             | B-          |
| Argentina           | Namqom                        | 14,508         | 0.71 ± 0.14                   | 0.37 ± 0.07 | 69.04 ± 4.69           | 64.66 ± 5.62  | 10.40 ± 2.62          | 24.16 ± 2.86 | 23.47 ± 5.03          | 22.44 ± 5.07  | 24.48 ± 4.94                   | 2.22 ± 0.53 |
| Bolivia             | Amazonian Lowlands            | 3,351          | 0.61 ± 0.13                   | 0 ± 0       | 68.90 ± 6.39           | 0 ± 0         | 11.14 ± 2.69          | 0 ± 0        | 23.20 ± 6.39          | 0 ± 0         | 24.12 ± 8.87                   | 0 ± 0       |
| Brazil              | Fortaleza, Ceará              | 9,881          | 0.59 ± 0.16                   | 0.59 ± 0.12 | 65.18 ± 6.19           | 54.80 ± 10.01 | 11.74 ± 3.64          | 14.76 ± 5.66 | 27.68 ± 6.64          | 36.94 ± 11.55 | 20.51 ± 7.32                   | 1.72 ± 1.01 |
| Peru                | Loreto                        | 6,723          | 0.61 ± 0.19                   | 0.48 ± 0.17 | 71.26 ± 4.79           | 64.15 ± 5.57  | 13.63 ± 3.22          | 15.99 ± 3.46 | 20.35 ± 4.92          | 26.74 ± 6.41  | 24.64 ± 7.65                   | 1.98 ± 0.68 |
| Australia           | Perth                         | 53,831         | 0.98 ± 0.24                   | 0.94 ± 0.16 | 63.24 ± 4.58           | 58.02 ± 10.77 | 29.43 ± 6.73          | 34.17 ± 6.98 | 21.42 ± 6.08          | 26.32 ± 10.71 | 10.84 ± 5.06                   | 2.61 ± 0.82 |
| Bangladesh          | Mirpur, Dhaka                 | 1,564          | 0.58 ± 0.15                   | 0.47 ± 0.15 | 65.30 ± 5.42           | 56.16 ± 12.40 | 11.44 ± 2.95          | 15.17 ± 3.19 | 27.76 ± 5.79          | 34.31 ± 12.66 | 18.45 ± 7.10                   | 1.28 ± 0.90 |
| India               | Vellore, Tamil Nadu           | 1,980          | 0.62 ± 0.16                   | 0.54 ± 0.16 | 62.94 ± 7.43           | 54.15 ± 9.78  | 10.78 ± 2.87          | 15.13 ± 4.15 | 29.92 ± 7.18          | 36.37 ± 9.16  | 19.32 ± 6.49                   | 1.17 ± 2.07 |
| Nepal               | Nubri Valley                  | 900            | 0.64 ± 0.13                   | 0.63 ± 0.24 | 62.23 ± 6.64           | 49.66 ± 19.50 | 14.31 ± 2.88          | 19.19 ± 4.04 | 28.42 ± 6.12          | 38.71 ± 19.37 | 12.82 ± 3.68                   | 0.99 ± 0.37 |
| Philippines         | Cebu                          | 2,982          | 0.62 ± 0.09                   | 0.51 ± 0.11 | 64.11 ± 9.35           | 60.90 ± 5.89  | 11.54 ± 2.34          | 16.11 ± 4.35 | 27.65 ± 9.94          | 28.74 ± 6.34  | 20.09 ± 5.37                   | 2.24 ± 0.36 |
| Gambia              |                               | 673            | 0.58 ± 0.18                   | 0.55 ± 0.17 | 53.63 ± 8.49           | 42.60 ± 16.81 | 13.85 ± 5.07          | 16.34 ± 5.76 | 36.62 ± 7.68          | 45.96 ± 16.20 | 18.49 ± 65.85                  | 1.69 ± 1.47 |
| Malawi              | Mangochi district             | 357            | 0.72 ± 0.20                   | 0.66 ± 0.20 | 62.01 ± 9.91           | 54.22 ± 16.59 | 12.21 ± 3.37          | 14.31 ± 5.61 | 29.92 ± 9.32          | 36.37 ± 15.11 | 20.54 ± 7.20                   | 1.32 ± 0.74 |
| Namibia             | Omuhonga Basin                | 5,516          | 0.52 ± 0.25                   | 0.47 ± 0.02 | 63.63 ± 10.08          | 57.52 ± 1.67  | 17.92 ± 4.0           | 25.43 ± 1.54 | 26.07 ± 8.41          | 26.93 ± 0.67  | 15.10 ± 10.04                  | 1.11 ± 0.03 |
| South Africa        | Thohoyandou, Limpopo Province | 6,120          | 0.56 ± 0.15                   | 0.51 ± 0.18 | 60.15 ± 7.71           | 50.95 ± 10.45 | 13.16 ± 3.26          | 15.20 ± 3.08 | 31.32 ± 7.69          | 39.58 ± 9.85  | 17.88 ± 5.84                   | 1.03 ± 0.74 |
| Poland              | Beskid Wyspowy Mtns           | 13,871         | 0.70 ± 0.22                   | 0.54 ± 0.09 | 63.58 ± 6.60           | 51.46 ± 6.98  | 10.69 ± 3.66          | 17.35 ± 6.01 | 29.13 ± 7.25          | 36.68 ± 9.3   | 18.86 ± 5.06                   | 1.20 ± 0.29 |
| United States       | Boston, Massachusetts         | 59,939         | 0.76 ± 0.25                   | 0.58 ± 0.27 | 62.44 ± 3.88           | 58.95 ± 4.89  | 12.73 ± 3.47          | 16.45 ± 2.88 | 29.40 ± 5.35          | 30.87 ± 5.70  | 18.41 ± 6.77                   | 2.87 ± 0.97 |
| United States Davis | Davis, California             | 59,939         | 0.72 ± 0.24                   | 0.65 ± 0.24 | 64.00 ± 5.86           | 59.92 ± 9.23  | 13.57 ± 4.40          | 19.41 ± 6.36 | 27.50 ± 5.98          | 29.10 ± 9.19  | 15.44 ± 7.19                   | 2.11 ± 1.52 |

<sup>1</sup>Gross Domestic Product (GDP) values for each country are representative of the year of collection. Values are presented as mean ± SD. All data collected was used for this analysis including data from the same mother at different time points of lactation. P values were obtained using Mann-Whitney tests.

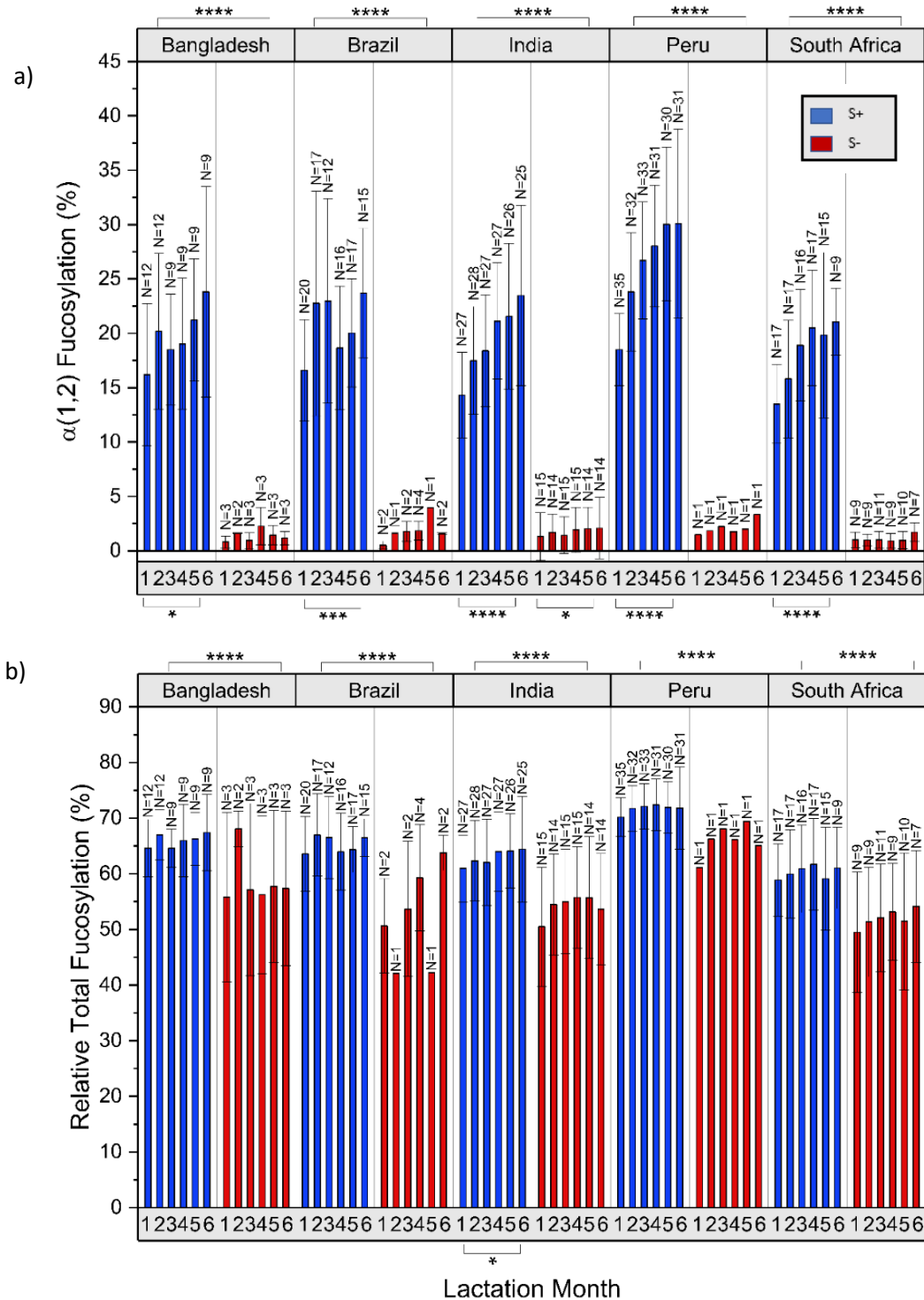


**Figure 2.6** Variations in Fucosylated HMOs during Lactation Between Geographical Sites. (A) Mean relative abundance of total  $\alpha(1,2)$ -fucose-containing HMOs in breastmilk samples as a function of lactation month (child's postnatal age) at sites with extensive longitudinal sampling. (B) Summed mean relative abundance of all fucose containing HMOs in the same samples (%)

Total Fucosylation). S- type producers (■) and S+ type producers (■). HMO abundance values correspond to HPLC-qTOF MS spectral abundance normalized to the mean of the total abundance of counts from each sample. Samples from multiple timepoints provided by a single mother as well as samples which only one time point was provided were included in this analysis. N values correspond to the number of samples. Error bars represent standard deviation. P values were obtained using Mann-Whitney tests with an  $\alpha$  correction of  $\alpha=0.05$ .

The proportion of  $\alpha(1,2)$ -fucosylated structures in secretors increased significantly between postnatal months 1-6, with statistical significance across all selected sites ( $P<0.05$ - $P<0.0001$ , Mann-Whitney). However, for S- milk, only the site with large sample size (India) achieved statistical significance. S+ milk had consistently higher abundances of  $\alpha(1,2)$ -fucosylated HMOs (ranging from 15-20% of total HMOs) compared to S- milk ( $<5\%$  of total HMOs;  $P<0.0001$ , Mann-Whitney). Interestingly S- milk, while containing very low abundances of  $\alpha(1,2)$ -fucosylated HMOs, at times had nonzero abundances slightly above the baseline ( $P<0.5$ ; Mann-Whitney). As 2-fucosyllactose is the most abundant of these structures, it increased over time as expected (**Figure 2.7**). Total fucosylation (oligosaccharides that contain fucose regardless of the linkage) increased between months 1 and 6 in all sites, however significance was only achieved in the India site and only for S+ milk ( $P<0.05$ , Mann-Whitney) (**Figure 2.6b**). Total fucosylation differed slightly between S+ and S- milk (**Figure 2.6b**). In general, S- milk had low abundances of fucosylated structures compared to S+ milk, reflecting the deficit in  $\alpha(1,2)$ -fucosylated HMOs, but partially compensated by increases in (1,3/4)-fucose linkages.

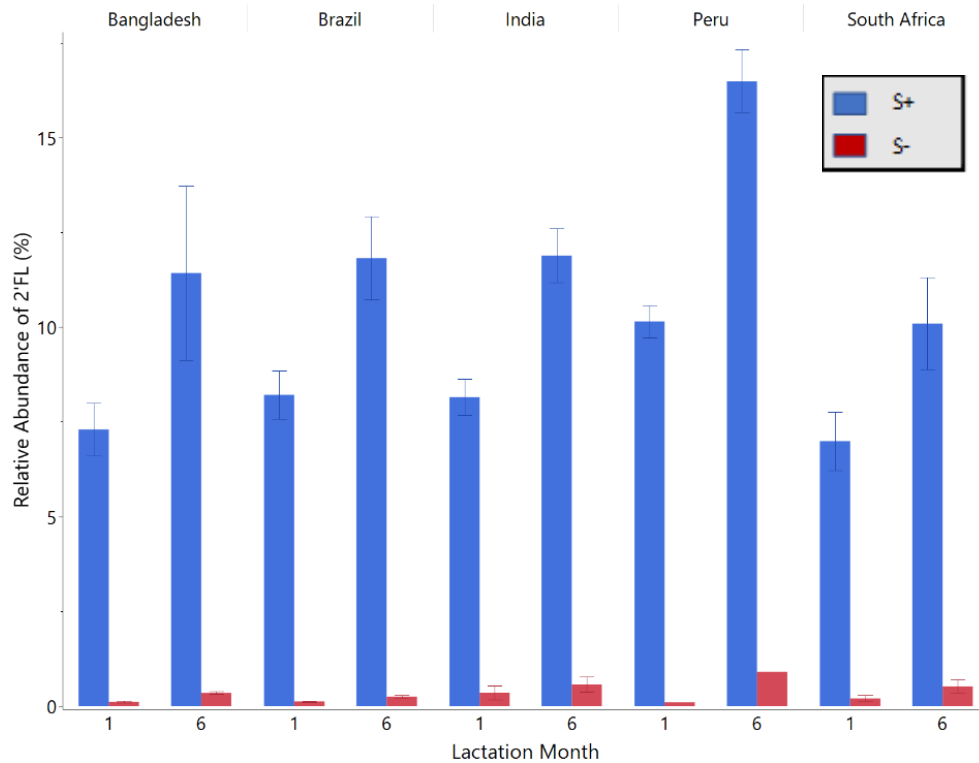


**Figure 2.7** Relative abundance of 2'FL at 1 and 6 month postpartum across 5 geographically diverse sites, where (■) corresponds to S+ producers and (■) corresponds to S- producers.

Variations in fucosylated structures were observed between milk from different countries within each secretor phenotype (**Figure 2.2**). Mothers with S+ milk from Nepal had significantly higher levels of DFLNH<sub>a</sub> ( $P < 0.0002$ , Mann-Whitney) and lower levels of 2'FL ( $P < 0.0001$ ) (both S+, secretor markers) compared to the other sites. Human milk obtained from mothers residing in the Boston-USA and Gambia sites had high relative abundances of LNFP I and LNFP III compared to all other sites, and low abundances of LNFP II. Milk from mothers residing in Perth-Australia had relatively high abundances of LSTc and LSTb compared to other sites. Interestingly, 2-fucosyllactose was not generally the most abundant in S+ milk among all countries. Australia, Boston-USA, and Namibia all had S+ milk with the most abundant  $\alpha(1-2)$ -fucosylated compound being LDFT ( $P = 0.005$ , Mann-Whitney).

**Sialylated HMOs.** Sialylated oligosaccharides generally had much lower abundances in human breast milk than fucosylated species. The mean abundances of sialylated HMOs in samples collected over the first 6 months postnatal from different study sites are shown in **Figure 2.8** and **Table 2.3**. Total abundances of sialylated HMOs were relatively constant throughout lactation for both S+ and S- phenotypes. Likewise, the relative abundances of sialylated HMOs were comparable across study sites with extensive sampling (Bangladesh, Bolivia, India, Peru, and South Africa) averaging  $12.3\% \pm 3.4$  of the total HMOs in S- milk and  $15.2\% \pm 3.8$  in S+ milk ( $P < 0.05$ - $P < 0.0001$ , Mann-Whitney). The most abundant sialylated HMOs when considering all samples were the combined group of LSTc+LSTb (in both S+ and S- samples) (**Figure 2.2**). Note however that the values from Peru for S- milk were obtained from samples provided by a single mother due to the very low prevalence of S- milk in this population. In populations with greater frequencies of S- milk, there was a greater relative abundance of sialylated structures in S- milk compared to S+ milk. In samples from India, Bangladesh and South Africa, the absolute abundances of sialylated HMOs in month 1 was nearly 15% greater in S- compared to S+ milk.

It is noteworthy that the sialylated HMO DSLNT, which has been shown to be protective against necrotizing enterocolitis in an animal model<sup>39</sup> and in a human preterm infant cohort<sup>40</sup> was often found in low abundance and was not one of the 60 HMOs found in all sites.

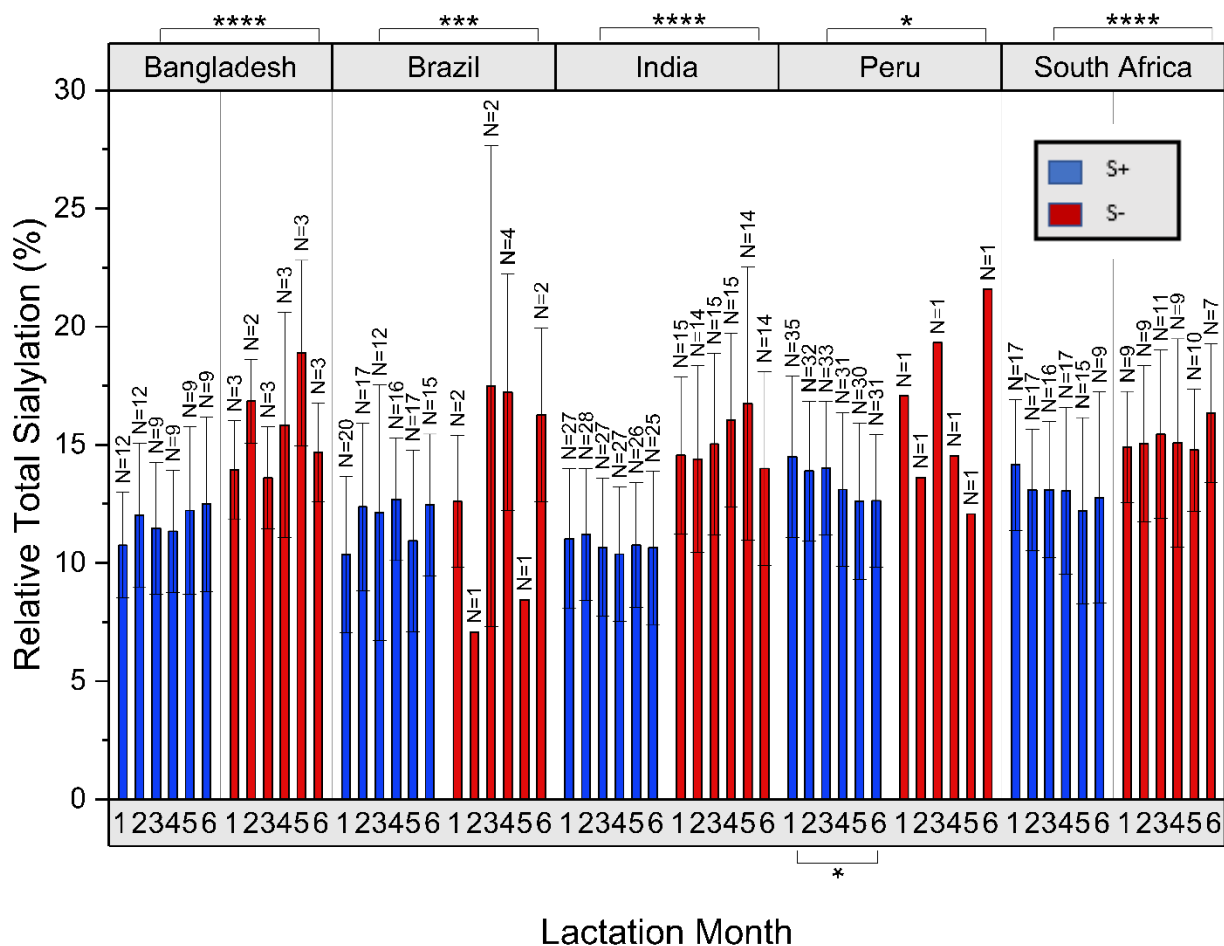


**Figure 2.8** Mean relative abundances of total sialic acid (Neu5Ac)-containing HMOs (% Total Sialylation) in breastmilk samples as a function of lactation month (child’s postnatal age) at sites with extensive longitudinal sampling. Samples from multiple timepoints provided by a single mother as well as samples from multiple mothers with one time point were all included in this analysis. HMO abundances corresponded to HPLC-qTOF MS abundances normalized to the mean of the total ion counts from each sample. Error bars represented standard deviation. P values were obtained using Mann-Whitney tests with an  $\alpha$  correction of  $\alpha=0.05$ .

**Undecorated (nonfucosylated and nonsialylated) HMOs.** The total abundances of undecorated HMOs (lacking both fucose and sialic acid) in milk from mothers at the various study sites were compared in **Figure 2.9** and **Table 2.3**. Undecorated HMOs were lower in S+ milk compared to S- milk ( $P=0.002$ , Mann-Whitney).<sup>41</sup> Between sites, overall relative abundances of undecorated HMOs were comparable ( $31.6\pm 8.9\%$ ) with the exception of Peru,

which exhibited significantly lower levels ( $20.5 \pm 5.2\%$ ) ( $P < 0.0001$ ) due to the higher amounts of fucosylation and diminished numbers of S- milk. Across all samples the most abundant undecorated HMO was the LNT/LNnT group (**Figure 2.2**).

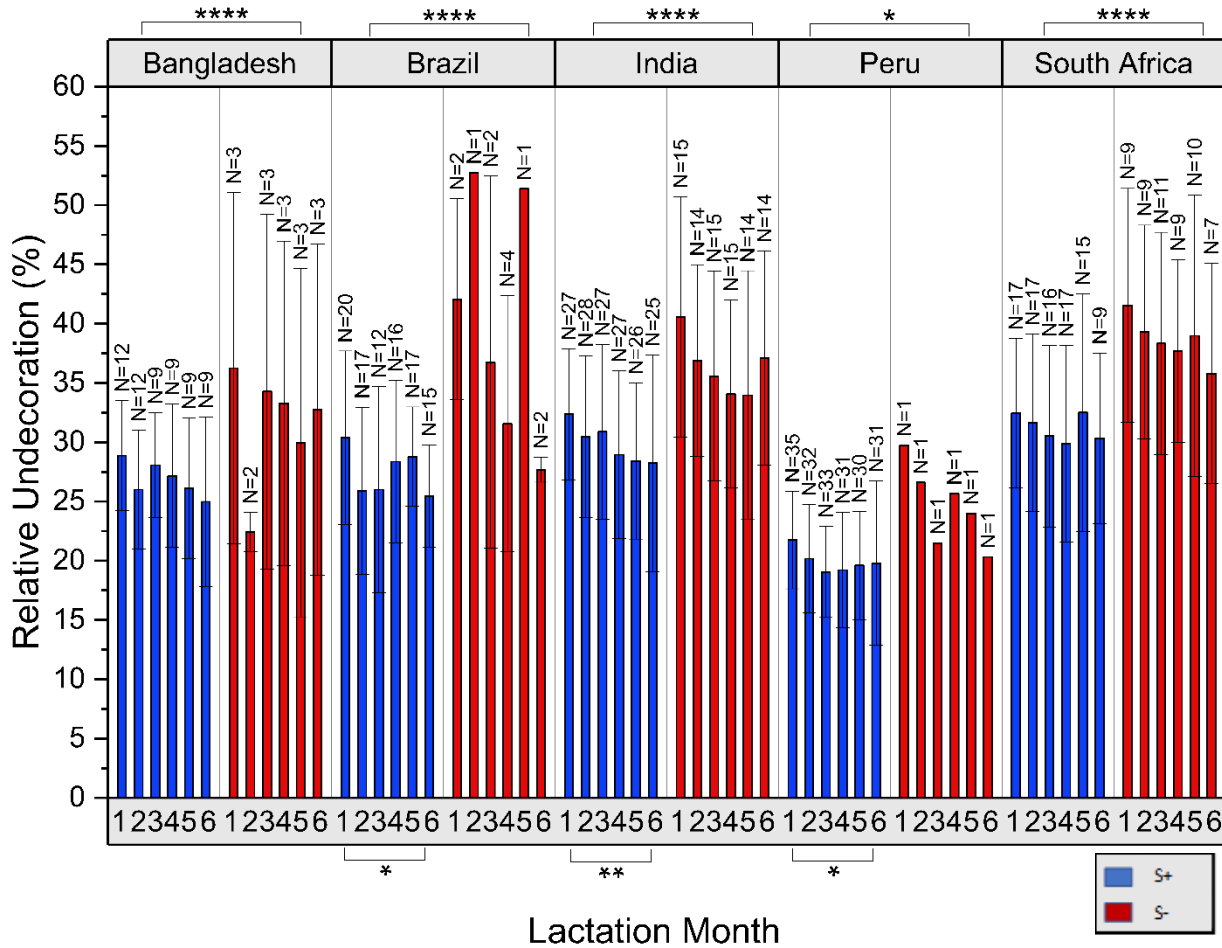


**Figure 2.9** Relative abundance of undecorated HMOs from regions with the most complete longitudinal samples, where (■) corresponds to S+ producers and (■) corresponds to S- producers. Samples from multiple timepoints provided by a single mother as well as samples which only one time point was provided were included in this analysis. N values correspond to the number of samples. Error bars represent standard deviation. P values were obtained using Mann-Whitney tests with an  $\alpha$  correction of  $\alpha=0.05$ .

### ***Global Variations of S+ and S- milk***

With the samples from different locations and the ability to distinguish S+ and S- milk, we determined the distribution of the two phenotypes globally. The sites are located on the map along with the fraction of S+ (blue) and S- (red) milk (**Figure 2.10**). The fraction of the mothers that produced S- milk was lower than those that produced S+ at every geographical site. High proportions of S- milk was found in Africa (37% in South Africa and 36% in The Gambia). These values contrast with other sites in Africa including Namibia (17%) and Malawi (25%) that had lower proportions of S- milk. Other sites with high levels of S- milk included those in India 35% and Nepal 29%. Bangladesh was lower with only 20% S- mothers. The USA sites (Davis, CA (22%) and Boston MA, 25%) were similar to the Poland (22%) site and the Australian site (19%). Low values were found in South America sites with Bolivia (0%), Peru (3%), Brazil (10%). The samples from these sites were obtained from indigenous populations. The other South American site, Argentina (15%) included nonindigenous populations.

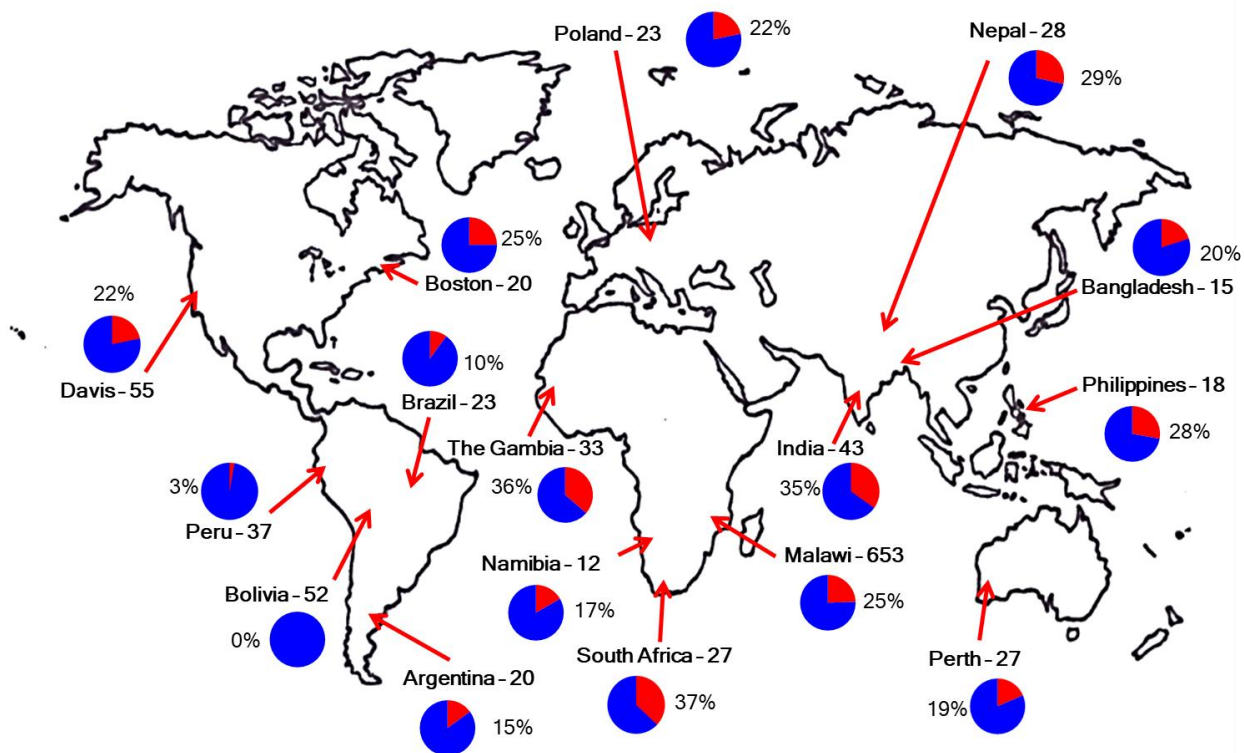


**Figure 2.10** Proportion of samples tested from each study location that were S+ type (i.e. secretor mothers, ■) and S- type (non-secretor mothers, ■). Labels presented as Country-Number of Mothers. If samples from multiple timepoints were provided by the same mother, the secretor status determination was concluded based on the majority of her samples. If there was no ‘majority milk type’, she was excluded from the statistical analysis (one mother from Davis, USA, two mothers from Malawi, and three mothers from Perth, Australia).

## DISCUSSION

The analyses of the HMO compositions of human milk samples collected from 16 sites around the world using a sensitive HPLC-qTOF-MS-based approach provided the most extensive dataset reported to date. While the samples were collected from different studies, the analytical method for each sample was the same. Unfortunately, absolute quantitation of total HMO and specific structures was not possible due to the low availability of standards in the earliest analysis.

This study significantly expands on our previous work at a single site in The Gambia.<sup>23</sup> The large number of samples from various geographical locations allowed us to further explore factors that may affect HMO production during lactation. Factors such as the age of the mother and the sex of the infant do not affect HMO abundances. The sex of the infant had been previously reported to affect milk compositions, suggesting that some components of human milk may be tailored to sex-differentiated developmental priorities.<sup>42</sup> However, examination of milk among all populations and within each site yielded no significant variations in total HMO abundances based on sex of a mother's child. Because neither dietary data nor maternal nutritional status were available for this study, we were not able to determine the extent to which these factors might influence abundances of individual structures nor levels of fucosylation and sialylation. However, the comparison of per capita gross domestic product (GDP) was obtained by comparing total abundances with published GDP. Interestingly, we observed some correlation between per capita GDP and total levels of HMOs from mothers living at the different sites. **(Figure 2.11)**. As shown, countries with high GDP per capita tended to have milk with the most abundant levels of HMOs. Likewise, mothers from sites with the low GDP per capita tended to have lower levels of HMOs. Among countries with low GDPs, there was a common minimum level of HMOs, while the trend towards higher abundances of HMOs did not appear to manifest until significantly higher GDPs were obtained. It would be difficult to make conclusions regarding GDP and HMO production as the amounts of HMOs fed to the infant can vary depending on feeding local feeding practices. Furthermore, the sample size, though large in totality, is still small at the local level and cannot fully represent the respective nation. However, we encourage further studies on societal effects on milk production.

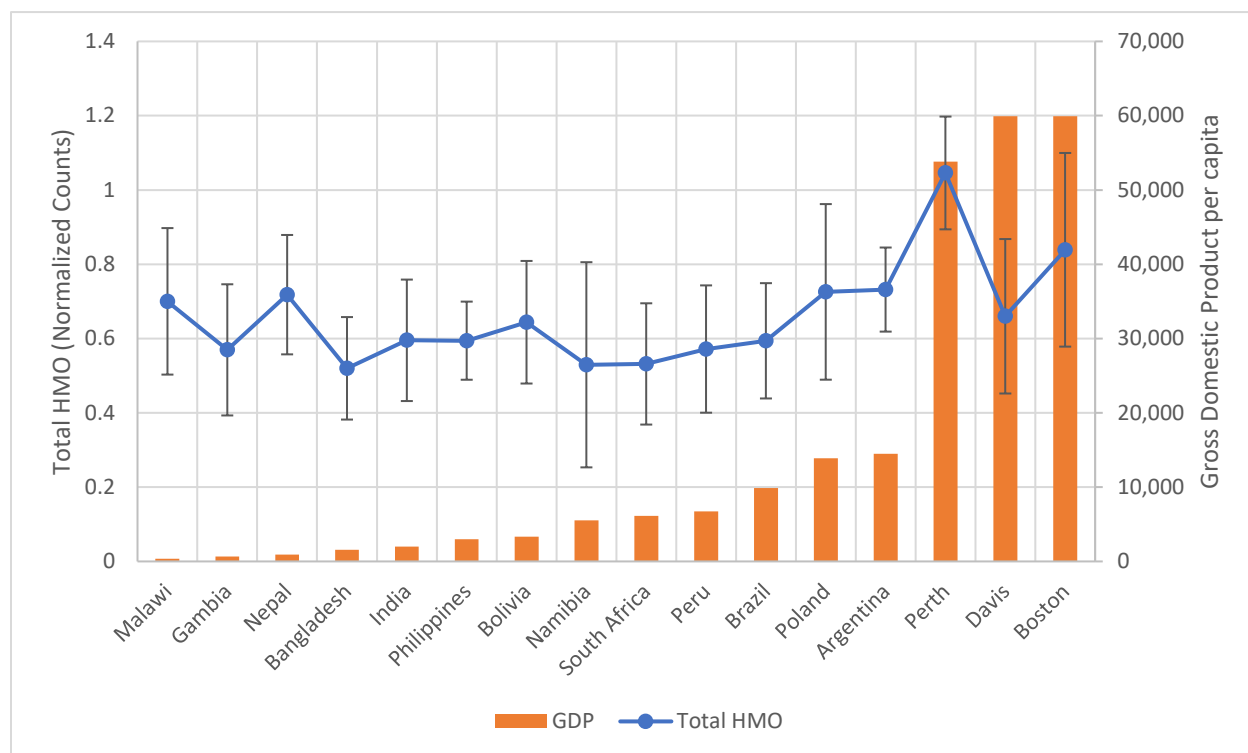


**Figure 2.11** (■) Gross domestic product per capita across all study sites (●) average abundance of HMOs found in mothers across all study sites. Samples from multiple timepoints provided by a single mother as well as samples which only one time point was provided were included in this analysis. Error bars represent standard deviation.

Genomic analysis has been previously used to obtain global distributions of secretors and nonsecretors.<sup>43</sup> While this approach uses obtains the genotypic status, the phenotype, i.e., the actual abundances of different structures and structural types in the milk, are those that affect infant health and developmental outcomes.<sup>44</sup> Hence, the concentrations of HMOs are crucial to understanding the health outcomes of infants providing information of distinct nutritional components that align with secretor status. Additionally, among secretors there are large variations in the abundances of fucosylated and sialylated species that are important contributors to infant development. The concentrations can then be used to phenotype milk based on the abundances of specific structures, namely  $\alpha(1,2)$ -fucosylated species, without genomic data. For

the purposes of this study, we therefore refer to milk that corresponds to high amounts of  $\alpha(1,2)$ -fucosylated structures as S+ milk, and milk corresponding to low abundances as S- milk.

The fraction of mothers who produce S- milk was nearly 40% in West and South Africa and South Asia, while nearly zero in parts of Latin America. The fraction of nonsecretor mothers (and hence S- milk) is often cited to be ~20%. However, this number is based primarily on studies of European and Euro-American mothers, which is consistent with our own results for sites in Europe and the USA. The USA sites (Davis CA, Boston MA), and Poland (the sole European site) had S- milk in proportions similar to those previously reported.<sup>34</sup> The rarity of S- milk among indigenous populations in South America suggests either founder effects during human migration into Beringia or selection from pathogen pressure. Many infectious diseases including cholera, whose severity is associated with blood type, can have devastating effects on populations.<sup>17</sup> As previously discussed, blood typing is similar to human milk in that the presence or absence of  $\alpha(1,2)$ -fucosylated structures is the key determinant. A study of the cholera outbreak in Peru in 1991 found that those with blood type O, which occurs at very high frequency among South American indigenous populations, had more severe symptoms and were eight times more likely to be hospitalized, emphasizing the relevance of glycosylation on infectious diseases.<sup>45</sup>

A distinguishing feature of humans and primates compared to other mammals is the high level of fucosylated structures with humans having the highest abundances.<sup>46</sup> Fucosylated structures, or the presence of at least one fucose, increased in relative abundances throughout lactation. Previous studies similarly noted that fucosylation increased throughout lactation for the first six months regardless of secretor status.<sup>41</sup> Fucosylation was generally higher in S+ milk. As a consequence of higher fucosylation in S+ milk, the amount of undecorated HMOs was lower

compared to S- negative milk, consistent with earlier findings.<sup>41</sup> In contrast, sialylation is the lowest among humans but is significantly greater in bovine and porcine milk.<sup>47</sup> In this study, though sialylated oligosaccharides in the human milk samples were still low, they were relatively higher in S- compared to S+ milk. Previous studies have also reported the higher abundances of sialylated HMOs in nonsecretor (S-) milk.<sup>41</sup>

The structural variety of HMOs and their different relative abundances have the potential to endow human milk from different mothers with distinct functional properties, including modulating its effect on the developing microbiota and its effects on infection/colonization with enteropathogens.<sup>48</sup> Members of the infant gut microbiota have specific glycosyl hydrolases and glycan-binding proteins that either promote the fitness of specific community members or block the host from infection. For example, HMOs promote the growth of *Bifidobacterium longum* subsp. *infantis*, a gut symbiont that is richly endowed with a suite of genes specifically adapted to import and utilize HMOs. The HMO composition of breastmilk thus has the potential to influence the fitness of strain-level variants of this and other related bifidobacterial species and to shape a program of normal postnatal community development (succession) that has been identified in healthy individuals and that is impaired in those with undernutrition<sup>13, 49</sup> Preclinical studies in gnotobiotic animals and clinical studies of the effects of repairing microbial community immaturity in children with acute malnutrition support the notion that healthy development of the microbiota is causally linked to healthy growth.<sup>13, 49</sup> Similarly, HMOs with  $\alpha(1-2)$  linked Fuc (S+ milk) are associated with decreased incidence and severity of diarrhea caused by *Campylobacter jejuni* and enteropathogenic *E. coli* - enteropathogens<sup>50, 51</sup> that are ubiquitous in many low income countries where childhood undernutrition is prevalent.<sup>52</sup> S- milk is enriched in HMOs that bind to *Helicobacter pylori*, and enteropathogenic *E. coli* preventing their attachment to gut epithelial

cells.<sup>53</sup> Individuals homozygous for *FUT2* mutations (non-secretors) also show resistance to norovirus infection<sup>54, 55</sup> or considering this relationship from the viewpoint of the pathogen, both rotavirus and norovirus (two of the most common causes of viral diarrhea in infants) appear to prefer the secretor host.<sup>32</sup> These mothers could in turn provide protection to their infant by delivering S- milk. Determining infant infectious disease risk should ideally include consideration of the secretor status of both the mother and the infant to address such key question as whether S+ milk is particularly beneficial for the non-secretor infant and vice versa.

The global results suggest that secretor status and the complement of HMO produced by a mother during lactation are influenced in part by adaptations shaped by ancestral nutritional and disease ecologies experienced by diverse human populations. Indeed, immunofactors in breastmilk are associated with subsistence practices that affect nutritional intake and pathogen exposure of diverse traditional societies and demonstrate the importance of considering populations within their contemporary, historical, and prehistorical contexts.<sup>45</sup> The “first-step” findings described here highlight the importance of multi-population studies to better characterize the relationships among maternal characteristics, HMO composition, early gut community development, the products of microbial metabolism of these HMOs, and measures of infant health status.<sup>46</sup> Delineation of these relationships, along with those mediated by other key constituents of breastmilk, e.g., secreted immunoglobulins and antibacterial proteins, will help guide the design of future prebiotic approaches based on purified milk components (or synthetically-produced mimetics) and/or synbiotics (prebiotics combined with a probiotic micro-organisms) that promote healthy gut community development healthy growth of infants , and even healthy immune and inflammatory responses over a lifetime.

## ACKNOWLEDGMENTS

We thank all of the mothers who participated, the communities who allowed the research and contributed samples. We also thank all the fieldworkers, staff and researchers, clinical staff, and laboratory technicians who collected the samples and data, and field assistant/translator John Jakurama.

We are grateful to the PIs and their colleagues who oversaw the studies at MAL-ED sites [Tahmeed Ahmed (icddr,b, Bangladesh), Aldo Lima (Universidade Federal do Ceará, Brazil), Margaret Kosek (Johns Hopkins School of Public Health, Iquitos, Peru), Gagandeep Kang (Christian Medical College, Vellore, India) and Pascale Bessong (University of Venda, South Africa)], We are grateful to the iLNS-DYAD-Malawi PIs and study team [Ken Maleta (University of Malawi College of Medicine), Per Ashorn (University of Tampere School of Medicine, Finland), Robin Bernstein (University of Colorado) and Jennifer T. Smilowitz and Kathryn Dewey (University of California, Davis)], We would like to thank Andrzej Galbarzyck for critical organizing at the Mogielica Human Ecology Study Site (Poland). The Argentine samples from Qom mothers (Qom field assistants and Fundación ECO). Milk samples from Nepal were collected among ethnic Tibetan mothers in northern Gorkha district (Jhangchuk Sangmo, Nyima Sangmo, Tsewang Palton Tibetan field assistants, Dr. Diki Bista, co-PI); milk samples from the Philippines were collected from mothers in rural and urban Cebu, Philippines (Office of Population Studies, University of San Carlos). The Argentine samples from Qom mothers (Qom field assistants and Fundación ECO).

**Author contributions:** L.D.K., M.M., E.A.Q., A.B., K.H., J.T.S., A.M.Z., M.J.B., J.I.G., M.A.U., C.V. and J.B.G. oversaw sample collection and provided samples. L.D.W., S.M.T., and J.C.C.D prepared samples. A.V., L.D.W., S.M.T., and J.C.C.D analyzed HMO data. A.V. and

J.C.C.D. performed statistical analyses on HMO data and infant disease metadata. C.B.L. designed the study and oversaw the analyses. A.V. and C.B.L. interpreted results and wrote the manuscript together with J.C.C.D., M.B. and J.I.G

**Funding:** This work was supported by grants from the Bill and Melinda Gates Foundation (J.C.C.D., C.B.L.), the NIH [grants AT007079 to D.A.M., HD061923 to C.B.L. , R01AG024119 to MG and HK , and AT008759 to D.A.M.], the Peter J. Shields Endowed Chair in Dairy Food Science (D.A.M.), and NSF DDIG 1233270 to MM. The Etiology, Risk Factors and Interactions of Enteric Infections and Malnutrition and the Consequences for Child Health and Development (MAL-ED) Project was carried out as a collaborative project supported by the Bill & Melinda Gates Foundation, the Foundation for the National Institutes of Health, and the Fogarty International Center. The iLiNS-DYAD study was funded by the Bill & Melinda Gates Foundation and FANTA-2 project, AED. The ENID trial was supported by the UK Medical Research Council (MRC) (MC-A760-5QX00) and the UK Department for International Development (DFID), under the MRC/DFID Concordat agreement.

**Data and materials availability:** Materials and correspondence should be directed to Carlito B. Lebrilla, [cblebrilla@ucdavis.edu](mailto:cblebrilla@ucdavis.edu).

## REFERENCES

1. Ballard, O.; Morrow, A., Human Milk Composition Nutrients and Bioactive Factors. *Pediatric clinics of North America* **2013**, *60*, 49-74.
2. Dorea, J. G., Selenium and breast-feeding. *British Journal of Nutrition* **2002**, *88* (5), 443-461.
3. Innis, S. M., Impact of maternal diet on human milk composition and neurological development of infants. *The American Journal of Clinical Nutrition* **2014**, *99* (3), 734S-741S.
4. Picciano, M. F., Nutrient Composition of Human Milk. *Pediatric Clinics of North America* **2001**, *48* (1), 53-67.
5. Hinde, K.; Milligan, L. A., Primate milk: Proximate mechanisms and ultimate perspectives. *Evolutionary Anthropology: Issues, News, and Reviews* **2011**, *20* (1), 9-23.
6. Ruhaak, L. R.; Lebrilla, C. B., Analysis and role of oligosaccharides in milk. *BMB Reports* **2012**, *45* (8), 442-451.
7. Wu, S.; Grimm, R.; German, J. B.; Lebrilla, C. B., Annotation and Structural Analysis of Sialylated Human Milk Oligosaccharides. *Journal of Proteome Research* **2011**, *10*, 856-868.
8. Wu, S.; Tao, N.; German, J. B.; Grimm, R.; Lebrilla, C. B., Development of an Annotated Library of Neutral Human Milk Oligosaccharides. *Journal of Proteome Research* **2010**, *9*, 4138-4151.
9. Newburg, D. S.; Neubauer, S. H., *Handbook of Milk Composition*. Academic Press, Inc.: 1995; p 919.
10. Engfer, M. B.; Stahl, B.; Finke, B.; Sawatzki, G.; Daniel, H., Human milk oligosaccharides are resistant to enzymatic hydrolysis in the upper gastrointestinal tract. *The American Journal of Clinical Nutrition* **2000**, *71*, 1589-1596.
11. Garrido, D.; Dallas, D. C.; Mills, D. A., Consumption of human milk glycoconjugates by infant-associated bifidobacteria: mechanisms and implications. *Microbiology* **2013**, *159*, 649-664.
12. LoCascio, R. G.; Ninonuevo, M. R.; Freeman, S. L.; Sela, D. A.; Grimm, R.; Lebrilla, C. B.; Mills, D. A.; German, J. B., Glycoprofiling of Bifidobacterial Consumption of Human Milk Oligosaccharides Demonstrates Strain Specific, Preferential Consumption of Small Chain Glycans Secreted in Early Human Lactation. *Journal of Agricultural and Food Chemistry* **2007**, *55*, 8914-8919.
13. Gehrig, J. L.; Venkatesh, S.; Chang, H.-W.; Hibberd, M. C.; Kung, V. L.; Cheng, J.; Chen, R. Y.; Subramanian, S.; Cowardin, C. A.; Meier, M. F.; O'Donnell, D.; Talcott, M.; Spears, L. D.; Semenkovich, C. F.; Henrissat, B.; Giannone, R. J.; Hettich, R. L.; Ilkayeva, O.; Muehlbauer, M.; Newgard, C. B.; Sawyer, C.; Head, R. D.; Rodionov, D. A.; Arzamasov, A. A.; Leyn, S. A.; Osterman, A. L.; Hossain, M. I.; Islam, M.; Choudhury, N.; Sarker, S. A.; Huq, S.; Mahmud, I.; Mostafa, I.; Mahfuz, M.; Barratt, M. J.; Ahmed, T.; Gordon, J. I., Effects of microbiota-directed foods in gnotobiotic animals and undernourished children. *Science* **2019**, *365* (6449), eaau4732.
14. Hinde, K.; Lewis, Z. T., Mother's littlest helpers. *Science* **2015**, *348* (6242), 1427-1428.
15. Ruhaak, L. R.; Stroble, C.; Underwood, M. A.; Lebrilla, C. B., Detection of milk oligosaccharides in plasma of infants. *Analytical and Bioanalytical Chemistry* **2014**, *406*, 5775-5784.

16. De Leoz, M. L. A.; Wu, S.; Strum, J. S.; Ninonuevo, M. R.; Gaerlan, S. C.; Mirmiran, M.; German, J. B.; Mills, D. A.; Lebrilla, C. B.; Underwood, M. A., A quantitative and comprehensive method to analyze human milk oligosaccharide structures in the urine and feces of infants. *Analytical and Bioanalytical Chemistry* **2013**, *405*, 4089-4105.
17. Coppa, G. V.; Zampini, L.; Galeazzi, T.; Facinelli, B.; Ferrante, L.; Capretti, R.; Orazio, G., Human Milk Oligosaccharides Inhibit the Adhesion to Caco-2 Cells of Diarrheal Pathogens: Escherichia coli, Vibrio cholerae, and Salmonella typhi. *Pediatric Research* **2006**, *59* (3), 377-382.
18. Hong, P.; Ninonuevo, M. R.; Lee, B.; Lebrilla, C.; Bode, L., Human milk oligosaccharides reduce HIV-1-gp120 binding to dendritic cell-specific ICAM3-grabbing non-integrin (DC-SIGN). *British Journal of Nutrition* **2008**, *101* (4), 482-486.
19. Eiwegger, T.; Stahl, B.; Haidl, P.; Schmitt, J.; Boehm, G.; Dehlink, E.; Urbanek, R.; Szépfalusi, Z., Prebiotic oligosaccharides: In vitro evidence for gastrointestinal epithelial transfer and immunomodulatory properties. *Pediatric Allergy and Immunology* **2010**, *21*, 1179-1188.
20. Wang, B., Sialic Acid is an Essential Nutrient for Brain Development and Cognition. *Annu. Rev. Nutr.* **2009**, *29*, 177-222.
21. Kunz, C.; Rudloff, S., Biological functions of oligosaccharides in human milk. *Acta Paediatr* **1993**, *82*, 903-912.
22. Urashima, T.; Kitaoka, M.; Asakuma, S.; Messer, M., Milk Oligosaccharides. In *Advanced Dairy Chemistry: Lactose, Water, Salts, and Minor Constituents*, McSweeney, P.; Fox, P., Eds. Springer Science: New York, 2009; pp 295-348.
23. Totten, S. M.; Zivkovic, A. M.; Wu, S.; Ngyuen, U.; Freeman, S. L.; Ruhaak, R. L.; Darboe, M. K.; German, J. B.; Prentice, A. M.; Lebrilla, C. B., Comprehensive Profiles of Human Milk Oligosaccharides Yield Highly Sensitive and Specific Markers for Determining Secretor Status in Lactating Mothers. *Journal of Proteome Research* **2012**, *11* (12), 6124-6133.
24. Brooks, S. A.; Dwek, M. V.; Schumacher, U., *Functional and Molecular Glycobiology*. BIOS Scientific Publishers Ltd: Oxford OX4 1RE, UK, 2002.
25. Thurl, S.; Henker, J.; Siegel, M.; Tovar, K.; Sawatzki, G., Detection of four human milk groups with respect to Lewis blood group dependent oligosaccharides. *Glycoconjugate Journal* **1997**, *14*, 795-799.
26. Mottram, L.; Wiklund, G.; Larson, G.; Qadri, F.; Svennerholm, A.-M., FUT2 non-secretor status is associated with altered susceptibility to symptomatic enterotoxigenic Escherichia coli infection in Bangladeshis. *Scientific Reports* **2017**, *7* (1), 10649.
27. Liu, Y.; Koda, Y.; Soejima, M.; Pang, H.; Schlaphoff, T.; du Toit, E. D.; Kimura, H., Extensive polymorphism of the FUT2 gene in an African (Xhosa) population of South Africa.
28. Kudo, T.; Iwasaki, H.; Nishihara, S.; Shinya, N.; Ando, T.; Narimatsu, I.; Narimatsu, H., Molecular Genetic Analysis of the Human Lewis Histo-blood Group System: II. SECRETOR GENE INACTIVATION BY A NOVEL SINGLE MISSENSE MUTATION A385T IN JAPANESE NONSECRETOR INDIVIDUALS. *Journal of Biological Chemistry* **1996**, *271* (16), 9830-9837.
29. Santos-Cortez, R. L. P.; Chiong, C. M.; Frank, D. N.; Ryan, A. F.; Giese, A. P. J.; Bootpetch Roberts, T.; Daly, K. A.; Steritz, M. J.; Szeremeta, W.; Pedro, M.; Pine, H.; Yarza, T. K. L.; Scholes, M. A.; Llanes, E.; Yousaf, S.; Friedman, N.; Tantoco, M. L. C.; Wine, T. M.; Labra, P. J.; Benoit, J.; Ruiz, A. G.; de la Cruz, R. A. R.; Greenlee, C.; Yousaf, A.; Cardwell, J.; Nonato, R. M. A.; Ray, D.; Ong, K. M. C.; So, E.; Robertson, C. E.; Dinwiddie, J.; Lagrana-Villagrancia, S. M.; Gubbels, S. P.; Shaikh, R. S.; Cass, S. P.; Einarsdottir, E.; Lee, N. R.;

- Schwartz, D. A.; Gloria-Cruz, T. L. I.; Bamshad, M. J.; Yang, I. V.; Kere, J.; Abes, G. T.; Prager, J. D.; Riazuddin, S.; Chan, A. L.; Yoon, P. J.; Nickerson, D. A.; Cutiongco-de la Paz, E. M.; Streubel, S. O.; Reyes-Quintos, M. R. T.; Jenkins, H. A.; Mattila, P.; Chan, K. H.; Mohlke, K. L.; Leal, S. M.; Hafrén, L.; Chonmaitree, T.; Sale, M. M.; Ahmed, Z. M., FUT2 Variants Confer Susceptibility to Familial Otitis Media. *Am J Hum Genet* **2018**, *103* (5), 679-690.
30. Smyth, D. J.; Cooper, J. D.; Howson, J. M. M.; Clarke, P.; Downes, K.; Mistry, T.; Stevens, H.; Walker, N. M.; Todd, J. A., *FUT2* Nonsecretor Status Links Type 1 Diabetes Susceptibility and Resistance to Infection. *Diabetes* **2011**, *60* (11), 3081.
31. Ye, B. D.; Kim, B. M.; Jung, S.; Lee, H. S.; Hong, M.; Kim, K.; Moon, J. W.; Baek, J.; Oh, E. H.; Hwang, S. W.; Park, S. H.; Yang, S. K.; Song, K., Association of FUT2 and ABO with Crohn's disease in Koreans. *J Gastroenterol Hepatol* **2020**, *35* (1), 104-109.
32. Rossouw, E.; Brauer, M.; Meyer, P.; du Plessis, N. M.; Avenant, T.; Mans, J., Virus Etiology, Diversity and Clinical Characteristics in South African Children Hospitalised with Gastroenteritis. *Viruses* **2021**, *13* (2).
33. Erney, R. M.; Malone, W. T.; Skelding, M. B.; Marcon, A. A.; Kleman-Leyer, K. M.; O'Ryan, M. L.; Ruiz-Palacios, G.; Hilty, M. D.; Pickering, L. K.; Prieto, P. A., Variability of Human Milk Neutral Oligosaccharides in a Diverse Population. *Journal of Pediatric Gastroenterology and Nutrition* **2000**, *30* (2), 181-192.
34. McGuire, M. K.; Meehan, C. L.; McGuire, M. A.; Williams, J. E.; Foster, J.; Sellen, D. W.; Kamau-Mbuthia, E. W.; Kamundia, E. W.; Mbugua, S.; Moore, S. E.; Prentice, A. M.; Kvist, L. J.; Otoo, G. E.; Brooker, S. L.; Price, W. J.; Shafii, B.; Placek, C.; Lackey, K. A.; Robertson, B.; Manzano, S.; Ruiz, L.; Rodríguez, J. M.; Pareja, R. G.; Bode, L., What's normal? Oligosaccharide concentrations and profiles in milk produced by healthy women vary geographically. *The American Journal of Clinical Nutrition* **2017**.
35. Plows, J. F.; Berger, P. K.; Jones, R. B.; Alderete, T. L.; Yonemitsu, C.; Najera, J. A.; Khwajazada, S.; Bode, L.; Goran, M. I., Longitudinal Changes in Human Milk Oligosaccharides (HMOs) Over the Course of 24 Months of Lactation. *J Nutr* **2021**, *151* (4), 876-882.
36. Ninonuevo, M. R.; Park, Y.; Yin, H.; Zhang, J.; Ward, R. E.; Clowers, B. H.; German, J. B.; Freeman, S. L.; Killeen, K.; Grimm, R.; Lebrilla, C. B., A Strategy for Annotating the Human Milk Glycome. *Journal of Agricultural and Food Chemistry* **2006**, *54*, 7471-7480.
37. Totten, S. M.; Wu, L. D.; Parker, E. A.; Davis, J. C. C.; Hua, S.; Stroble, C.; Ruhaak, L. R.; Smilowitz, J. T.; German, J. B.; Lebrilla, C. B., Rapid-throughput glycomics applied to human milk oligosaccharide profiling for large human studies. *Analytical and Bioanalytical Chemistry* **2014**, *406*, 7925-7935.
38. Kumazaki, T.; Yoshida, A., Biochemical evidences that secretor gene, Se, is a structural gene, coding a specific fucosyltransferase. *Proceedings of the National Academy of Sciences of the United States of America* **1984**, *81*, 4193-7.
39. Zhang, W.; He-Yang, J.; Zhuang, W.; Liu, J.; Zhou, X., Causative role of mast cell and mast cell-regulatory function of disialyllacto-N-tetraose in necrotizing enterocolitis. *Int Immunopharmacol* **2021**, *96*, 107597.
40. Masi, A. C.; Embleton, N. D.; Lamb, C. A.; Young, G.; Granger, C. L.; Najera, J.; Smith, D. P.; Hoffman, K. L.; Petrosino, J. F.; Bode, L.; Berrington, J. E.; Stewart, C. J., Human milk oligosaccharide DSLNT and gut microbiome in preterm infants predicts necrotising enterocolitis. *Gut* **2020**.

41. Xu, G.; Davis, J. C. C.; Goonatilleke, E.; Smilowitz, J. T.; German, J. B.; Lebrilla, C. B., Absolute Quantitation of Human Milk Oligosaccharides Reveals Phenotypic Variations during Lactation. *The Journal of Nutrition* **2016**, *147* (1), 117-124.
42. Galante, L.; Milan, A. M.; Reynolds, C. M.; Cameron-Smith, D.; Vickers, M. H.; Pundir, S. Sex-Specific Human Milk Composition: The Role of Infant Sex in Determining Early Life Nutrition *Nutrients* [Online], 2018. PubMed. <http://europepmc.org/abstract/MED/30200404>  
<https://doi.org/10.3390/nu10091194>  
<http://europepmc.org/articles/PMC6165076>  
<http://europepmc.org/articles/PMC6165076?pdf=render> (accessed 2018/09//).
43. Arrouzet, C. J.; Ellis, K.; Kambhampati, A.; Chen, Y.; Steele, M.; Lopman, B., Population-Level Human Secretor Status Is Associated With Genogroup 2 Type 4 Norovirus Predominance. *The Journal of Infectious Diseases* **2020**, *221* (11), 1855-1863.
44. Klein, L. D.; Huang, J.; Quinn, E. A.; Martin, M. A.; Breakey, A. A.; Gurven, M.; Kaplan, H.; Vaggia, C.; Jasienska, G.; Scelza, B.; Lebrilla, C. B.; Hinde, K., Variation among populations in the immune protein composition of mother's milk reflects subsistence pattern. *Evolution, Medicine, and Public Health* **2018**, *2018* (1), 230-245.
45. Swerdlow, D. L.; Mintz, E. D.; Rodriguez, M.; Tejada, E.; Ocampo, C.; Espejo, L.; Barrett, T. J.; Petzelt, J.; Bean, N. H.; Seminario, L.; Tauxe, R. V.
46. Tao, N.; Wu, S.; Kim, J.; An, H. J.; Hinde, K.; Power, M. L.; Gagneux, P.; German, J. B.; Lebrilla, C. B., Evolutionary glycomics: characterization of milk oligosaccharides in primates. *J Proteome Res* **2011**, *10* (4), 1548-57.
47. Tao, N.; DePeters, E. J.; German, J. B.; Grimm, R.; Lebrilla, C. B., Variations in bovine milk oligosaccharides during early and middle lactation stages analyzed by high-performance liquid chromatography-chip/mass spectrometry. *J Dairy Sci* **2009**, *92* (7), 2991-3001.
48. Underwood, M. A., Impact of probiotics on necrotizing enterocolitis. *Semin Perinatol* **2017**, *41* (1), 41-51.
49. Raman, A. S.; Gehrig, J. L.; Venkatesh, S.; Chang, H.-W.; Hibberd, M. C.; Subramanian, S.; Kang, G.; Bessong, P. O.; Lima, A. A. M.; Kosek, M. N.; Petri, W. A.; Rodionov, D. A.; Arzamasov, A. A.; Leyn, S. A.; Osterman, A. L.; Huq, S.; Mostafa, I.; Islam, M.; Mahfuz, M.; Haque, R.; Ahmed, T.; Barratt, M. J.; Gordon, J. I., A sparse covarying unit that describes healthy and impaired human gut microbiota development. *Science* **2019**, *365* (6449), eaau4735.
50. Newburg, D. S.; Ruiz-Palacios, G.; Altaye, M.; Chaturvedi, P.; Meinen-Derr, J.; de Lourdes guerrero, M.; Morrow, A. L., Innate protection conferred by fucosylated oligosaccharides of human milk against diarrhea in breastfed infants. *Glycobiology* **2004**, *14* (3), 253-263.
51. Morrow, A. L.; Ruiz-Palacios, G. M.; Altaye, M.; Jiang, X.; Guerrero, M. L.; Meinen-Derr, J. K.; Farkas, T.; Chaturvedi, P.; Pickering, L. K.; Newburg, D. S., Human Milk Oligosaccharide Blood Group Epitopes and Innate Immune Protection against *Campylobacter* and *Calicivirus* Diarrhea in Breastfed Infants. In *Protecting Infants through Human Milk*, Pickering, L. K.; Morrow, A. L.; Ruiz-Palacios, G. M.; Schanler, R. J., Eds. Springer US: 2004; pp 443-446.
52. Platts-Mills, J. A.; Liu, J.; Rogawski, E. T.; Kabir, F.; Lertsethtakarn, P.; Siguas, M.; Khan, S. S.; Praharaj, I.; Murei, A.; Nshama, R.; Mujaga, B.; Havt, A.; Maciel, I. A.; McMurry, T. L.; Operario, D. J.; Taniuchi, M.; Gratz, J.; Stroup, S. E.; Roberts, J. H.; Kalam, A.; Aziz, F.;

Qureshi, S.; Islam, M. O.; Sakpaisal, P.; Silapong, S.; Yori, P. P.; Rajendiran, R.; Benny, B.; McGrath, M.; McCormick, B. J. J.; Seidman, J. C.; Lang, D.; Gottlieb, M.; Guerrant, R. L.; Lima, A. A. M.; Leite, J. P.; Samie, A.; Bessong, P. O.; Page, N.; Bodhidatta, L.; Mason, C.; Shrestha, S.; Kiwelu, I.; Mduma, E. R.; Iqbal, N. T.; Bhutta, Z. A.; Ahmed, T.; Haque, R.; Kang, G.; Kosek, M. N.; Houpt, E. R.; Acosta, A. M.; Rios de Burga, R.; Chavez, C. B.; Flores, J. T.; Olotegui, M. P.; Pinedo, S. R.; Trigoso, D. R.; Vasquez, A. O.; Ahmed, I.; Alam, D.; Ali, A.; Rasheed, M.; Soofi, S.; Turab, A.; Yousafzai, A.; Zaidi, A. K. M.; Shrestha, B.; Rayamajhi, B. B.; Strand, T.; Ammu, G.; Babji, S.; Bose, A.; George, A. T.; Hariraju, D.; Jennifer, M. S.; John, S.; Kaki, S.; Karunakaran, P.; Koshy, B.; Lazarus, R. P.; Muliyl, J.; Ragasudha, P.; Raghava, M. V.; Raju, S.; Ramachandran, A.; Ramadas, R.; Ramanujam, K.; Rose, A.; Roshan, R.; Sharma, S. L.; Sundaram, S.; Thomas, R. J.; Pan, W. K.; Ambikapathi, R.; Carreon, J. D.; Doan, V.; Hoest, C.; Knobler, S.; Miller, M. A.; Psaki, S.; Rasmussen, Z.; Richard, S. A.; Tountas, K. H.; Svensen, E.; Amour, C.; Bayyo, E.; Mvungi, R.; Pascal, J.; Yarrot, L.; Barrett, L.; Dillingham, R.; Petri, W. A.; Scharf, R.; Ahmed, A. M. S.; Alam, M. A.; Haque, U.; Hossain, M. I.; Islam, M.; Mahfuz, M.; Mondal, D.; Nahar, B.; Tofail, F.; Chandyo, R. K.; Shrestha, P. S.; Shrestha, R.; Ulak, M.; Bauck, A.; Black, R.; Caulfield, L.; Checkley, W.; Lee, G.; Schulze, K.; Scott, S.; Murray-Kolb, L. E.; Ross, A. C.; Schaefer, B.; Simons, S.; Pendergast, L.; Abreu, C. B.; Costa, H.; Di Moura, A.; Filho, J. Q.; Leite, Á. M.; Lima, N. L.; Lima, I. F.; Maciel, B. L. L.; Medeiros, P. H. Q. S.; Moraes, M.; Mota, F. S.; Oriá, R. B.; Quetz, J.; Soares, A. M.; Mota, R. M. S.; Patil, C. L.; Mahopo, C.; Maphula, A.; Nyathi, E., Use of quantitative molecular diagnostic methods to assess the aetiology, burden, and clinical characteristics of diarrhoea in children in low-resource settings: a reanalysis of the MAL-ED cohort study. *The Lancet Global Health* **2018**, *6* (12), e1309-e1318.

53. Simon, P. M.; Goode, P. L.; Mobasser, A.; Zopf, D., Inhibition of *Helicobacter pylori* binding to gastrointestinal epithelial cells by sialic acid-containing oligosaccharides. *Infection and Immunity* **1997**, *65* (2), 750-7.

54. Thorven, M.; Grahn, A.; Hedlund, K. O.; Johansson, H.; Wahlfrid, C.; Larson, G.; Svensson, L., A homozygous nonsense mutation (428G-->A) in the human secretor (FUT2) gene provides resistance to symptomatic norovirus (GGII) infections. *J Virol* **2005**, *79* (24), 15351-5.

55. Larsson, M. M.; Rydell, G. E. P.; Grahn, A.; Rodríguez-Díaz, J.; Åkerlind, B.; Hutson, A. M.; Estes, M. K.; Larson, G.; Svensson, L., Antibody Prevalence and Titer to Norovirus (Genogroup II) Correlate with Secretor (FUT2) but Not with ABO Phenotype or Lewis (FUT3) Genotype. *Journal of Infectious Diseases* **2006**, *194* (10), 1422-1427.

## CHAPTER THREE

**Fetus Receives Breast Milk Carbohydrates in Utero: An LC-MS based method for HMO analysis in Amniotic Fluid**

## **ABSTRACT**

Human Milk Oligosaccharides (HMOs) are an abundant component of breast milk and have shown to be beneficial to the infant's development. Previous studies have found that HMOs are not only present in maternal milk but also present in the mother's serum and urine. Herein, we report the first comprehensive study of oligosaccharides present in amniotic fluid demonstrating direct interaction of HMOs with the developing fetus. An extensive library and analytical methods were developed that allow for accurate quantitation of oligosaccharides using high resolution mass spectrometry. This method was applied to over 500 mothers from different gestational periods, ethnicity/race, ages, and birth outcomes. We observed over 30 oligosaccharide structures present in the amniotic fluid, eight of which are exclusive to maternal milk. Structure specific changes in concentration of amniotic fluid throughout gestation were revealed. HMOs 2'FL and LDFT increased with increasing gestational age ( $p=9.9 \times 10^{-8}$  and 0.002, respectively) while other HMOs such as 3'SL decreased in concentration throughout gestation. These results provide insight into the potential roles of HMOs and provides evidence that the developing fetus is receiving breast milk components in utero.

## INTRODUCTION

Human breast milk consists of a diverse group of bioactive molecules that aid in the development of the infant. Nutrients can be categorized primarily into three major components: fats, proteins, and carbohydrates. Carbohydrates are the most abundant nutrient accounting for roughly 40% of the total calories provided by breast milk.<sup>1</sup> A unique subset of carbohydrates found in human breast milk are called human milk oligosaccharides (HMOs). HMOs are unique among the macronutrients because unlike lactose, proteins, or fats, they are not digestible nor absorbed, yet they remain as one of the most abundant components.<sup>2</sup> The base structure of every HMO consists of lactose (a disaccharide comprised of glucose and galactose) at the reducing end and elongated with further additions of L-fucose (Fuc), D-galactose (Gal), N-acetylglucosamine (GlcNAc) and N-acetylneuraminic acid (Sia). These additions vary in sequence and orientation, which accounts for the structural diversity of hundreds of unique oligosaccharides that have been identified in human milk to date.<sup>3, 4</sup>

The presence and considerable abundance of oligosaccharides in maternal milk strongly suggests an important functional role for these sugars in infant development. The structure-function relationships between individual HMO structures and infant health have not been completely explored, however scientists have shown that HMOs collectively provide many benefits to the developing infant including establishing gastrointestinal microbiome,<sup>5-11</sup> acting as a decoy for pathogenic infection,<sup>12 13</sup> and aiding in neurological and cognitive development.<sup>14</sup> More recent investigations have suggested that HMOs may benefit even the developing neonate as HMOs have been found in maternal blood,<sup>15</sup> urine,<sup>16</sup> and more recently amniotic fluid<sup>17</sup> of pregnant mothers. The presence of HMOs in amniotic fluid is particularly important because

amniotic fluid not only surrounds the fetus during pregnancy but is also involved in various intermembranous pathways that transfer fluid and solutes from maternal plasma to the fetus.<sup>18-20</sup>

Amniotic fluid initially was thought to provide primarily physical support and other benefits such as allowing room for fetal growth and development, acting as a mechanical cushion for protection, and temperature regulation, but more recently researchers have observed potential nutritive functions of amniotic fluid providing vital nutrients such as proteins, lipids, and carbohydrates.<sup>21, 22</sup> Unfortunately, due to the complexity of the matrix, low concentrations of the analytes and the difficulty in obtaining samples, there are limited studies on the composition of amniotic fluid and even less on the direct effects of the composition on fetal development at different stages of gestation.

Herein, we report the methodologies for extraction, isolation, and characterization of all quantifiable oligosaccharides (including non-HMO structures) in N=516 maternal amniotic fluid samples utilizing LC-MS, making this the most comprehensive study of amniotic fluid oligosaccharides to date. The methods and results detailed here aim to provide the first steps to understanding the biological role of oligosaccharides in the uterus and provide the analytical tools for further investigations to address the many unanswered questions regarding the role and composition of amniotic fluid.

## **METHODS**

### **Amniotic Fluid Collection**

Under IRB approval from the University of Texas (HSC-MS-07-0109), this study recruited gravid participants who were undergoing clinically indicated and/or maternal requested

genetic amniocentesis for prenatal diagnosis. Consistent with genetic diagnostic amniocentesis being performed in the mid-trimester, participants were recruited and sampled at 15-29 weeks gestation (mean gestational age 17.5  $\pm$  1.9) and underwent full and informed consent to allow an additional 3-5 ml of amniotic fluid to be sterilely collected as part of their planned clinical procedure using aseptic technique, transferred under sterile conditions to 1.5 ml screw top cryopreservation vials, and stored at -80 °C until future use in the current research studies. Briefly, after sterile preparation and draping of the lower gravid abdomen, a 20 to 22 G spinal needle was advanced perpendicular to the skin with the transducer beam at a 15- to 20-degree angle. In a single passage under continuous ultrasound visualization and guidance using aseptic techniques and with sterile handling maintained throughout the entirety of the procedure, a total of 30 to 45 mL of sterile amniotic fluid was collected in three steps. As a first step, an initial sterile 3 or 5 cc syringe was used to aspirate a small amount (1 to 3 mL) of amniotic fluid through the sheath to discard any potential maternal or skin contaminants. Caution was taken when entering the amniotic cavity to ensure no direct contact with the fetus. Second, without repositioning the sheath, sequential aspirations with 10 or 15 cc sterile syringes collected the 25 to 35 cc of amniotic fluid to be sent for clinical diagnostic purposes. Third, and again without repositioning the sheath, a final aliquot of 3-5 mL of amniotic fluid was aspirated with a 5 cc sterile syringe, using identical aseptic sterile technique under continuous ultrasound visualization. This final 3-5 mL of amniotic fluid was immediately transferred and aliquoted to sterile cryotubes for preservation at -80 °C. The prospective cohort was followed for later outcomes during the pregnancy, which were abstracted into an anonymized (coded, without identifying data) repository that accompanied the biobank. Data recorded included the week of amniocentesis, self-reported race and ethnicity of the mother, parity, indication for

amniocentesis, history of preterm birth, and delivery outcome inclusive of gestational age at delivery, spontaneous or indicated preterm birth and including preterm premature rupture of membranes. The outcome of the fetal karyotype was also included.

### **Oligosaccharide Extraction from Amniotic Fluid**

A total of 514 amniotic fluid (AF) samples were prepared for oligosaccharide profiling. Surrogate internal standard mix (xylo-oligosaccharides) was prepared in a large batch and added to individual samples prior to preparation. 100  $\mu$ L of AF was purified using a 10K allowance ultracentrifuge filter. The flow through was then cleaned up with solid phase extraction packed with C18 and sequentially processed through PGC. Eluant was dried and concentrated with water prior to analyses on a nano-HPLC-qTOF-MS (nano-HPLC: Model series 1200, QTOF: Model series 6220, Agilent Technologies). Separation was performed on a microfluidic chip packed with PGC via enrichment and analytical columns, respectively, using a binary gradient of solvent A [3% acetonitrile (ACN) in 0.1% formic acid] and solvent B (90% ACN in 0.1% formic acid). Optimized gradient composition as follows: 0.00–2.50 min, 2–7% B; 2.50–10 min, 7–10% B; 10.00–25.00 min, 10–16% B; 25.0–40.00 min, 16–35% B, 40.00–45.00 min, 35–100% B. Mass spec was set to operate in positive mode with parameters optimized in previous publication.<sup>23, 24</sup> Standard solutions of the most abundant HMOs were run prior to each batch with concentrations ranging from (0.03 fmol/mL to 15.75 nmol/mL). Blanks and quality controls were run every 6 samples.

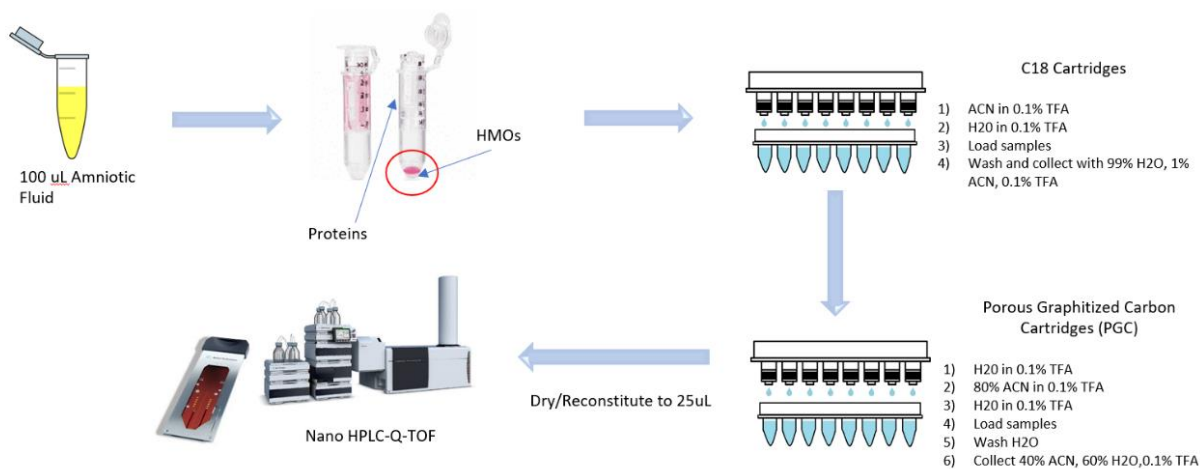
### **Statistical Analysis and Data Processing**

Data was collected using Agilent MassHunter Workstation Data Acquisition and then analyzed with Agilent MassHunter Qualitative Analysis software. Peak areas were assigned

using Profinder B.08.00. Calibration curves were constructed using Microsoft Excel 2016. Matrix correction factors were calculated by dividing the intensity of pure internal standard by the mean internal standard signal in the samples. Cohort normalization was performed between all batches to reduce batch-to-batch variability by normalizing each batch to the cohort mean. Limits of Quantitation (LOQ) and Limits of Detection (LOD) were defined as 6X and 3X the signal-to-noise ratio of the blanks respectively.

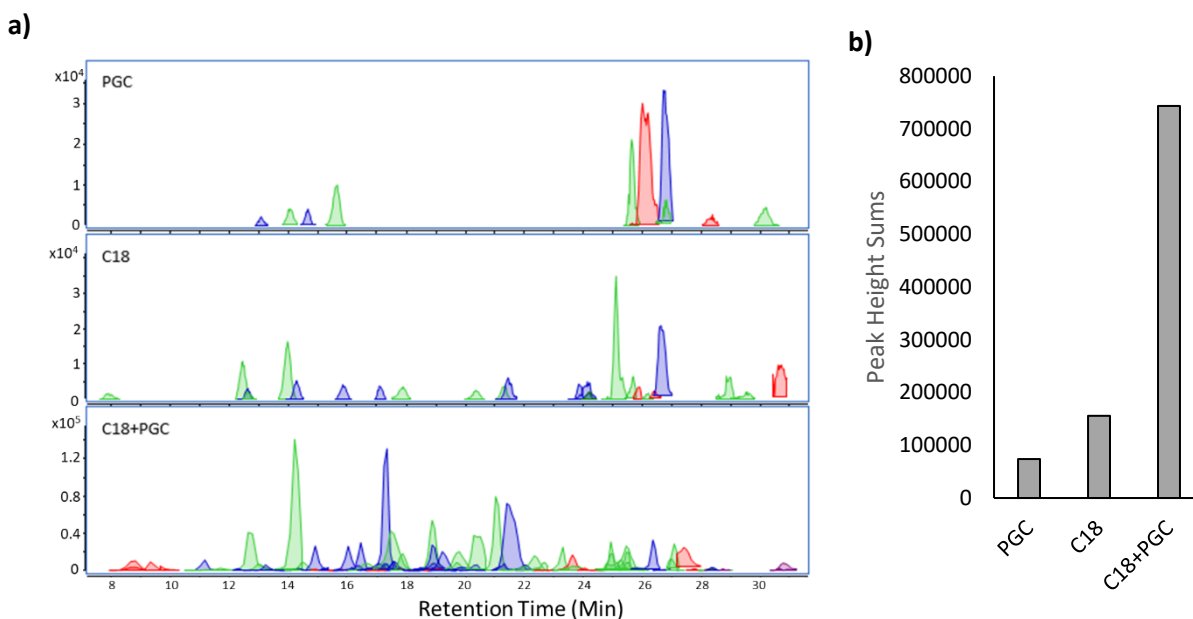
## RESULTS

Analysis of HMOs in amniotic fluid poses various challenges due to the diversity of structures and complexity of the fluid matrix. Additionally, due to their importance in fetal development and proximity to the fetus, samples even in minimal amounts, are difficult to obtain.



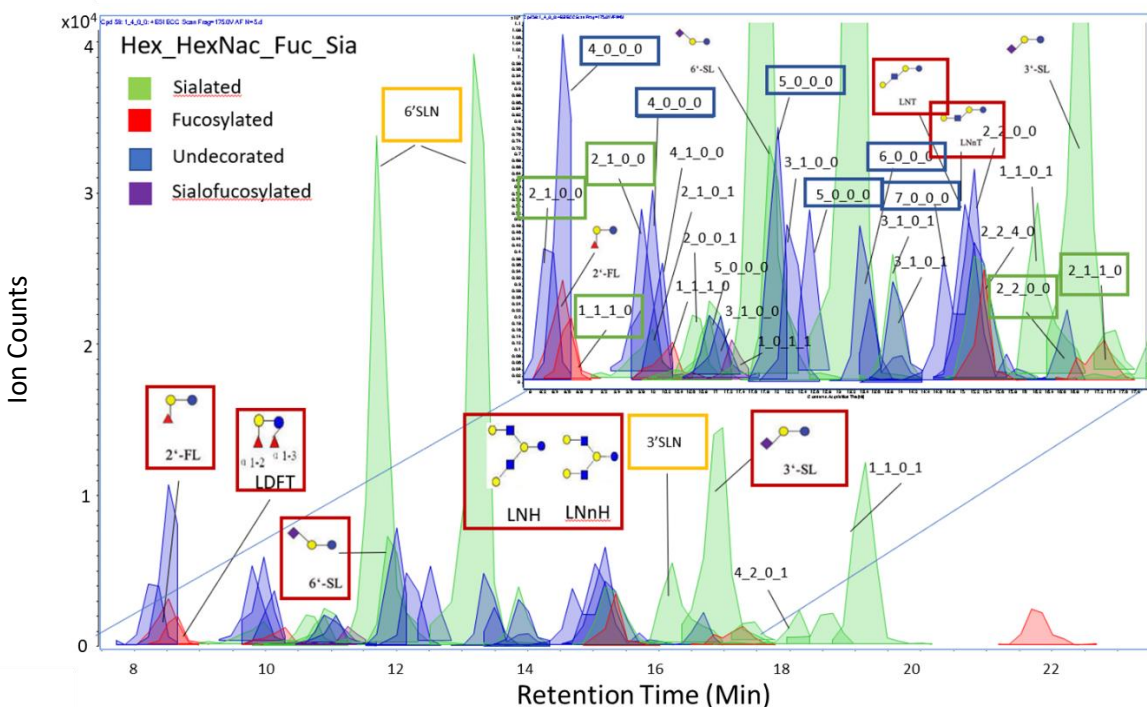
**Figure 3.1** Workflow for extraction, isolation, and profiling of oligosaccharides in amniotic fluid.

A method for isolation and extraction of oligosaccharides was developed specifically for amniotic fluid. A schematic of the extraction procedure is presented in **Figure 3.1**. The extraction procedure is unique from those published analyzing oligosaccharides in breast milk<sup>3, 5, 23-27</sup>, serum<sup>15, 28</sup>, plasma<sup>29</sup>, or urine<sup>16, 30, 31</sup> in that it required several isolation steps to separate the oligosaccharides from the other biological components. A 100  $\mu$ L aliquot of the fluid was first purified through a 10K allowance filter allowing the smaller molecules (<10 kDa), such as the oligosaccharides, to pass through. Larger molecules, such as proteins, were retained and separated from the oligosaccharides. The flow through (containing the HMOs) then went through two solid phase extractions, the first extraction with C18 and then sequentially with PGC. The C18 cartridge removed proteins, peptides or lipids potentially remaining in the sample after the filtration. PGC is commonly used for glycan retention through dispersive interactions and polar retention, allowing most nonpolar species and salts to be removed. Isolation of oligosaccharides from other biological fluids such as breast milk or serum often required a single SPE step; however, because of the complexity of the matrix, we found that performing two clean up steps provided the best glycan coverages (**Figure 3.2**). As shown, we observed up to a seven-fold increase in peak intensity when performing both C18 and PGC cleanups sequentially compared to using just one extraction technique. The enriched HMOs were dried down and concentrated to 4X the original concentration prior to analyses on a nano-HPLC-qTOF-MS.



**Figure 3.2 (a)** Extracted Ion Chromatograms of amniotic fluid samples extracted with PGC (top), C18 (middle), and C18 + PGC (bottom). Red indicates fucosylated oligosaccharides, green indicates sialylated oligosaccharides, blue indicates undecorated oligosaccharides. **(b)** Total peak height of oligosaccharides detected from the corresponding chromatograms.

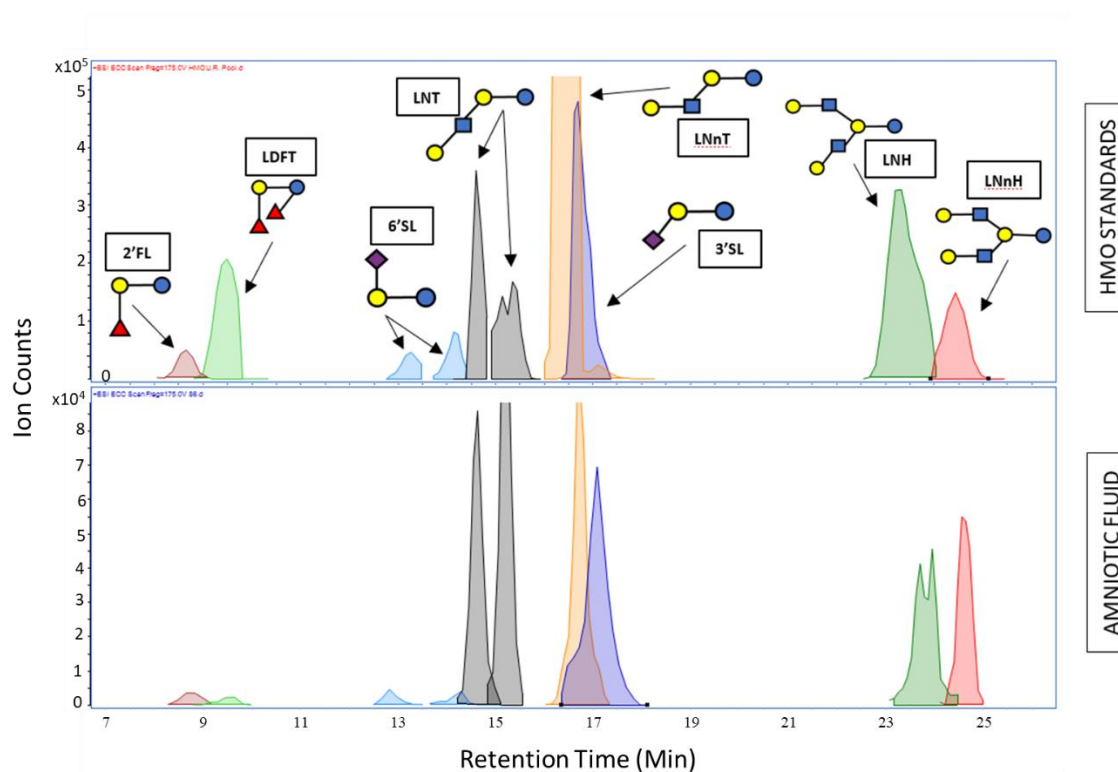
Amniotic fluid from N=4 mothers were pooled and analyzed on a nano-HPLC-Q-TOF-MS. Oligosaccharide peaks were filtered by matching the output data obtained on the LC-MS with an in-house library of exact masses and chemical compositions. Analysis on nano-HPLC-Q-TOF-MS revealed around 64 oligosaccharides present in amniotic fluid. **Figure 3.3** shows a representative chromatogram of the oligosaccharides detected from the pooled amniotic fluid sample.



**Figure 3.3** Extracted ion chromatograms of oligosaccharides in amniotic fluid. Monosaccharide composition of structures are given as Hex\_HexNac\_Fuc\_Neu5Ac and represented as glucose (●), galactose (●), N-acetylglucosamine (■), and fucose (▲). Color of chromatographic peak is characterized by decoration, green-sialylated, red-fucosylated, blue- undecorated, purple-sialofucosylated.

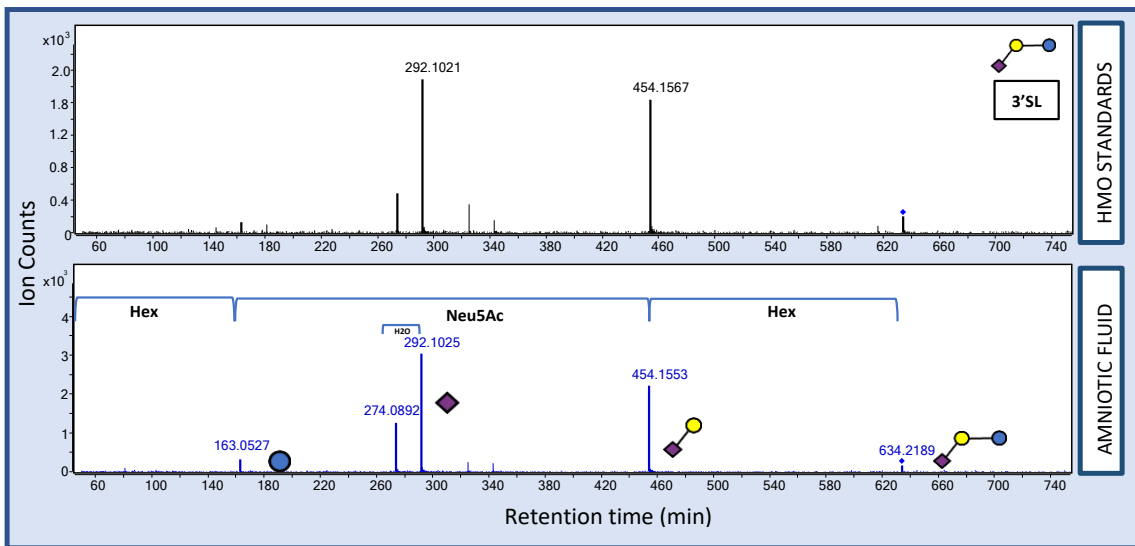
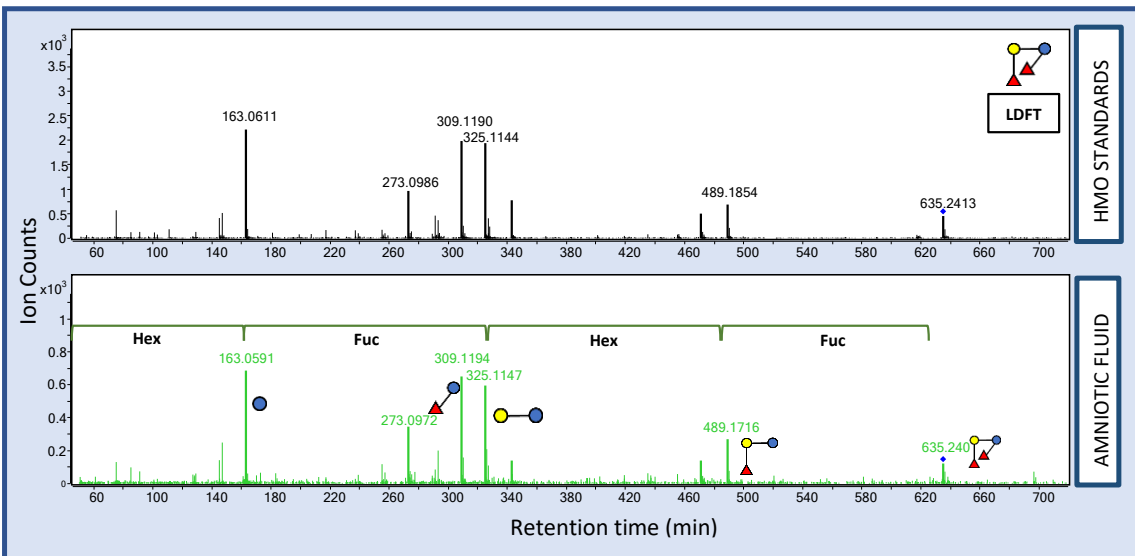
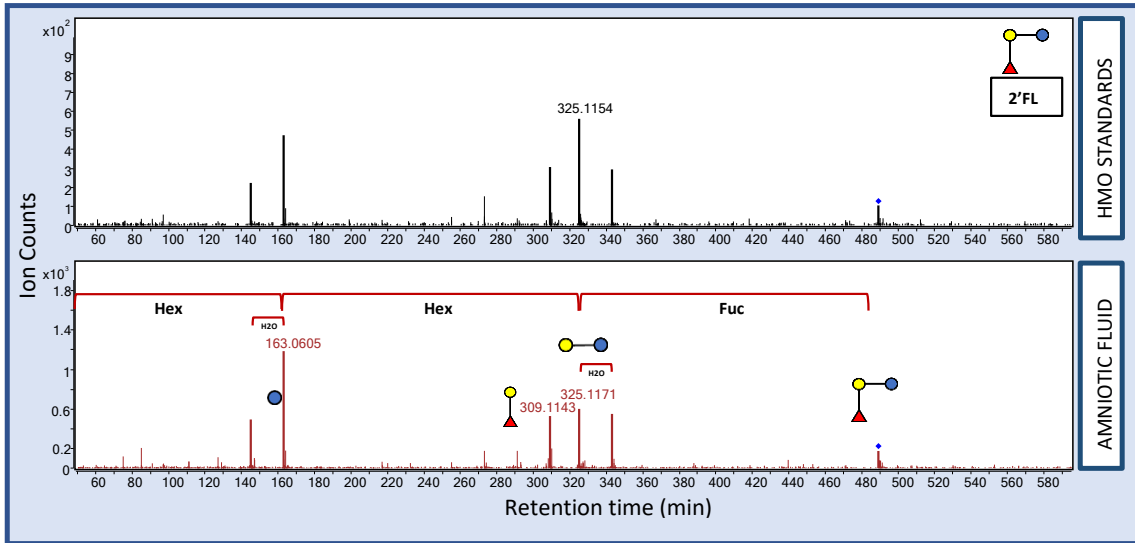
Of the total identified oligosaccharides, eight were common to human breast milk (represented by the red boxed structures in the chromatogram) including 2'-Fucosyllactose (2'-FL), Lactodifucotetraose (LDFT), Lacto-N-tetraose (LNT), Lacto-N-neotetraose (LNnT), 3'-Sialyllactose (3'-SL), 6'-Sialyllactose (6'-SL), Lacto-N-neohexaose (LNnH), Lacto-N-hexaose (LNH). Interestingly, we observed several non-HMO structures that had structures similar to HMOs as they contained a lactose core and were similarly elongated with sialic acid and fucose. The most abundant of these structures were 2\_1\_0\_0 and 2\_2\_0\_0. Surprisingly, 3'-Sialyl-N-acetylglucosamine (3'-SLN) and 6'-Sialyl-N-acetylglucosamine (6'-SLN) (represented by the yellow boxed structures in the chromatogram) were found to be one of the most abundant

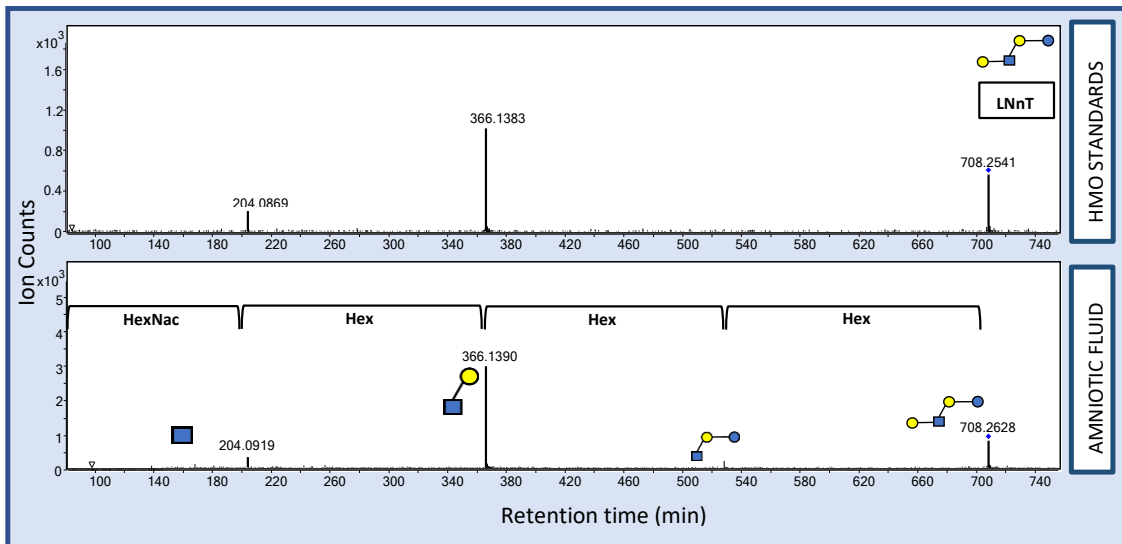
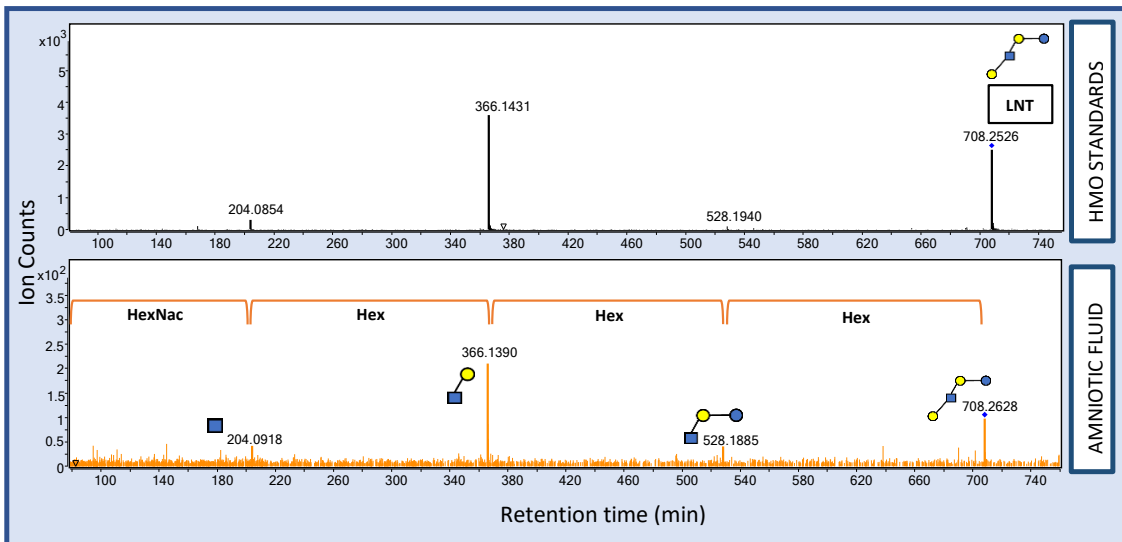
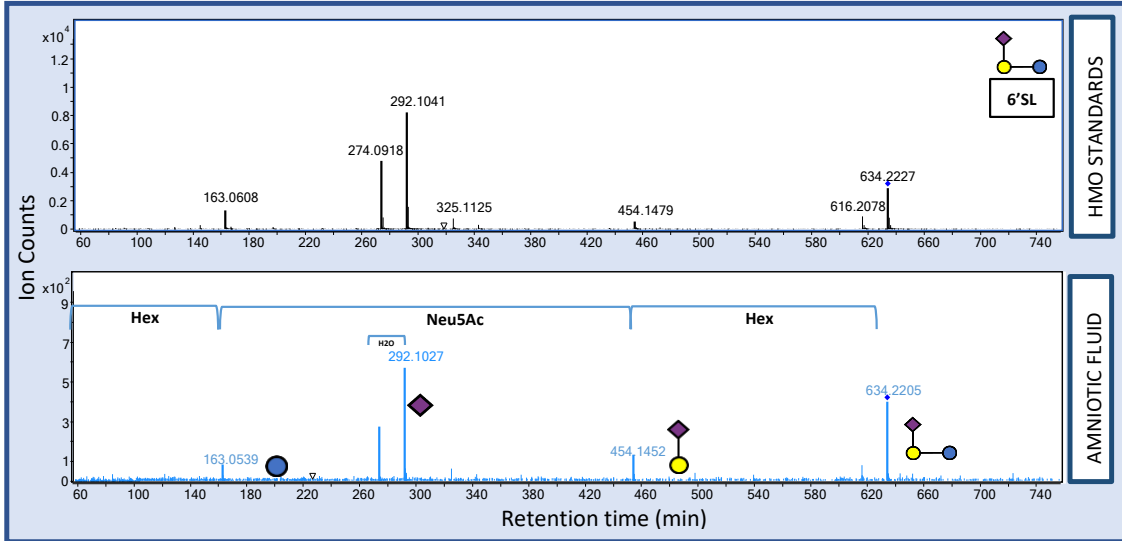
oligosaccharides in the amniotic fluid samples and have also been previously reported in infant urine and serum but are generally not found in maternal milk.<sup>15, 28</sup> Hexose containing structures, represented by the blue boxed structures in the chromatogram were also found in large abundance in a majority of the samples analyzed. We also observed the presence of oligosaccharides that appeared as fragments of larger HMO species (green boxed structures). They did not correspond to HMO structures but were similar in composition while missing one or two terminal sugars. Several more oligosaccharides were identified; however, many were either too low in abundance to elucidate the structure or were only found in a small subset of samples (not shown).



**Figure 3.4** nano-HPLC-Q-TOF-MS extracted ion chromatograms of (top) human milk oligosaccharide standard pool (bottom) human milk oligosaccharides in a representative amniotic fluid sample.

Identified human milk oligosaccharides were validated and measured against purified standards by comparing retention times (**Figure 3.4**) and fragmentation spectra (**Figure 3.5**). Retention time matching was conducted by comparing a pooled sample of purchased human milk oligosaccharides with the oligosaccharides found in amniotic fluid. Standards and samples were not reduced during sample preparation therefore some structures were observed to have two characteristic peaks representing both the  $\alpha$  and  $\beta$  configuration of the reducing end. Due to the nature of low flow systems, any small variations in temperature, solvent composition, or column compactness can cause significant retention time shifts. Thus, an HMO reference pool was run between every 6 samples to monitor and account for any retention time shifts.





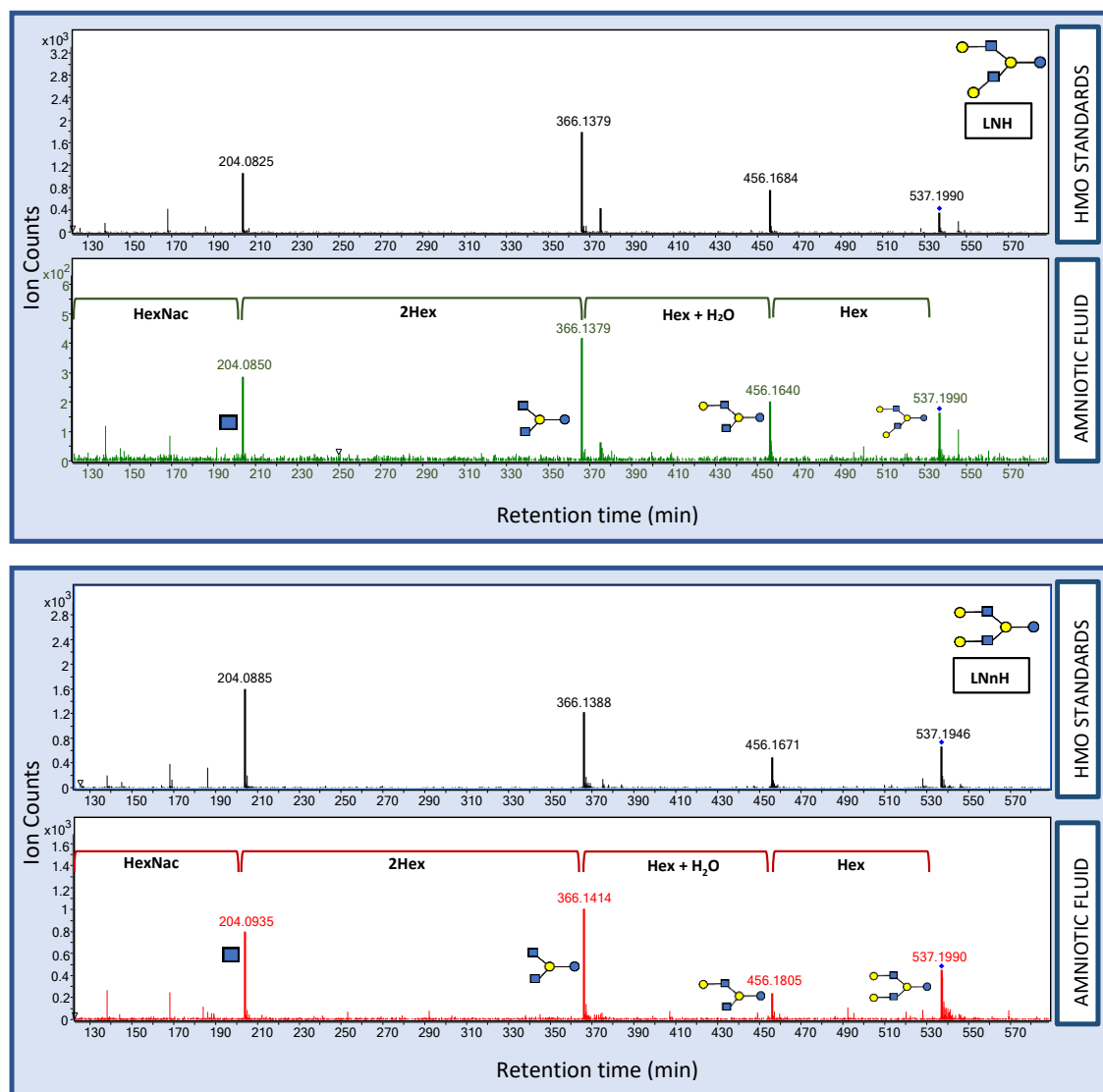


**Figure 3.5** Tandem MS/MS spectra comparing mass spectra of (top) purified HMO standard to (bottom) HMOs in amniotic fluid.

Tandem MS data of the standards validated the structures and compositions of the respective HMOs present in amniotic fluid samples. Due to the limitation of working with low abundance analytes, MS/MS data were not obtainable to validate peaks in every sample. In these instances, validation relied solely on exact mass, isotopic distributions, and retention time. **Table**

**3.1** presents a comprehensive list of observed oligosaccharides. A mass filter of 20 ppm was applied to the library scan. Retention times were averaged across samples but can shift up to 6 minutes between batches. Structures where standards were not available were confirmed by MS/MS fragmentation and labeled as follows: Hex\_HexNAc\_Fuc\_Neu5Ac.

**Table 3.1** comprehensive list of oligosaccharides found in amniotic fluid.

| hex | hexnac | fuc | sia | Neutral     |            |            | Compound | Formula     | MS/MS | RT   | Structure     |
|-----|--------|-----|-----|-------------|------------|------------|----------|-------------|-------|------|---------------|
|     |        |     |     | Mass        | (M+H)      | (M+2H)/2   |          |             |       |      |               |
| 1   | 1      | 0   | 1   | 674.2381774 | 675.24599  | 338.126895 | 1_1_0_1  | C25H42O19N2 | yes   | 13   | 6'SLN         |
| 1   | 1      | 0   | 1   | 674.2381774 | 675.24599  | 338.126895 | 1_1_0_1  | C25H42O19N2 | yes   | 16   |               |
| 1   | 1      | 0   | 1   | 674.2381774 | 675.24599  | 338.126895 | 1_1_0_1  | C25H42O19N2 | yes   | 14   |               |
| 1   | 1      | 0   | 1   | 674.2381774 | 675.24599  | 338.126895 | 1_1_0_1  | C25H42O19N2 | yes   | 20   | 3'SLN         |
| 2   | 0      | 0   | 1   | 634.2320294 | 635.23984  | 318.12382  | 2_0_2_0  | C24H42O19N0 | yes   | 10   | LDFT          |
| 2   | 0      | 0   | 1   | 634.2320294 | 635.23984  | 318.12382  | 2_0_2_0  | C24H42O19N0 | yes   | 11   |               |
| 2   | 0      | 1   | 0   | 634.2320294 | 635.23984  | 318.12382  | 2_0_2_0  | C24H42O19N0 | no    | 28   |               |
| 2   | 0      | 1   | 0   | 488.1741206 | 489.18193  | 245.094865 | 2_0_1_0  | C18H32O15N0 | yes   | 1.2  | 3'FL          |
| 2   | 0      | 1   | 0   | 488.1741206 | 489.18193  | 245.094865 | 2_0_1_0  | C18H32O15N0 | yes   | 8    |               |
| 2   | 0      | 2   | 0   | 488.1741206 | 489.18193  | 245.094865 | 2_0_1_0  | C18H32O15N0 | yes   | 9    | 2'FL          |
| 2   | 0      | 2   | 0   | 545.1955843 | 546.2034   | 273.6056   | 2_1_0_0  | C20H35O16N1 | yes   | 9    |               |
| 2   | 0      | 2   | 0   | 545.1955843 | 546.2034   | 273.6056   | 2_1_0_0  | C20H35O16N1 | yes   | 12   |               |
| 2   | 0      | 2   | 2   | 837.311402  | 838.31922  | 419.66351  | 2_1_2_0  | C32H55O24N1 | yes   | 4    |               |
| 2   | 0      | 2   | 2   | 633.2116283 | 634.21944  | 317.61362  | 2_0_0_1  | C23H39O19N1 | yes   | 13   | 6'SL          |
| 2   | 1      | 0   | 0   | 633.2116283 | 634.21944  | 317.61362  | 2_0_0_1  | C23H39O19N1 | yes   | 17   | 3'SL          |
| 2   | 1      | 0   | 0   | 1216.422863 | 1217.43068 | 609.21924  | 2_0_2_2  | C46H76O35N2 | no    | 18.5 |               |
| 2   | 1      | 2   | 0   | 1216.422863 | 1217.43068 | 609.21924  | 2_0_2_2  | C46H76O35N2 | yes   | 18   |               |
| 2   | 2      | 0   | 1   | 1039.370374 | 1040.3782  | 520.693    | 2_2_0_1  | C39H65O29N3 | yes   | 26   |               |
| 2   | 4      | 0   | 0   | 1154.433702 | 1155.44154 | 578.22467  | 2_4_0_0  | C44H74O31N4 | yes   | 25.5 |               |
| 3   | 0      | 0   | 0   | 504.1690352 | 505.17685  | 253.092325 | 3_0_0_0  | C18H32O16N0 | yes   | 1.5  |               |
| 3   | 0      | 0   | 0   | 504.1690352 | 505.17685  | 253.092325 | 3_0_0_0  | C18H32O16N0 | yes   | 5    |               |
| 3   | 0      | 0   | 0   | 504.1690352 | 505.17685  | 253.092325 | 3_0_0_0  | C18H32O16N0 | yes   | 17   |               |
| 3   | 0      | 0   | 0   | 504.1690352 | 505.17685  | 253.092325 | 3_0_0_0  | C18H32O16N0 | yes   | 10   |               |
| 3   | 0      | 1   | 0   | 650.2269441 | 651.23476  | 326.12128  | 3_0_1_0  | C24H42O20N0 | yes   | 3    |               |
| 3   | 1      | 0   | 0   | 707.2484078 | 708.25623  | 354.632015 | 3_1_0_0  | C26H45O21N1 | yes   | 17   | LNT &<br>LNnT |
| 3   | 1      | 0   | 1   | 853.3063167 | 854.31414  | 427.66097  | 3_1_1_0  | C32H55O25N1 | yes   | 11   | LNFP II       |

|   |   |   |   |             |            |            |         |              |     |    | LNFP III + |
|---|---|---|---|-------------|------------|------------|---------|--------------|-----|----|------------|
| 3 | 1 | 1 | 0 | 853.3063167 | 854.31414  | 427.66097  | 3_1_1_0 | C32H55O25N1  | yes | 15 | I          |
| 3 | 1 | 1 | 0 | 910.3277804 | 911.33561  | 456.171705 | 3_2_0_0 | C34H58O26N2  | yes | 11 |            |
| 3 | 2 | 0 | 0 | 910.3277804 | 911.33561  | 456.171705 | 3_2_0_0 | C34H58O26N2  | yes | 17 |            |
| 3 | 2 | 0 | 0 | 1056.385689 | 1057.39352 | 529.20066  | 3_2_1_0 | C40H68O30N2  | yes | 17 |            |
| 3 | 2 | 1 | 0 | 998.3438244 | 999.35165  | 500.179725 | 3_1_0_1 | C37H62O29N2  | yes | 26 |            |
| 3 | 2 | 2 | 1 | 1493.539015 | 1494.54685 | 747.777325 | 3_2_2_1 | C57H95O42N3  | yes | 24 |            |
| 4 | 0 | 0 | 0 | 1161.417049 | 1162.42488 | 581.71634  | 4_1_2_0 | C44H75O34N1  | yes | 26 |            |
| 4 | 0 | 0 | 0 | 1363.476021 | 1364.48386 | 682.74583  | 4_2_0_1 | C51H85O39N3  | yes | 25 |            |
| 4 | 1 | 0 | 0 | 869.3012313 | 870.30906  | 435.65843  | 4_1_0_0 | C32H55O26N1  | yes | 23 | LNH        |
| 4 | 1 | 0 | 0 | 869.3012313 | 870.30906  | 435.65843  | 4_1_0_0 | C32H55O26N1  | yes | 24 | LNnH       |
| 4 | 1 | 0 | 0 | 869.3012313 | 870.30906  | 435.65843  | 4_1_0_0 | C32H55O26N1  | yes | 18 |            |
| 4 | 1 | 2 | 0 | 1363.476021 | 1364.48386 | 682.74583  | 4_2_0_1 | C51H85O39N3  | yes | 18 |            |
| 4 | 2 | 0 | 0 | 1363.476021 | 1364.48386 | 682.74583  | 4_2_0_1 | C51H85O39N3  | yes | 25 |            |
| 4 | 2 | 0 | 0 | 1072.380604 | 1073.38844 | 537.19812  | 4_2_0_0 | C40H68O31N2  | yes | 14 |            |
| 4 | 2 | 0 | 0 | 1072.380604 | 1073.38844 | 537.19812  | 4_2_0_0 | C40H68O31N2  | yes | 17 |            |
| 4 | 2 | 0 | 1 | 1072.380604 | 1073.38844 | 537.19812  | 4_2_0_0 | C40H68O31N2  | yes | 22 |            |
| 4 | 2 | 0 | 1 | 1363.476021 | 1364.48386 | 682.74583  | 4_2_0_1 | C51H85O39N3  | yes | 18 |            |
| 4 | 2 | 0 | 1 | 1363.476021 | 1364.48386 | 682.74583  | 4_2_0_1 | C51H85O39N3  | yes | 25 |            |
| 4 | 2 | 0 | 1 | 1510.554331 | 1511.56217 | 756.284985 | 4_2_3_0 | C58H98O43N2  | yes | 18 |            |
| 4 | 2 | 0 | 1 | 702.24296   | 667.22968  | 334.11874  | 4_0_0_0 | C24H42O21N0  | yes | 10 |            |
| 4 | 2 | 3 | 0 | 702.24296   | 667.22968  | 334.11874  | 4_0_0_0 | C24H42O21N0  | yes | 25 |            |
| 5 | 0 | 0 | 0 | 1437.5128   | 1438.52065 | 719.764225 | 5_3_0_0 | C54H91O41N3  | yes | 22 |            |
| 5 | 2 | 0 | 2 | 1437.5128   | 1438.52065 | 719.764225 | 5_3_0_0 | C54H91O41N3  | yes | 18 |            |
| 5 | 2 | 0 | 2 | 1437.5128   | 1438.52065 | 719.764225 | 5_3_0_0 | C54H91O41N3  | yes | 27 |            |
| 5 | 2 | 2 | 0 | 1437.5128   | 1438.52065 | 719.764225 | 5_3_0_0 | C54H91O41N3  | yes | 11 |            |
| 5 | 3 | 0 | 0 | 1437.5128   | 1438.52065 | 719.764225 | 5_3_0_0 | C54H91O41N3  | yes | 17 |            |
| 5 | 3 | 0 | 0 | 828.2746822 | 829.28251  | 415.145155 | 5_0_0_0 | C30H52O26N0  | yes | 28 |            |
| 5 | 3 | 0 | 0 | 1526.549245 | 1527.55709 | 764.282445 | 5_2_2_0 | C58H98O44N2  | yes | 21 |            |
| 5 | 3 | 0 | 0 | 1728.608217 | 1729.61607 | 865.311935 | 5_3_0_1 | C65H108O49N4 | yes | 22 |            |
| 5 | 3 | 0 | 0 | 1816.624261 | 1817.63211 | 909.319955 | 5_2_0_2 | C68H112O52N4 | yes | 25 |            |

|   |   |   |   |             |            |             |         |              |     |    |
|---|---|---|---|-------------|------------|-------------|---------|--------------|-----|----|
| 5 | 3 | 0 | 1 | 1816.624261 | 1817.63211 | 909.319955  | 5_2_0_2 | C68H112O52N4 | yes | 29 |
| 5 | 4 | 0 | 1 | 1931.687589 | 1932.69545 | 966.851625  | 5_4_0_1 | C73H121O54N5 | yes | 23 |
| 6 | 0 | 0 | 0 | 1599.565624 | 1600.57348 | 800.79064   | 6_3_0_0 | C60H101O46N3 | no  | 18 |
| 6 | 1 | 2 | 0 | 990.3275057 | 991.33534  | 496.17157   | 6_0_0_0 | C36H62O31N0  | yes | 14 |
| 6 | 3 | 0 | 0 | 1485.522696 | 1486.53054 | 743.76917   | 6_1_2_0 | C56H95O44N1  | yes | 21 |
| 7 | 0 | 0 | 0 | 1152.380329 | 1153.38817 | 577.197985  | 7_0_0_0 | C42H72O36N0  | yes | 6  |
| 7 | 0 | 0 | 0 | 1152.380329 | 1153.38817 | 577.197985  | 7_0_0_0 | C42H72O36N0  | yes | 20 |
| 7 | 2 | 1 | 2 | 2286.787817 | 2287.79568 | 1144.40174  | 7_2_1_2 | C86H142O66N4 | yes | 23 |
| 8 | 2 | 1 | 2 | 2448.84064  | 2449.84851 | 1225.428155 | 8_2_1_2 | C92H152O71N4 | yes | 24 |

Analysis of all 514 samples remained the goal of this project, however a small set was performed in a pilot study to validate the method and evaluate feasibility of performing a larger scale analysis. A small set of N=51 (out of a total of 514) were analyzed for this validation study. Mothers selected for the pilot study varied in maternal characteristics (ethnicity/race, age), sampling characteristic (gestational age), and birth outcomes (spontaneous preterm birth (SPTB), indicated preterm birth (IPTB) and normal birth).

In order to evaluate the contribution of performing a larger scale analysis, we assessed whether any associations could be made with selected cohort characteristics and oligosaccharide profiles of the amniotic fluid samples that would warrant further investigation. Oligosaccharides were rapidly identified by aligning retention times, isotopic distributions, and exact masses with previously validated structures from **Table 3.1**. As a first assessment we compared the concentration of HMOs present in the amniotic fluid as a function of gestational age (**Figure 3.6**).

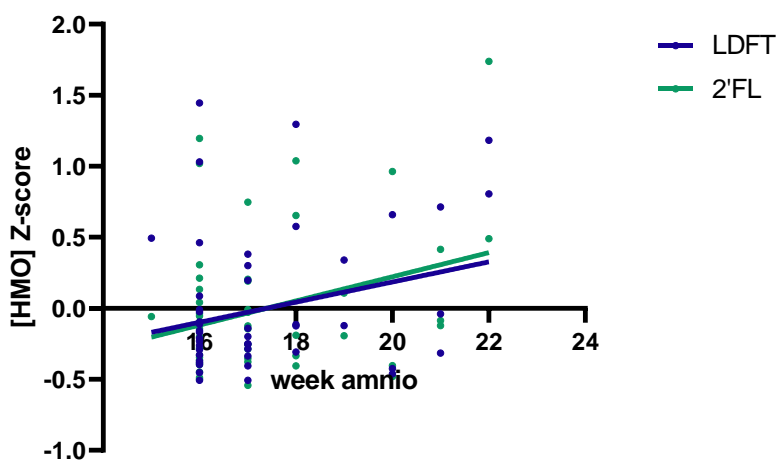


**Figure 3.6.** LDFT and 2'FL trends throughout gestation. HMOs were normalized via Z-scores such that the mean of HMO concentrations is zero. For LDFT,  $R = 0.26$ ,  $p = 0.06$ . For 2'FL,  $R=0.32$ ,  $p=0.02$ .

Preliminary findings showed that from the eight quantifiable HMOs, the most abundant, 2'FL and LDFT, significantly correlated with increasing gestational age ( $r= 0.32$  and  $0.26$ ,  $p=0.02$  and  $0.06$ , respectively, inclusive of linear analysis [2'FL,  $p=0.04$ ]) (**Figure 3.6**). Statistical significance was not achieved for the remaining HMOs (LNH, LNT, LNnT, 6'SL, 3'SL); however, these structures were present in much lower abundance making the search for systematic variations more difficult. Similarly, comparing other cohort characteristics such as race, maternal age, reason for 2nd trimester amniocentesis, or subsequent occurrence of PTB showed no associations with HMO abundance (not shown).

Inspired by the preliminary data showing compositional changes in oligosaccharides across gestation, we applied our methods to the larger cohort of  $N=516$  in efforts to further assess and identify potential trends and correlations that could have been lost due to the small sample size. **Table 3.2** summarizes important characteristics of the cohort. The average maternal age was 34.3 which is significantly higher than the nation average of 25.6. Maternal background, such as previous pregnancy (nulliparous) and history of premature deliveries, was also included. Amniocentesis was performed in the second trimester from 14 to 29 weeks and averaging 17.5 weeks. Amniocentesis can cause complications in the pregnancy and is only performed if certain indications are observed. These indications are detailed in **Table 3.2**.

**Table 3.2** Summary of demographics, gestational age and observed indications for study cohort (N=516).

|  | <b>Cohort</b>                  | <b>U.S. National Averages</b> |
|--|--------------------------------|-------------------------------|
| <b>Maternal Age (years)</b>                | <b>34.3 +/- 5.4 (17 to 44)</b> | <b>25.6</b>                   |
| <b>Ethnicity</b>                           |                                |                               |
| <b>Asian</b>                               | <b>227 (31.1%)</b>             |                               |
| <b>Hispanic</b>                            | <b>139 (19.1%)</b>             |                               |
| <b>African American</b>                    | <b>144 (19.8%)</b>             |                               |
| <b>White</b>                               | <b>219 (30.0%)</b>             |                               |
| <b>Nulliparous</b>                         | <b>200 (27.4%)</b>             | <b>~40%</b>                   |
| <b>History of preterm birth</b>            | <b>78 (10.7%)</b>              |                               |
| <b>Preterm Delivery</b>                    | <b>92 (12.6%)</b>              | <b>9.6%</b>                   |
| <b>Gestational Age at Sampling (weeks)</b> | <b>17.5 +/- 1.9 (14 to 29)</b> |                               |
| <b>Amniocentesis Indication</b>            |                                |                               |
| <b>Advanced Maternal Age (AMA)</b>         | <b>389</b>                     |                               |
| <b>+Mat. Serum Screen (+MSS)</b>           | <b>218</b>                     |                               |
| <b>Abnormal Ultrasound</b>                 | <b>40</b>                      |                               |
| <b>Multiples</b>                           | <b>82</b>                      |                               |

Absolute concentrations of HMOs in human milk have been measured previously, however these structures have not yet been quantified in amniotic fluid using LC-MS. The concentration of oligosaccharides in amniotic fluid can provide insight into the origin of these structures in the uterus. Thus, absolute quantitation was performed using external calibrations to quantify the most abundant HMOs observed. Calibration curves were run alongside every sample set. Because of the large matrix effects and retention time shifts observed in the pilot study, a surrogate plant-based internal standard mix, consisting of xylo-oligosaccharides (DP 4-7) was used to monitor retention times and normalize peak areas. **Figure 3.7** plots the instrument

responses versus concentration of six standards used to determine the concentrations present in amniotic fluid. LNT and LNnT were not able to be chromatographically separated in all samples, thus LNnT was used to approximate the concentrations of LNT and LNnT.

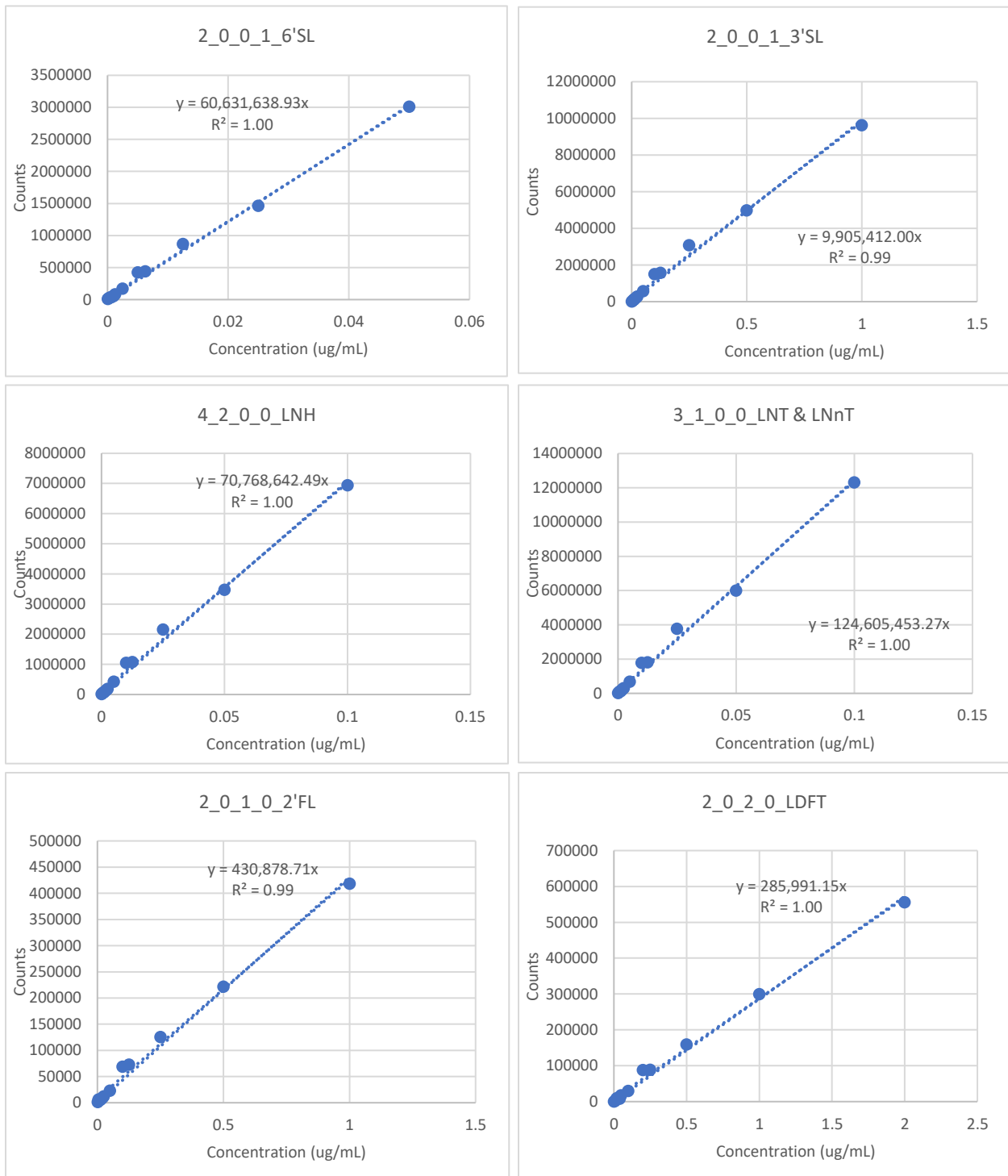


**Figure 3.7** Example Calibration curves for the six external standards used to quantify HMOs in amniotic fluid.

The linear range of the oligosaccharide standards spanned 3-4 orders of magnitude (approx.  $2 \times 10^2$ - $3 \times 10^6$  units). The LOD and LOQs were determined to be in the pico-femto molar ranges allowing for quantitation of low abundant compounds. Regression coefficients were excellent for all compounds ( $R^2 > 0.95$ ). **Table 3.3** presents the average concentration of each quantitated HMO observed in amniotic fluid. Total HMO concentrations observed ranged from 0.014-2.87 nmol/mL with an average concentration of 0.33 nmol/mL

**Table 3.3** Concentration of HMOs in Amniotic fluid. Limits of Quantitation (LOQ) and Limits of Detection (LOD) were defined as 6X and 3X the signal-to-noise ratio of the blanks respectively. Concentration given as ng/mL  $\pm$  SD.

| <i>HMO</i>      | Concentration (ng/mL) | LOD (counts) | LOQ (pg/mL) |
|-----------------|-----------------------|--------------|-------------|
| <i>2'FL</i>     | 88.52 $\pm$ 93.79     | 2472         | 11.474      |
| <i>LDFT</i>     | 88.95 $\pm$ 88.69     | 2934         | 20.518      |
| <i>6'SL</i>     | 0.39 $\pm$ .389       | 9630         | 0.3176      |
| <i>3'SL</i>     | 5.49 $\pm$ 6.03       | 7791         | 1.57        |
| <i>LNH</i>      | 0.65 $\pm$ 0.77       | 28248        | 0.15        |
| <i>LNT/LNnT</i> | 0.68 $\pm$ 0.81       | 9405         | 0.80        |

Correlations observed in the pilot study were also observed in the larger cohort. Namely, the most abundant HMOs (*2'FL* and *LDFT*) increased with increasing gestational age ( $r= 0.23$  and  $0.14$ ),  $p=9.9 \times 10^{-8}$  and  $0.002$ , respectively (**Figure 3.8**) Interestingly, analysis of the larger cohort revealed that *3'SL* decreased in concentration throughout gestation ( $r=-0.14$ ,  $p=0.002$ ),

which was not observed in the pilot study. No significant correlation was found with LNH or LNT/LnNT.

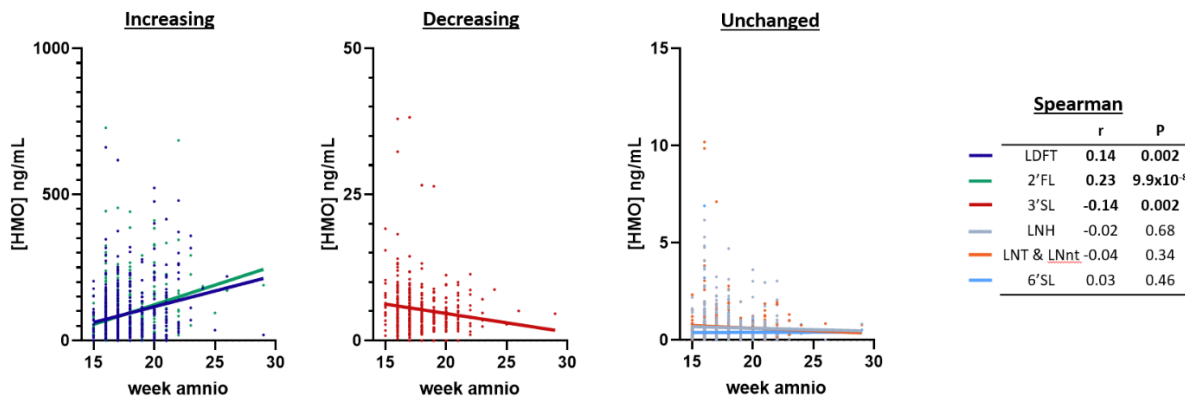


**Figure 3.8** Structure specific HMO correlations to gestational age. For LDFT,  $R = 0.14$ ,  $p = 0.002$ . For 2'FL,  $R=0.23$ ,  $p=9.9 \times 10^{-8}$ . For 3'SL,  $R=-0.014$ ,  $p=0.002$ . For LNH  $R=-0.02$ ,  $p=0.68$ . For LNT & LNnt,  $R=-0.04$ ,  $p=0.34$ . For 6'SL,  $R=0.03$ ,  $p=0.46$ .

Additionally, we investigated how maternal characteristics affected the oligosaccharide abundances and profile (**Figure 3.9**). Analysis of HMOs with maternal age, parity, race, history of premature delivery (Hx PTD), and reason for performing the amniocentesis revealed little to no correlation with HMO abundance. However, correlational analysis revealed HMO levels to be intercorrelated within subjects based on their glycan type. For example, samples that tended to have higher levels of 6'SL also tended to have higher levels of 3'SL (both sialylated species) ( $r=0.68$ ). Similar trends are observed with fucosylated species such as 2'FL and LDFT ( $r=0.74$ ) and undecorated structures LNH and LNT ( $r=0.48$ ).

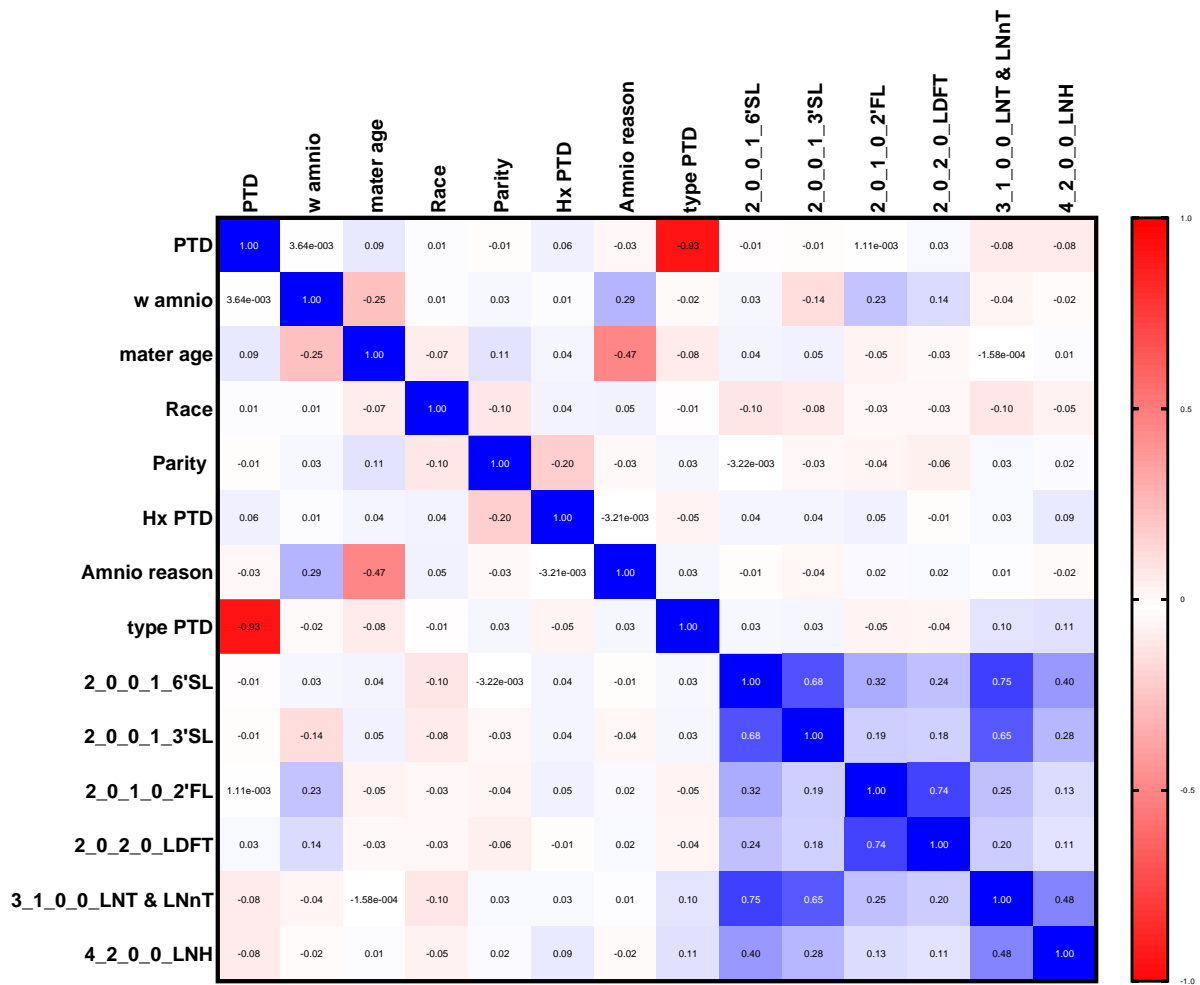


Figure 3.9 Correlation analysis between subjects and study characteristics.

## DISCUSSION

Oligosaccharides in mammalian milk are a highly evolutionarily preserved nutrient but are not digestible by the offspring that consume them. Rather, they are known to provide a growth advantage to beneficial microbes, act as “decoys” for pathogenic microbes, and promote a healthy gut epithelial barrier. HMOs have been presumed to be found and function solely in the postnatal period of infant development.<sup>5-14, 32, 33</sup> We demonstrate here that oligosaccharides, and HMOs in particular, are present in human amniotic fluid as early as the 2nd trimester.

The source or mechanism of transportation of these HMOs in the amniotic fluid has yet to be elucidated. The HMOs observed in amniotic fluid, although alike in structure, differ greatly in abundance compared to those found in maternal milk. Concentrations of HMOs in amniotic fluid were found to range from 0.014-2.87 nmol/mL, which is several orders of magnitude less than those found in maternal milk (approx. 20  $\mu$ mol/mL).<sup>34</sup> More so, only a small subset of the oligosaccharides commonly observed in milk was identified in the amniotic fluid, suggesting a distinct and important functional role of these select structures. Previous studies conducted in our lab have shown evidence of HMOs in maternal circulation during pregnancy.<sup>28</sup> Both the structures and concentrations of these HMOs in the blood resemble those found in amniotic fluid. This points towards the hypothesis that HMOs could be transported through permeability of the epithelial membrane.

The role that these HMOs play in fetal development is not yet clear. In this study, we report the first observation and characterization of other non-HMO oligosaccharides found in amniotic fluid, which could potentially provide further insight into the biological role of these structures in the uterus. We observed approximately 20 oligosaccharides found across most samples (>80%) that have structures similar to those found in maternal milk, in that they contain

a lactose core with terminations of fucose and sialic acid but differ by monosaccharide composition and/or linkage. Of these structures, a handful were found to resemble partial HMOs in that they contain the same monosaccharide composition as those found in maternal milk but lack one or two terminal sugars. Glycosylation involves several stepwise processes leading to groups of structures such as HMOs. The absence or down regulation of any transferase associated with the synthesis of any structure could affect the final product. The presence of partial structures could be due to an incomplete process of the formation of these oligosaccharides. For example, two “incomplete” structures were found in relatively large abundance in the amniotic fluid: 2hex\_2hexNac\_0Fuc\_0Sia (2\_2\_0\_0) and 2hex\_1hexNac\_0Fuc\_0Sia (2\_1\_0\_0). The absence or down regulation of a galactotransferase could potentially hinder the addition of terminal galactoses and therefore partially inhibit the formation of LNH (4\_2\_0\_0) and LNT (3\_1\_0\_0). Alternatively, if in fact amniotic fluid is not sterile<sup>35</sup>, these structures could be digestion products that are formed by an exogalactosidase which cleaved both terminal galactoses of LNH (4\_2\_0\_0) to form 2\_2\_0\_0 and the single terminal galactose in LNT (3\_1\_0\_0) to form (2\_1\_0\_0). Previously, our lab has analyzed fecal samples from exclusively breastfed infants and found that digested oligosaccharides in feces correspond to the action of glycosidases on HMOs.<sup>36</sup> Among other products, 2\_2\_0\_0 and 2\_1\_0\_0 was found in relatively large abundances in most fecal samples.

Additionally, 3'SLN and 6'SLN were the most abundant sialylated species found in amniotic fluid. Towards the end of the first trimester of gestation, as the infant begins to develop kidneys, amniotic fluid composition starts to resemble that of infant urine.<sup>20</sup> Our lab as well as others, have studied urine composition of exclusively breastfed infants.<sup>30</sup> In these studies, several sialylated HMOs including 3'SLN and 6'SLN were found in significant abundance in infant

urine that are not typically found in maternal milk suggesting synthesis in the proximal intestine.<sup>30</sup>

## **CONCLUSION**

We demonstrate for the first time a robust comprehensive method for quantitation of oligosaccharides in amniotic fluid using nano-LC chip-TOF MS. This study covers methodologies from sample preparation to data analysis. Analysis of 516 amniotic fluid samples revealed trends throughout gestation and opened the door to the possible roles that HMOs play in developmental nutrition; however, many unknowns remain. Further studies that elucidate the function of these HMOs in fetal development and explore the mechanism behind the formation of these structures are required.

## **ACKNOWLEDGEMENTS**

We thank all mothers and participants involved. We thank the doctors, clinical staff, researchers, and laboratory technicians who helped collect the samples. We thank the undergraduate students in our lab Kiley Cleland and Jessie Benedict for helping with the sample preparation and analysis. And our funding agencies for providing support for this project.

### **Author Contributions**

M.S. and K.M.A. oversaw sample collection and provided samples. A.V. and D.T. prepared samples. A.V., D.T. analyzed HMO data. A.V. and M.S. performed statistical analyses on HMO

data and metadata. C.B.L. and K.M.A. designed the study and oversaw the analyses. A.V. and C.B.L. interpreted results and wrote the manuscript.

## **Funding**

National Institute of Health (NIH)

Eunice Kennedy Shriver National Institute of Child Health & Human Development (NICHD)

Research Project (R01)

1R01HD091731

## REFERENCES

1. Prentice, P.; Ong, K. K.; Schoemaker, M. H.; van Tol, E. A.; Vervoort, J.; Hughes, I. A.; Acerini, C. L.; Dunger, D. B., Breast milk nutrient content and infancy growth. *Acta Paediatr* **2016**, *105* (6), 641-7.
2. Kunz, C.; Rudloff, S., Biological functions of oligosaccharides in human milk. *Acta Paediatr* **1993**, *82*, 903-912.
3. Wu, S.; Grimm, R.; German, J. B.; Lebrilla, C. B., Annotation and Structural Analysis of Sialylated Human Milk Oligosaccharides. *Journal of Proteome Research* **2011**, *10*, 856-868.
4. Wu, S.; Tao, N.; German, J. B.; Grimm, R.; Lebrilla, C. B., Development of an Annotated Library of Neutral Human Milk Oligosaccharides. *Journal of Proteome Research* **2010**, *9*, 4138-4151.
5. Cabrera-Rubio, R.; Kunz, C.; Rudloff, S.; García-Mantrana, I.; Crehuá-Gaudiza, E.; Martínez-Costa, C.; Collado, M. C., Association of Maternal Secretor Status and Human Milk Oligosaccharides With Milk Microbiota: An Observational Pilot Study. *J Pediatr Gastroenterol Nutr* **2019**, *68* (2), 256-263.
6. Casaburi, G.; Duar, R. M.; Vance, D. P.; Mitchell, R.; Contreras, L.; Frese, S. A.; Smilowitz, J. T.; Underwood, M. A., Early-life gut microbiome modulation reduces the abundance of antibiotic-resistant bacteria. *Antimicrobial Resistance & Infection Control* **2019**, *8* (1), 131.
7. Charbonneau, M. R.; O'Donnell, D.; Blanton, L. V.; Totten, S. M.; Davis, J. C.; Barratt, M. J.; Cheng, J.; Guruge, J.; Talcott, M.; Bain, J. R.; Muehlbauer, M. J.; Ilkayeva, O.; Wu, C.; Struckmeyer, T.; Barile, D.; Mangani, C.; Jorgensen, J.; Fan, Y. M.; Maleta, K.; Dewey, K. G.; Ashorn, P.; Newgard, C. B.; Lebrilla, C.; Mills, D. A.; Gordon, J. I., Sialylated Milk Oligosaccharides Promote Microbiota-Dependent Growth in Models of Infant Undernutrition. *Cell* **2016**, *164* (5), 859-71.
8. Garrido, D.; Dallas, D. C.; Mills, D. A., Consumption of human milk glycoconjugates by infant-associated bifidobacteria: mechanisms and implications. *Microbiology* **2013**, *159*, 649-664.
9. Lewis, Z. T.; Totten, S. M.; Smilowitz, J. T.; Popovic, M.; Parker, E.; Lemay, D. G.; Van Tassell, M. L.; Miller, M. J.; Jin, Y.-S.; German, J. B.; Lebrilla, C. B.; Mills, D. A., Maternal fucosyltransferase 2 status affects the gut bifidobacterial communities of breastfed infants. *Microbiome* **2015**, *3* (1), 13.
10. Sela, D. A.; Li, Y.; Lerno, L.; Wu, S.; Marcobal, A. M.; German, J. B.; Chen, X.; Lebrilla, C. B.; Mills, D. A., An Infant-associated Bacterial Commensal Utilizes Breast Milk Sialyloligosaccharides\*. *Journal of Biological Chemistry* **2011**, *286* (14), 11909-11918.
11. Zivkovic, A. M.; German, J. B.; Lebrilla, C. B.; Mills, D. A., Human milk glycobiome and its impact on the infant gastrointestinal microbiota. *Proceedings of the National Academy of Sciences* **2011**, *108* (Supplement 1), 4653.
12. Barboza, M.; Pinzon, J.; Wickramasinghe, S.; Froehlich, J. W.; Moeller, I.; Smilowitz, J. T.; Ruhaak, L. R.; Huang, J.; Lönnerdal, B.; German, J. B.; Medrano, J. F.; Weimer, B. C.; Lebrilla, C. B., Glycosylation of human milk lactoferrin exhibits dynamic changes during early lactation enhancing its role in pathogenic bacteria-host interactions. *Mol Cell Proteomics* **2012**, *11* (6), M111.015248.

13. Coppa, G. V.; Zampini, L.; Galeazzi, T.; Facinelli, B.; Ferrante, L.; Capretti, R.; Orazio, G., Human Milk Oligosaccharides Inhibit the Adhesion to Caco-2 Cells of Diarrheal Pathogens: *Escherichia coli*, *Vibrio cholerae*, and *Salmonella typhi*.
14. Wang, B.; Miller, J. B.; McNeil, Y.; McVeagh, P., Sialic acid concentration of brain gangliosides: variation among eight mammalian species. *Comp Biochem Physiol A Mol Integr Physiol* **1998**, *119* (1), 435-9.
15. Hirschmugl, B.; Brandl, W.; Csapo, B.; van Poppel, M.; Köfeler, H.; Desoye, G.; Wadsack, C.; Jantscher-Krenn, E., Evidence of Human Milk Oligosaccharides in Cord Blood and Maternal-to-Fetal Transport across the Placenta. *Nutrients* **2019**, *11* (11).
16. Hallgren, P.; Lindberg, B. S.; Lundblad, A., Quantitation of some urinary oligosaccharides during pregnancy and lactation. *Journal of Biological Chemistry* **1977**, *252* (3), 1034-1040.
17. Wise, A.; Robertson, B.; Choudhury, B.; Rautava, S.; Isolauri, E.; Salminen, S.; Bode, L., Infants Are Exposed to Human Milk Oligosaccharides Already in utero. *Frontiers in Pediatrics* **2018**, *6*, 270.
18. Gilbert, W. M.; Newman, P. S.; Eby-Wilkens, E.; Brace, R. A., Technetium Tc 99m rapidly crosses the ovine placenta and intramembranous pathway. *American Journal of Obstetrics and Gynecology* **1996**, *175* (6), 1557-1562.
19. BRACE, R. A., Physiology of Amniotic Fluid Volume Regulation. *Clinical Obstetrics and Gynecology* **1997**, *40* (2), 280-289.
20. Underwood, M. A.; Gilbert, W. M.; Sherman, M. P., Amniotic Fluid: Not Just Fetal Urine Anymore. *Journal of Perinatology* **2005**, *25* (5), 341-348.
21. Wooten, L.; Shulze, R. A.; Lancey, R. W.; Lietzow, M.; Linder, M. C., Ceruloplasmin is found in milk and amniotic fluid and may have a nutritional role. *The Journal of Nutritional Biochemistry* **1996**, *7* (11), 632-639.
22. Mulvihill, S. J.; Stone, M. M.; Debas, H. T.; Fonkalsrud, E. W., The role of amniotic fluid in fetal nutrition. *Journal of Pediatric Surgery* **1985**, *20* (6), 668-672.
23. Xu, G.; Davis, J. C. C.; Goonatileke, E.; Smilowitz, J. T.; German, J. B.; Lebrilla, C. B., Absolute Quantitation of Human Milk Oligosaccharides Reveals Phenotypic Variations during Lactation. *The Journal of Nutrition* **2017**, *147* (1), 117-124.
24. Vinjamuri, A.; Davis, J. C. C.; Totten, S. M.; Wu, L. D.; Klein, L. D.; Martin, M.; Quinn, E. A.; Scelza, B.; Breakey, A.; Gurven, M.; Jasienska, G.; Kaplan, H.; Vallengia, C.; Hinde, K.; Smilowitz, J. T.; Bernstein, R. M.; Zivkovic, A. M.; Barratt, M. J.; Gordon, J. I.; Underwood, M. A.; Mills, D. A.; German, J. B.; Lebrilla, C. B., Human Milk Oligosaccharide Compositions Illustrate Global Variations in Early Nutrition. *J Nutr* **2022**.
25. Totten, S. M.; Zivkovic, A. M.; Wu, S.; Ngyuen, U.; Freeman, S. L.; Ruhaak, R. L.; Darboe, M. K.; German, J. B.; Prentice, A. M.; Lebrilla, C. B., Comprehensive Profiles of Human Milk Oligosaccharides Yield Highly Sensitive and Specific Markers for Determining Secretor Status in Lactating Mothers. *Journal of Proteome Research* **2012**, *11* (12), 6124-6133.
26. Miller, E. M.; Aiello, M. O.; Fujita, M.; Hinde, K.; Milligan, L.; Quinn, E. A., Field and laboratory methods in human milk research. *American Journal of Human Biology* **2013**, *25* (1), 1-11.
27. Totten, S. M.; Wu, L. D.; Parker, E. A.; Davis, J. C. C.; Hua, S.; Stroble, C.; Ruhaak, L. R.; Smilowitz, J. T.; German, J. B.; Lebrilla, C. B., Rapid-throughput glycomics applied to human milk

- oligosaccharide profiling for large human studies. *Analytical and Bioanalytical Chemistry* **2014**, *406*, 7925-7935.
28. Jantscher-Krenn, E.; Aigner, J.; Reiter, B.; Köfeler, H.; Csapo, B.; Desoye, G.; Bode, L.; Poppel, M. N. M. v., Evidence of human milk oligosaccharides in maternal circulation already during pregnancy: a pilot study. *American Journal of Physiology-Endocrinology and Metabolism* **2019**, *316* (3), E347-E357.
29. Ruhaak, L. R.; Stroble, C.; Underwood, M. A.; Lebrilla, C. B., Detection of milk oligosaccharides in plasma of infants. *Analytical and Bioanalytical Chemistry* **2014**, *406* (24), 5775-5784.
30. De Leoz, M. L. A.; Wu, S.; Strum, J. S.; Ninonuevo, M. R.; Gaerlan, S. C.; Mirmiran, M.; German, J. B.; Mills, D. A.; Lebrilla, C. B.; Underwood, M. A., A quantitative and comprehensive method to analyze human milk oligosaccharide structures in the urine and feces of infants. *Analytical and Bioanalytical Chemistry* **2013**, *405*, 4089-4105.
31. Rudloff, S.; Pohlentz, G.; Diekmann, L.; Egge, H.; Kunz, C., Urinary excretion of lactose and oligosaccharides in preterm infants fed human milk or infant formula. *Acta Paediatrica* **1996**, *85* (5), 598-603.
32. Wang, B., Sialic Acid is an Essential Nutrient for Brain Development and Cognition. *Annu. Rev. Nutr.* **2009**, *29*, 177-222.
33. Wang, B.; Brand-Miller, J., The role and potential of sialic acid in human nutrition. *European Journal of Clinical Nutrition* **2003**, *57* (11), 1351-1369.
34. Xu, G.; Davis, J. C. C.; Goonatileke, E.; Smilowitz, J. T.; German, J. B.; Lebrilla, C. B., Absolute Quantitation of Human Milk Oligosaccharides Reveals Phenotypic Variations during Lactation. *The Journal of Nutrition* **2016**, *147* (1), 117-124.
35. Stinson, L. F.; Boyce, M. C.; Payne, M. S.; Keelan, J. A., The Not-so-Sterile Womb: Evidence That the Human Fetus Is Exposed to Bacteria Prior to Birth. *Frontiers in Microbiology* **2019**, *10*.
36. Davis, J. C.; Totten, S. M.; Huang, J. O.; Nagshbandi, S.; Kirmiz, N.; Garrido, D. A.; Lewis, Z. T.; Wu, L. D.; Smilowitz, J. T.; German, J. B.; Mills, D. A.; Lebrilla, C. B., Identification of Oligosaccharides in Feces of Breast-fed Infants and Their Correlation with the Gut Microbial Community. *Mol Cell Proteomics* **2016**, *15* (9), 2987-3002.

## **CHAPTER FOUR**

### **Host Cell Glycocalyx Remodeling Reveals SARS-Cov-2 Spike Protein Glycomic Binding Sites**

## ABSTRACT

Glycans on the host cell membrane and viral proteins play critical roles in pathogenesis. Highly glycosylated epithelial cells represent the primary boundary separating embedded host tissues from pathogens within the respiratory and intestinal tracts. SARS-CoV-2, the causative agent for the COVID-19 pandemic, reaches into the respiratory tract. We found purified human milk oligosaccharides (HMOs) inhibited the viral binding on cells. Spike (S) protein receptor binding domain (RBD) binding to host cells were partly blocked by co-incubation with exogenous HMOs, most by 2-6-sialyl-lactose (6'SL), supporting the notion that HMOs can function as decoys in defense against SARS-Cov2. To investigate the effect of host cell glycocalyx on viral adherence, we metabolically modified and confirmed with glycomic methods the cell surface glycome to enrich specific N-glycan types including those containing sialic acids, fucose, mannose, and terminal galactose. Additionally, Immunofluorescence studies demonstrated that the S protein preferentially binds to terminal sialic acids with  $\alpha$ -(2,6)-linkages. Furthermore, site-specific glycosylation of S protein RBD and its human receptor ACE2 were characterized using LC-MS/MS. We then performed molecular dynamics calculations on the interaction complex to further explore the interactive complex between ACE2 and the S protein. The results showed that hydrogen bonds mediated the interactions between ACE2 glycans and S protein with desialylated glycans forming significantly fewer hydrogen bonds. These results supported a mechanism where the virus binds initially to glycans on host cells preferring  $\alpha$ -(2,6)-sialic acids and finds ACE2 and with the proper orientation infects the cell.

## INTRODUCTION

Severe acute respiratory syndrome coronavirus-2 (SARS-CoV-2), the causative agent of COVID-19<sup>1</sup>, encodes an extensively glycosylated spike (S) protein that protrudes from the viral surface and binds angiotensin-converting enzyme 2 (ACE2) on host cells.<sup>2-6</sup> This novel SARS-CoV-2 was found to share similarities with the SARS-CoV, which was responsible for the SARS pandemic that occurred in 2002.<sup>7, 8</sup> ACE2 serves as the entry point for several coronaviruses into cells, including SARS-CoV and SARS-CoV-2.<sup>9, 10</sup> The receptor binding domain (RBD) of SARS-CoV-2 S protein has been limited to amino acid residues Arg319 to Phe541.<sup>11-13</sup> *In vitro* binding measurements also showed that the SARS-CoV-2 RBD binds to ACE2 with an affinity in the low nanomolar range, indicating that the RBD is a key functional component within the S1 subunit responsible for the binding of SARS-CoV-2 to ACE2.<sup>2, 13</sup> The plasma membrane protein ACE2 is abundantly expressed in humans tissues, including respiratory and intestinal epithelia, liver arteries, heart and kidney.<sup>14</sup>

Mammalian epithelial cells are highly glycosylated<sup>15, 16</sup> due to glycoproteins and glycolipids found on the cell membrane. Both the ACE2 receptor and the S protein are similarly extensively glycosylated. Several glycosylation sites are found near the binding interface.<sup>12, 17-19</sup> The role of glycosylation in the interaction between human ACE2 and SARS-CoV-2 S protein has been extensively studied, primarily using molecular dynamics (MD) simulations.<sup>12, 20, 21</sup> Human ACE2 variants have also been modeled, characterized, and examined for susceptibility to coronavirus interactions.<sup>22, 23</sup> Among ACE2 glycosylation sites, one of the most characterized positions for its role in S protein binding and viral infectivity is the asparagine on position 90 (N90). Recent genetic and biochemical studies showed that mutations that removed glycosylation on N90 site directly increased the susceptibility to SARS-CoV-2 infection.<sup>21, 23</sup> In contrast, glycans

present on N322 and N90 have the opposite effects on S protein binding. The N322 glycan interacts tightly with the RBD of the ACE2-bound S protein and strengthens the complex.<sup>20</sup> The S protein also contains glycosaminoglycan (GAG) binding motifs so that host surface GAGs contribute to cell entry by SARS-CoV-2.<sup>24</sup> Additionally, heparan sulfate has also been shown to promote Spike-ACE2 interaction.<sup>25</sup>

Pathogen adhesion is often mediated by highly specific lectin-glycan interactions. For example, *Escherichia coli* with type 1 fimbriae binds to cell surfaces exhibiting preference for high mannose glycans, while *Escherichia coli* with type S fimbriae has binding specificity for  $\alpha$ -(2,3)-linked sialic acids. Cell surface glycans have also been shown to act as a shield to mask its identity as a viable host to the pathogen. It was recently proposed that HMOs can prevent viral adhesion to intestinal epithelial cells via binding to the epithelial surface, causing structural changes in the receptor thereby impeding the virus from hijacking the host cell.<sup>26</sup> Breast-fed infants have significant amounts of HMOs lining the mucosal surface of their gastrointestinal tract. While the viral binding to glycans and HMO in particular have been studied, the direct interaction between the virus and host glycans remain relatively unexplored.

In this study, the role of host glycosylation and its effect on S protein binding was examined by identifying the host glycans that are involved in the binding. The study began with HMOs in a rapid assay to determine the broad details of the oligosaccharide that bind the virus. We then examined the impact of host cell glycosylation on S protein binding, by modifying the host glycosylation while leaving protein expression unchanged using transferase inhibitors. Using newly developed glycomic tools, we found that specific glycans on the host cell facilitate S protein binding and that binding depends more on the nature of glycans than it does on the membrane proteins.

This work has been published in the *Frontiers in Molecular Biology* and is included with permission in this thesis.

## **METHODS AND MATERIALS**

### **HMO Purification**

HMOs were obtained from breast milk samples using previously reported methods.<sup>27, 28</sup> Briefly, breast milk samples from 7 mothers were pooled. The pooled sample was defatted through centrifugation, proteins were precipitated with ethanol, and the resulting glycans were reduced with sodium borohydride (Sigma-Aldrich, St. Louis, MO). Solid phase extraction was performed on 25 mg graphitized carbon cartridges (ThermoFisher). Solvents were dried in vacuo using miVac (SP Scientific, PA) and purified HMOs were reconstituted and diluted prior to analysis.

### **Inhibition of HMO against SARS-CoV-2**

All HMO screens were performed with Vero E6 cells. Cells were plated in 96 well plates at 5e3 cells/well one day prior to infection. HMOs were diluted from stock to 50  $\mu$ M and an 8-point 1:2 dilution series was prepared in duplicate in Vero Media. Every compound dilution and control was normalized to contain the same concentration of drug vehicle (e.g., DMSO). Cell plates were pre-treated with drug for 2 h at 37 °C (5% CO<sub>2</sub>) prior to infection with diluted SARS-CoV-2 GFP for a final MOI of 0.1. In addition to plates that were infected, parallel plates were left uninfected to monitor cytotoxicity of drug alone, measured by CellTiter-Glo (CTG) assays as per the manufacturer's instructions (Promega, Madison, WI). Plates were then incubated at 37 °C (5% CO<sub>2</sub>) for 48 hours, followed by fixation with 4.0% paraformaldehyde, nuclear staining with Hoechst (Invitrogen, Carlsbad, CA), and data acquisition on a Celigo 5-channel Imaging

Cytometer (Nexcelom Bioscience, Lawrence, MA). The percent of infected cells was determined for each well based on GFP expression by manual gating using the Celigo software. For the CTG assays, luminescence was read on a BioTek Synergy HTX plate reader (BioTek Instruments Inc., Winooski, VT) using the Gen5 software (v7.07, Biotek Instruments Inc., Winooski, VT).

### **Cell culture and glycoalyx remodeling treatments**

Human liver hepatocellular carcinoma HepG2, lung carcinoma epithelial Calu-3, urinary bladder epithelial RT4 cells were obtained from American Type Culture Collection (ATCC, VA).

HepG2 and Calu-3 cells were grown in Eagle's Minimum Essential Medium (EMEM). RT4 cells were cultured in McCoy's 5a Medium. All media were supplemented with 10% (v/v) fetal bovine serum and 100 U mL<sup>-1</sup> penicillin and streptomycin. Cells were sub-cultured at 90% confluency and maintained at 37 °C in a humidified incubator with 5% CO<sub>2</sub>. At 50% cell confluency, the cells were either treated with 150 μM kifunensine, 2-fluoro-L-fucose, or 3-fluorinated sialic acid for 48 hours.

### **Sample Information**

Recombinant human angiotensin-converting enzyme 2(ACE2), SARS-CoV-2 Spike protein S1 Subunit RBD (Arg319-Phe541) and Spike protein S1 subunit (Val16-Arg685) derived from transfected human HEK293 cells were obtained from RayBiotech (Georgia, Product Number 230-30165, 230-30162) and Sino Biological (China, Product Number 40591-V08H), respectively.

### **Immunofluorescence**

The cells were seeded into FluoroDish™ cell culture dishes (WPI, FL) coated with poly-d-lysine with appropriate density using EMEM cell culture media. At 40% confluency, cells were treated with media either supplemented with 150 μM kifunensine, 2-fluoro-L-fucose, or 3-

fluorinated sialic acid for 48 hours. Control cell culture without treatment and treated cells were rinsed with phosphate-buffered saline (PBS), and fixed with 4% paraformaldehyde (Affymetrix, OH). Recombinant SARS-CoV-2 spike protein RBD and S1 subunits were conjugated to a fluorescent label with Alexa Fluor™ 555 according to manufacturing instructions (Microscale Protein Labeling Kit, Invitrogen, MA). Fixed control and glyco-modified cells were then incubated with fluorescent labelled S proteins or Anti-ACE2 antibody (Santa Cruz Biotechnology, TX) in PBS at 4 °C for 18 hours. Cells were stained for the nucleus with 1.6 µM Hoechst 33342 (Thermo Fisher Scientific, MA) followed by the staining for the plasma membrane with 1000-fold diluted CellMask™ Deep Red Plasma Membrane Stain (Thermo Fisher Scientific, MA), respectively at 37 °C for 10 min. Fluorescence images were captured using a Leica TCS SP8 STED 3X Super-Resolution Confocal Microscope (Wetzlar, Germany). Fluorescence intensity was quantified for selected cell area. Quantification was performed with software ImageJ.

### **Cell membrane extraction**

Cell membrane fractions were prepared as previously described.<sup>16,29,30</sup> Briefly, control and glycoengineered cells were collected and resuspended in homogenization buffer containing 0.25 M sucrose, 20 mM HEPES-KOH (pH 7.4), and protease inhibitor mixture (1:100; Calbiochem/EMD Chemicals). Cells were lysed on ice with five alternating on and off pulses in 5 and 10 second intervals using a probe sonicator (Qsonica, CT). Nuclear and mitochondrial fractions and cellular debris were pelleted and isolated by centrifugation at  $2000 \times g$  for 10 min. The supernatants were then ultra-centrifuged at  $200\,000 \times g$  for 45 min at 4 °C to extract the plasma membrane. The pellets of the cell membrane were resuspended in 500 µL of 0.2 M Na<sub>2</sub>CO<sub>3</sub> solution and 500 µL of water followed by two more ultracentrifugation treatments at  $200\,000 \times g$  for 45 min to wash off the endoplasmic reticulum (ER) and cytoplasmic fraction.

## **Enzymatic N-glycan release and purification of N-glycans**

Extracted cell membrane fractions or RNase B were suspended with 100  $\mu\text{L}$  of 100 mM  $\text{NH}_4\text{HCO}_3$  in 5 mM dithiothreitol and heated in boiling water for 2 minutes to denature the proteins. Solutions of with 2  $\mu\text{L}$  of peptide N-glycosidase F (New England Biolabs, MA) were added to the samples to release the N-glycans from proteins, and the resulting solutions were then incubated in a microwave reactor (CEM Corporation, NC) at 20 watts, 37  $^\circ\text{C}$  for 10 min. The samples were further placed in a 37  $^\circ\text{C}$  water bath for 18 hours. Ultracentrifugation at 200 000  $\times g$  for 30 min was performed to precipitate membrane fractions, and the supernatant containing N-glycans was collected and purified using porous graphitic carbon (PGC) on a 96-well SPE plate (Grace, IL). The plate was equilibrated with 80% (v/v) acetonitrile containing 0.1% (v/v) trifluoroacetic acid. The samples were loaded onto the plate and washed with nanopure water. N-Glycans were eluted with a solution of 40% (v/v) acetonitrile containing 0.05% (v/v) trifluoroacetic acid, and the samples were dried *in vacuo* using miVac (SP Scientific, PA) prior to mass spectrometric analysis.

## **Glycoprotein digestion and enrichment**

Details of the protein digestion have been described previously.<sup>30</sup> Extracted cell membrane proteins were reconstituted in 60  $\mu\text{L}$  of 8 M urea at room temperature. Recombinant proteins and dissolved cell membrane proteins were reduced with 2  $\mu\text{L}$  of 550 mM dithiothreitol, alkylated with 4  $\mu\text{L}$  of 450 mM iodoacetamide. A 420  $\mu\text{L}$  of 50 mM ammonium bicarbonate solution was added to dilute the urea concentration to 1 M and to adjust the pH value. The samples were incubated with 2  $\mu\text{g}$  trypsin at 37  $^\circ\text{C}$  for 18 hours. The resulting peptides were concentrated *in vacuo* using miVac (SP Scientific, PA). Glycopeptides were enriched by solid-phase extraction using iSPE®-HILIC cartridges (HILICON, Sweden). The cartridges were conditioned with 0.1% (v/v)

trifluoroacetic acid in acetonitrile, followed by 1% (v/v) trifluoroacetic acid and 80% (v/v) acetonitrile in water. The samples were loaded and washed with 1% (v/v) trifluoroacetic acid and 80% (v/v) acetonitrile in water. The enriched glycopeptides were eluted with water containing 0.1% (v/v) trifluoroacetic acid and dried prior to mass spectrometric analysis.

### **Glycomic analysis with LC-MS/MS**

Glycan samples were reconstituted with 30  $\mu$ L nanopure water and analyzed using an Agilent 6520 Accurate Mass Q-TOF LC/MS equipped with a PGC nano-chip (Agilent Technologies, CA). The glycan separation was performed at a constant flow rate of 300 nL min<sup>-1</sup>, and a binary gradient was applied using (A) 0.1% (v/v) formic acid in 3% acetonitrile and (B) 1% (v/v) formic acid in 90% acetonitrile: 0–2 min, 0–0% (B); 2–20 min, 0–16% (B); 20–40 min, 16%–72% (B); 40–42 min, 72–100% (B); 42–52 min, 100–100% (B); 52–54 min, 100–0% (B); 54–65 min, 0–0% (B). MS spectra were collected with a mass range of m/z 600–2000 at a rate of 1.5 s per spectrum in positive ionization mode. The most abundant precursor ions in each MS1 spectrum were subjected to fragmentation through collision-induced dissociation (CID) based on the equation  $V_{\text{collision}} = 1.8 \times (m/z) / 100 V - 2.4 V$ .

### **Glycomic data analysis**

Extraction of the compound chromatographs of glycans from cells was obtained via the MassHunter Qualitative Analysis B08 software (Agilent, CA). N-Glycan compositions were identified according to accurate masses using an in-house library constructed based on the knowledge of N-glycan biosynthetic pathways and previously obtained in-house structures of N-glycans. Relative abundances were determined by integrating peak areas for observed glycan masses and normalizing to the summed peak areas of all glycans detected.

## **Glycoproteomic analysis with LC-MS/MS**

The enriched glycopeptide samples were reconstituted with nanopure water and directly characterized using UltiMate™ WPS-3000RS nanoLC 980 system coupled to the Nanospray Flex ion source of an Orbitrap Fusion Lumos Tribrid Mass Spectrometer system (Thermo Fisher Scientific, MA). The analytes were separated on an Acclaim™ PepMap™ 100 C18 LC Column (3 μm, 0.075 mm x 150 mm, ThermoFisher Scientific). A binary gradient was applied using 0.1% (v/v) formic acid in (A) water and (B) 80% acetonitrile: 0–5 min, 4–4% (B); 5–133 min, 4–32% (B); 133–152 min, 32%–48% (B); 152–155 min, 48–100% (B); 155–170 min, 100–100% (B); 170–171 min, 100–4% (B); 171–180 min, 4–4% (B). The instrument was run in data-dependent mode with 1.8kV spray voltage, 275 °C ion transfer capillary temperature, and the acquisition was performed with the full MS scanned from 700 to 2000 in positive ionization mode. Stepped higher-energy C-trap dissociation (HCD) at 30±10% was applied to obtain tandem MS/MS spectra with m/z values starting from 120.

## **Glycoproteomic data analysis**

Glycopeptide fragmentation spectra were annotated using Byonic software (Protein Metrics, CA) against the reviewed UniProt Severe acute respiratory syndrome coronavirus 2 spike protein database. Carbamidomethyl modification at cysteine residues and oxidation at methionine were assigned as the modification.

## **Molecular dynamic simulation of S protein on ACE2**

The 3D structure of S protein and ACE2 complex was obtained from PDB (PDB code 7DF4).<sup>31</sup> The most abundant glycans for each ACE2 glycosite were modeled and attached to the protein using CHARMM-GUI.<sup>32</sup> Additionally, the fully-desialylated glycans were modeled and

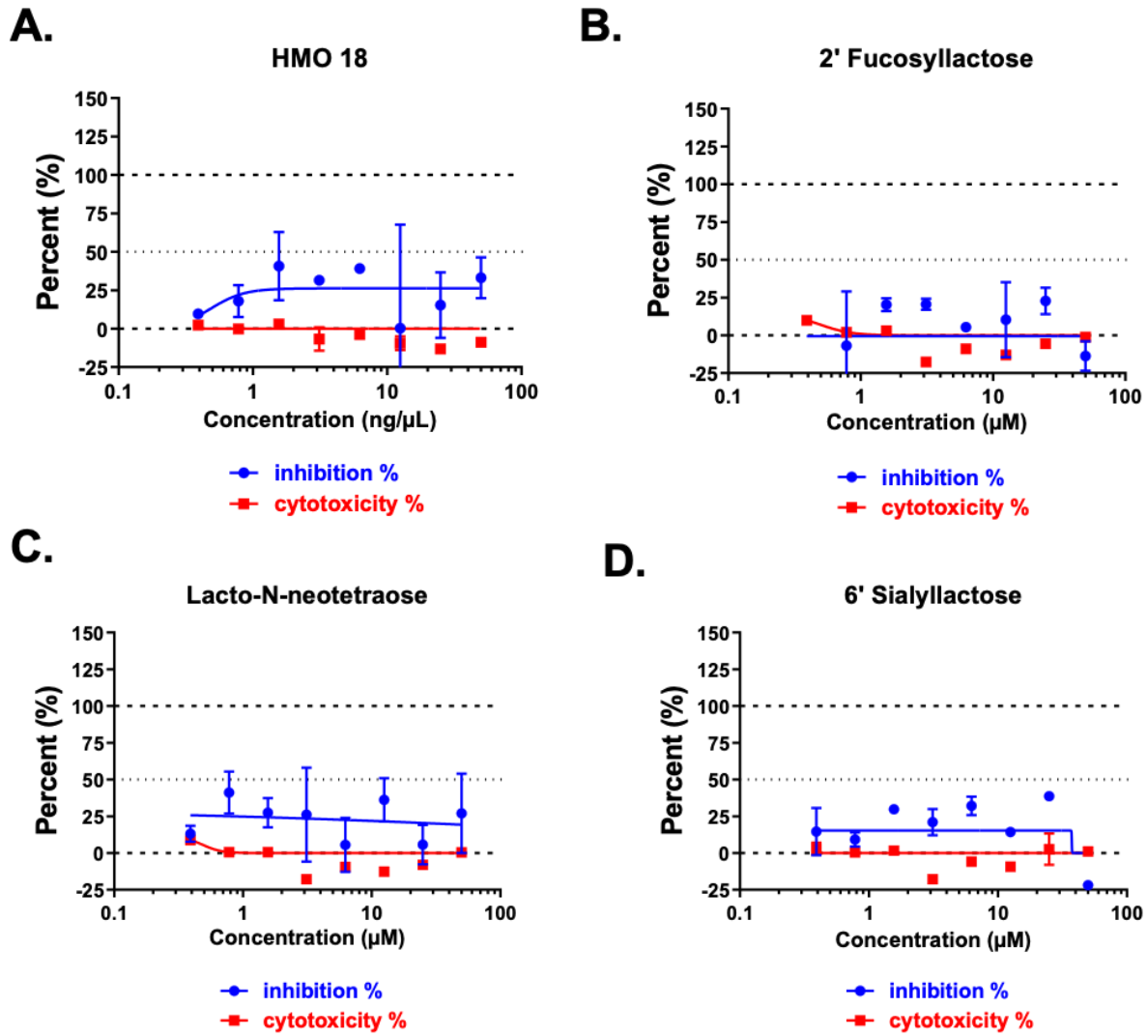
attached to generate a fully-desialylated homolog of the ACE2 glycoprotein. The models were solvated using the TIP3P water model, and counterions were added to neutralize the system. The CHARMM carbohydrate force field<sup>33</sup> and CHARMM36m force field<sup>34</sup> were used for the carbohydrate and protein structures. Equilibration was performed at 303.15 K over 10 ps. Molecular dynamics simulation was performed using NAMD software package version 2.13<sup>35</sup> at 303.15 K under NPT conditions over 5 ns with an output every 10 ps. Long-range electrostatics were evaluated using the particle-mesh Ewald (PME) method.<sup>36</sup> Covalent bonds involving hydrogen were constrained with the SHAKE algorithm.<sup>37</sup> After dynamics simulations, trajectories were loaded onto VMD for visualization and analysis.<sup>38</sup> Specifically, the intermolecular hydrogen-bonding interactions (donor-acceptor distance 3.0 Å, angle cutoff 20°) of each glycan in the fully-sialylated and desialylated forms were compared over the simulation period.

## RESULTS

### Inhibition of virus binding by human milk oligosaccharides

Human milk oligosaccharides (HMOs) contain a number of unique structures that can be used to rapidly screen the glycan specificity of the virus. We tested whether SARS-CoV-2 virus could be inhibited by HMOs. We first examined whether pooled samples of purified HMOs from seven different mothers could affect the binding of SARS-CoV-2 virus on Vero E6 cells. **Figure 4.1a** showed that the binding capability was affected by the HMO mixture to about 25%. HMOs contain compounds with terminal fucose, sialic acid and galactose. To identify the functional components that could specifically affect binding, we further tested individual compounds that contained these terminal saccharides. The HMOs 2'-fucosyllactose (2'-FL), 6'-sialyllactose (6'-SL), and lacto-N-neotetraose (LNnT) were selected for this study because they represent many of

the structures and are abundant in mothers' milk. 2'-FL and 6'-SL were produced by adding fucose or a N-acetylneuraminic acid (Neu5Ac)<sup>39</sup> to the lactose core, respectively. Lacto-N-neotetraose (LNnT) is a neutral HMO with a galactose terminus and contained neither fucose nor sialic acid. The infection studies showed that 2'-FL did not diminish infection, however both 6'-SL and LNnT showed some diminished infection to a similar extent as the pooled sample (**Figure 4.1**).



| IC50 | CC50 | SI  |
|------|------|-----|
| N/A  | >50  | N/A |

**Figure 4.1** Viral infection on cells and cytotoxicity assays. Cell plates were pre-treated with pooled HMOs(A), 2'-FL(B), LNnT(C), and 6'-SL(C), respectively. The treatment was performed for 2 h at 37°C (5% CO<sub>2</sub>) prior to infection. The percent of infected cells was determined for each well based on GFP expression. All samples were run in triplicate on both an assay plate and a toxicity plate.

Due to limitations with working on the whole intact virus, we used the S protein as a surrogate for the virus. To validate this model, we performed the experiments on the S protein using the fluorescent labeling and immunofluorescence imaging. SARS-CoV-2 enters host cells via the angiotensin-converting enzyme 2 (ACE2) receptor, which binds the receptor binding domain (RBD) of the S protein.<sup>12</sup> *The Human Protein Atlas* (HPA), a website resource for protein expression profiles in cells, tissues and organs (<https://www.proteinatlas.org/>)<sup>40, 41</sup> was used to select the host cell with ACE2 expression. HepG2 was selected after confirming ACE2 expression with labeled antibody and immunofluorescence on the cell membrane (**Figure 4.2**).

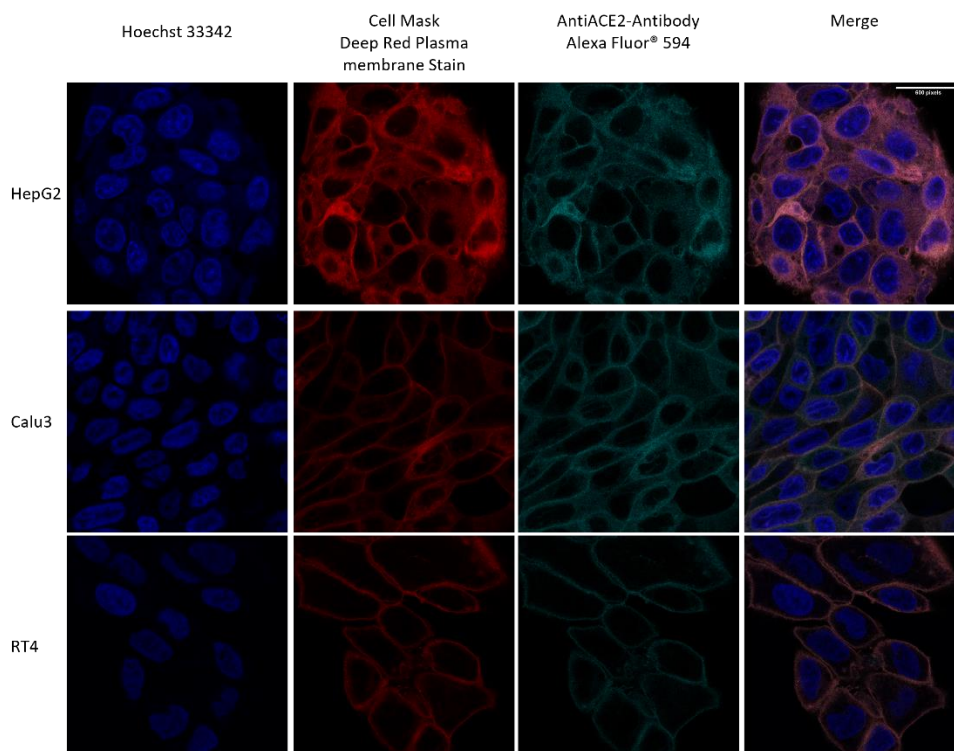


**Figure 4.2** Validating the expression of ACE2 in HepG2 cells using immunofluorescence. Cells were incubated with mouse monoclonal antibody. The images show HepG2, Calu3 and RT4 cells expressing huACE2. The columns (from left to right) show staining of nuclear acid (Hoechst 33342), plasma membrane (CellMask™ Deep Red), anti-ACE2 antibody, and merged image. Scale bar, 600 pixels.

To verify further whether HMOs block viral adhesion, we tested the ability of the selected HMO compounds to inhibit RBD binding to HepG2 cells with immunofluorescence. Preincubating HepG2 cells with HMOs did not decrease the binding between the RBD and the cells suggesting that the HMOs did not block binding sites on the host cell surface (**Figure 4.S2**). We then tested whether the HMOs could block or alter the RBD of the virus by preincubating the RBD and the HMOs before introduction to HepG2 cells. Fluorescently labelled RBD was preincubated with 2'-FL, LNnT and 6'-SL separately then allowed to interact with host cells (**Figure 4.3A**). Quantitation of fluorescent signal intensity showed that HMOs blocked binding of RBD to cells presumably reflecting the behavior of the intact virus. The RBD was blocked only slightly by 2'FL (not statistically significant), more by LNnT (significant), and the most by 6'SL (**Figure 4.3B**). The data further showed that HMOs can potentially function as decoys to affect SARS-CoV-2 adherence.

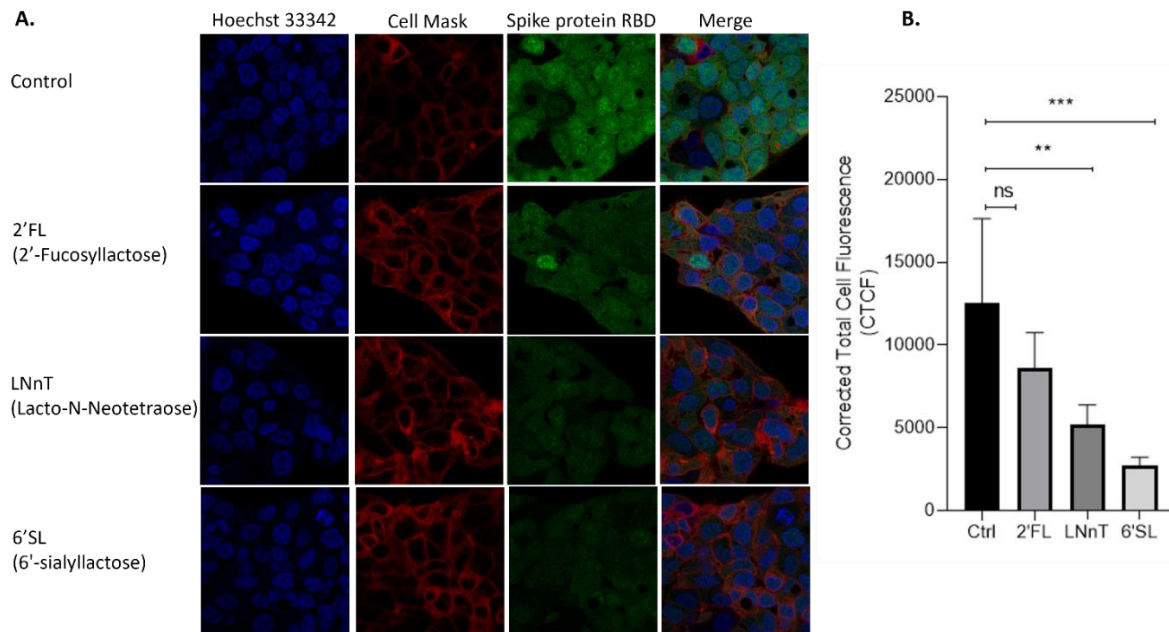


**Figure 4.3** Inhibition of HMOs on the binding between HepG2 cells and Spike protein RBD. Fluorescent labelled proteins were preincubated with 1 mg per mL 2'-FL, 6'-SL, and LNnT, respectively. The preincubation was performed at room temperature for 30 min. (A) Immunofluorescence for S protein RBD binding. The columns (from left to right) show staining of nuclear acid (Hoechst 33342), plasma membrane (CellMask™ Deep Red), S protein RBD, and merged image. Scale bar, 496 pixels. (B) Quantification of fluorescent intensity of Spike protein RBD binding. Fluorescence intensity was quantified for selected cell area. Quantification was performed with software ImageJ. Asterisks indicate the statistical significance between groups compared (\*\* $p < 0.01$ ; \*\*\* $p < 0.001$ ; ns  $p < 0.05$ ).

## Determining SARS-CoV-2 binding through variable glycoalyx expression

The notable decrease in binding caused by 6'-SL drew our attention to sialic acids as potential receptors on the cell surface. To further investigate the effects of cell surface glycans on RBD binding, we altered the cell membrane glycans through transferase inhibitors. We first characterized the glycan of the cell membrane and ACE2 on the native cell line. For this analysis, complex and hybrid type glycans were combined to distinguish them from oligomannose type. The N-glycan profile showed a notable abundance of sialylated and sialyfucoylated structures (**Figure 4.4A**). The most abundant N-glycan compositions had multiple fucose and sialic acid (N-acetylneuraminic acid or Neu5Ac) residues such as Hex<sub>6</sub>HexNAc<sub>5</sub>Fuc<sub>2</sub>NeuAc<sub>3</sub>, Hex<sub>6</sub>HexNAc<sub>5</sub>Fuc<sub>1</sub>NeuAc<sub>3</sub> and Hex<sub>5</sub>HexNAc<sub>4</sub>Fuc<sub>1</sub>NeuAc<sub>2</sub>. Glycoproteomic analysis of the cell membrane revealed seven glycosites on the ACE2 protein of HepG2 cells. The N-glycoforms of the ACE2 protein extracted from HepG2 cells were diverse and the most common structures were both fucosylated and sialylated (**Figure 4.4B, Table S4.1**). For comparison, we analyzed the glycosylation of commercial recombinant ACE2 protein expressed from HEK293 (**Figure 4.5, Table S4.2**) and found them to be similar to those expressed by HepG2 (**Table 4.1**). Both proteins were highly sialylated and fucosylated with limited amounts of high-mannose glycans.

**Table 4.1 Summary of Glycoproteomic Profiles of ACE2 proteins.** The number of glycoforms is shown in Table 1.

| Subtype of N-Glycans detected on glycosites | Fucosylated | Sialyfucoylated | Undecorated | Sialylated | HM |
|---|-------------|-----------------|-------------|------------|----|
| Recombinant Human ACE2                      | 147         | 175             | 68          | 119        | 16 |
| ACE2 from HepG2 cells                       | 100         | 120             | 38          | 65         | 5  |

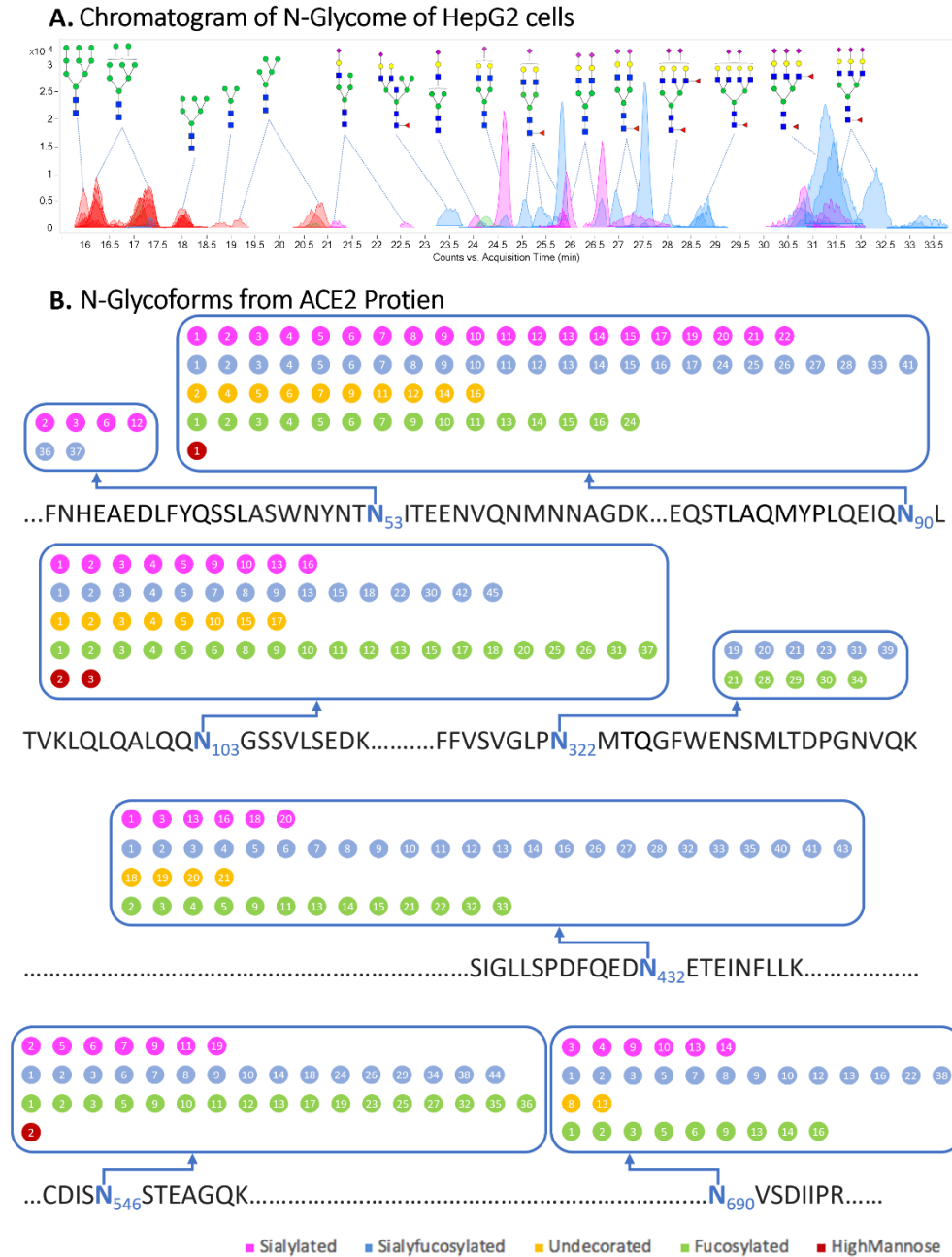


**Figure 4.4** Cell membrane N-glycome and site-specific occupancy of ACE2 receptor in HepG2 cells. (A) Individual N-glycan species of HepG2 host cells. LC-MS peaks were color coded to assign glycan subtype. Abundant peaks are annotated with putative structures. Symbol nomenclature is used for representing glycan structures (<https://www.ncbi.nlm.nih.gov/glycans/snfg.html>). (B) Site-specific occupancy of ACE2 receptor in HepG2 cells. The N-glycoforms from ACE2 protein extracted from HepG2 cells are distributed on 7 glycosites. The labeled numbers inside dots denote identified individual glycan and the details were shown in Table S2.

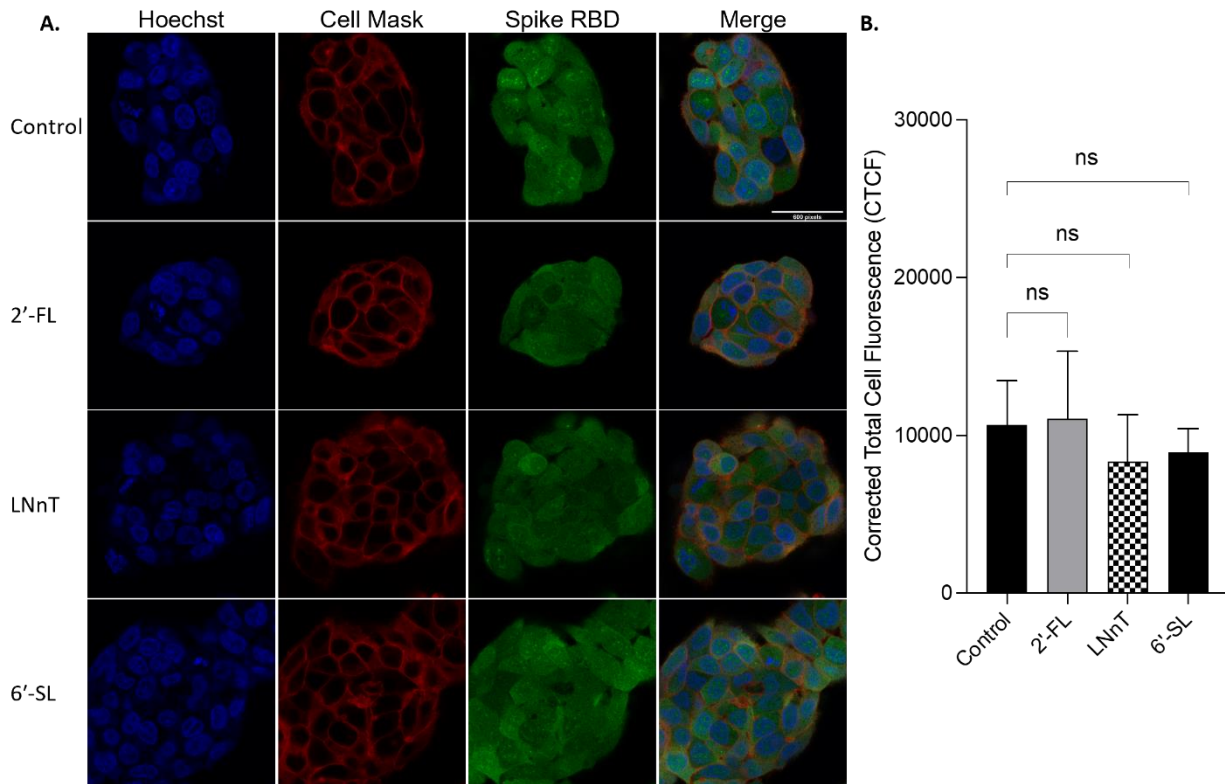


**Figure 4.5** Effect of HMOs on the binding between HepG2 cells and Spike protein RBD. HepG2 cells were preincubated with 1 mg per mL 2'-FL, 6'-SL, and LNnT, respectively. After 30 min-preincubation at room temperature, cells were washed with PBS to remove exogenous decoys before fixation. (A) Immunofluorescence for S protein RBD binding with HepG2 cells. The columns (from left to right) show staining of nuclear acid (Hoechst 33342), plasma membrane (CellMask™ Deep Red), S protein RBD, and merged image. Scale bar, 600 pixels. (B) Quantification of fluorescent intensity of Spike protein RBD binding. Fluorescence intensity was quantified for selected cell area. Quantification was performed with software ImageJ. Asterisks indicate the statistical significance between groups compared (ns  $p < 0.05$ ).

We metabolically altered the cell surface glycome to enrich for sialic acids, fucoses and mannoses, respectively. To determine whether these changes in glycosylation affected ACE2 expression on the cell membrane, we probed the cells with fluorescently labeled antibodies (**Figure 4.6**) These experiments showed no significant changes in protein expression for ACE2 in any of the glycan modification procedures. To diminish fucosylation on the HepG2 cell surface, we employed a fucosyltransferase inhibitor, 2-fluoro-L-fucose (2F-Fucose). To inhibit sialylation, a sialyltransferase inhibitor 3-fluorinated sialic acid(3-F-Sia) was used.

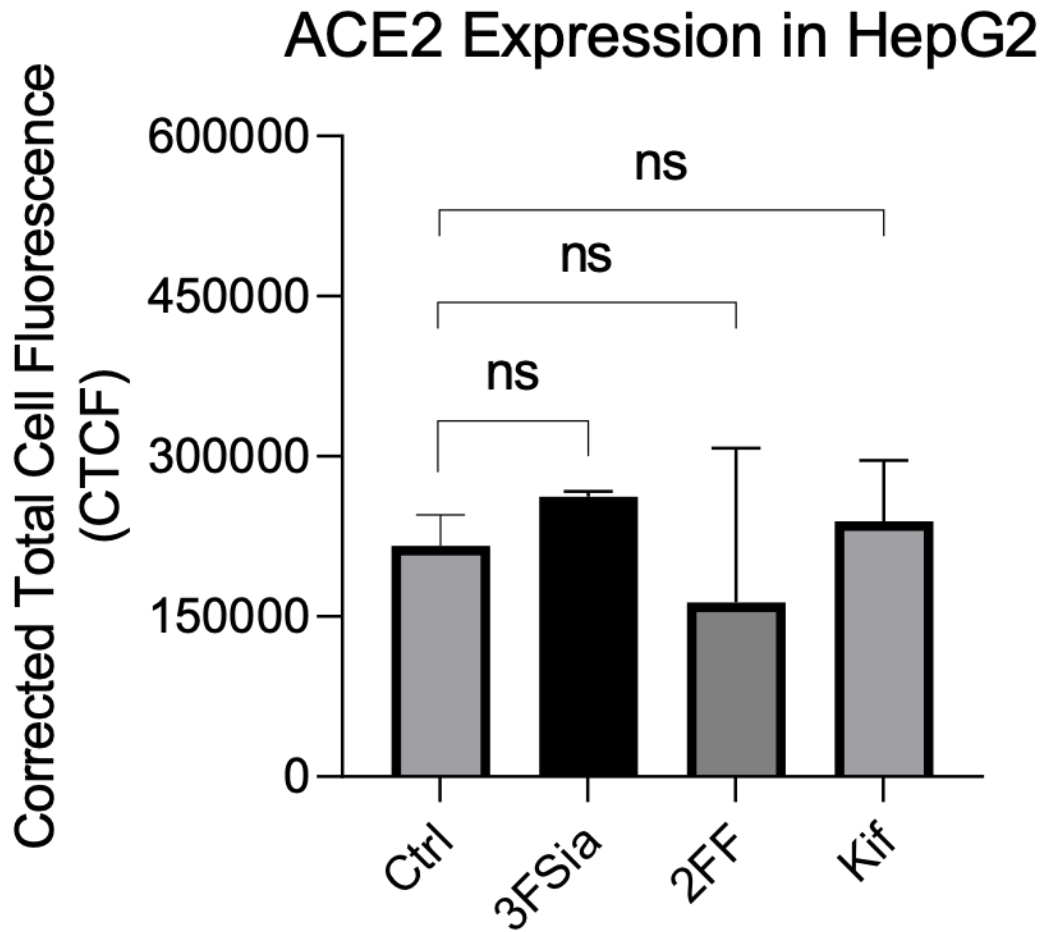
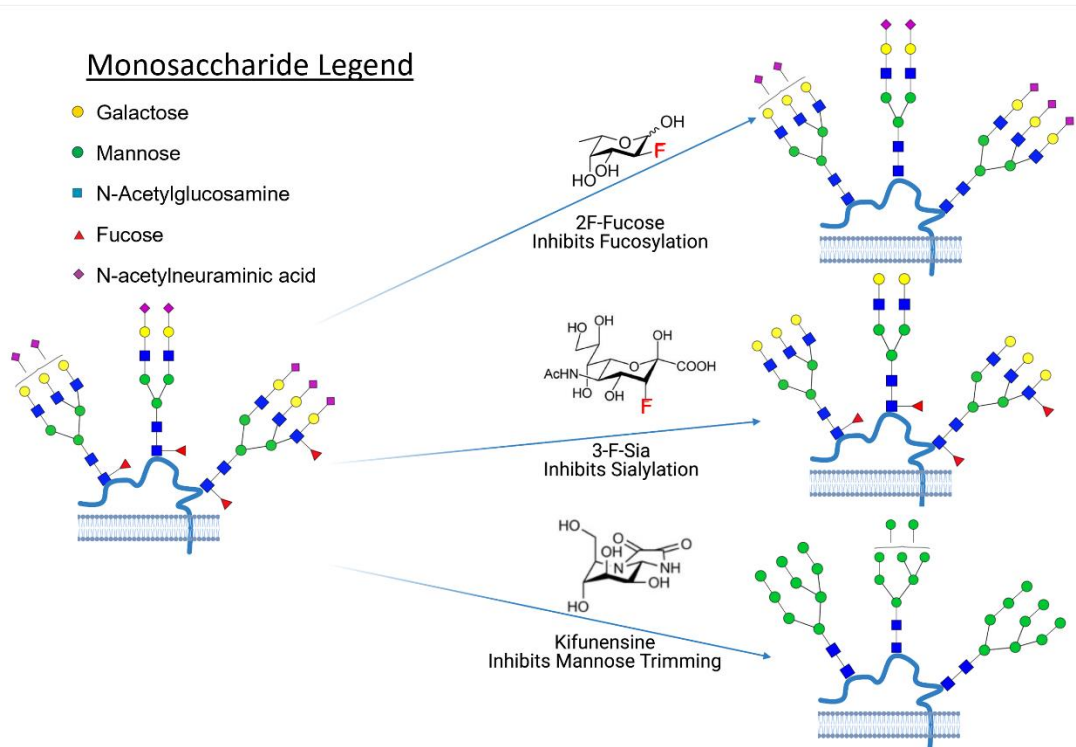


**Figure 4.6** Host cell glyocalyx remodeling not altering ACE2 expression on HepG2 cells. Quantification of fluorescent intensity of anti-ACE2 antibodies on HepG2 cells. Fluorescence intensity was quantified for selected cell area. Quantification was performed with software ImageJ. Asterisks indicate the statistical significance between groups compared (ns  $p < 0.05$ ).

The predicted behavior of each substrate is shown in **Figure 4.7**. Compositional profiles were generated for the modified cells, using the sum of the intensities for similar glycan types from the LC-MS analysis. These inhibitors have recently been applied for altering cell surface glycosylation to yield similar results (**Figure 4.7B**).<sup>42</sup> 2F-Fucose inhibits fucosylation by being converted to the sugar nucleotide GDP-2F-Fuc.<sup>43</sup> It then accumulates in the cell and binds to the transferase and prohibits the enzyme from adding fucose to the nascent chain, thereby decreasing fucose expression on the cell surface.<sup>44</sup> The sialyfucoylated N-glycans decreased from 75% to 10% after inhibition with 2F-Fucose treatment. The sialyfucoylated N-glycans were converted to sialylated (only) ones. For example, the abundant sialyfucoylated compound Hex<sub>5</sub>HexNAc<sub>4</sub>Fuc<sub>1</sub>NeuAc decreased (9.6% to 1.9%, relative abundance) relative to the unfucosylated species Hex<sub>5</sub>HexNAc<sub>4</sub>Fuc<sub>0</sub>NeuAc<sub>2</sub> which increased in abundance from 3.7% to 19% (**Table 4.S3**). The sialylation pathway was inhibited using 3-F-Sia, a fluorinated sialic acid substrate [cytidine monophosphate (CMP)–SiaFAc]<sup>45</sup>, which binds more strongly to the enzyme thereby prohibiting the transfer of sialic acids. Treatment with 3-F-Sia decreased the relative abundance of all sialyfucoylated N-glycans from 75% to 34%. Simultaneously, the relative abundance of fucosylated (only) species increased from 1 % to 27 %. Thus, it appears that the inhibitors are highly effective diminishing fucosylated and sialylated structures, respectively.

## A. Schematic Representation of Modifying Host Cell Surface Glycosylation



## B. Relative Abundance of N-Glycan Subtypes from Modified HepG2 Cells

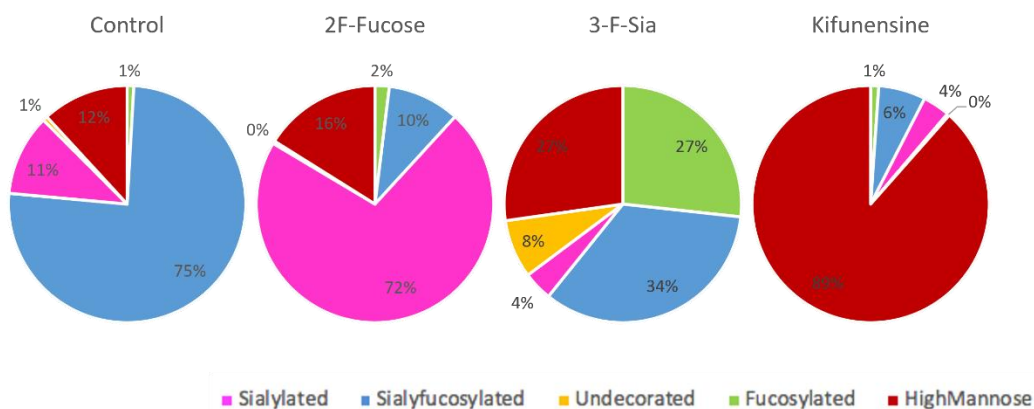


**Figure 4.7** Host Cell Surface Glycome Modification. 2F-Fucose (Fucosyltransferase Inhibitor); 3-F-Sia (Sialyltransferase Inhibitor). (A) Metabolic engineering strategy for altering host cell glycosylation. Symbol nomenclature is used for representing glycan structures (<https://www.ncbi.nlm.nih.gov/glycans/snfg.html>). (B) N-Glycome Profiles of unmodified and modified HepG2 cells from LC-MS analysis. Compound list and details are shown in Table S3. Pie charts were color coded to assign glycan subtype. Numbers inside pie charts denote the relative abundance of each identified glycan subtype.

After confirming that glycan alteration had taken place in host cell, immunofluorescence analysis was used to observe the effect of the host glycome on viral binding. Treatment of 2F-Fucose did not affect RBD binding to the cell significantly as observed by immunofluorescence imaging (**Figure 4.8A**). However, inhibition of sialylation by 3-F-Sia decreased the S protein RBD binding with HepG2 cells by 64% (**Figure 4.8B**), indicating that the binding was likely mediated by sialic acid residues on the host cell surface. Similar trends were observed in other cell lines with ACE2 expression, namely Calu3 and RT4 (**Figure 4.8B**). Desialylation inhibited the binding from S protein RBD significantly, and decreased fucosylation did not change the extent of the binding.

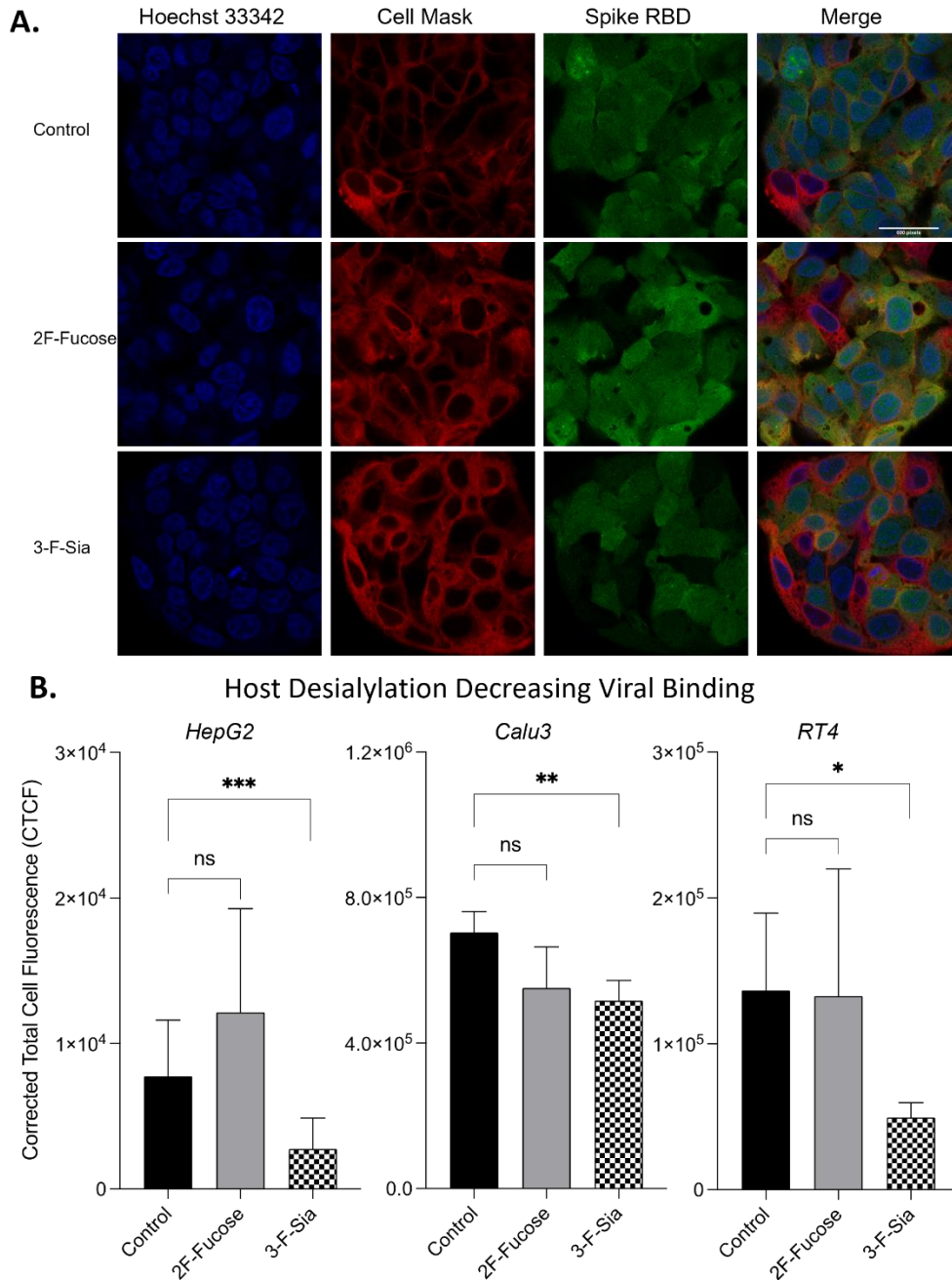


**Figure 4.8** Remodeling host glycome alters binding between host cells and Spike protein RBD. 2F-Fucose (Fucosyltransferase Inhibitor); 3-F-Sia (Sialyltransferase Inhibitor). (A) Immunofluorescence for S protein RBD binding with modified cells. The columns (from left to right) show staining of nuclear acid (Hoechst 33342), plasma membrane (CellMask™ Deep Red), S protein RBD, and merged image. Scale bar, 600 pixels. (B) Quantification of fluorescent intensity of Spike protein RBD binding. Fluorescence intensity was quantified for selected cell area. Quantification was performed with software ImageJ. Asterisks indicate the statistical significance between groups compared (\* $p < 0.05\%$ ; \*\* $p < 0.01\%$ ; \*\*\* $p < 0.001\%$ ; ns  $p < 0.05$ ).

In mammalian cells, terminal sialic acids are commonly found in  $\alpha$ -glycosidic linkages to the C-3 or C-6 hydroxyl of galactose via  $\alpha$ -(2,3)- or  $\alpha$ -(2,6)-linkage for N-glycans.<sup>46</sup> In nasal mucosa,  $\alpha$ -(2-6)-sialic acids are dominant<sup>47</sup> with significantly less detected in the lung.<sup>48</sup> We further investigated linkage specificities for RBD binding by preincubating the RBD with sialylated HMOs. Preincubation with 3'- sialyllactose (3'-SL) did not decrease the binding, while a significant decrease was observed after preincubation with 6'-SL, confirming S protein RBD prefers binding with  $\alpha$ -(2-6) sialic acids (**Figure 4.9**).

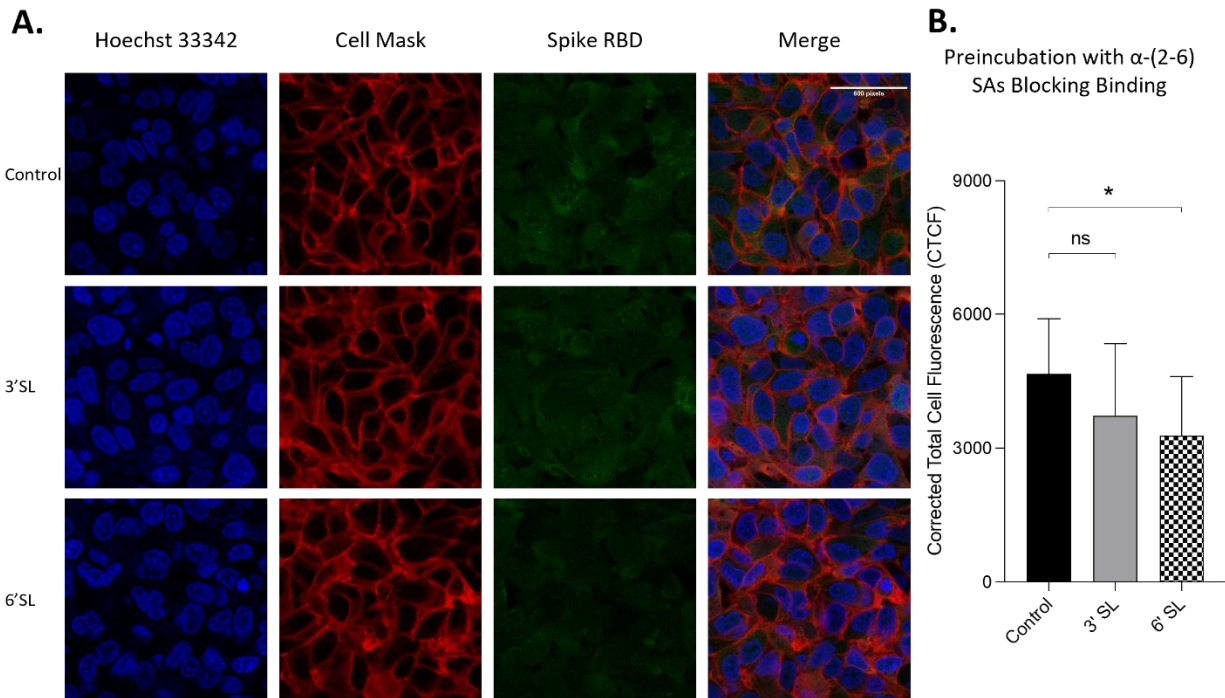


**Figure 4.9** Sialylated 6'-SL HMOs inhibited binding of Spike protein RBD to HepG2 Cells. Fluorescent labelled proteins were preincubated with 1 mg per mL 3'-FL(3'-sialyllactose) and 6'-SL(6'-sialyllactose) respectively at room temperature. (A) Immunofluorescence for S protein RBD binding with cells. The columns (from left to right) show staining of nuclear acid (Hoechst 33342), plasma membrane (CellMask™ Deep Red), S protein RBD, and merged image. Scale bar, 600 pixels. (B) Quantification of fluorescent intensity of Spike protein RBD binding. Fluorescence intensity was quantified for selected cell area. Quantification was performed with software ImageJ. Asterisks indicate the statistical significance between groups compared (\*p < 0.05%; ns p < 0.05).

Fucosylated glycans were also observed on ACE2 proteins in HepG2 cells (**Table S1**). Terminal  $\alpha$ -(1,2) and  $\alpha$ -(1,3)-fucose residues are commonly found in mammalian cells.<sup>49, 50</sup> To confirm that fucosylation is less important, 2'-FL and 3'-fucosyllactose (3'-FL), components of HMOs, were used.<sup>39</sup> Preincubating the S protein RBD with 2'-FL or 3'-FL did not significantly alter binding (**Figure 4.10**). The S protein RBD again showed little affinity to terminal fucose residues on host cells.

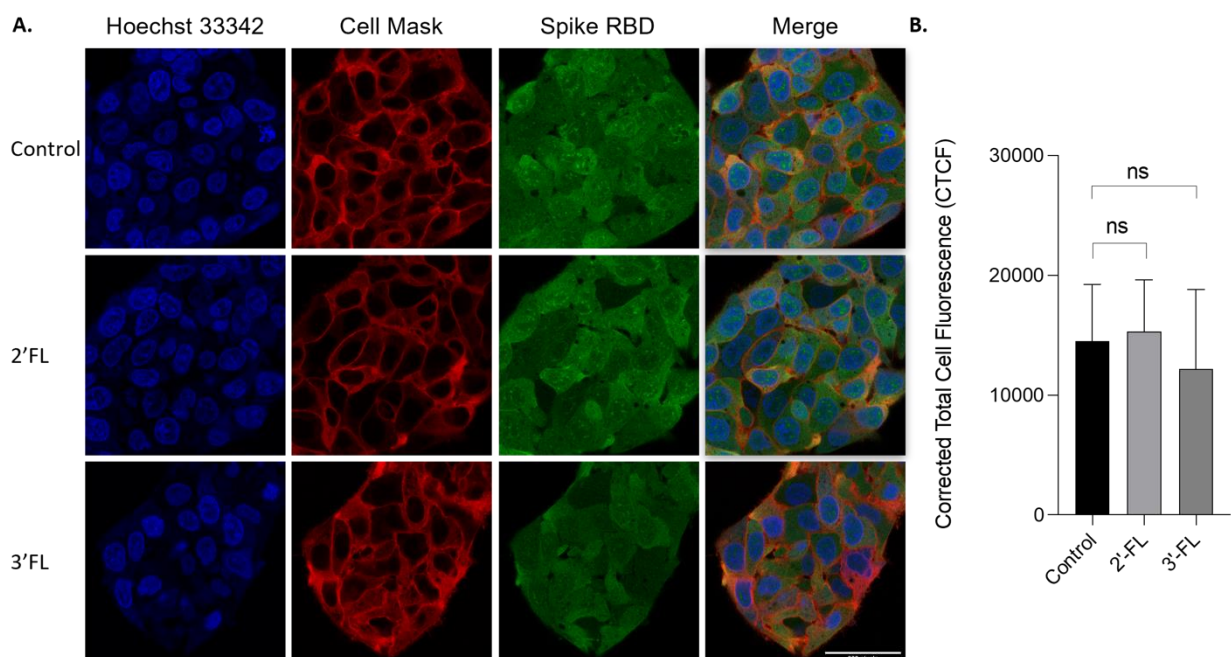


**Figure 4.10** Effect of fucosylated HMOs on the binding between HepG2 cells and Spike protein RBD. S protein RBD with 2'-FL or 3'-FL for 30 min at room temperature. (A) Immunofluorescence for S protein RBD binding with HepG2 cells. The columns (from left to right) show staining of nuclear acid (Hoechst 33342), plasma membrane (CellMask™ Deep Red), S protein RBD, and merged image. Scale bar, 600 pixels. (B) Quantification of fluorescent intensity of Spike protein RBD binding. Fluorescence intensity was quantified for selected cell area. Quantification was performed with software ImageJ. Asterisks indicate the statistical significance between groups compared (ns p<0.05).

Glycosylation of HepG2 included primarily complex and hybrid type structures with fewer high mannose structures. The latter have been reported as important mediators in host-virus binding for human coronaviruses HKU1<sup>51</sup> and severe acute respiratory syndrome (SARS).<sup>52</sup> We remodeled the cell surface to produce primarily oligomannose and determined its effects on SARS-CoV-2 binding. Kifunensine (Kif) is commonly used to inhibit the  $\alpha$ -mannosidase-I<sup>53</sup>, thereby preventing mannose trimming to increase oligomannose-type glycans.<sup>52, 54</sup> Our LC/MS data also proved its increasing the relative abundance of oligomannose to 89% in whole cell N-glycome as shown in **Figure 4.4**. Introduction of Kif to the cell resulted in a fourfold increase in the binding as measured by immunofluorescence imaging (**Figure 4.11A, 4.11B**). N-Glycans, released from RNase B, were also employed to examine high mannose type binding. Preincubation with the oligomannose decreased the binding of S protein RBD with host cells (**Figure 4.11C**). This effect was dose dependent with higher concentrations preventing binding more strongly. High mannose glycans on the host cell surface can therefore increase the adherence of S protein RBD.

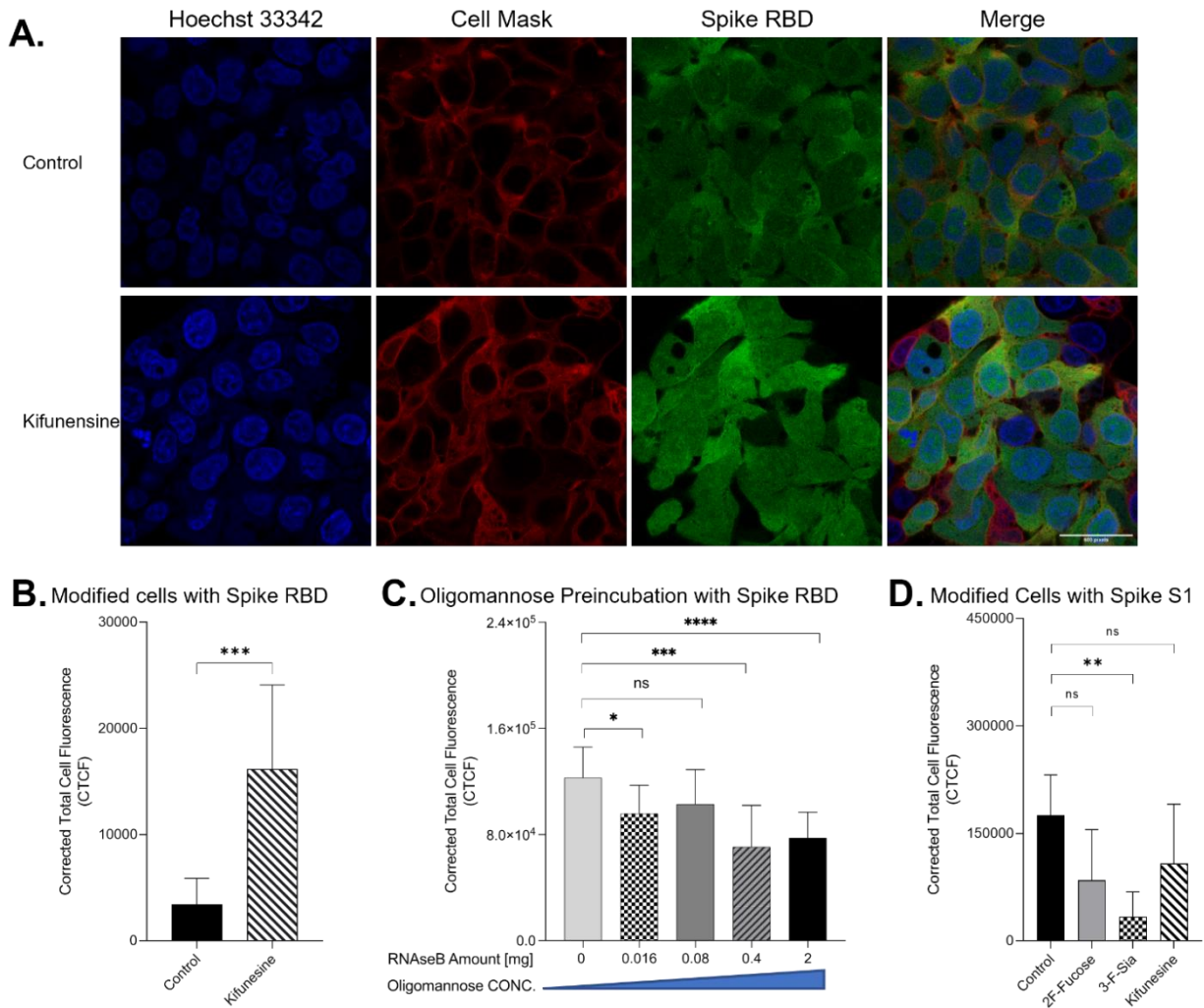


**Figure 4.11** Introducing high mannose glycans into viral binding. (A) Immunofluorescence for S protein RBD binding with modified cells. The columns (from left to right) show staining of nuclear acid (Hoechst 33342), plasma membrane (CellMask™ Deep Red), S protein RBD, and merged image. Scale bar, 600 pixels. Quantification of fluorescent intensity of Spike protein RBD (B) (C) or S1 subunit (D) binding. (C) Fluorescent labelled proteins were preincubated with purified high mannose at room temperature for 30 min before binding. Fluorescence intensity was quantified for selected cell area. Quantification was performed with software ImageJ. Asterisks indicate the statistical significance between groups compared (\* $p < 0.05$ ; \*\* $p < 0.01$ ; \*\*\* $p < 0.001$ ; \*\*\*\* $p < 0.0001$ ; ns  $p < 0.05$ ).

To further validate the binding of the spike protein with the host glyocalyx, we used spike protein S1 subunit, a longer polypeptide segment of the S protein and includes the sequence of RBD. Treatment of the cell line with 2F-Fucose did not change the binding between S1 subunit and host cells (**Figure 4.11D**). Similarly, the use of 3-F-Sia significant decreased the fluorescent intensity of the assay demonstrating again that the spike protein binds to sialic acids. Surprisingly, the use of Kif on the S1 subunit no longer increased binding. The binding studies showed that there was no significant change in binding relative to the control.

### **Molecular Dynamics Calculations of ACE2 and S Protein Interactions**

To gain further insight into the interactions between the primary receptor ACE2<sup>12, 55, 56</sup> and the SARS-CoV-2 S protein, we performed molecular dynamics calculations on the interacting complex. Based on the glycoproteomic results for ACE2 from the HepG2 cell line (**Table S4.1**), we constructed a model with selected glycoforms on ACE2. ACE2 contained seven occupied N-glycan sites corresponding to Asn 53, 90, 103, 322, 432, 546, and 690 (**Figure 4.12A**).

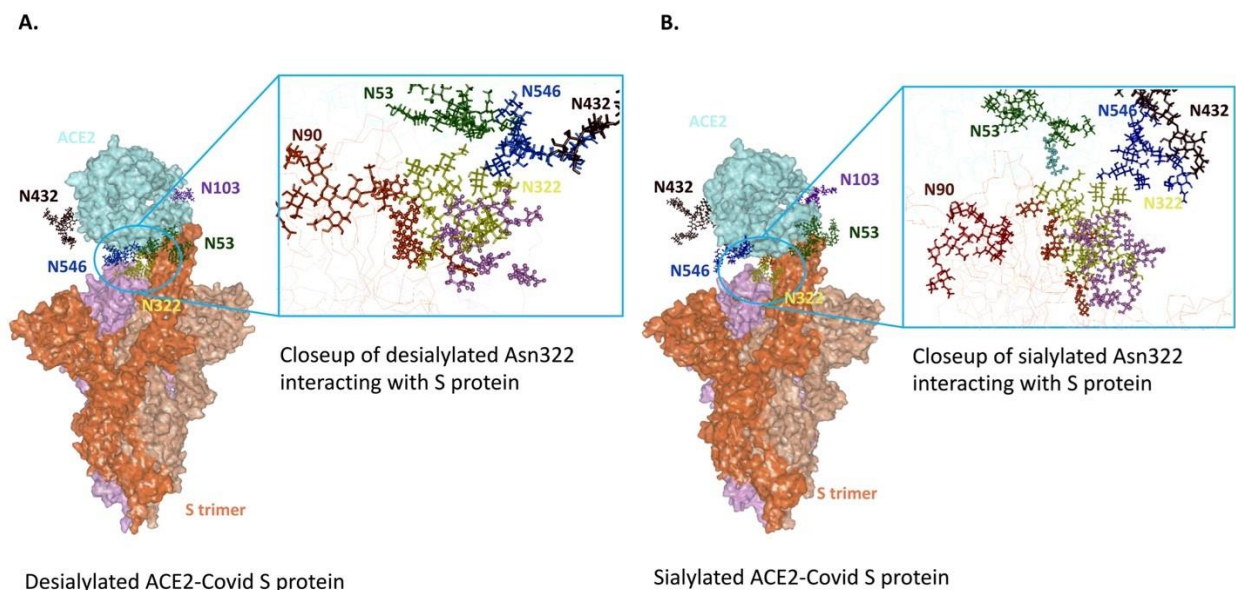


**Figure 4.12** Modelled sialylated and desialylated ACE2-Covid S protein complexes. 3D structural modeling of glycosylated ACE2 interacting with S-protein. Results from glycomics and glycoproteomics of HEPG2 cell lines were used to generate (A) fully-desialylated and (B) fully-sialylated homologs of ACE2, interacting with S-protein.

From the quantitative glycoproteomic results and the Protein Data Bank-derived complex (PDB ID: 7DF4)<sup>31</sup>, the most abundant glycan at each site were modelled with CHARMM-GUI.<sup>32</sup> The resulting structure, shown in the “up” conformation, was selected because it represented the activated complex prior to invasion. Molecular dynamics simulations were performed on the complex with solvent and associated ions for 5 ns (See Methods Section). After the simulations, the number of hydrogen bonds formed between the ACE2 glycans and S protein determined. For comparison, the same calculations were performed on the fully desialylated ACE2 homologs (**Figure 4.12B**). The results showed that many of the glycans on ACE2 interacted with the S protein through hydrogen bonding interactions. Comparison of the fully sialylated and desialylated glycans showed significantly lower number of hydrogen bonds (based on 3 Å, donor-acceptor

distances) particularly on Asn 90 (22 hydrogen bonds by glycan) and Asn 322 (51 hydrogen bonds by glycan) of the desialylated homolog (**Figure 4.13A**). These results are consistent with earlier simulations performed by Zhao et al on ACE2 - S who noted that both glycan sites were also the most interactive in the complex.<sup>21</sup> Furthermore, when the sialic acids were considered relative to other monosaccharide residues (3 by sialic acid at Asn 90, 15 by sialic acid at Asn 322), their contributions to the overall interactions were proportionally larger (**Figure 4.9B**).

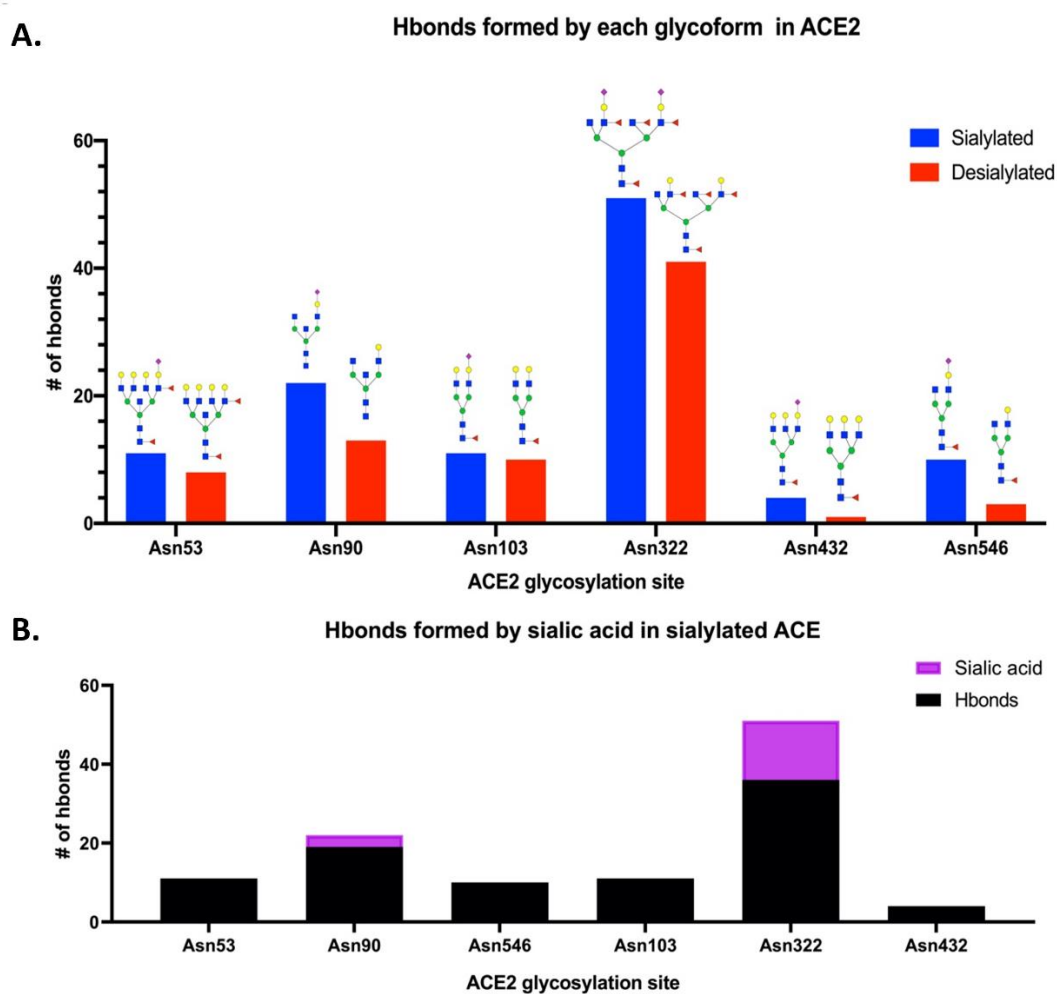


**Figure 4.13** Interactions of glycosylated ACE2 and S-protein were revealed using molecular dynamics simulations. (A) The number of intramolecular hydrogen bonds was drastically higher for each fully-sialylated N-glycan compared to the desialylated glycoform. (B) For Asn 90 and Asn 322, the sialic acid residue in the glycoform accounted for ~10% of hydrogen bonds.

## DISCUSSION

Glycans on the host cell membrane and on viral proteins play key roles in the infection of SARS-CoV-2. Viral glycosylation has been the primary focus of glycomic studies related to the virus. Indeed, the virus is highly glycosylated with at least 17 N-glycosylation and 2 O-glycosylation sites identified.<sup>19</sup> We found two occupied N-glycosites on Spike RBD (**Table S4.4**) consistent with earlier findings. However, the host cells were also highly glycosylated. The LC-MS glycomic profile of HepG2 shows cell membrane with an abundance of high mannose-type glycans as well as complex-type structures with a high degree of sialylation. These structures are also branched with a combination of bi, tri, and higher antennary structures. The HepG2 cell lines was selected for its expression of ACE2, and these highly sialylated branched structures were similarly present in the protein further alluding to the importance of sialylation in at least the host-virus adhesion process.

The results showed that sialic acid in human milk oligosaccharides (HMOs) can block the binding of virus on the cell membrane. These results are further supported by recent findings that show similar deflecting properties of sialylated HMOs toward the S protein of SARS-CoV-2<sup>26</sup> and illustrating further the protective nature of human milk against these pathogens. HMOs are similar to O-glycans in structure; however, N-glycans on membrane proteins similarly provide sialic acid on their termini. Altering the glycans on the cell membrane, while maintaining the expression levels of proteins such as ACE2, shows that sialic acid on the cell surface induces stronger binding to the virus. ACE2 is itself highly sialylated, in the cell line used in this study and from commercial sources (mainly from HEK293). ACE2 expressed recombinantly in other cell lines have similar glycosylation profiles that are similarly rich in sialylation. Deeper structural analysis showed that the binding prefers a specific linkage, namely  $\alpha$ -(2,6)-sialic acids. Interestingly, the human

influenza virus has a similar preference for binding.<sup>57-59</sup> Perhaps not coincidentally, the human epithelium is rich in  $\alpha$ -(2,6)-sialic acid, which is also more abundant than the isomer  $\alpha$ -(2,3)-sialic acid, the binding site of avian bird flu.

The binding of sialic acid point to specific protective measures by the host. In breastfed infants, HMOs provide some protection. Human milk is also full of proteins that are highly sialylated, such as the immunoglobulins and lactoferrins.<sup>60-63</sup> In adults, pathogen deflection is performed by the mucus layer in the lungs and gastrointestinal tract. SARS-CoV-2 is a respiratory disease reaching deep into the respiratory tract and the lungs. It also infects the intestine<sup>64</sup>, with both types of tissues protected by a mucus layer constructed around high molecular weight glycoproteins called mucins.<sup>65</sup> Mucin are expressed in epithelial surfaces of gastrointestinal, genitourinary, and respiratory tracts, where they also shield the surface against chemical and physical damages<sup>46</sup>. While mucins are covered primarily by O-glycans that are similar to human milk oligosaccharides, they contain the same sialic acid termini as N-glycans. The mucus layer therefore presents a myriad of potential binding sites for commensal and pathogenic microbes<sup>66</sup>,<sup>67</sup>, and shedding mucins is a defense strategy against pathogen infection.

High mannose glycans were also investigated as potential inhibitors of viral infections. The high mannose glycans were also strongly bound in the shorter version (RBD) of the S protein. However, in the longer homolog (S1 subunit) this binding was diminished. These results suggest that that there is a high mannose binding site on the S protein that is potentially shielded in the longer homolog. On the other hand, high mannose glycans are typically not found on epithelial cells<sup>16</sup> and are not abundant in the blood. However, they are much more abundant in the tissue samples compared to serum. These glycans are found in cancer cells<sup>68, 69</sup> and stem cells.<sup>70</sup> The levels of several oligomannose type glycans are upregulated in tumor tissue.<sup>71, 72</sup> The role of

mannose residue as a host receptor has been studied and proved in the microbe-host interactions, such as *Salmonella enterica* subsp. *enterica* serovar typhimurium (*S. typhimurium*)<sup>73</sup>, influenza virus<sup>74, 75</sup>, dengue virus<sup>76</sup> and human immunodeficiency virus (HIV).<sup>77</sup> Mannan is usually employed for studying mannose binding with virus.<sup>51, 52, 75, 78</sup> The mannans are highly heterogeneous in length and branching. The repeating  $\alpha$ -(1,6)-linked mannose backbone is usually branched by short chains of  $\alpha$ -(1-2) and  $\alpha$ -(1-3)-linked mannose structures.<sup>79</sup> In this study, we used oligomannose released from RNase B<sup>80</sup> instead of mannan. The released high mannose glycans were determined with mass spectrometry (**Figure 4.14**), and all those structures have been found in human cell glycomes.

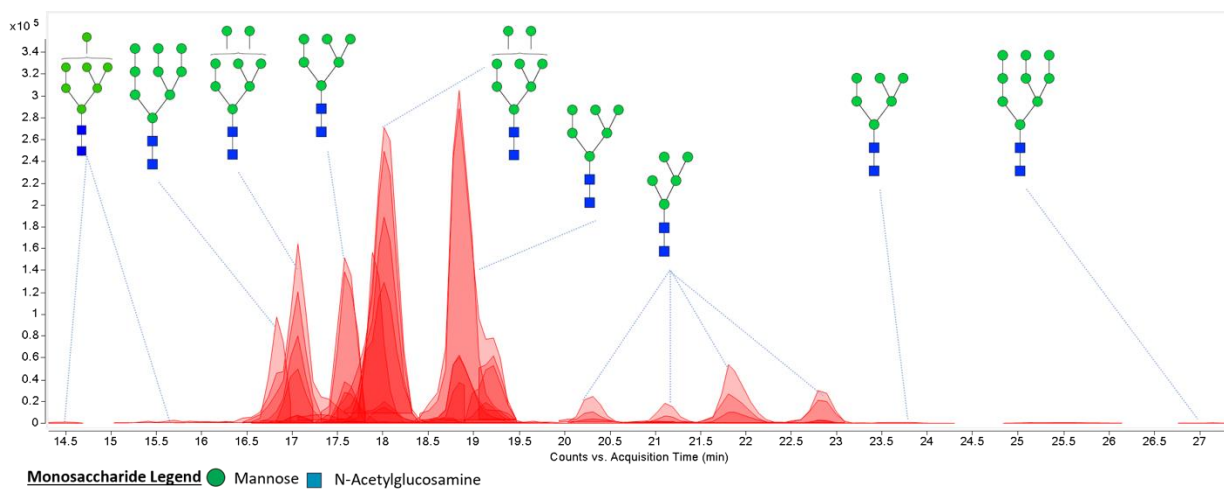


**Figure 4.14** Chromatogram of high mannose N-glycans released from RNase B. Abundant peaks are annotated with putative structures. Symbol nomenclature is used for representing glycan structures (<https://www.ncbi.nlm.nih.gov/glycans/snfg.html>).

The integrated method developed here, which includes alteration of cell surface glycan products through specific inhibitors, coupled with the enrichment of the membrane proteins and extensive glycomic and glycoproteomic analysis provides a new platform for obtaining structural specificity in host-microbe interactions. Glycans are common targets for many commensals and pathogens. This method will have great utility in identifying glycan targets of individual microbes

and even toxins that bind glycans. The method is made possible by recent advancements in novel glycosyl transferase inhibitors that produce specifically glycosylated membrane proteins. I should be noted that the conversion to a glycan type is never fully complete. There are residual endogenous glycans due to the differences in turnover of different glycoproteoform.<sup>81</sup> However, the ability to perform glycomic profiling with LC-MS provides a guiding assay to examine the extent of the glycomic transformation.

## CONCLUSIONS

The study supports a mechanism for binding of SARS-CoV-2 to the cell membrane that is primarily mediated by glycans. The preferred target of the S protein is sialylated glycans with  $\alpha$ -(2,6)-sialic acids on the termini positions. The virus likely binds to cells and tissues rich in sialylated glycans, whether N-, O-, and potentially even glycolipids that are found in the surface of the epithelial surface. The airway epithelium is rich in sialic acids and in particular,  $\alpha$ -(2,6)-sialic acids. In this regard, the human influenza virus and SARS-CoV-2 have the same binding preference on host membranes. Invasion of SARS-CoV-2 likely occurs when the virus fortuitously binds to the ACE2 protein, which itself is highly sialylated. The alignment between the S and the ACE2 protein is further facilitated by hydrogen binding interactions between the sialylated glycans of the host cell and the polypeptide of the S protein.

**Table S4.1** Glycoproteomic information of ACE2 derived from HepG2 cells

| Peptide Sequence                                      | Modification                                    | Modified Amino Acid | Modification Position | Glycans                           | Label in Figure 3 | Relative Abundance | Glycan Subtype  |
|---|---|---------------------|-----------------------|-----------------------------------|-------------------|--------------------|-----------------|
| FNHEAEDL<br>FYQSSLAS<br>WNYNTNIT<br>EENVQNM<br>NNAGDK | NGlycan/31<br>39.1366                           | N                   | 53                    | HexNAc(7)Hex(7)<br>Fuc(2)NeuAc(1) | 36                | 0.0326             | Sialyucosylated |
| FNHEAEDL<br>FYQSSLAS<br>WNYNTNIT<br>EENVQNM<br>NNAGDK | NGlycan/29<br>92.0834                           | N                   | 53                    | HexNAc(5)Hex(5)<br>Fuc(4)NeuAc(2) | 37                | 0.0298             | Sialyucosylated |
| FNHEAEDL<br>FYQSSLAS<br>WNYNTNIT<br>EENVQNM<br>NNAGDK | NGlycan/19<br>54.7036                           | N                   | 53                    | HexNAc(5)Hex(4)<br>Fuc(0)NeuAc(1) | 2                 | 0.0235             | Sialylated      |
| FNHEAEDL<br>FYQSSLAS<br>WNYNTNIT<br>EENVQNM<br>NNAGDK | NGlycan/21<br>57.7829                           | N                   | 53                    | HexNAc(6)Hex(4)<br>Fuc(0)NeuAc(1) | 12                | 0.0227             | Sialylated      |
| FNHEAEDL<br>FYQSSLAS<br>WNYNTNIT<br>EENVQNM<br>NNAGDK | NGlycan/23<br>19.8358;<br>Deamidated<br>/0.9840 | N,N                 | 53,58                 | HexNAc(6)Hex(5)<br>Fuc(0)NeuAc(1) | 6                 | 0.00539            | Sialylated      |
| FNHEAEDL<br>FYQSSLAS<br>WNYNTNIT<br>EENVQNM<br>NNAGDK | NGlycan/21<br>16.7564                           | N                   | 53                    | HexNAc(5)Hex(5)<br>Fuc(0)NeuAc(1) | 3                 | 0.0253             | Sialylated      |

|                              |  |     |       |                               |   |        |                 |
|------------------------------|--|-----|-------|-------------------------------|---|--------|-----------------|
| EQSTLAQM<br>YPLQEIQN<br>LTVK | NGlycan/20<br>59.7349                                | N   | 90    | HexNAc(4)Hex(5)Fuc(1)NeuAc(1) | 1 | 0.592  | Sialyucosylated |
| EQSTLAQM<br>YPLQEIQN<br>LTVK | Glu->pyro-Glu/-<br>18.0106;<br>NGlycan/20<br>59.7349 | E,N | 75,90 | HexNAc(4)Hex(5)Fuc(1)NeuAc(1) | 1 | 0.0441 | Sialyucosylated |
| EQSTLAQM<br>YPLQEIQN<br>LTVK | NGlycan/23<br>50.8304                                | N   | 90    | HexNAc(4)Hex(5)Fuc(1)NeuAc(2) | 2 | 0.275  | Sialyucosylated |
| EQSTLAQM<br>YPLQEIQN<br>LTVK | Glu->pyro-Glu/-<br>18.0106;<br>NGlycan/23<br>50.8304 | E,N | 75,90 | HexNAc(4)Hex(5)Fuc(1)NeuAc(2) | 2 | 0.0259 | Sialyucosylated |
| EQSTLAQM<br>YPLQEIQN<br>LTVK | NGlycan/18<br>97.6821                                | N   | 90    | HexNAc(4)Hex(4)Fuc(1)NeuAc(1) | 3 | 0.7    | Sialyucosylated |
| EQSTLAQM<br>YPLQEIQN<br>LTVK | Glu->pyro-Glu/-<br>18.0106;<br>NGlycan/18<br>97.6821 | E,N | 75,90 | HexNAc(4)Hex(4)Fuc(1)NeuAc(1) | 3 | 0.0349 | Sialyucosylated |
| EQSTLAQM<br>YPLQEIQN<br>LTVK | Deamidated /0.9840;<br>NGlycan/18<br>97.6821         | Q,N | 76,90 | HexNAc(4)Hex(4)Fuc(1)NeuAc(1) | 3 | 0.0126 | Sialyucosylated |
| EQSTLAQM<br>YPLQEIQN<br>LTVK | NGlycan/23<br>67.8457                                | N   | 90    | HexNAc(4)Hex(6)Fuc(2)NeuAc(1) | 4 | 0.0617 | Sialyucosylated |
| EQSTLAQM<br>YPLQEIQN<br>LTVK | Glu->pyro-Glu/-<br>18.0106;<br>NGlycan/23<br>67.8457 | E,N | 75,90 | HexNAc(4)Hex(6)Fuc(2)NeuAc(1) | 4 | 0.0223 | Sialyucosylated |

|                              |  |     |       |                               |    |        |                 |
|------------------------------|--|-----|-------|-------------------------------|----|--------|-----------------|
| EQSTLAQM<br>YPLQEIQN<br>LTVK | NGlycan/22<br>05.7928                                | N   | 90    | HexNAc(4)Hex(5)Fuc(2)NeuAc(1) | 5  | 0.0237 | Sialyucosylated |
| EQSTLAQM<br>YPLQEIQN<br>LTVK | NGlycan/27<br>89.9993                                | N   | 90    | HexNAc(6)Hex(7)Fuc(1)NeuAc(1) | 6  | 0.328  | Sialyucosylated |
| EQSTLAQM<br>YPLQEIQN<br>LTVK | NGlycan/24<br>24.8671                                | N   | 90    | HexNAc(5)Hex(6)Fuc(1)NeuAc(1) | 7  | 0.218  | Sialyucosylated |
| EQSTLAQM<br>YPLQEIQN<br>LTVK | Glu->pyro-Glu/-<br>18.0106;<br>NGlycan/24<br>24.8671 | E,N | 75,90 | HexNAc(5)Hex(6)Fuc(1)NeuAc(1) | 7  | 0.0155 | Sialyucosylated |
| EQSTLAQM<br>YPLQEIQN<br>LTVK | NGlycan/27<br>15.9625                                | N   | 90    | HexNAc(5)Hex(6)Fuc(1)NeuAc(2) | 8  | 0.221  | Sialyucosylated |
| EQSTLAQM<br>YPLQEIQN<br>LTVK | Glu->pyro-Glu/-<br>18.0106;<br>NGlycan/27<br>15.9625 | E,N | 75,90 | HexNAc(5)Hex(6)Fuc(1)NeuAc(2) | 8  | 0.0392 | Sialyucosylated |
| EQSTLAQM<br>YPLQEIQN<br>LTVK | NGlycan/22<br>62.8143                                | N   | 90    | HexNAc(5)Hex(5)Fuc(1)NeuAc(1) | 9  | 0.212  | Sialyucosylated |
| EQSTLAQM<br>YPLQEIQN<br>LTVK | NGlycan/21<br>00.7615                                | N   | 90    | HexNAc(5)Hex(4)Fuc(1)NeuAc(1) | 10 | 0.149  | Sialyucosylated |
| EQSTLAQM<br>YPLQEIQN<br>LTVK | NGlycan/30<br>81.0947                                | N   | 90    | HexNAc(6)Hex(7)Fuc(1)NeuAc(2) | 11 | 0.0402 | Sialyucosylated |
| EQSTLAQM<br>YPLQEIQN<br>LTVK | Glu->pyro-Glu/-<br>18.0106;<br>NGlycan/27<br>32.9779 | E,N | 75,90 | HexNAc(5)Hex(7)Fuc(2)NeuAc(1) | 12 | 0.177  | Sialyucosylated |

|                              |  |     |       |                               |    |        |                 |
|------------------------------|--|-----|-------|-------------------------------|----|--------|-----------------|
| EQSTLAQM<br>YPLQEIQN<br>LTVK | NGlycan/27<br>32.9779                                | N   | 90    | HexNAc(5)Hex(7)Fuc(2)NeuAc(1) | 12 | 0.127  | Sialyucosylated |
| EQSTLAQM<br>YPLQEIQN<br>LTVK | NGlycan/30<br>07.0580                                | N   | 90    | HexNAc(5)Hex(6)Fuc(1)NeuAc(3) | 13 | 0.0612 | Sialyucosylated |
| EQSTLAQM<br>YPLQEIQN<br>LTVK | NGlycan/25<br>53.9097                                | N   | 90    | HexNAc(5)Hex(5)Fuc(1)NeuAc(2) | 14 | 0.153  | Sialyucosylated |
| EQSTLAQM<br>YPLQEIQN<br>LTVK | Glu->pyro-Glu/-<br>18.0106;<br>NGlycan/25<br>53.9097 | E,N | 75,90 | HexNAc(5)Hex(5)Fuc(1)NeuAc(2) | 14 | 0.0247 | Sialyucosylated |
| EQSTLAQM<br>YPLQEIQN<br>LTVK | NGlycan/22<br>21.7878                                | N   | 90    | HexNAc(4)Hex(6)Fuc(1)NeuAc(1) | 15 | 0.0205 | Sialyucosylated |
| EQSTLAQM<br>YPLQEIQN<br>LTVK | NGlycan/30<br>24.0733                                | N   | 90    | HexNAc(5)Hex(7)Fuc(2)NeuAc(2) | 16 | 0.034  | Sialyucosylated |
| EQSTLAQM<br>YPLQEIQN<br>LTVK | Glu->pyro-Glu/-<br>18.0106;<br>NGlycan/30<br>82.1151 | E,N | 75,90 | HexNAc(6)Hex(7)Fuc(3)NeuAc(1) | 17 | 0.124  | Sialyucosylated |
| EQSTLAQM<br>YPLQEIQN<br>LTVK | NGlycan/24<br>65.8937                                | N   | 90    | HexNAc(6)Hex(5)Fuc(1)NeuAc(1) | 24 | 0.0757 | Sialyucosylated |
| EQSTLAQM<br>YPLQEIQN<br>LTVK | Glu->pyro-Glu/-<br>18.0106;<br>NGlycan/27<br>74.0044 | E,N | 75,90 | HexNAc(6)Hex(6)Fuc(2)NeuAc(1) | 25 | 0.075  | Sialyucosylated |
| EQSTLAQM<br>YPLQEIQN<br>LTVK | NGlycan/26<br>27.9465                                | N   | 90    | HexNAc(6)Hex(6)Fuc(1)NeuAc(1) | 26 | 0.0389 | Sialyucosylated |

|                              |  |     |       |                               |    |        |                     |
|------------------------------|--|-----|-------|-------------------------------|----|--------|---------------------|
| EQSTLAQM<br>YPLQEIQN<br>LTVK | NGlycan/33<br>72.1902                                    | N   | 90    | HexNAc(6)Hex(7)Fuc(1)NeuAc(3) | 27 | 0.0246 | Sialyfu<br>osylated |
| EQSTLAQM<br>YPLQEIQN<br>LTVK | NGlycan/29<br>19.0419                                    | N   | 90    | HexNAc(6)Hex(6)Fuc(1)NeuAc(2) | 28 | 0.0411 | Sialyfu<br>osylated |
| EQSTLAQM<br>YPLQEIQN<br>LTVK | NGlycan/25<br>70.9250                                    | N   | 90    | HexNAc(5)Hex(6)Fuc(2)NeuAc(1) | 33 | 0.0272 | Sialyfu<br>osylated |
| EQSTLAQM<br>YPLQEIQN<br>LTVK | Glu->pyro-<br>Glu/-<br>18.0106;<br>NGlycan/25<br>70.9250 | E,N | 75,90 | HexNAc(5)Hex(6)Fuc(2)NeuAc(1) | 33 | 0.0225 | Sialyfu<br>osylated |
| EQSTLAQM<br>YPLQEIQN<br>LTVK | NGlycan/32<br>10.1373                                    | N   | 90    | HexNAc(6)Hex(6)Fuc(1)NeuAc(3) | 41 | 0.0106 | Sialyfu<br>osylated |
| EQSTLAQM<br>YPLQEIQN<br>LTVK | NGlycan/20<br>75.7298                                    | N   | 90    | HexNAc(4)Hex(6)Fuc(0)NeuAc(1) | 1  | 0.0551 | Sialylate<br>d      |
| EQSTLAQM<br>YPLQEIQN<br>LTVK | NGlycan/19<br>54.7036                                    | N   | 90    | HexNAc(5)Hex(4)Fuc(0)NeuAc(1) | 2  | 2.02   | Sialylate<br>d      |
| EQSTLAQM<br>YPLQEIQN<br>LTVK | Glu->pyro-<br>Glu/-<br>18.0106;<br>NGlycan/19<br>54.7036 | E,N | 75,90 | HexNAc(5)Hex(4)Fuc(0)NeuAc(1) | 2  | 0.123  | Sialylate<br>d      |
| EQSTLAQM<br>YPLQEIQN<br>LTVK | NGlycan/21<br>16.7564                                    | N   | 90    | HexNAc(5)Hex(5)Fuc(0)NeuAc(1) | 3  | 2      | Sialylate<br>d      |
| EQSTLAQM<br>YPLQEIQN<br>LTVK | Glu->pyro-<br>Glu/-<br>18.0106;<br>NGlycan/21<br>16.7564 | E,N | 75,90 | HexNAc(5)Hex(5)Fuc(0)NeuAc(1) | 3  | 0.11   | Sialylate<br>d      |

|                              |  |     |       |                                   |   |        |            |
|------------------------------|--|-----|-------|-----------------------------------|---|--------|------------|
| EQSTLAQM<br>YPLQEIQN<br>LTVK | NGlycan/19<br>13.6770                                | N   | 90    | HexNAc(4)Hex(5)<br>Fuc(0)NeuAc(1) | 4 | 0.51   | Sialylated |
| EQSTLAQM<br>YPLQEIQN<br>LTVK | Glu->pyro-Glu/-<br>18.0106;<br>NGlycan/19<br>13.6770 | E,N | 75,90 | HexNAc(4)Hex(5)<br>Fuc(0)NeuAc(1) | 4 | 0.0556 | Sialylated |
| EQSTLAQM<br>YPLQEIQN<br>LTVK | NGlycan/24<br>07.8518                                | N   | 90    | HexNAc(5)Hex(5)<br>Fuc(0)NeuAc(2) | 5 | 0.748  | Sialylated |
| EQSTLAQM<br>YPLQEIQN<br>LTVK | Glu->pyro-Glu/-<br>18.0106;<br>NGlycan/24<br>07.8518 | E,N | 75,90 | HexNAc(5)Hex(5)<br>Fuc(0)NeuAc(2) | 5 | 0.134  | Sialylated |
| EQSTLAQM<br>YPLQEIQN<br>LTVK | NGlycan/23<br>19.8358                                | N   | 90    | HexNAc(6)Hex(5)<br>Fuc(0)NeuAc(1) | 6 | 0.587  | Sialylated |
| EQSTLAQM<br>YPLQEIQN<br>LTVK | NGlycan/27<br>72.9840                                | N   | 90    | HexNAc(6)Hex(6)<br>Fuc(0)NeuAc(2) | 7 | 0.552  | Sialylated |
| EQSTLAQM<br>YPLQEIQN<br>LTVK | Glu->pyro-Glu/-<br>18.0106;<br>NGlycan/27<br>72.9840 | E,N | 75,90 | HexNAc(6)Hex(6)<br>Fuc(0)NeuAc(2) | 7 | 0.0723 | Sialylated |
| EQSTLAQM<br>YPLQEIQN<br>LTVK | NGlycan/24<br>81.8886                                | N   | 90    | HexNAc(6)Hex(6)<br>Fuc(0)NeuAc(1) | 8 | 0.49   | Sialylated |
| EQSTLAQM<br>YPLQEIQN<br>LTVK | NGlycan/17<br>51.6242                                | N   | 90    | HexNAc(4)Hex(4)<br>Fuc(0)NeuAc(1) | 9 | 0.47   | Sialylated |
| EQSTLAQM<br>YPLQEIQN<br>LTVK | Glu->pyro-Glu/-<br>18.0106;                          | E,N | 75,90 | HexNAc(4)Hex(4)<br>Fuc(0)NeuAc(1) | 9 | 0.0279 | Sialylated |

|                              |  |     |       |                                   |    |        |            |
|------------------------------|--|-----|-------|-----------------------------------|----|--------|------------|
|                              | NGlycan/17<br>51.6242                        |     |       |                                   |    |        |            |
| EQSTLAQM<br>YPLQEIQN<br>LTVK | NGlycan/22<br>04.7724                        | N   | 90    | HexNAc(4)Hex(5)<br>Fuc(0)NeuAc(2) | 10 | 0.125  | Sialylated |
| EQSTLAQM<br>YPLQEIQN<br>LTVK | NGlycan/26<br>10.9312                        | N   | 90    | HexNAc(6)Hex(5)<br>Fuc(0)NeuAc(2) | 11 | 0.437  | Sialylated |
| EQSTLAQM<br>YPLQEIQN<br>LTVK | NGlycan/21<br>57.7829                        | N   | 90    | HexNAc(6)Hex(4)<br>Fuc(0)NeuAc(1) | 12 | 0.418  | Sialylated |
| EQSTLAQM<br>YPLQEIQN<br>LTVK | NGlycan/22<br>78.8092                        | N   | 90    | HexNAc(5)Hex(6)<br>Fuc(0)NeuAc(1) | 13 | 0.136  | Sialylated |
| EQSTLAQM<br>YPLQEIQN<br>LTVK | NGlycan/25<br>69.9046                        | N   | 90    | HexNAc(5)Hex(6)<br>Fuc(0)NeuAc(2) | 14 | 0.122  | Sialylated |
| EQSTLAQM<br>YPLQEIQN<br>LTVK | NGlycan/29<br>76.0634                        | N   | 90    | HexNAc(7)Hex(6)<br>Fuc(0)NeuAc(2) | 15 | 0.0988 | Sialylated |
| EQSTLAQM<br>YPLQEIQN<br>LTVK | NGlycan/27<br>31.9575                        | N   | 90    | HexNAc(5)Hex(7)<br>Fuc(0)NeuAc(2) | 17 | 0.0226 | Sialylated |
| EQSTLAQM<br>YPLQEIQN<br>LTVK | NGlycan/15<br>48.5448                        | N   | 90    | HexNAc(3)Hex(4)<br>Fuc(0)NeuAc(1) | 19 | 0.0133 | Sialylated |
| EQSTLAQM<br>YPLQEIQN<br>LTVK | Deamidated /0.9840;<br>NGlycan/24<br>40.8620 | Q,N | 89,90 | HexNAc(5)Hex(7)<br>Fuc(0)NeuAc(1) | 20 | 0.0193 | Sialylated |
| EQSTLAQM<br>YPLQEIQN<br>LTVK | Deamidated /0.9840;<br>NGlycan/24<br>40.8620 | Q,N | 81,90 | HexNAc(5)Hex(7)<br>Fuc(0)NeuAc(1) | 20 | 0.0181 | Sialylated |

|                              |  |     |       |                               |    |        |             |
|------------------------------|--|-----|-------|-------------------------------|----|--------|-------------|
| EQSTLAQM<br>YPLQEIQN<br>LTVK | NGlycan/29<br>35.0368                                | N   | 90    | HexNAc(6)Hex(7)Fuc(0)NeuAc(2) | 21 | 0.0184 | Sialylated  |
| EQSTLAQM<br>YPLQEIQN<br>LTVK | NGlycan/28<br>61.0001                                | N   | 90    | HexNAc(5)Hex(6)Fuc(0)NeuAc(3) | 22 | 0.0142 | Sialylated  |
| EQSTLAQM<br>YPLQEIQN<br>LTVK | NGlycan/14<br>44.5339                                | N   | 90    | HexNAc(4)Hex(3)Fuc(1)NeuAc(0) | 1  | 0.112  | Fucosylated |
| EQSTLAQM<br>YPLQEIQN<br>LTVK | NGlycan/16<br>06.5867                                | N   | 90    | HexNAc(4)Hex(4)Fuc(1)NeuAc(0) | 2  | 0.428  | Fucosylated |
| EQSTLAQM<br>YPLQEIQN<br>LTVK | NGlycan/17<br>68.6395                                | N   | 90    | HexNAc(4)Hex(5)Fuc(1)NeuAc(0) | 3  | 0.251  | Fucosylated |
| EQSTLAQM<br>YPLQEIQN<br>LTVK | NGlycan/20<br>76.7502                                | N   | 90    | HexNAc(4)Hex(6)Fuc(2)NeuAc(0) | 4  | 0.297  | Fucosylated |
| EQSTLAQM<br>YPLQEIQN<br>LTVK | Glu->pyro-Glu/-<br>18.0106;<br>NGlycan/21<br>33.7717 | E,N | 75,90 | HexNAc(5)Hex(6)Fuc(1)NeuAc(0) | 5  | 1.13   | Fucosylated |
| EQSTLAQM<br>YPLQEIQN<br>LTVK | NGlycan/21<br>33.7717                                | N   | 90    | HexNAc(5)Hex(6)Fuc(1)NeuAc(0) | 5  | 0.0772 | Fucosylated |
| EQSTLAQM<br>YPLQEIQN<br>LTVK | NGlycan/19<br>14.6974                                | N   | 90    | HexNAc(4)Hex(5)Fuc(2)NeuAc(0) | 6  | 0.315  | Fucosylated |
| EQSTLAQM<br>YPLQEIQN<br>LTVK | Glu->pyro-Glu/-<br>18.0106;<br>NGlycan/26<br>44.9618 | E,N | 75,90 | HexNAc(6)Hex(7)Fuc(2)NeuAc(0) | 7  | 0.365  | Fucosylated |
| EQSTLAQM<br>YPLQEIQN<br>LTVK | NGlycan/18<br>09.6661                                | N   | 90    | HexNAc(5)Hex(4)Fuc(1)NeuAc(0) | 9  | 0.224  | Fucosylated |

|                              |  |     |       |                                   |    |        |             |
|------------------------------|--|-----|-------|-----------------------------------|----|--------|-------------|
| EQSTLAQM<br>YPLQEIQN<br>LTVK | NGlycan/17<br>52.6446                                | N   | 90    | HexNAc(4)Hex(4)<br>Fuc(2)NeuAc(0) | 10 | 0.0827 | Fucosylated |
| EQSTLAQM<br>YPLQEIQN<br>LTVK | Glu->pyro-Glu/-<br>18.0106;<br>NGlycan/22<br>79.8296 | E,N | 75,90 | HexNAc(5)Hex(6)<br>Fuc(2)NeuAc(0) | 11 | 0.334  | Fucosylated |
| EQSTLAQM<br>YPLQEIQN<br>LTVK | NGlycan/22<br>79.8296                                | N   | 90    | HexNAc(5)Hex(6)<br>Fuc(2)NeuAc(0) | 11 | 0.101  | Fucosylated |
| EQSTLAQM<br>YPLQEIQN<br>LTVK | NGlycan/19<br>71.7189                                | N   | 90    | HexNAc(5)Hex(5)<br>Fuc(1)NeuAc(0) | 13 | 0.136  | Fucosylated |
| EQSTLAQM<br>YPLQEIQN<br>LTVK | Glu->pyro-Glu/-<br>18.0106;<br>NGlycan/19<br>71.7189 | E,N | 75,90 | HexNAc(5)Hex(5)<br>Fuc(1)NeuAc(0) | 13 | 0.0362 | Fucosylated |
| EQSTLAQM<br>YPLQEIQN<br>LTVK | NGlycan/24<br>41.8824                                | N   | 90    | HexNAc(5)Hex(7)<br>Fuc(2)NeuAc(0) | 14 | 0.0567 | Fucosylated |
| EQSTLAQM<br>YPLQEIQN<br>LTVK | Glu->pyro-Glu/-<br>18.0106;<br>NGlycan/21<br>17.7768 | E,N | 75,90 | HexNAc(5)Hex(5)<br>Fuc(2)NeuAc(0) | 15 | 0.138  | Fucosylated |
| EQSTLAQM<br>YPLQEIQN<br>LTVK | NGlycan/21<br>17.7768                                | N   | 90    | HexNAc(5)Hex(5)<br>Fuc(2)NeuAc(0) | 15 | 0.0945 | Fucosylated |
| EQSTLAQM<br>YPLQEIQN<br>LTVK | Deamidated /0.9840;<br>NGlycan/21<br>17.7768         | Q,N | 86,90 | HexNAc(5)Hex(5)<br>Fuc(2)NeuAc(0) | 15 | 0.0191 | Fucosylated |
| EQSTLAQM<br>YPLQEIQN<br>LTVK | NGlycan/19<br>30.6923                                | N   | 90    | HexNAc(4)Hex(6)<br>Fuc(1)NeuAc(0) | 16 | 0.135  | Fucosylated |

|                              |  |     |       |                                   |    |             |                 |
|------------------------------|--|-----|-------|-----------------------------------|----|-------------|-----------------|
| EQSTLAQM<br>YPLQEIQN<br>LTVK | Glu->pyro-<br>Glu/-<br>18.0106;<br>NGlycan/19<br>30.6923 | E,N | 75,90 | HexNAc(4)Hex(6)<br>Fuc(1)NeuAc(0) | 16 | 0.0975      | Fucosyl<br>ated |
| EQSTLAQM<br>YPLQEIQN<br>LTVK | NGlycan/20<br>92.7452                                    | N   | 90    | HexNAc(4)Hex(7)<br>Fuc(1)NeuAc(0) | 24 | 0.0493      | Fucosyl<br>ated |
| EQSTLAQM<br>YPLQEIQN<br>LTVK | NGlycan/16<br>22.5816                                    | N   | 90    | HexNAc(4)Hex(5)<br>Fuc(0)NeuAc(0) | 2  | 0.455       | Undecor<br>ated |
| EQSTLAQM<br>YPLQEIQN<br>LTVK | Deamidated<br>/0.9840;<br>NGlycan/16<br>22.5816          | Q,N | 86,90 | HexNAc(4)Hex(5)<br>Fuc(0)NeuAc(0) | 2  | 0.181       | Undecor<br>ated |
| EQSTLAQM<br>YPLQEIQN<br>LTVK | NGlycan/16<br>63.6082                                    | N   | 90    | HexNAc(5)Hex(4)<br>Fuc(0)NeuAc(0) | 4  | 1.22        | Undecor<br>ated |
| EQSTLAQM<br>YPLQEIQN<br>LTVK | Deamidated<br>/0.9840;<br>NGlycan/16<br>63.6082          | Q,N | 89,90 | HexNAc(5)Hex(4)<br>Fuc(0)NeuAc(0) | 4  | 0.015       | Undecor<br>ated |
| EQSTLAQM<br>YPLQEIQN<br>LTVK | NGlycan/18<br>25.6610                                    | N   | 90    | HexNAc(5)Hex(5)<br>Fuc(0)NeuAc(0) | 5  | 0.659       | Undecor<br>ated |
| EQSTLAQM<br>YPLQEIQN<br>LTVK | Deamidated<br>/0.9840;<br>NGlycan/18<br>25.6610          | Q,N | 86,90 | HexNAc(5)Hex(5)<br>Fuc(0)NeuAc(0) | 5  | 0.0298      | Undecor<br>ated |
| EQSTLAQM<br>YPLQEIQN<br>LTVK | NGlycan/15<br>01.5553                                    | N   | 90    | HexNAc(5)Hex(3)<br>Fuc(0)NeuAc(0) | 6  | 0.433       | Undecor<br>ated |
| EQSTLAQM<br>YPLQEIQN<br>LTVK | Deamidated<br>/0.9840;<br>NGlycan/15<br>01.5553          | Q,N | 89,90 | HexNAc(5)Hex(3)<br>Fuc(0)NeuAc(0) | 6  | 0.0037<br>9 | Undecor<br>ated |

|   |  |     |         |                                   |    |        |                   |
|---|--|-----|---------|-----------------------------------|----|--------|-------------------|
| EQSTLAQM<br>YPLQEIQN<br>LTVK                                | NGlycan/14<br>60.5288                                | N   | 90      | HexNAc(4)Hex(4)<br>Fuc(0)NeuAc(0) | 7  | 0.351  | Undecorated       |
| EQSTLAQM<br>YPLQEIQN<br>LTVK                                | NGlycan/18<br>66.6875                                | N   | 90      | HexNAc(6)Hex(4)<br>Fuc(0)NeuAc(0) | 9  | 0.195  | Undecorated       |
| EQSTLAQM<br>YPLQEIQN<br>LTVK                                | NGlycan/20<br>28.7404                                | N   | 90      | HexNAc(6)Hex(5)<br>Fuc(0)NeuAc(0) | 11 | 0.133  | Undecorated       |
| EQSTLAQM<br>YPLQEIQN<br>LTVK                                | NGlycan/21<br>90.7932                                | N   | 90      | HexNAc(6)Hex(6)<br>Fuc(0)NeuAc(0) | 12 | 0.0716 | Undecorated       |
| EQSTLAQM<br>YPLQEIQN<br>LTVK                                | NGlycan/19<br>87.7138                                | N   | 90      | HexNAc(5)Hex(6)<br>Fuc(0)NeuAc(0) | 14 | 0.0451 | Undecorated       |
| EQSTLAQM<br>YPLQEIQN<br>LTVK                                | NGlycan/12<br>98.4760                                | N   | 90      | HexNAc(4)Hex(3)<br>Fuc(0)NeuAc(0) | 16 | 0.0407 | Undecorated       |
| EQSTLAQM<br>YPLQEIQN<br>LTVK                                | Glu->pyro-Glu/-<br>18.0106;<br>NGlycan/17<br>02.5813 | E,N | 75,90   | HexNAc(2)Hex(8)<br>Fuc(0)NeuAc(0) | 1  | 0.114  | High Mannose      |
| EQSTLAQM<br>YPLQEIQN<br>LTVK<br>LQKLQ<br>ALQQNGSS<br>VLSEDK | Glu->pyro-Glu/-<br>18.0106;<br>NGlycan/25<br>69.9046 | E,N | 75,90   | HexNAc(5)Hex(6)<br>Fuc(0)NeuAc(2) | 14 | 0.0386 | Sialylated        |
| LQLQALQQ<br>NGSSVLSE<br>DK                                  | NGlycan/20<br>59.7349                                | N   | 103     | HexNAc(4)Hex(5)<br>Fuc(1)NeuAc(1) | 1  | 5.19   | Sialylfucosylated |
| LQLQALQQ<br>NGSSVLSE<br>DK                                  | Deamidated /0.9840;<br>NGlycan/20<br>59.7349         | Q,N | 101,103 | HexNAc(4)Hex(5)<br>Fuc(1)NeuAc(1) | 1  | 0.0322 | Sialylfucosylated |

|                            |   |     |         |                                   |   |         |                      |
|----------------------------|---|-----|---------|-----------------------------------|---|---------|----------------------|
| LQLQALQQ<br>NGSSVLSE<br>DK | NGlycan/23<br>50.8304                           | N   | 103     | HexNAc(4)Hex(5)<br>Fuc(1)NeuAc(2) | 2 | 3.91    | Sialyfu-<br>osylated |
| LQLQALQQ<br>NGSSVLSE<br>DK | NGlycan/18<br>97.6821                           | N   | 103     | HexNAc(4)Hex(4)<br>Fuc(1)NeuAc(1) | 3 | 1.79    | Sialyfu-<br>osylated |
| LQLQALQQ<br>NGSSVLSE<br>DK | Deamidated<br>/0.9840;<br>NGlycan/18<br>97.6821 | Q,N | 98,103  | HexNAc(4)Hex(4)<br>Fuc(1)NeuAc(1) | 3 | 0.0119  | Sialyfu-<br>osylated |
| LQLQALQQ<br>NGSSVLSE<br>DK | Deamidated<br>/0.9840;<br>NGlycan/18<br>97.6821 | Q,N | 101,103 | HexNAc(4)Hex(4)<br>Fuc(1)NeuAc(1) | 3 | 0.0118  | Sialyfu-<br>osylated |
| LQLQALQQ<br>NGSSVLSE<br>DK | Deamidated<br>/0.9840;<br>NGlycan/18<br>97.6821 | Q,N | 102,103 | HexNAc(4)Hex(4)<br>Fuc(1)NeuAc(1) | 3 | 0.00758 | Sialyfu-<br>osylated |
| LQLQALQQ<br>NGSSVLSE<br>DK | NGlycan/23<br>67.8457                           | N   | 103     | HexNAc(4)Hex(6)<br>Fuc(2)NeuAc(1) | 4 | 1.47    | Sialyfu-<br>osylated |
| LQLQALQQ<br>NGSSVLSE<br>DK | Deamidated<br>/0.9840;<br>NGlycan/23<br>67.8457 | Q,N | 101,103 | HexNAc(4)Hex(6)<br>Fuc(2)NeuAc(1) | 4 | 0.0161  | Sialyfu-<br>osylated |
| LQLQALQQ<br>NGSSVLSE<br>DK | NGlycan/22<br>05.7928                           | N   | 103     | HexNAc(4)Hex(5)<br>Fuc(2)NeuAc(1) | 5 | 0.595   | Sialyfu-<br>osylated |
| LQLQALQQ<br>NGSSVLSE<br>DK | NGlycan/24<br>24.8671                           | N   | 103     | HexNAc(5)Hex(6)<br>Fuc(1)NeuAc(1) | 7 | 0.0542  | Sialyfu-<br>osylated |
| LQLQALQQ<br>NGSSVLSE<br>DK | NGlycan/27<br>15.9625                           | N   | 103     | HexNAc(5)Hex(6)<br>Fuc(1)NeuAc(2) | 8 | 0.0695  | Sialyfu-<br>osylated |
| LQLQALQQ<br>NGSSVLSE<br>DK | NGlycan/22<br>62.8143                           | N   | 103     | HexNAc(5)Hex(5)<br>Fuc(1)NeuAc(1) | 9 | 0.0782  | Sialyfu-<br>osylated |

|                            |   |     |             |                               |    |             |                     |
|----------------------------|---|-----|-------------|-------------------------------|----|-------------|---------------------|
| LQLQALQQ<br>NGSSVLSE<br>DK | NGlycan/30<br>07.0580                           | N   | 103         | HexNAc(5)Hex(6)Fuc(1)NeuAc(3) | 13 | 0.0252      | Sialyfu<br>osylated |
| LQLQALQQ<br>NGSSVLSE<br>DK | Deamidated<br>/0.9840;<br>NGlycan/22<br>21.7878 | Q,N | 101,10<br>3 | HexNAc(4)Hex(6)Fuc(1)NeuAc(1) | 15 | 0.153       | Sialyfu<br>osylated |
| LQLQALQQ<br>NGSSVLSE<br>DK | NGlycan/16<br>94.6027                           | N   | 103         | HexNAc(3)Hex(4)Fuc(1)NeuAc(1) | 18 | 0.0109      | Sialyfu<br>osylated |
| LQLQALQQ<br>NGSSVLSE<br>DK | NGlycan/27<br>16.9829                           | N   | 103         | HexNAc(5)Hex(6)Fuc(3)NeuAc(1) | 22 | 0.0145      | Sialyfu<br>osylated |
| LQLQALQQ<br>NGSSVLSE<br>DK | NGlycan/23<br>91.8569                           | N   | 103         | HexNAc(5)Hex(4)Fuc(1)NeuAc(2) | 30 | 0.0604      | Sialyfu<br>osylated |
| LQLQALQQ<br>NGSSVLSE<br>DK | NGlycan/24<br>08.8722                           | N   | 103         | HexNAc(5)Hex(5)Fuc(2)NeuAc(1) | 42 | 0.0177      | Sialyfu<br>osylated |
| LQLQALQQ<br>NGSSVLSE<br>DK | Deamidated<br>/0.9840;<br>NGlycan/24<br>08.8722 | Q,N | 101,10<br>3 | HexNAc(5)Hex(5)Fuc(2)NeuAc(1) | 42 | 0.0098<br>4 | Sialyfu<br>osylated |
| LQLQALQQ<br>NGSSVLSE<br>DK | NGlycan/25<br>86.9200                           | N   | 103         | HexNAc(5)Hex(7)Fuc(1)NeuAc(1) | 45 | 0.0061<br>9 | Sialyfu<br>osylated |
| LQLQALQQ<br>NGSSVLSE<br>DK | Deamidated<br>/0.9840;<br>NGlycan/20<br>75.7298 | Q,N | 98,103      | HexNAc(4)Hex(6)Fuc(0)NeuAc(1) | 1  | 2.24        | Sialylate<br>d      |
| LQLQALQQ<br>NGSSVLSE<br>DK | NGlycan/19<br>54.7036                           | N   | 103         | HexNAc(5)Hex(4)Fuc(0)NeuAc(1) | 2  | 0.0519      | Sialylate<br>d      |
| LQLQALQQ<br>NGSSVLSE<br>DK | Deamidated<br>/0.9840;<br>NGlycan/21<br>16.7564 | Q,N | 101,10<br>3 | HexNAc(5)Hex(5)Fuc(0)NeuAc(1) | 3  | 0.0274      | Sialylate<br>d      |

|                            |  |     |         |                                   |    |        |            |
|----------------------------|--|-----|---------|-----------------------------------|----|--------|------------|
| LQLQALQQ<br>NGSSVLSE<br>DK | NGlycan/21<br>16.7564                        | N   | 103     | HexNAc(5)Hex(5)<br>Fuc(0)NeuAc(1) | 3  | 0.174  | Sialylated |
| LQLQALQQ<br>NGSSVLSE<br>DK | Deamidated /0.9840;<br>NGlycan/19<br>13.6770 | Q,N | 98,103  | HexNAc(4)Hex(5)<br>Fuc(0)NeuAc(1) | 4  | 0.44   | Sialylated |
| LQLQALQQ<br>NGSSVLSE<br>DK | Deamidated /0.9840;<br>NGlycan/19<br>13.6770 | Q,N | 102,103 | HexNAc(4)Hex(5)<br>Fuc(0)NeuAc(1) | 4  | 0.429  | Sialylated |
| LQLQALQQ<br>NGSSVLSE<br>DK | NGlycan/19<br>13.6770                        | N   | 103     | HexNAc(4)Hex(5)<br>Fuc(0)NeuAc(1) | 4  | 0.0206 | Sialylated |
| LQLQALQQ<br>NGSSVLSE<br>DK | Deamidated /0.9840;<br>NGlycan/19<br>13.6770 | Q,N | 101,103 | HexNAc(4)Hex(5)<br>Fuc(0)NeuAc(1) | 4  | 0.0057 | Sialylated |
| LQLQALQQ<br>NGSSVLSE<br>DK | NGlycan/24<br>07.8518                        | N   | 103     | HexNAc(5)Hex(5)<br>Fuc(0)NeuAc(2) | 5  | 0.0204 | Sialylated |
| LQLQALQQ<br>NGSSVLSE<br>DK | NGlycan/17<br>51.6242                        | N   | 103     | HexNAc(4)Hex(4)<br>Fuc(0)NeuAc(1) | 9  | 0.317  | Sialylated |
| LQLQALQQ<br>NGSSVLSE<br>DK | NGlycan/22<br>04.7724                        | N   | 103     | HexNAc(4)Hex(5)<br>Fuc(0)NeuAc(2) | 10 | 0.469  | Sialylated |
| LQLQALQQ<br>NGSSVLSE<br>DK | NGlycan/22<br>78.8092                        | N   | 103     | HexNAc(5)Hex(6)<br>Fuc(0)NeuAc(1) | 13 | 0.0777 | Sialylated |
| LQLQALQQ<br>NGSSVLSE<br>DK | Deamidated /0.9840;<br>NGlycan/22<br>78.8092 | Q,N | 98,103  | HexNAc(5)Hex(6)<br>Fuc(0)NeuAc(1) | 13 | 0.0382 | Sialylated |
| LQLQALQQ<br>NGSSVLSE<br>DK | NGlycan/23<br>66.8253                        | N   | 103     | HexNAc(4)Hex(6)<br>Fuc(0)NeuAc(2) | 16 | 0.012  | Sialylated |

|                            |  |     |         |                               |   |        |             |
|----------------------------|--|-----|---------|-------------------------------|---|--------|-------------|
| LQLQALQQ<br>NGSSVLSE<br>DK | NGlycan/14<br>44.5339                        | N   | 103     | HexNAc(4)Hex(3)Fuc(1)NeuAc(0) | 1 | 5.02   | Fucosylated |
| LQLQALQQ<br>NGSSVLSE<br>DK | Deamidated /0.9840;<br>NGlycan/14<br>44.5339 | Q,N | 101,103 | HexNAc(4)Hex(3)Fuc(1)NeuAc(0) | 1 | 0.0661 | Fucosylated |
| LQLQALQQ<br>NGSSVLSE<br>DK | Deamidated /0.9840;<br>NGlycan/14<br>44.5339 | Q,N | 98,103  | HexNAc(4)Hex(3)Fuc(1)NeuAc(0) | 1 | 0.0119 | Fucosylated |
| LQLQALQQ<br>NGSSVLSE<br>DK | NGlycan/16<br>06.5867                        | N   | 103     | HexNAc(4)Hex(4)Fuc(1)NeuAc(0) | 2 | 3.26   | Fucosylated |
| LQLQALQQ<br>NGSSVLSE<br>DK | Deamidated /0.9840;<br>NGlycan/16<br>06.5867 | Q,N | 101,103 | HexNAc(4)Hex(4)Fuc(1)NeuAc(0) | 2 | 0.0406 | Fucosylated |
| LQLQALQQ<br>NGSSVLSE<br>DK | NGlycan/17<br>68.6395                        | N   | 103     | HexNAc(4)Hex(5)Fuc(1)NeuAc(0) | 3 | 2.65   | Fucosylated |
| LQLQALQQ<br>NGSSVLSE<br>DK | Deamidated /0.9840;<br>NGlycan/17<br>68.6395 | Q,N | 101,103 | HexNAc(4)Hex(5)Fuc(1)NeuAc(0) | 3 | 1.14   | Fucosylated |
| LQLQALQQ<br>NGSSVLSE<br>DK | Deamidated /0.9840;<br>NGlycan/17<br>68.6395 | Q,N | 96,103  | HexNAc(4)Hex(5)Fuc(1)NeuAc(0) | 3 | 0.0296 | Fucosylated |
| LQLQALQQ<br>NGSSVLSE<br>DK | NGlycan/20<br>76.7502                        | N   | 103     | HexNAc(4)Hex(6)Fuc(2)NeuAc(0) | 4 | 2.04   | Fucosylated |
| LQLQALQQ<br>NGSSVLSE<br>DK | NGlycan/21<br>33.7717                        | N   | 103     | HexNAc(5)Hex(6)Fuc(1)NeuAc(0) | 5 | 0.0536 | Fucosylated |

|                            |   |     |             |                                   |    |        |                 |
|----------------------------|---|-----|-------------|-----------------------------------|----|--------|-----------------|
| LQLQALQQ<br>NGSSVLSE<br>DK | NGlycan/19<br>14.6974                           | N   | 103         | HexNAc(4)Hex(5)<br>Fuc(2)NeuAc(0) | 6  | 0.497  | Fucosyl<br>ated |
| LQLQALQQ<br>NGSSVLSE<br>DK | Deamidated<br>/0.9840;<br>NGlycan/19<br>14.6974 | Q,N | 101,10<br>3 | HexNAc(4)Hex(5)<br>Fuc(2)NeuAc(0) | 6  | 0.0298 | Fucosyl<br>ated |
| LQLQALQQ<br>NGSSVLSE<br>DK | Deamidated<br>/0.9840;<br>NGlycan/19<br>14.6974 | Q,N | 98,103      | HexNAc(4)Hex(5)<br>Fuc(2)NeuAc(0) | 6  | 0.0209 | Fucosyl<br>ated |
| LQLQALQQ<br>NGSSVLSE<br>DK | NGlycan/22<br>22.8082                           | N   | 103         | HexNAc(4)Hex(6)<br>Fuc(3)NeuAc(0) | 8  | 0.348  | Fucosyl<br>ated |
| LQLQALQQ<br>NGSSVLSE<br>DK | NGlycan/18<br>09.6661                           | N   | 103         | HexNAc(5)Hex(4)<br>Fuc(1)NeuAc(0) | 9  | 0.187  | Fucosyl<br>ated |
| LQLQALQQ<br>NGSSVLSE<br>DK | NGlycan/17<br>52.6446                           | N   | 103         | HexNAc(4)Hex(4)<br>Fuc(2)NeuAc(0) | 10 | 0.334  | Fucosyl<br>ated |
| LQLQALQQ<br>NGSSVLSE<br>DK | Deamidated<br>/0.9840;<br>NGlycan/17<br>52.6446 | Q,N | 102,10<br>3 | HexNAc(4)Hex(4)<br>Fuc(2)NeuAc(0) | 10 | 0.141  | Fucosyl<br>ated |
| LQLQALQQ<br>NGSSVLSE<br>DK | NGlycan/22<br>79.8296                           | N   | 103         | HexNAc(5)Hex(6)<br>Fuc(2)NeuAc(0) | 11 | 0.0819 | Fucosyl<br>ated |
| LQLQALQQ<br>NGSSVLSE<br>DK | NGlycan/16<br>47.6132                           | N   | 103         | HexNAc(5)Hex(3)<br>Fuc(1)NeuAc(0) | 12 | 0.212  | Fucosyl<br>ated |
| LQLQALQQ<br>NGSSVLSE<br>DK | NGlycan/19<br>71.7189                           | N   | 103         | HexNAc(5)Hex(5)<br>Fuc(1)NeuAc(0) | 13 | 0.121  | Fucosyl<br>ated |
| LQLQALQQ<br>NGSSVLSE<br>DK | NGlycan/21<br>17.7768                           | N   | 103         | HexNAc(5)Hex(5)<br>Fuc(2)NeuAc(0) | 15 | 0.0524 | Fucosyl<br>ated |

|                            |  |     |             |                                   |    |              |             |
|----------------------------|--|-----|-------------|-----------------------------------|----|--------------|-------------|
| LQLQALQQ<br>NGSSVLSE<br>DK | NGlycan/12<br>41.4545                        | N   | 103         | HexNAc(3)Hex(3)<br>Fuc(1)NeuAc(0) | 17 | 0.0676       | Fucosylated |
| LQLQALQQ<br>NGSSVLSE<br>DK | NGlycan/20<br>60.7553                        | N   | 103         | HexNAc(4)Hex(5)<br>Fuc(3)NeuAc(0) | 18 | 0.114        | Fucosylated |
| LQLQALQQ<br>NGSSVLSE<br>DK | NGlycan/22<br>63.8347                        | N   | 103         | HexNAc(5)Hex(5)<br>Fuc(3)NeuAc(0) | 20 | 0.0615       | Fucosylated |
| LQLQALQQ<br>NGSSVLSE<br>DK | NGlycan/14<br>03.5073                        | N   | 103         | HexNAc(3)Hex(4)<br>Fuc(1)NeuAc(0) | 25 | 0.0489       | Fucosylated |
| LQLQALQQ<br>NGSSVLSE<br>DK | NGlycan/24<br>25.8875                        | N   | 103         | HexNAc(5)Hex(6)<br>Fuc(3)NeuAc(0) | 26 | 0.0459       | Fucosylated |
| LQLQALQQ<br>NGSSVLSE<br>DK | NGlycan/19<br>55.7240                        | N   | 103         | HexNAc(5)Hex(4)<br>Fuc(2)NeuAc(0) | 31 | 0.0246       | Fucosylated |
| LQLQALQQ<br>NGSSVLSE<br>DK | NGlycan/23<br>45.8878                        | N   | 103         | HexNAc(7)Hex(3)<br>Fuc(3)NeuAc(0) | 37 | 0.0007<br>33 | Fucosylated |
| LQLQALQQ<br>NGSSVLSE<br>DK | NGlycan/14<br>60.5288                        | N   | 103         | HexNAc(4)Hex(4)<br>Fuc(0)NeuAc(0) | 1  | 4.24         | Undecorated |
| LQLQALQQ<br>NGSSVLSE<br>DK | Deamidated /0.9840;<br>NGlycan/14<br>60.5288 | Q,N | 101,10<br>3 | HexNAc(4)Hex(4)<br>Fuc(0)NeuAc(0) | 1  | 2.61         | Undecorated |
| LQLQALQQ<br>NGSSVLSE<br>DK | Deamidated /0.9840;<br>NGlycan/14<br>60.5288 | Q,N | 98,103      | HexNAc(4)Hex(4)<br>Fuc(0)NeuAc(0) | 1  | 2.61         | Undecorated |
| LQLQALQQ<br>NGSSVLSE<br>DK | Deamidated /0.9840;<br>NGlycan/14<br>60.5288 | Q,N | 102,10<br>3 | HexNAc(4)Hex(4)<br>Fuc(0)NeuAc(0) | 1  | 2.55         | Undecorated |

|                            |  |     |         |                                   |   |       |             |
|----------------------------|--|-----|---------|-----------------------------------|---|-------|-------------|
| LQLQALQQ<br>NGSSVLSE<br>DK | NGlycan/16<br>22.5816                        | N   | 103     | HexNAc(4)Hex(5)<br>Fuc(0)NeuAc(0) | 2 | 3.29  | Undecorated |
| LQLQALQQ<br>NGSSVLSE<br>DK | Deamidated /0.9840;<br>NGlycan/16<br>22.5816 | Q,N | 98,103  | HexNAc(4)Hex(5)<br>Fuc(0)NeuAc(0) | 2 | 1.93  | Undecorated |
| LQLQALQQ<br>NGSSVLSE<br>DK | Deamidated /0.9840;<br>NGlycan/16<br>22.5816 | Q,N | 101,103 | HexNAc(4)Hex(5)<br>Fuc(0)NeuAc(0) | 2 | 1.88  | Undecorated |
| LQLQALQQ<br>NGSSVLSE<br>DK | Deamidated /0.9840;<br>NGlycan/17<br>84.6344 | Q,N | 101,103 | HexNAc(4)Hex(6)<br>Fuc(0)NeuAc(0) | 3 | 1.75  | Undecorated |
| LQLQALQQ<br>NGSSVLSE<br>DK | Deamidated /0.9840;<br>NGlycan/16<br>63.6082 | Q,N | 102,103 | HexNAc(5)Hex(4)<br>Fuc(0)NeuAc(0) | 4 | 0.142 | Undecorated |
| LQLQALQQ<br>NGSSVLSE<br>DK | Deamidated /0.9840;<br>NGlycan/16<br>63.6082 | Q,N | 98,103  | HexNAc(5)Hex(4)<br>Fuc(0)NeuAc(0) | 4 | 0.142 | Undecorated |
| LQLQALQQ<br>NGSSVLSE<br>DK | NGlycan/16<br>63.6082                        | N   | 103     | HexNAc(5)Hex(4)<br>Fuc(0)NeuAc(0) | 4 | 0.094 | Undecorated |
| LQLQALQQ<br>NGSSVLSE<br>DK | NGlycan/18<br>25.6610                        | N   | 103     | HexNAc(5)Hex(5)<br>Fuc(0)NeuAc(0) | 5 | 0.319 | Undecorated |
| LQLQALQQ<br>NGSSVLSE<br>DK | Deamidated /0.9840;<br>NGlycan/18<br>25.6610 | Q,N | 101,103 | HexNAc(5)Hex(5)<br>Fuc(0)NeuAc(0) | 5 | 0.113 | Undecorated |
| LQLQALQQ<br>NGSSVLSE<br>DK | Deamidated /0.9840;<br>NGlycan/18<br>25.6610 | Q,N | 102,103 | HexNAc(5)Hex(5)<br>Fuc(0)NeuAc(0) | 5 | 0.113 | Undecorated |

|                              |  |     |         |                                |    |         |                |
|------------------------------|--|-----|---------|--------------------------------|----|---------|----------------|
| LQLQALQQ<br>NGSSVLSE<br>DK   | NGlycan/15<br>01.5553                        | N   | 103     | HexNAc(5)Hex(3)Fuc(0)NeuAc(0)  | 10 | 0.135   | Undecorated    |
| LQLQALQQ<br>NGSSVLSE<br>DK   | Deamidated /0.9840;<br>NGlycan/12<br>57.4494 | Q,N | 98,103  | HexNAc(3)Hex(4)Fuc(0)NeuAc(0)  | 15 | 0.0438  | Undecorated    |
| LQLQALQQ<br>NGSSVLSE<br>DK   | NGlycan/12<br>98.4760                        | N   | 103     | HexNAc(4)Hex(3)Fuc(0)NeuAc(0)  | 17 | 0.036   | Undecorated    |
| LQLQALQQ<br>NGSSVLSE<br>DK   | Deamidated /0.9840;<br>NGlycan/12<br>98.4760 | Q,N | 101,103 | HexNAc(4)Hex(3)Fuc(0)NeuAc(0)  | 17 | 0.0216  | Undecorated    |
| LQLQALQQ<br>NGSSVLSE<br>DK   | NGlycan/21<br>88.7398                        | N   | 103     | HexNAc(2)Hex(11)Fuc(0)NeuAc(0) | 3  | 0.00855 | High Mannose   |
| LQLQALQQ<br>NGSSVLSE<br>DK   | Deamidated /0.9840;<br>NGlycan/12<br>16.4229 | Q,N | 101,103 | HexNAc(2)Hex(5)Fuc(0)NeuAc(0)  | 2  | 0.00151 | High Mannose   |
| LQLQALQQ<br>NGSSVLSE<br>DK   | Deamidated /0.9840;<br>NGlycan/12<br>16.4229 | Q,N | 102,103 | HexNAc(2)Hex(5)Fuc(0)NeuAc(0)  | 2  | 0.00151 | High Mannose   |
| LQLQALQQ<br>NGSSVLSE<br>DKSK | NGlycan/20<br>59.7349                        | N   | 103     | HexNAc(4)Hex(5)Fuc(1)NeuAc(1)  | 1  | 0.175   | Sialyfosylated |
| LQLQALQQ<br>NGSSVLSE<br>DKSK | NGlycan/23<br>50.8304                        | N   | 103     | HexNAc(4)Hex(5)Fuc(1)NeuAc(2)  | 2  | 0.143   | Sialyfosylated |
| LQLQALQQ<br>NGSSVLSE<br>DKSK | NGlycan/18<br>97.6821                        | N   | 103     | HexNAc(4)Hex(4)Fuc(1)NeuAc(1)  | 3  | 0.0589  | Sialyfosylated |
| LQLQALQQ<br>NGSSVLSE<br>DKSK | NGlycan/22<br>05.7928                        | N   | 103     | HexNAc(4)Hex(5)Fuc(2)NeuAc(1)  | 5  | 0.0213  | Sialyfosylated |

|  |  |     |         |                               |    |         |                |
|--|--|-----|---------|-------------------------------|----|---------|----------------|
| LQLQALQQ<br>NGSSVLSE<br>DKSK             | NGlycan/14<br>44.5339                        | N   | 103     | HexNAc(4)Hex(3)Fuc(1)NeuAc(0) | 1  | 0.21    | Fucosylated    |
| LQLQALQQ<br>NGSSVLSE<br>DKSK             | Deamidated /0.9840;<br>NGlycan/14<br>44.5339 | Q,N | 102,103 | HexNAc(4)Hex(3)Fuc(1)NeuAc(0) | 1  | 0.00489 | Fucosylated    |
| LQLQALQQ<br>NGSSVLSE<br>DKSK             | NGlycan/16<br>06.5867                        | N   | 103     | HexNAc(4)Hex(4)Fuc(1)NeuAc(0) | 2  | 0.153   | Fucosylated    |
| LQLQALQQ<br>NGSSVLSE<br>DKSK             | NGlycan/17<br>68.6395                        | N   | 103     | HexNAc(4)Hex(5)Fuc(1)NeuAc(0) | 3  | 0.113   | Fucosylated    |
| LQLQALQQ<br>NGSSVLSE<br>DKSK             | NGlycan/19<br>14.6974                        | N   | 103     | HexNAc(4)Hex(5)Fuc(2)NeuAc(0) | 6  | 0.0273  | Fucosylated    |
| LQLQALQQ<br>NGSSVLSE<br>DKSK             | NGlycan/17<br>52.6446                        | N   | 103     | HexNAc(4)Hex(4)Fuc(2)NeuAc(0) | 10 | 0.0213  | Fucosylated    |
| FFVSVGLP<br>NMTQGF<br>WENSMLTDP<br>GNVQK | NGlycan/31<br>95.1628                        | N   | 322     | HexNAc(6)Hex(5)Fuc(4)NeuAc(2) | 19 | 0.0995  | Sialyfosylated |
| FFVSVGLP<br>NMTQGF<br>WENSMLTDP<br>GNVQK | NGlycan/25<br>38.9352                        | N   | 322     | HexNAc(5)Hex(4)Fuc(4)NeuAc(1) | 20 | 0.0957  | Sialyfosylated |
| FFVSVGLP<br>NMTQGF<br>WENSMLTDP<br>GNVQK | NGlycan/28<br>31.0259                        | N   | 322     | HexNAc(7)Hex(6)Fuc(1)NeuAc(1) | 21 | 0.0878  | Sialyfosylated |
| FFVSVGLP<br>NMTQGF<br>WENSMLTDP<br>GNVQK | NGlycan/24<br>98.9039;<br>Deamidated /0.9840 | N,Q | 322,325 | HexNAc(6)Hex(7)Fuc(1)NeuAc(0) | 21 | 0.00397 | Fucosylated    |

|  |                       |   |     |                               |    |        |                     |
|--|-----------------------|---|-----|-------------------------------|----|--------|---------------------|
| FFVSVGLP<br>NMTQGF<br>W<br>ENSMLTDP<br>GNVQK | NGlycan/27<br>42.0146 | N | 322 | HexNAc(6)Hex(4)Fuc(4)NeuAc(1) | 23 | 0.0757 | Sialyfu<br>osylated |
| FFVSVGLP<br>NMTQGF<br>W<br>ENSMLTDP<br>GNVQK | NGlycan/20<br>85.7870 | N | 322 | HexNAc(5)Hex(3)Fuc(4)NeuAc(0) | 28 | 0.0423 | Fucosyl<br>ated     |
| FFVSVGLP<br>NMTQGF<br>W<br>ENSMLTDP<br>GNVQK | NGlycan/22<br>88.8663 | N | 322 | HexNAc(6)Hex(3)Fuc(4)NeuAc(0) | 29 | 0.0334 | Fucosyl<br>ated     |
| FFVSVGLP<br>NMTQGF<br>W<br>ENSMLTDP<br>GNVQK | NGlycan/24<br>50.9192 | N | 322 | HexNAc(6)Hex(4)Fuc(4)NeuAc(0) | 30 | 0.0261 | Fucosyl<br>ated     |
| FFVSVGLP<br>NMTQGF<br>W<br>ENSMLTDP<br>GNVQK | NGlycan/29<br>04.0674 | N | 322 | HexNAc(6)Hex(5)Fuc(4)NeuAc(1) | 31 | 0.0576 | Sialyfu<br>osylated |
| FFVSVGLP<br>NMTQGF<br>W<br>ENSMLTDP<br>GNVQK | NGlycan/26<br>12.9720 | N | 322 | HexNAc(6)Hex(5)Fuc(4)NeuAc(0) | 34 | 0.0181 | Fucosyl<br>ated     |
| FFVSVGLP<br>NMTQGF<br>W<br>ENSMLTDP<br>GNVQK | NGlycan/22<br>46.8194 | N | 322 | HexNAc(5)Hex(4)Fuc(2)NeuAc(1) | 39 | 0.0279 | Sialyfu<br>osylated |
| SIGLLSPDF<br>QEDNETEI<br>NFLK                | NGlycan/20<br>59.7349 | N | 432 | HexNAc(4)Hex(5)Fuc(1)NeuAc(1) | 1  | 0.253  | Sialyfu<br>osylated |
| SIGLLSPDF<br>QEDNETEI<br>NFLK                | NGlycan/23<br>50.8304 | N | 432 | HexNAc(4)Hex(5)Fuc(1)NeuAc(2) | 2  | 0.223  | Sialyfu<br>osylated |
| SIGLLSPDF<br>QEDNETEI<br>NFLK                | NGlycan/18<br>97.6821 | N | 432 | HexNAc(4)Hex(4)Fuc(1)NeuAc(1) | 3  | 0.0157 | Sialyfu<br>osylated |

|                               |                       |   |     |                               |    |        |                 |
|-------------------------------|-----------------------|---|-----|-------------------------------|----|--------|-----------------|
| SIGLLSPDF<br>QEDNETEI<br>NFLK | NGlycan/23<br>67.8457 | N | 432 | HexNAc(4)Hex(6)Fuc(2)NeuAc(1) | 4  | 0.0248 | Sialyucosylated |
| SIGLLSPDF<br>QEDNETEI<br>NFLK | NGlycan/22<br>05.7928 | N | 432 | HexNAc(4)Hex(5)Fuc(2)NeuAc(1) | 5  | 0.0243 | Sialyucosylated |
| SIGLLSPDF<br>QEDNETEI<br>NFLK | NGlycan/27<br>89.9993 | N | 432 | HexNAc(6)Hex(7)Fuc(1)NeuAc(1) | 6  | 0.141  | Sialyucosylated |
| SIGLLSPDF<br>QEDNETEI<br>NFLK | NGlycan/24<br>24.8671 | N | 432 | HexNAc(5)Hex(6)Fuc(1)NeuAc(1) | 7  | 0.287  | Sialyucosylated |
| SIGLLSPDF<br>QEDNETEI<br>NFLK | NGlycan/27<br>15.9625 | N | 432 | HexNAc(5)Hex(6)Fuc(1)NeuAc(2) | 8  | 0.282  | Sialyucosylated |
| SIGLLSPDF<br>QEDNETEI<br>NFLK | NGlycan/22<br>62.8143 | N | 432 | HexNAc(5)Hex(5)Fuc(1)NeuAc(1) | 9  | 0.193  | Sialyucosylated |
| SIGLLSPDF<br>QEDNETEI<br>NFLK | NGlycan/21<br>00.7615 | N | 432 | HexNAc(5)Hex(4)Fuc(1)NeuAc(1) | 10 | 0.0708 | Sialyucosylated |
| SIGLLSPDF<br>QEDNETEI<br>NFLK | NGlycan/30<br>81.0947 | N | 432 | HexNAc(6)Hex(7)Fuc(1)NeuAc(2) | 11 | 0.206  | Sialyucosylated |
| SIGLLSPDF<br>QEDNETEI<br>NFLK | NGlycan/27<br>32.9779 | N | 432 | HexNAc(5)Hex(7)Fuc(2)NeuAc(1) | 12 | 0.189  | Sialyucosylated |
| SIGLLSPDF<br>QEDNETEI<br>NFLK | NGlycan/30<br>07.0580 | N | 432 | HexNAc(5)Hex(6)Fuc(1)NeuAc(3) | 13 | 0.181  | Sialyucosylated |
| SIGLLSPDF<br>QEDNETEI<br>NFLK | NGlycan/25<br>53.9097 | N | 432 | HexNAc(5)Hex(5)Fuc(1)NeuAc(2) | 14 | 0.062  | Sialyucosylated |
| SIGLLSPDF<br>QEDNETEI<br>NFLK | NGlycan/30<br>24.0733 | N | 432 | HexNAc(5)Hex(7)Fuc(2)NeuAc(2) | 16 | 0.139  | Sialyucosylated |

|                               |   |     |             |                                   |    |             |                     |
|-------------------------------|---|-----|-------------|-----------------------------------|----|-------------|---------------------|
| SIGLLSPDF<br>QEDNETEI<br>NFLK | NGlycan/26<br>27.9465                           | N   | 432         | HexNAc(6)Hex(6)<br>Fuc(1)NeuAc(1) | 26 | 0.0683      | Sialyfu<br>osylated |
| SIGLLSPDF<br>QEDNETEI<br>NFLK | NGlycan/33<br>72.1902                           | N   | 432         | HexNAc(6)Hex(7)<br>Fuc(1)NeuAc(3) | 27 | 0.0659      | Sialyfu<br>osylated |
| SIGLLSPDF<br>QEDNETEI<br>NFLK | NGlycan/29<br>19.0419                           | N   | 432         | HexNAc(6)Hex(6)<br>Fuc(1)NeuAc(2) | 28 | 0.0651      | Sialyfu<br>osylated |
| SIGLLSPDF<br>QEDNETEI<br>NFLK | NGlycan/29<br>36.0572                           | N   | 432         | HexNAc(6)Hex(7)<br>Fuc(2)NeuAc(1) | 32 | 0.049       | Sialyfu<br>osylated |
| SIGLLSPDF<br>QEDNETEI<br>NFLK | NGlycan/25<br>70.9250                           | N   | 432         | HexNAc(5)Hex(6)<br>Fuc(2)NeuAc(1) | 33 | 0.0436      | Sialyfu<br>osylated |
| SIGLLSPDF<br>QEDNETEI<br>NFLK | NGlycan/32<br>27.1527                           | N   | 432         | HexNAc(6)Hex(7)<br>Fuc(2)NeuAc(2) | 35 | 0.0339      | Sialyfu<br>osylated |
| SIGLLSPDF<br>QEDNETEI<br>NFLK | NGlycan/28<br>62.0205                           | N   | 432         | HexNAc(5)Hex(6)<br>Fuc(2)NeuAc(2) | 40 | 0.0234      | Sialyfu<br>osylated |
| SIGLLSPDF<br>QEDNETEI<br>NFLK | NGlycan/32<br>10.1373                           | N   | 432         | HexNAc(6)Hex(6)<br>Fuc(1)NeuAc(3) | 41 | 0.021       | Sialyfu<br>osylated |
| SIGLLSPDF<br>QEDNETEI<br>NFLK | NGlycan/28<br>79.0358                           | N   | 432         | HexNAc(5)Hex(7)<br>Fuc(3)NeuAc(1) | 43 | 0.0164      | Sialyfu<br>osylated |
| SIGLLSPDF<br>QEDNETEI<br>NFLK | NGlycan/20<br>75.7298;<br>Deamidated<br>/0.9840 | N,N | 432,43<br>7 | HexNAc(4)Hex(6)<br>Fuc(0)NeuAc(1) | 1  | 0.0065<br>7 | Sialylate<br>d      |
| SIGLLSPDF<br>QEDNETEI<br>NFLK | Deamidated<br>/0.9840;<br>NGlycan/21<br>16.7564 | Q,N | 429,43<br>2 | HexNAc(5)Hex(5)<br>Fuc(0)NeuAc(1) | 3  | 0.0045<br>8 | Sialylate<br>d      |

|                                |   |     |             |                                   |    |             |             |
|--------------------------------|---|-----|-------------|-----------------------------------|----|-------------|-------------|
| SIGLLSPDF<br>QEDNETEI<br>NFLLK | NGlycan/22<br>78.8092;<br>Deamidated<br>/0.9840 | N,N | 432,43<br>7 | HexNAc(5)Hex(6)<br>Fuc(0)NeuAc(1) | 13 | 0.0152      | Sialylated  |
| SIGLLSPDF<br>QEDNETEI<br>NFLLK | NGlycan/23<br>66.8253;<br>Deamidated<br>/0.9840 | N,N | 432,43<br>7 | HexNAc(4)Hex(6)<br>Fuc(0)NeuAc(2) | 16 | 0.0239      | Sialylated  |
| SIGLLSPDF<br>QEDNETEI<br>NFLLK | NGlycan/26<br>43.9414                           | N   | 432         | HexNAc(6)Hex(7)<br>Fuc(0)NeuAc(1) | 18 | 0.0218      | Sialylated  |
| SIGLLSPDF<br>QEDNETEI<br>NFLLK | Deamidated<br>/0.9840;<br>NGlycan/24<br>40.8620 | Q,N | 429,43<br>2 | HexNAc(5)Hex(7)<br>Fuc(0)NeuAc(1) | 20 | 0.0046<br>2 | Sialylated  |
| SIGLLSPDF<br>QEDNETEI<br>NFLLK | NGlycan/16<br>06.5867                           | N   | 432         | HexNAc(4)Hex(4)<br>Fuc(1)NeuAc(0) | 2  | 0.0226      | Fucosylated |
| SIGLLSPDF<br>QEDNETEI<br>NFLLK | NGlycan/17<br>68.6395                           | N   | 432         | HexNAc(4)Hex(5)<br>Fuc(1)NeuAc(0) | 3  | 0.0729      | Fucosylated |
| SIGLLSPDF<br>QEDNETEI<br>NFLLK | NGlycan/20<br>76.7502                           | N   | 432         | HexNAc(4)Hex(6)<br>Fuc(2)NeuAc(0) | 4  | 0.113       | Fucosylated |
| SIGLLSPDF<br>QEDNETEI<br>NFLLK | NGlycan/21<br>33.7717                           | N   | 432         | HexNAc(5)Hex(6)<br>Fuc(1)NeuAc(0) | 5  | 0.164       | Fucosylated |
| SIGLLSPDF<br>QEDNETEI<br>NFLLK | Deamidated<br>/0.9840;<br>NGlycan/21<br>33.7717 | Q,N | 429,43<br>2 | HexNAc(5)Hex(6)<br>Fuc(1)NeuAc(0) | 5  | 0.0263      | Fucosylated |
| SIGLLSPDF<br>QEDNETEI<br>NFLLK | NGlycan/18<br>09.6661                           | N   | 432         | HexNAc(5)Hex(4)<br>Fuc(1)NeuAc(0) | 9  | 0.0374      | Fucosylated |
| SIGLLSPDF<br>QEDNETEI<br>NFLLK | NGlycan/22<br>79.8296                           | N   | 432         | HexNAc(5)Hex(6)<br>Fuc(2)NeuAc(0) | 11 | 0.0759      | Fucosylated |

|                                |   |     |         |                               |    |         |             |
|--------------------------------|---|-----|---------|-------------------------------|----|---------|-------------|
| SIGLLSPDF<br>QEDNETEI<br>NFLLK | NGlycan/19<br>71.7189                           | N   | 432     | HexNAc(5)Hex(5)Fuc(1)NeuAc(0) | 13 | 0.0896  | Fucosylated |
| SIGLLSPDF<br>QEDNETEI<br>NFLLK | NGlycan/24<br>41.8824                           | N   | 432     | HexNAc(5)Hex(7)Fuc(2)NeuAc(0) | 14 | 0.173   | Fucosylated |
| SIGLLSPDF<br>QEDNETEI<br>NFLLK | NGlycan/21<br>17.7768                           | N   | 432     | HexNAc(5)Hex(5)Fuc(2)NeuAc(0) | 15 | 0.0209  | Fucosylated |
| SIGLLSPDF<br>QEDNETEI<br>NFLLK | NGlycan/24<br>98.9039                           | N   | 432     | HexNAc(6)Hex(7)Fuc(1)NeuAc(0) | 21 | 0.0564  | Fucosylated |
| SIGLLSPDF<br>QEDNETEI<br>NFLLK | NGlycan/23<br>36.8511                           | N   | 432     | HexNAc(6)Hex(6)Fuc(1)NeuAc(0) | 22 | 0.0541  | Fucosylated |
| SIGLLSPDF<br>QEDNETEI<br>NFLLK | NGlycan/21<br>74.7983                           | N   | 432     | HexNAc(6)Hex(5)Fuc(1)NeuAc(0) | 32 | 0.0231  | Fucosylated |
| SIGLLSPDF<br>QEDNETEI<br>NFLLK | NGlycan/22<br>95.8245                           | N   | 432     | HexNAc(5)Hex(7)Fuc(1)NeuAc(0) | 33 | 0.0235  | Fucosylated |
| SIGLLSPDF<br>QEDNETEI<br>NFLLK | Deamidated<br>/0.9840;<br>NGlycan/21<br>49.7666 | Q,N | 429,432 | HexNAc(5)Hex(7)Fuc(0)NeuAc(0) | 18 | 0.0203  | Undecorated |
| SIGLLSPDF<br>QEDNETEI<br>NFLLK | NGlycan/17<br>84.6344;<br>Deamidated<br>/0.9840 | N,N | 432,437 | HexNAc(4)Hex(6)Fuc(0)NeuAc(0) | 19 | 0.0164  | Undecorated |
| SIGLLSPDF<br>QEDNETEI<br>NFLLK | Deamidated<br>/0.9840;<br>NGlycan/18<br>25.6610 | Q,N | 429,432 | HexNAc(5)Hex(5)Fuc(0)NeuAc(0) | 20 | 0.0116  | Undecorated |
| SIGLLSPDF<br>QEDNETEI<br>NFLLK | Deamidated<br>/0.9840;<br>NGlycan/23<br>52.8460 | Q,N | 429,432 | HexNAc(6)Hex(7)Fuc(0)NeuAc(0) | 21 | 0.00396 | Undecorated |

|                  |                       |   |     |                               |    |        |                     |
|------------------|-----------------------|---|-----|-------------------------------|----|--------|---------------------|
| CDISNSTE<br>AGQK | NGlycan/20<br>59.7349 | N | 546 | HexNAc(4)Hex(5)Fuc(1)NeuAc(1) | 1  | 0.463  | Sialyfu<br>osylated |
| CDISNSTE<br>AGQK | NGlycan/23<br>50.8304 | N | 546 | HexNAc(4)Hex(5)Fuc(1)NeuAc(2) | 2  | 0.126  | Sialyfu<br>osylated |
| CDISNSTE<br>AGQK | NGlycan/18<br>97.6821 | N | 546 | HexNAc(4)Hex(4)Fuc(1)NeuAc(1) | 3  | 0.691  | Sialyfu<br>osylated |
| CDISNSTE<br>AGQK | NGlycan/27<br>89.9993 | N | 546 | HexNAc(6)Hex(7)Fuc(1)NeuAc(1) | 6  | 0.0137 | Sialyfu<br>osylated |
| CDISNSTE<br>AGQK | NGlycan/24<br>24.8671 | N | 546 | HexNAc(5)Hex(6)Fuc(1)NeuAc(1) | 7  | 0.0957 | Sialyfu<br>osylated |
| CDISNSTE<br>AGQK | NGlycan/27<br>15.9625 | N | 546 | HexNAc(5)Hex(6)Fuc(1)NeuAc(2) | 8  | 0.0422 | Sialyfu<br>osylated |
| CDISNSTE<br>AGQK | NGlycan/22<br>62.8143 | N | 546 | HexNAc(5)Hex(5)Fuc(1)NeuAc(1) | 9  | 0.17   | Sialyfu<br>osylated |
| CDISNSTE<br>AGQK | NGlycan/21<br>00.7615 | N | 546 | HexNAc(5)Hex(4)Fuc(1)NeuAc(1) | 10 | 0.208  | Sialyfu<br>osylated |
| CDISNSTE<br>AGQK | NGlycan/25<br>53.9097 | N | 546 | HexNAc(5)Hex(5)Fuc(1)NeuAc(2) | 14 | 0.0278 | Sialyfu<br>osylated |
| CDISNSTE<br>AGQK | NGlycan/16<br>94.6027 | N | 546 | HexNAc(3)Hex(4)Fuc(1)NeuAc(1) | 18 | 0.112  | Sialyfu<br>osylated |
| CDISNSTE<br>AGQK | NGlycan/24<br>65.8937 | N | 546 | HexNAc(6)Hex(5)Fuc(1)NeuAc(1) | 24 | 0.0382 | Sialyfu<br>osylated |
| CDISNSTE<br>AGQK | NGlycan/26<br>27.9465 | N | 546 | HexNAc(6)Hex(6)Fuc(1)NeuAc(1) | 26 | 0.0266 | Sialyfu<br>osylated |

|                  |                       |   |     |                               |    |             |                     |
|------------------|-----------------------|---|-----|-------------------------------|----|-------------|---------------------|
| CDISNSTE<br>AGQK | NGlycan/18<br>56.6556 | N | 546 | HexNAc(3)Hex(5)Fuc(1)NeuAc(1) | 29 | 0.0629      | Sialyfu<br>osylated |
| CDISNSTE<br>AGQK | NGlycan/23<br>03.8409 | N | 546 | HexNAc(6)Hex(4)Fuc(1)NeuAc(1) | 34 | 0.0426      | Sialyfu<br>osylated |
| CDISNSTE<br>AGQK | NGlycan/23<br>51.8508 | N | 546 | HexNAc(4)Hex(5)Fuc(3)NeuAc(1) | 38 | 0.0296      | Sialyfu<br>osylated |
| CDISNSTE<br>AGQK | NGlycan/27<br>56.9891 | N | 546 | HexNAc(6)Hex(5)Fuc(1)NeuAc(2) | 44 | 0.0135      | Sialyfu<br>osylated |
| CDISNSTE<br>AGQK | NGlycan/19<br>54.7036 | N | 546 | HexNAc(5)Hex(4)Fuc(0)NeuAc(1) | 2  | 0.289       | Sialylate<br>d      |
| CDISNSTE<br>AGQK | NGlycan/24<br>07.8518 | N | 546 | HexNAc(5)Hex(5)Fuc(0)NeuAc(2) | 5  | 0.144       | Sialylate<br>d      |
| CDISNSTE<br>AGQK | NGlycan/23<br>19.8358 | N | 546 | HexNAc(6)Hex(5)Fuc(0)NeuAc(1) | 6  | 0.0090<br>9 | Sialylate<br>d      |
| CDISNSTE<br>AGQK | NGlycan/27<br>72.9840 | N | 546 | HexNAc(6)Hex(6)Fuc(0)NeuAc(2) | 7  | 0.0157      | Sialylate<br>d      |
| CDISNSTE<br>AGQK | NGlycan/17<br>51.6242 | N | 546 | HexNAc(4)Hex(4)Fuc(0)NeuAc(1) | 9  | 0.0345      | Sialylate<br>d      |
| CDISNSTE<br>AGQK | NGlycan/26<br>10.9312 | N | 546 | HexNAc(6)Hex(5)Fuc(0)NeuAc(2) | 11 | 0.0285      | Sialylate<br>d      |
| CDISNSTE<br>AGQK | NGlycan/15<br>48.5448 | N | 546 | HexNAc(3)Hex(4)Fuc(0)NeuAc(1) | 19 | 0.0206      | Sialylate<br>d      |
| CDISNSTE<br>AGQK | NGlycan/14<br>44.5339 | N | 546 | HexNAc(4)Hex(3)Fuc(1)NeuAc(0) | 1  | 0.418       | Fucosyl<br>ated     |

|                  |                       |   |     |                               |    |        |             |
|------------------|-----------------------|---|-----|-------------------------------|----|--------|-------------|
| CDISNSTE<br>AGQK | NGlycan/16<br>06.5867 | N | 546 | HexNAc(4)Hex(4)Fuc(1)NeuAc(0) | 2  | 1.06   | Fucosylated |
| CDISNSTE<br>AGQK | NGlycan/17<br>68.6395 | N | 546 | HexNAc(4)Hex(5)Fuc(1)NeuAc(0) | 3  | 0.251  | Fucosylated |
| CDISNSTE<br>AGQK | NGlycan/21<br>33.7717 | N | 546 | HexNAc(5)Hex(6)Fuc(1)NeuAc(0) | 5  | 0.0436 | Fucosylated |
| CDISNSTE<br>AGQK | NGlycan/18<br>09.6661 | N | 546 | HexNAc(5)Hex(4)Fuc(1)NeuAc(0) | 9  | 0.343  | Fucosylated |
| CDISNSTE<br>AGQK | NGlycan/17<br>52.6446 | N | 546 | HexNAc(4)Hex(4)Fuc(2)NeuAc(0) | 10 | 0.0208 | Fucosylated |
| CDISNSTE<br>AGQK | NGlycan/22<br>79.8296 | N | 546 | HexNAc(5)Hex(6)Fuc(2)NeuAc(0) | 11 | 0.0738 | Fucosylated |
| CDISNSTE<br>AGQK | NGlycan/16<br>47.6132 | N | 546 | HexNAc(5)Hex(3)Fuc(1)NeuAc(0) | 12 | 0.141  | Fucosylated |
| CDISNSTE<br>AGQK | NGlycan/19<br>71.7189 | N | 546 | HexNAc(5)Hex(5)Fuc(1)NeuAc(0) | 13 | 0.182  | Fucosylated |
| CDISNSTE<br>AGQK | NGlycan/12<br>41.4545 | N | 546 | HexNAc(3)Hex(3)Fuc(1)NeuAc(0) | 17 | 0.129  | Fucosylated |
| CDISNSTE<br>AGQK | NGlycan/15<br>65.5601 | N | 546 | HexNAc(3)Hex(5)Fuc(1)NeuAc(0) | 19 | 0.0644 | Fucosylated |
| CDISNSTE<br>AGQK | NGlycan/18<br>50.6926 | N | 546 | HexNAc(6)Hex(3)Fuc(1)NeuAc(0) | 23 | 0.0496 | Fucosylated |
| CDISNSTE<br>AGQK | NGlycan/14<br>03.5073 | N | 546 | HexNAc(3)Hex(4)Fuc(1)NeuAc(0) | 25 | 0.0427 | Fucosylated |

|                  |                       |   |     |                               |    |         |                |
|------------------|-----------------------|---|-----|-------------------------------|----|---------|----------------|
| CDISNSTE<br>AGQK | NGlycan/20<br>12.7454 | N | 546 | HexNAc(6)Hex(4)Fuc(1)NeuAc(0) | 27 | 0.0454  | Fucosylated    |
| CDISNSTE<br>AGQK | NGlycan/21<br>74.7983 | N | 546 | HexNAc(6)Hex(5)Fuc(1)NeuAc(0) | 32 | 0.024   | Fucosylated    |
| CDISNSTE<br>AGQK | NGlycan/18<br>98.7025 | N | 546 | HexNAc(4)Hex(4)Fuc(3)NeuAc(0) | 35 | 0.00866 | Fucosylated    |
| CDISNSTE<br>AGQK | NGlycan/17<br>27.6130 | N | 546 | HexNAc(3)Hex(6)Fuc(1)NeuAc(0) | 36 | 0.00721 | Fucosylated    |
| CDISNSTE<br>AGQK | NGlycan/12<br>16.4229 | N | 546 | HexNAc(2)Hex(5)Fuc(0)NeuAc(0) | 2  | 0.0209  | High Mannose   |
| NVSDIIPR         | NGlycan/20<br>59.7349 | N | 690 | HexNAc(4)Hex(5)Fuc(1)NeuAc(1) | 1  | 1.75    | Sialyfosylated |
| NVSDIIPR         | NGlycan/23<br>50.8304 | N | 690 | HexNAc(4)Hex(5)Fuc(1)NeuAc(2) | 2  | 0.52    | Sialyfosylated |
| NVSDIIPR         | NGlycan/18<br>97.6821 | N | 690 | HexNAc(4)Hex(4)Fuc(1)NeuAc(1) | 3  | 0.61    | Sialyfosylated |
| NVSDIIPR         | NGlycan/22<br>05.7928 | N | 690 | HexNAc(4)Hex(5)Fuc(2)NeuAc(1) | 5  | 0.0253  | Sialyfosylated |
| NVSDIIPR         | NGlycan/24<br>24.8671 | N | 690 | HexNAc(5)Hex(6)Fuc(1)NeuAc(1) | 7  | 0.202   | Sialyfosylated |
| NVSDIIPR         | NGlycan/27<br>15.9625 | N | 690 | HexNAc(5)Hex(6)Fuc(1)NeuAc(2) | 8  | 0.179   | Sialyfosylated |
| NVSDIIPR         | NGlycan/22<br>62.8143 | N | 690 | HexNAc(5)Hex(5)Fuc(1)NeuAc(1) | 9  | 0.0468  | Sialyfosylated |

|          |                       |   |     |                               |    |             |                     |
|----------|-----------------------|---|-----|-------------------------------|----|-------------|---------------------|
| NVSDIIPR | NGlycan/21<br>00.7615 | N | 690 | HexNAc(5)Hex(4)Fuc(1)NeuAc(1) | 10 | 0.0335      | Sialyfu<br>osylated |
| NVSDIIPR | NGlycan/27<br>32.9779 | N | 690 | HexNAc(5)Hex(7)Fuc(2)NeuAc(1) | 12 | 0.134       | Sialyfu<br>osylated |
| NVSDIIPR | NGlycan/30<br>07.0580 | N | 690 | HexNAc(5)Hex(6)Fuc(1)NeuAc(3) | 13 | 0.0296      | Sialyfu<br>osylated |
| NVSDIIPR | NGlycan/30<br>24.0733 | N | 690 | HexNAc(5)Hex(7)Fuc(2)NeuAc(2) | 16 | 0.0197      | Sialyfu<br>osylated |
| NVSDIIPR | NGlycan/27<br>16.9829 | N | 690 | HexNAc(5)Hex(6)Fuc(3)NeuAc(1) | 22 | 0.0858      | Sialyfu<br>osylated |
| NVSDIIPR | NGlycan/23<br>51.8508 | N | 690 | HexNAc(4)Hex(5)Fuc(3)NeuAc(1) | 38 | 0.0033<br>9 | Sialyfu<br>osylated |
| NVSDIIPR | NGlycan/21<br>16.7564 | N | 690 | HexNAc(5)Hex(5)Fuc(0)NeuAc(1) | 3  | 0.0204      | Sialylate<br>d      |
| NVSDIIPR | NGlycan/19<br>13.6770 | N | 690 | HexNAc(4)Hex(5)Fuc(0)NeuAc(1) | 4  | 0.756       | Sialylate<br>d      |
| NVSDIIPR | NGlycan/17<br>51.6242 | N | 690 | HexNAc(4)Hex(4)Fuc(0)NeuAc(1) | 9  | 0.193       | Sialylate<br>d      |
| NVSDIIPR | NGlycan/22<br>04.7724 | N | 690 | HexNAc(4)Hex(5)Fuc(0)NeuAc(2) | 10 | 0.101       | Sialylate<br>d      |
| NVSDIIPR | NGlycan/22<br>78.8092 | N | 690 | HexNAc(5)Hex(6)Fuc(0)NeuAc(1) | 13 | 0.0671      | Sialylate<br>d      |
| NVSDIIPR | NGlycan/25<br>69.9046 | N | 690 | HexNAc(5)Hex(6)Fuc(0)NeuAc(2) | 14 | 0.0422      | Sialylate<br>d      |

|          |                       |   |     |                               |    |        |             |
|----------|-----------------------|---|-----|-------------------------------|----|--------|-------------|
| NVSDIIPR | NGlycan/14<br>44.5339 | N | 690 | HexNAc(4)Hex(3)Fuc(1)NeuAc(0) | 1  | 0.0189 | Fucosylated |
| NVSDIIPR | NGlycan/16<br>06.5867 | N | 690 | HexNAc(4)Hex(4)Fuc(1)NeuAc(0) | 2  | 0.322  | Fucosylated |
| NVSDIIPR | NGlycan/17<br>68.6395 | N | 690 | HexNAc(4)Hex(5)Fuc(1)NeuAc(0) | 3  | 0.817  | Fucosylated |
| NVSDIIPR | NGlycan/21<br>33.7717 | N | 690 | HexNAc(5)Hex(6)Fuc(1)NeuAc(0) | 5  | 0.113  | Fucosylated |
| NVSDIIPR | NGlycan/19<br>14.6974 | N | 690 | HexNAc(4)Hex(5)Fuc(2)NeuAc(0) | 6  | 0.0243 | Fucosylated |
| NVSDIIPR | NGlycan/18<br>09.6661 | N | 690 | HexNAc(5)Hex(4)Fuc(1)NeuAc(0) | 9  | 0.0703 | Fucosylated |
| NVSDIIPR | NGlycan/19<br>71.7189 | N | 690 | HexNAc(5)Hex(5)Fuc(1)NeuAc(0) | 13 | 0.0882 | Fucosylated |
| NVSDIIPR | NGlycan/24<br>41.8824 | N | 690 | HexNAc(5)Hex(7)Fuc(2)NeuAc(0) | 14 | 0.0876 | Fucosylated |
| NVSDIIPR | NGlycan/19<br>30.6923 | N | 690 | HexNAc(4)Hex(6)Fuc(1)NeuAc(0) | 16 | 0.0822 | Fucosylated |
| NVSDIIPR | NGlycan/16<br>22.5816 | N | 690 | HexNAc(4)Hex(5)Fuc(0)NeuAc(0) | 8  | 0.2    | Undecorated |
| NVSDIIPR | NGlycan/14<br>60.5288 | N | 690 | HexNAc(4)Hex(4)Fuc(0)NeuAc(0) | 13 | 0.0604 | Undecorated |

**Table S4.2 Site-specific occupancy of recombinant ACE2 derived from HEK293 cells**

| <b>Glycans</b>                | <b>Peptide Sequence</b>                       | <b>Glyco site</b> | <b>Glycan Subtype</b> |
|-------------------------------|---|-------------------|-----------------------|
| HexNAc(5)Hex(5)Fuc(3)NeuAc(0) | K.FNHEAEDLFYQSSLASWNYNTNITEE<br>NVQNMNNAGDK.W | 53                | Fucosylated           |
| HexNAc(5)Hex(4)Fuc(1)NeuAc(0) | K.FNHEAEDLFYQSSLASWNYNTNITEE<br>NVQNMNNAGDK.W | 53                | Fucosylated           |
| HexNAc(9)Hex(9)Fuc(1)NeuAc(0) | K.FNHEAEDLFYQSSLASWNYNTNITEE<br>NVQNMNNAGDK.W | 53                | Fucosylated           |
| HexNAc(6)Hex(5)Fuc(4)NeuAc(2) | K.FNHEAEDLFYQSSLASWNYNTNITEE<br>NVQNMNNAGDK.W | 53                | Sialyfuco<br>sylated  |
| HexNAc(5)Hex(4)Fuc(4)NeuAc(1) | K.FNHEAEDLFYQSSLASWNYNTNITEE<br>NVQNMNNAGDK.W | 53                | Sialyfuco<br>sylated  |
| HexNAc(5)Hex(5)Fuc(2)NeuAc(2) | K.FNHEAEDLFYQSSLASWNYNTNITEE<br>NVQNMNNAGDK.W | 53                | Sialyfuco<br>sylated  |
| HexNAc(5)Hex(5)Fuc(4)NeuAc(1) | K.FNHEAEDLFYQSSLASWNYNTNITEE<br>NVQNMNNAGDK.W | 53                | Sialyfuco<br>sylated  |
| HexNAc(7)Hex(7)Fuc(1)NeuAc(1) | K.FNHEAEDLFYQSSLASWNYNTNITEE<br>NVQNMNNAGDK.W | 53                | Sialyfuco<br>sylated  |
| HexNAc(5)Hex(6)Fuc(1)NeuAc(3) | K.FNHEAEDLFYQSSLASWNYNTNITEE<br>NVQNMNNAGDK.W | 53                | Sialyfuco<br>sylated  |
| HexNAc(7)Hex(7)Fuc(2)NeuAc(1) | K.FNHEAEDLFYQSSLASWNYNTNITEE<br>NVQNMNNAGDK.W | 53                | Sialyfuco<br>sylated  |
| HexNAc(7)Hex(8)Fuc(1)NeuAc(1) | K.FNHEAEDLFYQSSLASWNYNTNITEE<br>NVQNMNNAGDK.W | 53                | Sialyfuco<br>sylated  |
| HexNAc(5)Hex(7)Fuc(3)NeuAc(2) | K.FNHEAEDLFYQSSLASWNYNTNITEE<br>NVQNMNNAGDK.W | 53                | Sialyfuco<br>sylated  |
| HexNAc(7)Hex(8)Fuc(0)NeuAc(1) | K.FNHEAEDLFYQSSLASWNYNTNITEE<br>NVQNMNNAGDK.W | 53                | Sialylated            |
| HexNAc(5)Hex(4)Fuc(0)NeuAc(1) | K.FNHEAEDLFYQSSLASWNYNTNITEE<br>NVQNMNNAGDK.W | 53                | Sialylated            |

|                               |   |    |            |
|-------------------------------|---|----|------------|
| HexNAc(5)Hex(5)Fuc(0)NeuAc(1) | K.FNHEAEDLFYQSSLASWNYNTNITEE<br>NVQNMNNAGDK.W | 53 | Sialylated |
| HexNAc(6)Hex(4)Fuc(0)NeuAc(1) | K.FNHEAEDLFYQSSLASWNYNTNITEE<br>NVQNMNNAGDK.W | 53 | Sialylated |
| HexNAc(4)Hex(7)Fuc(0)NeuAc(1) | K.FNHEAEDLFYQSSLASWNYNTNITEE<br>NVQNMNNAGDK.W | 53 | Sialylated |
| HexNAc(6)Hex(5)Fuc(0)NeuAc(1) | K.FNHEAEDLFYQSSLASWNYNTNITEE<br>NVQNMNNAGDK.W | 53 | Sialylated |
| HexNAc(7)Hex(4)Fuc(0)NeuAc(1) | K.FNHEAEDLFYQSSLASWNYNTNITEE<br>NVQNMNNAGDK.W | 53 | Sialylated |
| HexNAc(5)Hex(5)Fuc(0)NeuAc(2) | K.FNHEAEDLFYQSSLASWNYNTNITEE<br>NVQNMNNAGDK.W | 53 | Sialylated |
| HexNAc(6)Hex(6)Fuc(0)NeuAc(1) | K.FNHEAEDLFYQSSLASWNYNTNITEE<br>NVQNMNNAGDK.W | 53 | Sialylated |
| HexNAc(7)Hex(5)Fuc(0)NeuAc(1) | K.FNHEAEDLFYQSSLASWNYNTNITEE<br>NVQNMNNAGDK.W | 53 | Sialylated |
| HexNAc(6)Hex(5)Fuc(0)NeuAc(2) | K.FNHEAEDLFYQSSLASWNYNTNITEE<br>NVQNMNNAGDK.W | 53 | Sialylated |
| HexNAc(6)Hex(6)Fuc(0)NeuAc(2) | K.FNHEAEDLFYQSSLASWNYNTNITEE<br>NVQNMNNAGDK.W | 53 | Sialylated |
| HexNAc(7)Hex(5)Fuc(0)NeuAc(2) | K.FNHEAEDLFYQSSLASWNYNTNITEE<br>NVQNMNNAGDK.W | 53 | Sialylated |
| HexNAc(7)Hex(7)Fuc(0)NeuAc(1) | K.FNHEAEDLFYQSSLASWNYNTNITEE<br>NVQNMNNAGDK.W | 53 | Sialylated |
| HexNAc(7)Hex(6)Fuc(0)NeuAc(2) | K.FNHEAEDLFYQSSLASWNYNTNITEE<br>NVQNMNNAGDK.W | 53 | Sialylated |
| HexNAc(6)Hex(6)Fuc(0)NeuAc(3) | K.FNHEAEDLFYQSSLASWNYNTNITEE<br>NVQNMNNAGDK.W | 53 | Sialylated |
| HexNAc(7)Hex(7)Fuc(0)NeuAc(2) | K.FNHEAEDLFYQSSLASWNYNTNITEE<br>NVQNMNNAGDK.W | 53 | Sialylated |
| HexNAc(7)Hex(7)Fuc(0)NeuAc(3) | K.FNHEAEDLFYQSSLASWNYNTNITEE<br>NVQNMNNAGDK.W | 53 | Sialylated |

|                               |   |    |             |
|-------------------------------|---|----|-------------|
| HexNAc(5)Hex(3)Fuc(0)NeuAc(0) | K.FNHEAEDLFYQSSLASWNYNTNITEE<br>NVQNMNNAGDK.W | 53 | Undecorated |
| HexNAc(5)Hex(4)Fuc(0)NeuAc(0) | K.FNHEAEDLFYQSSLASWNYNTNITEE<br>NVQNMNNAGDK.W | 53 | Undecorated |
| HexNAc(6)Hex(3)Fuc(0)NeuAc(0) | K.FNHEAEDLFYQSSLASWNYNTNITEE<br>NVQNMNNAGDK.W | 53 | Undecorated |
| HexNAc(6)Hex(4)Fuc(0)NeuAc(0) | K.FNHEAEDLFYQSSLASWNYNTNITEE<br>NVQNMNNAGDK.W | 53 | Undecorated |
| HexNAc(7)Hex(3)Fuc(0)NeuAc(0) | K.FNHEAEDLFYQSSLASWNYNTNITEE<br>NVQNMNNAGDK.W | 53 | Undecorated |
| HexNAc(4)Hex(7)Fuc(0)NeuAc(0) | K.FNHEAEDLFYQSSLASWNYNTNITEE<br>NVQNMNNAGDK.W | 53 | Undecorated |
| HexNAc(7)Hex(4)Fuc(0)NeuAc(0) | K.FNHEAEDLFYQSSLASWNYNTNITEE<br>NVQNMNNAGDK.W | 53 | Undecorated |
| HexNAc(5)Hex(4)Fuc(3)NeuAc(0) | K.EQSTLAQMYPLQEIQNLTVK.L                      | 90 | Fucosylated |
| HexNAc(5)Hex(3)Fuc(3)NeuAc(0) | K.EQSTLAQMYPLQEIQNLTVK.L                      | 90 | Fucosylated |
| HexNAc(6)Hex(3)Fuc(3)NeuAc(0) | K.EQSTLAQMYPLQEIQNLTVK.L                      | 90 | Fucosylated |
| HexNAc(6)Hex(4)Fuc(3)NeuAc(0) | K.EQSTLAQMYPLQEIQNLTVK.L                      | 90 | Fucosylated |
| HexNAc(6)Hex(6)Fuc(3)NeuAc(0) | K.EQSTLAQMYPLQEIQNLTVK.L                      | 90 | Fucosylated |
| HexNAc(4)Hex(5)Fuc(3)NeuAc(0) | K.EQSTLAQMYPLQEIQNLTVK.L                      | 90 | Fucosylated |
| HexNAc(6)Hex(5)Fuc(3)NeuAc(0) | K.EQSTLAQMYPLQEIQNLTVK.L                      | 90 | Fucosylated |
| HexNAc(5)Hex(5)Fuc(3)NeuAc(0) | K.EQSTLAQMYPLQEIQNLTVK.L                      | 90 | Fucosylated |
| HexNAc(4)Hex(4)Fuc(2)NeuAc(0) | K.EQSTLAQMYPLQEIQNLTVK.L                      | 90 | Fucosylated |

|                               |                          |    |             |
|-------------------------------|--------------------------|----|-------------|
| HexNAc(5)Hex(3)Fuc(2)NeuAc(0) | K.EQSTLAQMYPLQEIQNLTVK.L | 90 | Fucosylated |
| HexNAc(5)Hex(4)Fuc(2)NeuAc(0) | K.EQSTLAQMYPLQEIQNLTVK.L | 90 | Fucosylated |
| HexNAc(4)Hex(6)Fuc(2)NeuAc(0) | K.EQSTLAQMYPLQEIQNLTVK.L | 90 | Fucosylated |
| HexNAc(7)Hex(7)Fuc(2)NeuAc(0) | K.EQSTLAQMYPLQEIQNLTVK.L | 90 | Fucosylated |
| HexNAc(5)Hex(6)Fuc(2)NeuAc(0) | K.EQSTLAQMYPLQEIQNLTVK.L | 90 | Fucosylated |
| HexNAc(6)Hex(6)Fuc(2)NeuAc(0) | K.EQSTLAQMYPLQEIQNLTVK.L | 90 | Fucosylated |
| HexNAc(6)Hex(7)Fuc(2)NeuAc(0) | K.EQSTLAQMYPLQEIQNLTVK.L | 90 | Fucosylated |
| HexNAc(6)Hex(3)Fuc(2)NeuAc(0) | K.EQSTLAQMYPLQEIQNLTVK.L | 90 | Fucosylated |
| HexNAc(4)Hex(3)Fuc(2)NeuAc(0) | K.EQSTLAQMYPLQEIQNLTVK.L | 90 | Fucosylated |
| HexNAc(6)Hex(4)Fuc(2)NeuAc(0) | K.EQSTLAQMYPLQEIQNLTVK.L | 90 | Fucosylated |
| HexNAc(4)Hex(4)Fuc(1)NeuAc(0) | K.EQSTLAQMYPLQEIQNLTVK.L | 90 | Fucosylated |
| HexNAc(4)Hex(3)Fuc(1)NeuAc(0) | K.EQSTLAQMYPLQEIQNLTVK.L | 90 | Fucosylated |
| HexNAc(4)Hex(5)Fuc(1)NeuAc(0) | K.EQSTLAQMYPLQEIQNLTVK.L | 90 | Fucosylated |
| HexNAc(5)Hex(4)Fuc(1)NeuAc(0) | K.EQSTLAQMYPLQEIQNLTVK.L | 90 | Fucosylated |
| HexNAc(6)Hex(6)Fuc(1)NeuAc(0) | K.EQSTLAQMYPLQEIQNLTVK.L | 90 | Fucosylated |
| HexNAc(5)Hex(3)Fuc(1)NeuAc(0) | K.EQSTLAQMYPLQEIQNLTVK.L | 90 | Fucosylated |

|                               |                          |    |                 |
|-------------------------------|--------------------------|----|-----------------|
| HexNAc(5)Hex(6)Fuc(1)NeuAc(0) | K.EQSTLAQMYPLQEIQNLTVK.L | 90 | Fucosylated     |
| HexNAc(5)Hex(5)Fuc(1)NeuAc(0) | K.EQSTLAQMYPLQEIQNLTVK.L | 90 | Fucosylated     |
| HexNAc(4)Hex(6)Fuc(1)NeuAc(0) | K.EQSTLAQMYPLQEIQNLTVK.L | 90 | Fucosylated     |
| HexNAc(4)Hex(7)Fuc(1)NeuAc(0) | K.EQSTLAQMYPLQEIQNLTVK.L | 90 | Fucosylated     |
| HexNAc(7)Hex(6)Fuc(1)NeuAc(0) | K.EQSTLAQMYPLQEIQNLTVK.L | 90 | Fucosylated     |
| HexNAc(6)Hex(5)Fuc(1)NeuAc(0) | K.EQSTLAQMYPLQEIQNLTVK.L | 90 | Fucosylated     |
| HexNAc(2)Hex(8)Fuc(0)NeuAc(0) | K.EQSTLAQMYPLQEIQNLTVK.L | 90 | High Mannose    |
| HexNAc(2)Hex(9)Fuc(0)NeuAc(0) | K.EQSTLAQMYPLQEIQNLTVK.L | 90 | High Mannose    |
| HexNAc(6)Hex(4)Fuc(4)NeuAc(1) | K.EQSTLAQMYPLQEIQNLTVK.L | 90 | Sialyfucoylated |
| HexNAc(5)Hex(4)Fuc(3)NeuAc(1) | K.EQSTLAQMYPLQEIQNLTVK.L | 90 | Sialyfucoylated |
| HexNAc(6)Hex(5)Fuc(3)NeuAc(1) | K.EQSTLAQMYPLQEIQNLTVK.L | 90 | Sialyfucoylated |
| HexNAc(6)Hex(4)Fuc(3)NeuAc(1) | K.EQSTLAQMYPLQEIQNLTVK.L | 90 | Sialyfucoylated |
| HexNAc(7)Hex(6)Fuc(3)NeuAc(1) | K.EQSTLAQMYPLQEIQNLTVK.L | 90 | Sialyfucoylated |
| HexNAc(6)Hex(7)Fuc(3)NeuAc(1) | K.EQSTLAQMYPLQEIQNLTVK.L | 90 | Sialyfucoylated |
| HexNAc(5)Hex(4)Fuc(2)NeuAc(1) | K.EQSTLAQMYPLQEIQNLTVK.L | 90 | Sialyfucoylated |
| HexNAc(4)Hex(5)Fuc(2)NeuAc(1) | K.EQSTLAQMYPLQEIQNLTVK.L | 90 | Sialyfucoylated |

|                               |                          |    |                      |
|-------------------------------|--------------------------|----|----------------------|
| HexNAc(4)Hex(6)Fuc(2)NeuAc(1) | K.EQSTLAQMYPLQEIQNLTVK.L | 90 | Sialyfuco<br>sylated |
| HexNAc(6)Hex(5)Fuc(2)NeuAc(1) | K.EQSTLAQMYPLQEIQNLTVK.L | 90 | Sialyfuco<br>sylated |
| HexNAc(6)Hex(4)Fuc(2)NeuAc(1) | K.EQSTLAQMYPLQEIQNLTVK.L | 90 | Sialyfuco<br>sylated |
| HexNAc(5)Hex(5)Fuc(2)NeuAc(1) | K.EQSTLAQMYPLQEIQNLTVK.L | 90 | Sialyfuco<br>sylated |
| HexNAc(5)Hex(7)Fuc(2)NeuAc(1) | K.EQSTLAQMYPLQEIQNLTVK.L | 90 | Sialyfuco<br>sylated |
| HexNAc(4)Hex(4)Fuc(1)NeuAc(1) | K.EQSTLAQMYPLQEIQNLTVK.L | 90 | Sialyfuco<br>sylated |
| HexNAc(4)Hex(5)Fuc(1)NeuAc(1) | K.EQSTLAQMYPLQEIQNLTVK.L | 90 | Sialyfuco<br>sylated |
| HexNAc(4)Hex(5)Fuc(1)NeuAc(2) | K.EQSTLAQMYPLQEIQNLTVK.L | 90 | Sialyfuco<br>sylated |
| HexNAc(5)Hex(5)Fuc(1)NeuAc(1) | K.EQSTLAQMYPLQEIQNLTVK.L | 90 | Sialyfuco<br>sylated |
| HexNAc(5)Hex(4)Fuc(1)NeuAc(1) | K.EQSTLAQMYPLQEIQNLTVK.L | 90 | Sialyfuco<br>sylated |
| HexNAc(5)Hex(6)Fuc(1)NeuAc(3) | K.EQSTLAQMYPLQEIQNLTVK.L | 90 | Sialyfuco<br>sylated |
| HexNAc(5)Hex(6)Fuc(1)NeuAc(2) | K.EQSTLAQMYPLQEIQNLTVK.L | 90 | Sialyfuco<br>sylated |
| HexNAc(5)Hex(6)Fuc(1)NeuAc(1) | K.EQSTLAQMYPLQEIQNLTVK.L | 90 | Sialyfuco<br>sylated |
| HexNAc(5)Hex(5)Fuc(1)NeuAc(2) | K.EQSTLAQMYPLQEIQNLTVK.L | 90 | Sialyfuco<br>sylated |
| HexNAc(5)Hex(4)Fuc(1)NeuAc(2) | K.EQSTLAQMYPLQEIQNLTVK.L | 90 | Sialyfuco<br>sylated |
| HexNAc(6)Hex(5)Fuc(1)NeuAc(2) | K.EQSTLAQMYPLQEIQNLTVK.L | 90 | Sialyfuco<br>sylated |

|                               |  |    |                       |
|-------------------------------|--|----|-----------------------|
| HexNAc(3)Hex(4)Fuc(1)NeuAc(1) | K.EQSTLAQMYPLQEIQNLTVK.L                       | 90 | Sialyfuco<br>slylated |
| HexNAc(5)Hex(6)Fuc(0)NeuAc(2) | K.EQSTLAQMYPLQEIQNLTVKLQLQA<br>LQQNGSSVLSEDK.S | 90 | Sialylated            |
| HexNAc(4)Hex(4)Fuc(0)NeuAc(1) | K.EQSTLAQMYPLQEIQNLTVK.L                       | 90 | Sialylated            |
| HexNAc(4)Hex(5)Fuc(0)NeuAc(1) | K.EQSTLAQMYPLQEIQNLTVK.L                       | 90 | Sialylated            |
| HexNAc(4)Hex(6)Fuc(0)NeuAc(1) | K.EQSTLAQMYPLQEIQNLTVK.L                       | 90 | Sialylated            |
| HexNAc(4)Hex(5)Fuc(0)NeuAc(2) | K.EQSTLAQMYPLQEIQNLTVK.L                       | 90 | Sialylated            |
| HexNAc(5)Hex(5)Fuc(0)NeuAc(1) | K.EQSTLAQMYPLQEIQNLTVK.L                       | 90 | Sialylated            |
| HexNAc(5)Hex(4)Fuc(0)NeuAc(1) | K.EQSTLAQMYPLQEIQNLTVK.L                       | 90 | Sialylated            |
| HexNAc(5)Hex(5)Fuc(0)NeuAc(2) | K.EQSTLAQMYPLQEIQNLTVK.L                       | 90 | Sialylated            |
| HexNAc(5)Hex(7)Fuc(0)NeuAc(2) | K.EQSTLAQMYPLQEIQNLTVK.L                       | 90 | Sialylated            |
| HexNAc(6)Hex(5)Fuc(0)NeuAc(1) | K.EQSTLAQMYPLQEIQNLTVK.L                       | 90 | Sialylated            |
| HexNAc(6)Hex(6)Fuc(0)NeuAc(1) | K.EQSTLAQMYPLQEIQNLTVK.L                       | 90 | Sialylated            |
| HexNAc(7)Hex(5)Fuc(0)NeuAc(1) | K.EQSTLAQMYPLQEIQNLTVK.L                       | 90 | Sialylated            |
| HexNAc(6)Hex(4)Fuc(0)NeuAc(1) | K.EQSTLAQMYPLQEIQNLTVK.L                       | 90 | Sialylated            |
| HexNAc(6)Hex(5)Fuc(0)NeuAc(2) | K.EQSTLAQMYPLQEIQNLTVK.L                       | 90 | Sialylated            |
| HexNAc(6)Hex(6)Fuc(0)NeuAc(2) | K.EQSTLAQMYPLQEIQNLTVK.L                       | 90 | Sialylated            |

|                               |                          |    |             |
|-------------------------------|--------------------------|----|-------------|
| HexNAc(5)Hex(6)Fuc(0)NeuAc(1) | K.EQSTLAQMYPLQEIQNLTVK.L | 90 | Sialylated  |
| HexNAc(3)Hex(4)Fuc(0)NeuAc(1) | K.EQSTLAQMYPLQEIQNLTVK.L | 90 | Sialylated  |
| HexNAc(4)Hex(6)Fuc(0)NeuAc(2) | K.EQSTLAQMYPLQEIQNLTVK.L | 90 | Sialylated  |
| HexNAc(4)Hex(7)Fuc(0)NeuAc(1) | K.EQSTLAQMYPLQEIQNLTVK.L | 90 | Sialylated  |
| HexNAc(7)Hex(4)Fuc(0)NeuAc(1) | K.EQSTLAQMYPLQEIQNLTVK.L | 90 | Sialylated  |
| HexNAc(6)Hex(7)Fuc(0)NeuAc(1) | K.EQSTLAQMYPLQEIQNLTVK.L | 90 | Sialylated  |
| HexNAc(6)Hex(6)Fuc(0)NeuAc(3) | K.EQSTLAQMYPLQEIQNLTVK.L | 90 | Sialylated  |
| HexNAc(6)Hex(3)Fuc(0)NeuAc(1) | K.EQSTLAQMYPLQEIQNLTVK.L | 90 | Sialylated  |
| HexNAc(4)Hex(4)Fuc(0)NeuAc(0) | K.EQSTLAQMYPLQEIQNLTVK.L | 90 | Undecorated |
| HexNAc(4)Hex(5)Fuc(0)NeuAc(0) | K.EQSTLAQMYPLQEIQNLTVK.L | 90 | Undecorated |
| HexNAc(4)Hex(3)Fuc(0)NeuAc(0) | K.EQSTLAQMYPLQEIQNLTVK.L | 90 | Undecorated |
| HexNAc(5)Hex(3)Fuc(0)NeuAc(0) | K.EQSTLAQMYPLQEIQNLTVK.L | 90 | Undecorated |
| HexNAc(4)Hex(6)Fuc(0)NeuAc(0) | K.EQSTLAQMYPLQEIQNLTVK.L | 90 | Undecorated |
| HexNAc(5)Hex(4)Fuc(0)NeuAc(0) | K.EQSTLAQMYPLQEIQNLTVK.L | 90 | Undecorated |
| HexNAc(5)Hex(5)Fuc(0)NeuAc(0) | K.EQSTLAQMYPLQEIQNLTVK.L | 90 | Undecorated |
| HexNAc(6)Hex(3)Fuc(0)NeuAc(0) | K.EQSTLAQMYPLQEIQNLTVK.L | 90 | Undecorated |

|                               |                          |     |             |
|-------------------------------|--------------------------|-----|-------------|
| HexNAc(6)Hex(4)Fuc(0)NeuAc(0) | K.EQSTLAQMYPLQEIQNLTVK.L | 90  | Undecorated |
| HexNAc(6)Hex(5)Fuc(0)NeuAc(0) | K.EQSTLAQMYPLQEIQNLTVK.L | 90  | Undecorated |
| HexNAc(6)Hex(6)Fuc(0)NeuAc(0) | K.EQSTLAQMYPLQEIQNLTVK.L | 90  | Undecorated |
| HexNAc(3)Hex(3)Fuc(0)NeuAc(0) | K.EQSTLAQMYPLQEIQNLTVK.L | 90  | Undecorated |
| HexNAc(7)Hex(6)Fuc(0)NeuAc(0) | K.EQSTLAQMYPLQEIQNLTVK.L | 90  | Undecorated |
| HexNAc(7)Hex(3)Fuc(0)NeuAc(0) | K.EQSTLAQMYPLQEIQNLTVK.L | 90  | Undecorated |
| HexNAc(7)Hex(4)Fuc(4)NeuAc(0) | K.LQLQALQQNGSSVLSEDK.S   | 103 | Fucosylated |
| HexNAc(5)Hex(5)Fuc(4)NeuAc(0) | K.LQLQALQQNGSSVLSEDK.S   | 103 | Fucosylated |
| HexNAc(5)Hex(3)Fuc(4)NeuAc(0) | K.LQLQALQQNGSSVLSEDK.S   | 103 | Fucosylated |
| HexNAc(7)Hex(3)Fuc(4)NeuAc(0) | K.LQLQALQQNGSSVLSEDK.S   | 103 | Fucosylated |
| HexNAc(4)Hex(4)Fuc(3)NeuAc(0) | K.LQLQALQQNGSSVLSEDK.S   | 103 | Fucosylated |
| HexNAc(4)Hex(5)Fuc(3)NeuAc(0) | K.LQLQALQQNGSSVLSEDK.S   | 103 | Fucosylated |
| HexNAc(4)Hex(3)Fuc(3)NeuAc(0) | K.LQLQALQQNGSSVLSEDK.S   | 103 | Fucosylated |
| HexNAc(4)Hex(6)Fuc(3)NeuAc(0) | K.LQLQALQQNGSSVLSEDK.S   | 103 | Fucosylated |
| HexNAc(6)Hex(5)Fuc(3)NeuAc(0) | K.LQLQALQQNGSSVLSEDK.S   | 103 | Fucosylated |
| HexNAc(7)Hex(4)Fuc(2)NeuAc(0) | K.LQLQALQQNGSSVLSEDK.S   | 103 | Fucosylated |

|                               |                        |     |             |
|-------------------------------|------------------------|-----|-------------|
| HexNAc(4)Hex(4)Fuc(2)NeuAc(0) | K.LQLQALQQNGSSVLSEDK.S | 103 | Fucosylated |
| HexNAc(4)Hex(5)Fuc(2)NeuAc(0) | K.LQLQALQQNGSSVLSEDK.S | 103 | Fucosylated |
| HexNAc(5)Hex(4)Fuc(2)NeuAc(0) | K.LQLQALQQNGSSVLSEDK.S | 103 | Fucosylated |
| HexNAc(3)Hex(4)Fuc(2)NeuAc(0) | K.LQLQALQQNGSSVLSEDK.S | 103 | Fucosylated |
| HexNAc(5)Hex(5)Fuc(2)NeuAc(0) | K.LQLQALQQNGSSVLSEDK.S | 103 | Fucosylated |
| HexNAc(4)Hex(6)Fuc(2)NeuAc(0) | K.LQLQALQQNGSSVLSEDK.S | 103 | Fucosylated |
| HexNAc(5)Hex(6)Fuc(2)NeuAc(0) | K.LQLQALQQNGSSVLSEDK.S | 103 | Fucosylated |
| HexNAc(6)Hex(6)Fuc(2)NeuAc(0) | K.LQLQALQQNGSSVLSEDK.S | 103 | Fucosylated |
| HexNAc(5)Hex(7)Fuc(2)NeuAc(0) | K.LQLQALQQNGSSVLSEDK.S | 103 | Fucosylated |
| HexNAc(3)Hex(5)Fuc(2)NeuAc(0) | K.LQLQALQQNGSSVLSEDK.S | 103 | Fucosylated |
| HexNAc(6)Hex(7)Fuc(2)NeuAc(0) | K.LQLQALQQNGSSVLSEDK.S | 103 | Fucosylated |
| HexNAc(3)Hex(4)Fuc(1)NeuAc(0) | K.LQLQALQQNGSSVLSEDK.S | 103 | Fucosylated |
| HexNAc(4)Hex(4)Fuc(1)NeuAc(0) | K.LQLQALQQNGSSVLSEDK.S | 103 | Fucosylated |
| HexNAc(4)Hex(3)Fuc(1)NeuAc(0) | K.LQLQALQQNGSSVLSEDK.S | 103 | Fucosylated |
| HexNAc(3)Hex(3)Fuc(1)NeuAc(0) | K.LQLQALQQNGSSVLSEDK.S | 103 | Fucosylated |
| HexNAc(5)Hex(4)Fuc(1)NeuAc(0) | K.LQLQALQQNGSSVLSEDK.S | 103 | Fucosylated |

|                                |                          |     |              |
|--------------------------------|--------------------------|-----|--------------|
| HexNAc(5)Hex(3)Fuc(1)NeuAc(0)  | K.LQLQALQQNGSSVLSEDK.S   | 103 | Fucosylated  |
| HexNAc(4)Hex(5)Fuc(1)NeuAc(0)  | K.LQLQALQQNGSSVLSEDK.S   | 103 | Fucosylated  |
| HexNAc(5)Hex(5)Fuc(1)NeuAc(0)  | K.LQLQALQQNGSSVLSEDK.S   | 103 | Fucosylated  |
| HexNAc(5)Hex(6)Fuc(1)NeuAc(0)  | K.LQLQALQQNGSSVLSEDK.S   | 103 | Fucosylated  |
| HexNAc(6)Hex(5)Fuc(1)NeuAc(0)  | K.LQLQALQQNGSSVLSEDK.S   | 103 | Fucosylated  |
| HexNAc(3)Hex(6)Fuc(1)NeuAc(0)  | K.LQLQALQQNGSSVLSEDK.S   | 103 | Fucosylated  |
| HexNAc(6)Hex(4)Fuc(1)NeuAc(0)  | K.LQLQALQQNGSSVLSEDK.S   | 103 | Fucosylated  |
| HexNAc(6)Hex(7)Fuc(1)NeuAc(0)  | K.LQLQALQQNGSSVLSEDK.S   | 103 | Fucosylated  |
| HexNAc(4)Hex(6)Fuc(1)NeuAc(0)  | K.LQLQALQQNGSSVLSEDK.S   | 103 | Fucosylated  |
| HexNAc(7)Hex(4)Fuc(1)NeuAc(0)  | K.LQLQALQQNGSSVLSEDK.S   | 103 | Fucosylated  |
| HexNAc(5)Hex(4)Fuc(3)NeuAc(0)  | K.LQLQALQQNGSSVLSEDKSK.R | 103 | Fucosylated  |
| HexNAc(2)Hex(11)Fuc(0)NeuAc(0) | K.LQLQALQQNGSSVLSEDK.S   | 103 | High Mannose |
| HexNAc(2)Hex(5)Fuc(0)NeuAc(0)  | K.LQLQALQQNGSSVLSEDK.S   | 103 | High Mannose |
| HexNAc(2)Hex(7)Fuc(0)NeuAc(0)  | K.LQLQALQQNGSSVLSEDK.S   | 103 | High Mannose |
| HexNAc(2)Hex(10)Fuc(0)NeuAc(0) | K.LQLQALQQNGSSVLSEDK.S   | 103 | High Mannose |
| HexNAc(2)Hex(9)Fuc(0)NeuAc(0)  | K.LQLQALQQNGSSVLSEDK.S   | 103 | High Mannose |

|                               |                        |     |                 |
|-------------------------------|------------------------|-----|-----------------|
| HexNAc(2)Hex(8)Fuc(0)NeuAc(0) | K.LQLQALQQNGSSVLSEDK.S | 103 | High Mannose    |
| HexNAc(4)Hex(4)Fuc(3)NeuAc(1) | K.LQLQALQQNGSSVLSEDK.S | 103 | Sialyfucoylated |
| HexNAc(5)Hex(4)Fuc(3)NeuAc(1) | K.LQLQALQQNGSSVLSEDK.S | 103 | Sialyfucoylated |
| HexNAc(5)Hex(5)Fuc(3)NeuAc(1) | K.LQLQALQQNGSSVLSEDK.S | 103 | Sialyfucoylated |
| HexNAc(4)Hex(6)Fuc(3)NeuAc(1) | K.LQLQALQQNGSSVLSEDK.S | 103 | Sialyfucoylated |
| HexNAc(5)Hex(6)Fuc(3)NeuAc(1) | K.LQLQALQQNGSSVLSEDK.S | 103 | Sialyfucoylated |
| HexNAc(5)Hex(7)Fuc(3)NeuAc(2) | K.LQLQALQQNGSSVLSEDK.S | 103 | Sialyfucoylated |
| HexNAc(4)Hex(5)Fuc(2)NeuAc(1) | K.LQLQALQQNGSSVLSEDK.S | 103 | Sialyfucoylated |
| HexNAc(9)Hex(9)Fuc(2)NeuAc(4) | K.LQLQALQQNGSSVLSEDK.S | 103 | Sialyfucoylated |
| HexNAc(4)Hex(6)Fuc(2)NeuAc(1) | K.LQLQALQQNGSSVLSEDK.S | 103 | Sialyfucoylated |
| HexNAc(5)Hex(5)Fuc(2)NeuAc(1) | K.LQLQALQQNGSSVLSEDK.S | 103 | Sialyfucoylated |
| HexNAc(4)Hex(4)Fuc(2)NeuAc(1) | K.LQLQALQQNGSSVLSEDK.S | 103 | Sialyfucoylated |
| HexNAc(5)Hex(6)Fuc(2)NeuAc(1) | K.LQLQALQQNGSSVLSEDK.S | 103 | Sialyfucoylated |
| HexNAc(4)Hex(5)Fuc(2)NeuAc(2) | K.LQLQALQQNGSSVLSEDK.S | 103 | Sialyfucoylated |
| HexNAc(5)Hex(4)Fuc(2)NeuAc(1) | K.LQLQALQQNGSSVLSEDK.S | 103 | Sialyfucoylated |
| HexNAc(4)Hex(6)Fuc(2)NeuAc(2) | K.LQLQALQQNGSSVLSEDK.S | 103 | Sialyfucoylated |

|                               |                        |     |                      |
|-------------------------------|------------------------|-----|----------------------|
| HexNAc(6)Hex(4)Fuc(2)NeuAc(1) | K.LQLQALQQNGSSVLSEDK.S | 103 | Sialyfuco<br>sylated |
| HexNAc(4)Hex(4)Fuc(1)NeuAc(1) | K.LQLQALQQNGSSVLSEDK.S | 103 | Sialyfuco<br>sylated |
| HexNAc(4)Hex(5)Fuc(1)NeuAc(1) | K.LQLQALQQNGSSVLSEDK.S | 103 | Sialyfuco<br>sylated |
| HexNAc(3)Hex(4)Fuc(1)NeuAc(1) | K.LQLQALQQNGSSVLSEDK.S | 103 | Sialyfuco<br>sylated |
| HexNAc(4)Hex(5)Fuc(1)NeuAc(2) | K.LQLQALQQNGSSVLSEDK.S | 103 | Sialyfuco<br>sylated |
| HexNAc(5)Hex(6)Fuc(1)NeuAc(1) | K.LQLQALQQNGSSVLSEDK.S | 103 | Sialyfuco<br>sylated |
| HexNAc(5)Hex(5)Fuc(1)NeuAc(1) | K.LQLQALQQNGSSVLSEDK.S | 103 | Sialyfuco<br>sylated |
| HexNAc(5)Hex(6)Fuc(1)NeuAc(2) | K.LQLQALQQNGSSVLSEDK.S | 103 | Sialyfuco<br>sylated |
| HexNAc(5)Hex(4)Fuc(1)NeuAc(1) | K.LQLQALQQNGSSVLSEDK.S | 103 | Sialyfuco<br>sylated |
| HexNAc(4)Hex(6)Fuc(1)NeuAc(1) | K.LQLQALQQNGSSVLSEDK.S | 103 | Sialyfuco<br>sylated |
| HexNAc(4)Hex(6)Fuc(1)NeuAc(2) | K.LQLQALQQNGSSVLSEDK.S | 103 | Sialyfuco<br>sylated |
| HexNAc(5)Hex(6)Fuc(1)NeuAc(3) | K.LQLQALQQNGSSVLSEDK.S | 103 | Sialyfuco<br>sylated |
| HexNAc(5)Hex(5)Fuc(1)NeuAc(2) | K.LQLQALQQNGSSVLSEDK.S | 103 | Sialyfuco<br>sylated |
| HexNAc(7)Hex(4)Fuc(1)NeuAc(1) | K.LQLQALQQNGSSVLSEDK.S | 103 | Sialyfuco<br>sylated |
| HexNAc(5)Hex(4)Fuc(1)NeuAc(2) | K.LQLQALQQNGSSVLSEDK.S | 103 | Sialyfuco<br>sylated |
| HexNAc(4)Hex(4)Fuc(0)NeuAc(1) | K.LQLQALQQNGSSVLSEDK.S | 103 | Sialylated           |

|                               |                        |     |            |
|-------------------------------|------------------------|-----|------------|
| HexNAc(4)Hex(5)Fuc(0)NeuAc(1) | K.LQLQALQQNGSSVLSEDK.S | 103 | Sialylated |
| HexNAc(7)Hex(4)Fuc(0)NeuAc(1) | K.LQLQALQQNGSSVLSEDK.S | 103 | Sialylated |
| HexNAc(5)Hex(5)Fuc(0)NeuAc(1) | K.LQLQALQQNGSSVLSEDK.S | 103 | Sialylated |
| HexNAc(4)Hex(5)Fuc(0)NeuAc(2) | K.LQLQALQQNGSSVLSEDK.S | 103 | Sialylated |
| HexNAc(5)Hex(4)Fuc(0)NeuAc(1) | K.LQLQALQQNGSSVLSEDK.S | 103 | Sialylated |
| HexNAc(6)Hex(6)Fuc(0)NeuAc(1) | K.LQLQALQQNGSSVLSEDK.S | 103 | Sialylated |
| HexNAc(5)Hex(5)Fuc(0)NeuAc(2) | K.LQLQALQQNGSSVLSEDK.S | 103 | Sialylated |
| HexNAc(6)Hex(6)Fuc(0)NeuAc(2) | K.LQLQALQQNGSSVLSEDK.S | 103 | Sialylated |
| HexNAc(3)Hex(4)Fuc(0)NeuAc(1) | K.LQLQALQQNGSSVLSEDK.S | 103 | Sialylated |
| HexNAc(4)Hex(5)Fuc(0)NeuAc(3) | K.LQLQALQQNGSSVLSEDK.S | 103 | Sialylated |
| HexNAc(5)Hex(6)Fuc(0)NeuAc(1) | K.LQLQALQQNGSSVLSEDK.S | 103 | Sialylated |
| HexNAc(6)Hex(4)Fuc(0)NeuAc(1) | K.LQLQALQQNGSSVLSEDK.S | 103 | Sialylated |
| HexNAc(6)Hex(5)Fuc(0)NeuAc(1) | K.LQLQALQQNGSSVLSEDK.S | 103 | Sialylated |
| HexNAc(4)Hex(6)Fuc(0)NeuAc(1) | K.LQLQALQQNGSSVLSEDK.S | 103 | Sialylated |
| HexNAc(6)Hex(3)Fuc(0)NeuAc(1) | K.LQLQALQQNGSSVLSEDK.S | 103 | Sialylated |
| HexNAc(5)Hex(7)Fuc(0)NeuAc(1) | K.LQLQALQQNGSSVLSEDK.S | 103 | Sialylated |

|                               |                        |     |             |
|-------------------------------|------------------------|-----|-------------|
| HexNAc(5)Hex(3)Fuc(0)NeuAc(0) | K.LQLQALQQNGSSVLSEDK.S | 103 | Undecorated |
| HexNAc(4)Hex(3)Fuc(0)NeuAc(0) | K.LQLQALQQNGSSVLSEDK.S | 103 | Undecorated |
| HexNAc(4)Hex(4)Fuc(0)NeuAc(0) | K.LQLQALQQNGSSVLSEDK.S | 103 | Undecorated |
| HexNAc(4)Hex(5)Fuc(0)NeuAc(0) | K.LQLQALQQNGSSVLSEDK.S | 103 | Undecorated |
| HexNAc(5)Hex(4)Fuc(0)NeuAc(0) | K.LQLQALQQNGSSVLSEDK.S | 103 | Undecorated |
| HexNAc(6)Hex(7)Fuc(0)NeuAc(0) | K.LQLQALQQNGSSVLSEDK.S | 103 | Undecorated |
| HexNAc(5)Hex(5)Fuc(0)NeuAc(0) | K.LQLQALQQNGSSVLSEDK.S | 103 | Undecorated |
| HexNAc(7)Hex(8)Fuc(0)NeuAc(0) | K.LQLQALQQNGSSVLSEDK.S | 103 | Undecorated |
| HexNAc(6)Hex(3)Fuc(0)NeuAc(0) | K.LQLQALQQNGSSVLSEDK.S | 103 | Undecorated |
| HexNAc(6)Hex(4)Fuc(0)NeuAc(0) | K.LQLQALQQNGSSVLSEDK.S | 103 | Undecorated |
| HexNAc(6)Hex(5)Fuc(0)NeuAc(0) | K.LQLQALQQNGSSVLSEDK.S | 103 | Undecorated |
| HexNAc(4)Hex(6)Fuc(0)NeuAc(0) | K.LQLQALQQNGSSVLSEDK.S | 103 | Undecorated |
| HexNAc(3)Hex(4)Fuc(0)NeuAc(0) | K.LQLQALQQNGSSVLSEDK.S | 103 | Undecorated |
| HexNAc(3)Hex(5)Fuc(0)NeuAc(0) | K.LQLQALQQNGSSVLSEDK.S | 103 | Undecorated |
| HexNAc(6)Hex(6)Fuc(0)NeuAc(0) | K.LQLQALQQNGSSVLSEDK.S | 103 | Undecorated |
| HexNAc(5)Hex(6)Fuc(0)NeuAc(0) | K.LQLQALQQNGSSVLSEDK.S | 103 | Undecorated |

|                               |                                      |     |              |
|-------------------------------|--------------------------------------|-----|--------------|
| HexNAc(7)Hex(6)Fuc(5)NeuAc(0) | K.FFVSVGLPNMTQGFWENSMLTDPGNVQK.A     | 322 | Fucosylated  |
| HexNAc(5)Hex(3)Fuc(4)NeuAc(0) | K.EAEKFFVSVGLPNMTQGFWENSMLTDPGNVQK.A | 322 | Fucosylated  |
| HexNAc(5)Hex(4)Fuc(4)NeuAc(0) | K.FFVSVGLPNMTQGFWENSMLTDPGNVQK.A     | 322 | Fucosylated  |
| HexNAc(6)Hex(4)Fuc(4)NeuAc(0) | K.FFVSVGLPNMTQGFWENSMLTDPGNVQK.A     | 322 | Fucosylated  |
| HexNAc(6)Hex(6)Fuc(3)NeuAc(0) | K.FFVSVGLPNMTQGFWENSMLTDPGNVQK.A     | 322 | Fucosylated  |
| HexNAc(6)Hex(3)Fuc(3)NeuAc(0) | K.FFVSVGLPNMTQGFWENSMLTDPGNVQK.A     | 322 | Fucosylated  |
| HexNAc(7)Hex(3)Fuc(2)NeuAc(0) | K.FFVSVGLPNMTQGFWENSMLTDPGNVQK.A     | 322 | Fucosylated  |
| HexNAc(3)Hex(4)Fuc(2)NeuAc(0) | K.FFVSVGLPNMTQGFWENSMLTDPGNVQK.A     | 322 | Fucosylated  |
| HexNAc(5)Hex(3)Fuc(2)NeuAc(0) | K.FFVSVGLPNMTQGFWENSMLTDPGNVQK.A     | 322 | Fucosylated  |
| HexNAc(7)Hex(4)Fuc(2)NeuAc(0) | K.FFVSVGLPNMTQGFWENSMLTDPGNVQK.A     | 322 | Fucosylated  |
| HexNAc(4)Hex(4)Fuc(2)NeuAc(0) | K.FFVSVGLPNMTQGFWENSMLTDPGNVQK.A     | 322 | Fucosylated  |
| HexNAc(4)Hex(5)Fuc(1)NeuAc(0) | K.FFVSVGLPNMTQGFWENSMLTDPGNVQK.A     | 322 | Fucosylated  |
| HexNAc(4)Hex(7)Fuc(1)NeuAc(0) | K.FFVSVGLPNMTQGFWENSMLTDPGNVQK.A     | 322 | Fucosylated  |
| HexNAc(4)Hex(6)Fuc(1)NeuAc(0) | K.FFVSVGLPNMTQGFWENSMLTDPGNVQK.A     | 322 | Fucosylated  |
| HexNAc(3)Hex(5)Fuc(1)NeuAc(0) | K.FFVSVGLPNMTQGFWENSMLTDPGNVQK.A     | 322 | Fucosylated  |
| HexNAc(2)Hex(6)Fuc(0)NeuAc(0) | K.EAEKFFVSVGLPNMTQGFWENSMLTDPGNVQK.A | 322 | High Mannose |

|                                |  |     |                            |
|--------------------------------|--|-----|----------------------------|
| HexNAc(2)Hex(11)Fuc(0)NeuAc(0) | K.FFVSVGLPNMTQGFWENSMLTDPGN<br>VQK.A     | 322 | High<br>Mannose            |
| HexNAc(2)Hex(4)Fuc(0)NeuAc(0)  | K.FFVSVGLPNMTQGFWENSMLTDPGN<br>VQK.A     | 322 | High<br>Mannose            |
| HexNAc(7)Hex(5)Fuc(5)NeuAc(2)  | K.FFVSVGLPNMTQGFWENSMLTDPGN<br>VQK.A     | 322 | Sialyfuco-<br>syla-<br>ted |
| HexNAc(6)Hex(4)Fuc(5)NeuAc(1)  | K.FFVSVGLPNMTQGFWENSMLTDPGN<br>VQK.A     | 322 | Sialyfuco-<br>syla-<br>ted |
| HexNAc(6)Hex(4)Fuc(4)NeuAc(1)  | K.EAEKFFVSVGLPNMTQGFWENSMLT<br>DPGNVQK.A | 322 | Sialyfuco-<br>syla-<br>ted |
| HexNAc(5)Hex(4)Fuc(4)NeuAc(1)  | K.FFVSVGLPNMTQGFWENSMLTDPGN<br>VQK.A     | 322 | Sialyfuco-<br>syla-<br>ted |
| HexNAc(6)Hex(5)Fuc(4)NeuAc(2)  | K.FFVSVGLPNMTQGFWENSMLTDPGN<br>VQK.A     | 322 | Sialyfuco-<br>syla-<br>ted |
| HexNAc(6)Hex(5)Fuc(4)NeuAc(1)  | K.FFVSVGLPNMTQGFWENSMLTDPGN<br>VQK.A     | 322 | Sialyfuco-<br>syla-<br>ted |
| HexNAc(7)Hex(5)Fuc(4)NeuAc(1)  | K.FFVSVGLPNMTQGFWENSMLTDPGN<br>VQK.A     | 322 | Sialyfuco-<br>syla-<br>ted |
| HexNAc(5)Hex(4)Fuc(3)NeuAc(1)  | K.FFVSVGLPNMTQGFWENSMLTDPGN<br>VQK.A     | 322 | Sialyfuco-<br>syla-<br>ted |
| HexNAc(6)Hex(4)Fuc(3)NeuAc(1)  | K.FFVSVGLPNMTQGFWENSMLTDPGN<br>VQK.A     | 322 | Sialyfuco-<br>syla-<br>ted |
| HexNAc(9)Hex(9)Fuc(3)NeuAc(1)  | K.FFVSVGLPNMTQGFWENSMLTDPGN<br>VQK.A     | 322 | Sialyfuco-<br>syla-<br>ted |
| HexNAc(6)Hex(6)Fuc(3)NeuAc(2)  | K.FFVSVGLPNMTQGFWENSMLTDPGN<br>VQK.A     | 322 | Sialyfuco-<br>syla-<br>ted |
| HexNAc(7)Hex(5)Fuc(3)NeuAc(1)  | K.FFVSVGLPNMTQGFWENSMLTDPGN<br>VQK.A     | 322 | Sialyfuco-<br>syla-<br>ted |
| HexNAc(4)Hex(7)Fuc(3)NeuAc(1)  | K.FFVSVGLPNMTQGFWENSMLTDPGN<br>VQK.A     | 322 | Sialyfuco-<br>syla-<br>ted |
| HexNAc(6)Hex(4)Fuc(2)NeuAc(1)  | K.EAEKFFVSVGLPNMTQGFWENSMLT<br>DPGNVQK.A | 322 | Sialyfuco-<br>syla-<br>ted |

|                               |                                      |     |                      |
|-------------------------------|--------------------------------------|-----|----------------------|
| HexNAc(6)Hex(3)Fuc(2)NeuAc(1) | K.EAEKFFVSVGLPNMTQGFWENSMLTDPGNVQK.A | 322 | Sialyfuco<br>sylated |
| HexNAc(4)Hex(4)Fuc(2)NeuAc(1) | K.EAEKFFVSVGLPNMTQGFWENSMLTDPGNVQK.A | 322 | Sialyfuco<br>sylated |
| HexNAc(6)Hex(5)Fuc(2)NeuAc(1) | K.FFVSVGLPNMTQGFWENSMLTDPGNVQK.A     | 322 | Sialyfuco<br>sylated |
| HexNAc(5)Hex(4)Fuc(2)NeuAc(1) | K.FFVSVGLPNMTQGFWENSMLTDPGNVQK.A     | 322 | Sialyfuco<br>sylated |
| HexNAc(8)Hex(8)Fuc(2)NeuAc(1) | K.FFVSVGLPNMTQGFWENSMLTDPGNVQK.A     | 322 | Sialyfuco<br>sylated |
| HexNAc(5)Hex(7)Fuc(2)NeuAc(2) | K.FFVSVGLPNMTQGFWENSMLTDPGNVQK.A     | 322 | Sialyfuco<br>sylated |
| HexNAc(7)Hex(5)Fuc(2)NeuAc(1) | K.FFVSVGLPNMTQGFWENSMLTDPGNVQK.A     | 322 | Sialyfuco<br>sylated |
| HexNAc(4)Hex(7)Fuc(2)NeuAc(2) | K.FFVSVGLPNMTQGFWENSMLTDPGNVQK.A     | 322 | Sialyfuco<br>sylated |
| HexNAc(3)Hex(4)Fuc(2)NeuAc(1) | K.FFVSVGLPNMTQGFWENSMLTDPGNVQK.A     | 322 | Sialyfuco<br>sylated |
| HexNAc(7)Hex(4)Fuc(2)NeuAc(1) | K.FFVSVGLPNMTQGFWENSMLTDPGNVQK.A     | 322 | Sialyfuco<br>sylated |
| HexNAc(3)Hex(5)Fuc(1)NeuAc(1) | K.FFVSVGLPNMTQGFWENSMLTDPGNVQK.A     | 322 | Sialyfuco<br>sylated |
| HexNAc(5)Hex(6)Fuc(1)NeuAc(1) | K.FFVSVGLPNMTQGFWENSMLTDPGNVQK.A     | 322 | Sialyfuco<br>sylated |
| HexNAc(6)Hex(3)Fuc(1)NeuAc(2) | K.FFVSVGLPNMTQGFWENSMLTDPGNVQK.A     | 322 | Sialyfuco<br>sylated |
| HexNAc(7)Hex(5)Fuc(1)NeuAc(2) | K.FFVSVGLPNMTQGFWENSMLTDPGNVQK.A     | 322 | Sialyfuco<br>sylated |
| HexNAc(7)Hex(4)Fuc(1)NeuAc(1) | K.FFVSVGLPNMTQGFWENSMLTDPGNVQK.A     | 322 | Sialyfuco<br>sylated |
| HexNAc(3)Hex(6)Fuc(1)NeuAc(1) | K.FFVSVGLPNMTQGFWENSMLTDPGNVQK.A     | 322 | Sialyfuco<br>sylated |

|                               |                                      |     |             |
|-------------------------------|--------------------------------------|-----|-------------|
| HexNAc(4)Hex(6)Fuc(0)NeuAc(1) | K.FFVSVGLPNMTQGFWENSMLTDPGN<br>VQK.A | 322 | Sialylated  |
| HexNAc(3)Hex(4)Fuc(0)NeuAc(1) | K.FFVSVGLPNMTQGFWENSMLTDPGN<br>VQK.A | 322 | Sialylated  |
| HexNAc(4)Hex(4)Fuc(0)NeuAc(1) | K.FFVSVGLPNMTQGFWENSMLTDPGN<br>VQK.A | 322 | Sialylated  |
| HexNAc(4)Hex(6)Fuc(0)NeuAc(2) | K.FFVSVGLPNMTQGFWENSMLTDPGN<br>VQK.A | 322 | Sialylated  |
| HexNAc(4)Hex(7)Fuc(0)NeuAc(2) | K.FFVSVGLPNMTQGFWENSMLTDPGN<br>VQK.A | 322 | Sialylated  |
| HexNAc(4)Hex(5)Fuc(0)NeuAc(1) | K.FFVSVGLPNMTQGFWENSMLTDPGN<br>VQK.A | 322 | Sialylated  |
| HexNAc(7)Hex(5)Fuc(0)NeuAc(1) | K.FFVSVGLPNMTQGFWENSMLTDPGN<br>VQK.A | 322 | Sialylated  |
| HexNAc(6)Hex(3)Fuc(0)NeuAc(1) | K.FFVSVGLPNMTQGFWENSMLTDPGN<br>VQK.A | 322 | Sialylated  |
| HexNAc(5)Hex(4)Fuc(0)NeuAc(1) | K.FFVSVGLPNMTQGFWENSMLTDPGN<br>VQK.A | 322 | Sialylated  |
| HexNAc(5)Hex(5)Fuc(0)NeuAc(2) | K.FFVSVGLPNMTQGFWENSMLTDPGN<br>VQK.A | 322 | Sialylated  |
| HexNAc(3)Hex(5)Fuc(0)NeuAc(1) | K.FFVSVGLPNMTQGFWENSMLTDPGN<br>VQK.A | 322 | Sialylated  |
| HexNAc(6)Hex(3)Fuc(0)NeuAc(0) | K.FFVSVGLPNMTQGFWENSMLTDPGN<br>VQK.A | 322 | Undecorated |
| HexNAc(7)Hex(6)Fuc(0)NeuAc(0) | K.FFVSVGLPNMTQGFWENSMLTDPGN<br>VQK.A | 322 | Undecorated |
| HexNAc(4)Hex(5)Fuc(3)NeuAc(0) | K.SIGLLSPDFQEDNETEINFLK.Q            | 432 | Fucosylated |
| HexNAc(5)Hex(4)Fuc(3)NeuAc(0) | K.SIGLLSPDFQEDNETEINFLK.Q            | 432 | Fucosylated |
| HexNAc(5)Hex(6)Fuc(3)NeuAc(0) | K.SIGLLSPDFQEDNETEINFLK.Q            | 432 | Fucosylated |

|                               |                           |     |             |
|-------------------------------|---------------------------|-----|-------------|
| HexNAc(5)Hex(5)Fuc(3)NeuAc(0) | K.SIGLLSPDFQEDNETEINFLK.Q | 432 | Fucosylated |
| HexNAc(5)Hex(6)Fuc(2)NeuAc(0) | K.SIGLLSPDFQEDNETEINFLK.Q | 432 | Fucosylated |
| HexNAc(4)Hex(6)Fuc(2)NeuAc(0) | K.SIGLLSPDFQEDNETEINFLK.Q | 432 | Fucosylated |
| HexNAc(5)Hex(5)Fuc(2)NeuAc(0) | K.SIGLLSPDFQEDNETEINFLK.Q | 432 | Fucosylated |
| HexNAc(5)Hex(7)Fuc(2)NeuAc(0) | K.SIGLLSPDFQEDNETEINFLK.Q | 432 | Fucosylated |
| HexNAc(5)Hex(6)Fuc(1)NeuAc(0) | K.SIGLLSPDFQEDNETEINFLK.Q | 432 | Fucosylated |
| HexNAc(5)Hex(5)Fuc(1)NeuAc(0) | K.SIGLLSPDFQEDNETEINFLK.Q | 432 | Fucosylated |
| HexNAc(6)Hex(7)Fuc(1)NeuAc(0) | K.SIGLLSPDFQEDNETEINFLK.Q | 432 | Fucosylated |
| HexNAc(6)Hex(5)Fuc(1)NeuAc(0) | K.SIGLLSPDFQEDNETEINFLK.Q | 432 | Fucosylated |
| HexNAc(4)Hex(5)Fuc(1)NeuAc(0) | K.SIGLLSPDFQEDNETEINFLK.Q | 432 | Fucosylated |
| HexNAc(5)Hex(4)Fuc(1)NeuAc(0) | K.SIGLLSPDFQEDNETEINFLK.Q | 432 | Fucosylated |
| HexNAc(6)Hex(6)Fuc(1)NeuAc(0) | K.SIGLLSPDFQEDNETEINFLK.Q | 432 | Fucosylated |
| HexNAc(5)Hex(3)Fuc(1)NeuAc(0) | K.SIGLLSPDFQEDNETEINFLK.Q | 432 | Fucosylated |
| HexNAc(6)Hex(4)Fuc(1)NeuAc(0) | K.SIGLLSPDFQEDNETEINFLK.Q | 432 | Fucosylated |
| HexNAc(4)Hex(4)Fuc(1)NeuAc(0) | K.SIGLLSPDFQEDNETEINFLK.Q | 432 | Fucosylated |
| HexNAc(4)Hex(3)Fuc(1)NeuAc(0) | K.SIGLLSPDFQEDNETEINFLK.Q | 432 | Fucosylated |

|                               |                           |     |                      |
|-------------------------------|---------------------------|-----|----------------------|
| HexNAc(6)Hex(7)Fuc(4)NeuAc(2) | K.SIGLLSPDFQEDNETEINFLK.Q | 432 | Sialyfuco<br>sylated |
| HexNAc(4)Hex(5)Fuc(3)NeuAc(1) | K.SIGLLSPDFQEDNETEINFLK.Q | 432 | Sialyfuco<br>sylated |
| HexNAc(4)Hex(4)Fuc(3)NeuAc(1) | K.SIGLLSPDFQEDNETEINFLK.Q | 432 | Sialyfuco<br>sylated |
| HexNAc(5)Hex(6)Fuc(2)NeuAc(1) | K.SIGLLSPDFQEDNETEINFLK.Q | 432 | Sialyfuco<br>sylated |
| HexNAc(4)Hex(5)Fuc(2)NeuAc(1) | K.SIGLLSPDFQEDNETEINFLK.Q | 432 | Sialyfuco<br>sylated |
| HexNAc(6)Hex(7)Fuc(2)NeuAc(2) | K.SIGLLSPDFQEDNETEINFLK.Q | 432 | Sialyfuco<br>sylated |
| HexNAc(4)Hex(6)Fuc(2)NeuAc(1) | K.SIGLLSPDFQEDNETEINFLK.Q | 432 | Sialyfuco<br>sylated |
| HexNAc(6)Hex(7)Fuc(2)NeuAc(1) | K.SIGLLSPDFQEDNETEINFLK.Q | 432 | Sialyfuco<br>sylated |
| HexNAc(6)Hex(6)Fuc(2)NeuAc(1) | K.SIGLLSPDFQEDNETEINFLK.Q | 432 | Sialyfuco<br>sylated |
| HexNAc(5)Hex(6)Fuc(2)NeuAc(2) | K.SIGLLSPDFQEDNETEINFLK.Q | 432 | Sialyfuco<br>sylated |
| HexNAc(6)Hex(7)Fuc(2)NeuAc(3) | K.SIGLLSPDFQEDNETEINFLK.Q | 432 | Sialyfuco<br>sylated |
| HexNAc(5)Hex(7)Fuc(2)NeuAc(1) | K.SIGLLSPDFQEDNETEINFLK.Q | 432 | Sialyfuco<br>sylated |
| HexNAc(5)Hex(7)Fuc(2)NeuAc(2) | K.SIGLLSPDFQEDNETEINFLK.Q | 432 | Sialyfuco<br>sylated |
| HexNAc(4)Hex(5)Fuc(2)NeuAc(2) | K.SIGLLSPDFQEDNETEINFLK.Q | 432 | Sialyfuco<br>sylated |
| HexNAc(4)Hex(5)Fuc(1)NeuAc(2) | K.SIGLLSPDFQEDNETEINFLK.Q | 432 | Sialyfuco<br>sylated |
| HexNAc(5)Hex(6)Fuc(1)NeuAc(1) | K.SIGLLSPDFQEDNETEINFLK.Q | 432 | Sialyfuco<br>sylated |

|                               |                           |     |                      |
|-------------------------------|---------------------------|-----|----------------------|
| HexNAc(6)Hex(6)Fuc(1)NeuAc(1) | K.SIGLLSPDFQEDNETEINFLK.Q | 432 | Sialyfuco<br>sylated |
| HexNAc(5)Hex(6)Fuc(1)NeuAc(2) | K.SIGLLSPDFQEDNETEINFLK.Q | 432 | Sialyfuco<br>sylated |
| HexNAc(5)Hex(5)Fuc(1)NeuAc(1) | K.SIGLLSPDFQEDNETEINFLK.Q | 432 | Sialyfuco<br>sylated |
| HexNAc(6)Hex(7)Fuc(1)NeuAc(3) | K.SIGLLSPDFQEDNETEINFLK.Q | 432 | Sialyfuco<br>sylated |
| HexNAc(6)Hex(6)Fuc(1)NeuAc(2) | K.SIGLLSPDFQEDNETEINFLK.Q | 432 | Sialyfuco<br>sylated |
| HexNAc(4)Hex(5)Fuc(1)NeuAc(1) | K.SIGLLSPDFQEDNETEINFLK.Q | 432 | Sialyfuco<br>sylated |
| HexNAc(4)Hex(4)Fuc(1)NeuAc(1) | K.SIGLLSPDFQEDNETEINFLK.Q | 432 | Sialyfuco<br>sylated |
| HexNAc(6)Hex(7)Fuc(1)NeuAc(2) | K.SIGLLSPDFQEDNETEINFLK.Q | 432 | Sialyfuco<br>sylated |
| HexNAc(5)Hex(6)Fuc(1)NeuAc(3) | K.SIGLLSPDFQEDNETEINFLK.Q | 432 | Sialyfuco<br>sylated |
| HexNAc(6)Hex(7)Fuc(1)NeuAc(1) | K.SIGLLSPDFQEDNETEINFLK.Q | 432 | Sialyfuco<br>sylated |
| HexNAc(6)Hex(7)Fuc(1)NeuAc(4) | K.SIGLLSPDFQEDNETEINFLK.Q | 432 | Sialyfuco<br>sylated |
| HexNAc(5)Hex(4)Fuc(1)NeuAc(1) | K.SIGLLSPDFQEDNETEINFLK.Q | 432 | Sialyfuco<br>sylated |
| HexNAc(5)Hex(5)Fuc(1)NeuAc(2) | K.SIGLLSPDFQEDNETEINFLK.Q | 432 | Sialyfuco<br>sylated |
| HexNAc(5)Hex(4)Fuc(1)NeuAc(2) | K.SIGLLSPDFQEDNETEINFLK.Q | 432 | Sialyfuco<br>sylated |
| HexNAc(6)Hex(5)Fuc(1)NeuAc(1) | K.SIGLLSPDFQEDNETEINFLK.Q | 432 | Sialyfuco<br>sylated |
| HexNAc(6)Hex(6)Fuc(1)NeuAc(3) | K.SIGLLSPDFQEDNETEINFLK.Q | 432 | Sialyfuco<br>sylated |

|                               |                              |     |                 |
|-------------------------------|------------------------------|-----|-----------------|
| HexNAc(6)Hex(5)Fuc(1)NeuAc(2) | K.SIGLLSPDFQEDNETEINFLK.Q    | 432 | Sialyfucoylated |
| HexNAc(6)Hex(5)Fuc(0)NeuAc(2) | K.HLKSIGLLSPDFQEDNETEINFLK.Q | 432 | Sialylated      |
| HexNAc(7)Hex(6)Fuc(0)NeuAc(2) | K.HLKSIGLLSPDFQEDNETEINFLK.Q | 432 | Sialylated      |
| HexNAc(4)Hex(5)Fuc(0)NeuAc(1) | K.SIGLLSPDFQEDNETEINFLK.Q    | 432 | Sialylated      |
| HexNAc(5)Hex(6)Fuc(0)NeuAc(1) | K.SIGLLSPDFQEDNETEINFLK.Q    | 432 | Sialylated      |
| HexNAc(4)Hex(4)Fuc(0)NeuAc(1) | K.SIGLLSPDFQEDNETEINFLK.Q    | 432 | Sialylated      |
| HexNAc(5)Hex(5)Fuc(0)NeuAc(1) | K.SIGLLSPDFQEDNETEINFLK.Q    | 432 | Sialylated      |
| HexNAc(6)Hex(7)Fuc(0)NeuAc(3) | K.SIGLLSPDFQEDNETEINFLK.Q    | 432 | Sialylated      |
| HexNAc(7)Hex(7)Fuc(0)NeuAc(2) | K.SIGLLSPDFQEDNETEINFLK.Q    | 432 | Sialylated      |
| HexNAc(6)Hex(6)Fuc(0)NeuAc(3) | K.SIGLLSPDFQEDNETEINFLK.Q    | 432 | Sialylated      |
| HexNAc(5)Hex(5)Fuc(0)NeuAc(2) | K.SIGLLSPDFQEDNETEINFLK.Q    | 432 | Sialylated      |
| HexNAc(7)Hex(7)Fuc(0)NeuAc(3) | K.SIGLLSPDFQEDNETEINFLK.Q    | 432 | Sialylated      |
| HexNAc(6)Hex(6)Fuc(0)NeuAc(2) | K.SIGLLSPDFQEDNETEINFLK.Q    | 432 | Sialylated      |
| HexNAc(6)Hex(6)Fuc(0)NeuAc(1) | K.SIGLLSPDFQEDNETEINFLK.Q    | 432 | Sialylated      |
| HexNAc(5)Hex(4)Fuc(0)NeuAc(1) | K.SIGLLSPDFQEDNETEINFLK.Q    | 432 | Sialylated      |
| HexNAc(5)Hex(6)Fuc(0)NeuAc(2) | K.SIGLLSPDFQEDNETEINFLK.Q    | 432 | Sialylated      |

|                               |                           |     |             |
|-------------------------------|---------------------------|-----|-------------|
| HexNAc(6)Hex(7)Fuc(0)NeuAc(1) | K.SIGLLSPDFQEDNETEINFLK.Q | 432 | Sialylated  |
| HexNAc(6)Hex(5)Fuc(0)NeuAc(1) | K.SIGLLSPDFQEDNETEINFLK.Q | 432 | Sialylated  |
| HexNAc(5)Hex(4)Fuc(0)NeuAc(0) | K.SIGLLSPDFQEDNETEINFLK.Q | 432 | Undecorated |
| HexNAc(6)Hex(4)Fuc(0)NeuAc(0) | K.SIGLLSPDFQEDNETEINFLK.Q | 432 | Undecorated |
| HexNAc(5)Hex(5)Fuc(0)NeuAc(0) | K.SIGLLSPDFQEDNETEINFLK.Q | 432 | Undecorated |
| HexNAc(4)Hex(6)Fuc(0)NeuAc(0) | K.SIGLLSPDFQEDNETEINFLK.Q | 432 | Undecorated |
| HexNAc(4)Hex(4)Fuc(3)NeuAc(0) | K.CDISNSTEAGQK.L          | 546 | Fucosylated |
| HexNAc(5)Hex(5)Fuc(3)NeuAc(0) | K.CDISNSTEAGQK.L          | 546 | Fucosylated |
| HexNAc(4)Hex(5)Fuc(3)NeuAc(0) | K.CDISNSTEAGQK.L          | 546 | Fucosylated |
| HexNAc(5)Hex(6)Fuc(3)NeuAc(0) | K.CDISNSTEAGQK.L          | 546 | Fucosylated |
| HexNAc(5)Hex(4)Fuc(3)NeuAc(0) | K.CDISNSTEAGQK.L          | 546 | Fucosylated |
| HexNAc(4)Hex(4)Fuc(2)NeuAc(0) | K.CDISNSTEAGQK.L          | 546 | Fucosylated |
| HexNAc(5)Hex(6)Fuc(2)NeuAc(0) | K.CDISNSTEAGQK.L          | 546 | Fucosylated |
| HexNAc(5)Hex(4)Fuc(2)NeuAc(0) | K.CDISNSTEAGQK.L          | 546 | Fucosylated |
| HexNAc(4)Hex(5)Fuc(2)NeuAc(0) | K.CDISNSTEAGQK.L          | 546 | Fucosylated |
| HexNAc(3)Hex(4)Fuc(2)NeuAc(0) | K.CDISNSTEAGQK.L          | 546 | Fucosylated |

|                               |                  |     |             |
|-------------------------------|------------------|-----|-------------|
| HexNAc(4)Hex(6)Fuc(2)NeuAc(0) | K.CDISNSTEAGQK.L | 546 | Fucosylated |
| HexNAc(5)Hex(3)Fuc(2)NeuAc(0) | K.CDISNSTEAGQK.L | 546 | Fucosylated |
| HexNAc(4)Hex(3)Fuc(1)NeuAc(0) | K.CDISNSTEAGQK.L | 546 | Fucosylated |
| HexNAc(4)Hex(4)Fuc(1)NeuAc(0) | K.CDISNSTEAGQK.L | 546 | Fucosylated |
| HexNAc(3)Hex(4)Fuc(1)NeuAc(0) | K.CDISNSTEAGQK.L | 546 | Fucosylated |
| HexNAc(3)Hex(5)Fuc(1)NeuAc(0) | K.CDISNSTEAGQK.L | 546 | Fucosylated |
| HexNAc(4)Hex(5)Fuc(1)NeuAc(0) | K.CDISNSTEAGQK.L | 546 | Fucosylated |
| HexNAc(5)Hex(5)Fuc(1)NeuAc(0) | K.CDISNSTEAGQK.L | 546 | Fucosylated |
| HexNAc(5)Hex(6)Fuc(1)NeuAc(0) | K.CDISNSTEAGQK.L | 546 | Fucosylated |
| HexNAc(3)Hex(3)Fuc(1)NeuAc(0) | K.CDISNSTEAGQK.L | 546 | Fucosylated |
| HexNAc(5)Hex(4)Fuc(1)NeuAc(0) | K.CDISNSTEAGQK.L | 546 | Fucosylated |
| HexNAc(6)Hex(4)Fuc(1)NeuAc(0) | K.CDISNSTEAGQK.L | 546 | Fucosylated |
| HexNAc(6)Hex(6)Fuc(1)NeuAc(0) | K.CDISNSTEAGQK.L | 546 | Fucosylated |
| HexNAc(5)Hex(3)Fuc(1)NeuAc(0) | K.CDISNSTEAGQK.L | 546 | Fucosylated |
| HexNAc(6)Hex(3)Fuc(1)NeuAc(0) | K.CDISNSTEAGQK.L | 546 | Fucosylated |
| HexNAc(6)Hex(7)Fuc(1)NeuAc(0) | K.CDISNSTEAGQK.L | 546 | Fucosylated |

|                                |                  |     |                 |
|--------------------------------|------------------|-----|-----------------|
| HexNAc(6)Hex(5)Fuc(1)NeuAc(0)  | K.CDISNSTEAGQK.L | 546 | Fucosylated     |
| HexNAc(3)Hex(6)Fuc(1)NeuAc(0)  | K.CDISNSTEAGQK.L | 546 | Fucosylated     |
| HexNAc(2)Hex(8)Fuc(0)NeuAc(0)  | K.CDISNSTEAGQK.L | 546 | High Mannose    |
| HexNAc(2)Hex(5)Fuc(0)NeuAc(0)  | K.CDISNSTEAGQK.L | 546 | High Mannose    |
| HexNAc(2)Hex(7)Fuc(0)NeuAc(0)  | K.CDISNSTEAGQK.L | 546 | High Mannose    |
| HexNAc(2)Hex(6)Fuc(0)NeuAc(0)  | K.CDISNSTEAGQK.L | 546 | High Mannose    |
| HexNAc(2)Hex(11)Fuc(0)NeuAc(0) | K.CDISNSTEAGQK.L | 546 | High Mannose    |
| HexNAc(5)Hex(4)Fuc(4)NeuAc(1)  | K.CDISNSTEAGQK.L | 546 | Sialyfucoylated |
| HexNAc(6)Hex(4)Fuc(4)NeuAc(1)  | K.CDISNSTEAGQK.L | 546 | Sialyfucoylated |
| HexNAc(5)Hex(6)Fuc(3)NeuAc(1)  | K.CDISNSTEAGQK.L | 546 | Sialyfucoylated |
| HexNAc(5)Hex(5)Fuc(3)NeuAc(1)  | K.CDISNSTEAGQK.L | 546 | Sialyfucoylated |
| HexNAc(6)Hex(7)Fuc(3)NeuAc(1)  | K.CDISNSTEAGQK.L | 546 | Sialyfucoylated |
| HexNAc(4)Hex(5)Fuc(3)NeuAc(1)  | K.CDISNSTEAGQK.L | 546 | Sialyfucoylated |
| HexNAc(4)Hex(6)Fuc(2)NeuAc(1)  | K.CDISNSTEAGQK.L | 546 | Sialyfucoylated |
| HexNAc(4)Hex(5)Fuc(2)NeuAc(1)  | K.CDISNSTEAGQK.L | 546 | Sialyfucoylated |
| HexNAc(4)Hex(5)Fuc(1)NeuAc(2)  | K.CDISNSTEAGQK.L | 546 | Sialyfucoylated |

|                               |                  |     |                      |
|-------------------------------|------------------|-----|----------------------|
| HexNAc(4)Hex(4)Fuc(1)NeuAc(1) | K.CDISNSTEAGQK.L | 546 | Sialyfuco<br>sylated |
| HexNAc(4)Hex(5)Fuc(1)NeuAc(1) | K.CDISNSTEAGQK.L | 546 | Sialyfuco<br>sylated |
| HexNAc(5)Hex(5)Fuc(1)NeuAc(1) | K.CDISNSTEAGQK.L | 546 | Sialyfuco<br>sylated |
| HexNAc(5)Hex(4)Fuc(1)NeuAc(1) | K.CDISNSTEAGQK.L | 546 | Sialyfuco<br>sylated |
| HexNAc(3)Hex(4)Fuc(1)NeuAc(1) | K.CDISNSTEAGQK.L | 546 | Sialyfuco<br>sylated |
| HexNAc(5)Hex(6)Fuc(1)NeuAc(1) | K.CDISNSTEAGQK.L | 546 | Sialyfuco<br>sylated |
| HexNAc(6)Hex(5)Fuc(1)NeuAc(1) | K.CDISNSTEAGQK.L | 546 | Sialyfuco<br>sylated |
| HexNAc(6)Hex(4)Fuc(1)NeuAc(1) | K.CDISNSTEAGQK.L | 546 | Sialyfuco<br>sylated |
| HexNAc(5)Hex(6)Fuc(1)NeuAc(2) | K.CDISNSTEAGQK.L | 546 | Sialyfuco<br>sylated |
| HexNAc(3)Hex(5)Fuc(1)NeuAc(1) | K.CDISNSTEAGQK.L | 546 | Sialyfuco<br>sylated |
| HexNAc(6)Hex(6)Fuc(1)NeuAc(2) | K.CDISNSTEAGQK.L | 546 | Sialyfuco<br>sylated |
| HexNAc(6)Hex(7)Fuc(1)NeuAc(1) | K.CDISNSTEAGQK.L | 546 | Sialyfuco<br>sylated |
| HexNAc(5)Hex(5)Fuc(1)NeuAc(2) | K.CDISNSTEAGQK.L | 546 | Sialyfuco<br>sylated |
| HexNAc(6)Hex(6)Fuc(1)NeuAc(1) | K.CDISNSTEAGQK.L | 546 | Sialyfuco<br>sylated |
| HexNAc(6)Hex(7)Fuc(1)NeuAc(2) | K.CDISNSTEAGQK.L | 546 | Sialyfuco<br>sylated |
| HexNAc(6)Hex(7)Fuc(1)NeuAc(3) | K.CDISNSTEAGQK.L | 546 | Sialyfuco<br>sylated |

|                               |                  |     |                      |
|-------------------------------|------------------|-----|----------------------|
| HexNAc(5)Hex(6)Fuc(1)NeuAc(3) | K.CDISNSTEAGQK.L | 546 | Sialyfuco<br>sylated |
| HexNAc(3)Hex(6)Fuc(1)NeuAc(1) | K.CDISNSTEAGQK.L | 546 | Sialyfuco<br>sylated |
| HexNAc(6)Hex(6)Fuc(1)NeuAc(3) | K.CDISNSTEAGQK.L | 546 | Sialyfuco<br>sylated |
| HexNAc(6)Hex(5)Fuc(1)NeuAc(2) | K.CDISNSTEAGQK.L | 546 | Sialyfuco<br>sylated |
| HexNAc(5)Hex(4)Fuc(0)NeuAc(1) | K.CDISNSTEAGQK.L | 546 | Sialylated           |
| HexNAc(4)Hex(4)Fuc(0)NeuAc(1) | K.CDISNSTEAGQK.L | 546 | Sialylated           |
| HexNAc(5)Hex(5)Fuc(0)NeuAc(1) | K.CDISNSTEAGQK.L | 546 | Sialylated           |
| HexNAc(5)Hex(5)Fuc(0)NeuAc(2) | K.CDISNSTEAGQK.L | 546 | Sialylated           |
| HexNAc(6)Hex(5)Fuc(0)NeuAc(1) | K.CDISNSTEAGQK.L | 546 | Sialylated           |
| HexNAc(6)Hex(6)Fuc(0)NeuAc(1) | K.CDISNSTEAGQK.L | 546 | Sialylated           |
| HexNAc(3)Hex(4)Fuc(0)NeuAc(1) | K.CDISNSTEAGQK.L | 546 | Sialylated           |
| HexNAc(7)Hex(5)Fuc(0)NeuAc(1) | K.CDISNSTEAGQK.L | 546 | Sialylated           |
| HexNAc(6)Hex(3)Fuc(0)NeuAc(1) | K.CDISNSTEAGQK.L | 546 | Sialylated           |
| HexNAc(6)Hex(5)Fuc(0)NeuAc(2) | K.CDISNSTEAGQK.L | 546 | Sialylated           |
| HexNAc(6)Hex(4)Fuc(0)NeuAc(1) | K.CDISNSTEAGQK.L | 546 | Sialylated           |
| HexNAc(6)Hex(6)Fuc(0)NeuAc(2) | K.CDISNSTEAGQK.L | 546 | Sialylated           |

|                               |                  |     |             |
|-------------------------------|------------------|-----|-------------|
| HexNAc(7)Hex(4)Fuc(0)NeuAc(1) | K.CDISNSTEAGQK.L | 546 | Sialylated  |
| HexNAc(4)Hex(5)Fuc(0)NeuAc(1) | K.CDISNSTEAGQK.L | 546 | Sialylated  |
| HexNAc(6)Hex(6)Fuc(0)NeuAc(3) | K.CDISNSTEAGQK.L | 546 | Sialylated  |
| HexNAc(3)Hex(5)Fuc(0)NeuAc(1) | K.CDISNSTEAGQK.L | 546 | Sialylated  |
| HexNAc(7)Hex(6)Fuc(0)NeuAc(1) | K.CDISNSTEAGQK.L | 546 | Sialylated  |
| HexNAc(7)Hex(7)Fuc(0)NeuAc(3) | K.CDISNSTEAGQK.L | 546 | Sialylated  |
| HexNAc(7)Hex(6)Fuc(0)NeuAc(2) | K.CDISNSTEAGQK.L | 546 | Sialylated  |
| HexNAc(5)Hex(3)Fuc(0)NeuAc(0) | K.CDISNSTEAGQK.L | 546 | Undecorated |
| HexNAc(6)Hex(3)Fuc(0)NeuAc(0) | K.CDISNSTEAGQK.L | 546 | Undecorated |
| HexNAc(4)Hex(4)Fuc(0)NeuAc(0) | K.CDISNSTEAGQK.L | 546 | Undecorated |
| HexNAc(5)Hex(5)Fuc(0)NeuAc(0) | K.CDISNSTEAGQK.L | 546 | Undecorated |
| HexNAc(5)Hex(4)Fuc(0)NeuAc(0) | K.CDISNSTEAGQK.L | 546 | Undecorated |
| HexNAc(4)Hex(3)Fuc(0)NeuAc(0) | K.CDISNSTEAGQK.L | 546 | Undecorated |
| HexNAc(3)Hex(5)Fuc(0)NeuAc(0) | K.CDISNSTEAGQK.L | 546 | Undecorated |
| HexNAc(6)Hex(5)Fuc(0)NeuAc(0) | K.CDISNSTEAGQK.L | 546 | Undecorated |
| HexNAc(6)Hex(4)Fuc(0)NeuAc(0) | K.CDISNSTEAGQK.L | 546 | Undecorated |

|                               |   |     |             |
|-------------------------------|---|-----|-------------|
| HexNAc(3)Hex(4)Fuc(0)NeuAc(0) | K.CDISNSTEAGQK.L                              | 546 | Undecorated |
| HexNAc(3)Hex(6)Fuc(0)NeuAc(0) | K.CDISNSTEAGQK.L                              | 546 | Undecorated |
| HexNAc(4)Hex(5)Fuc(0)NeuAc(0) | K.CDISNSTEAGQK.L                              | 546 | Undecorated |
| HexNAc(6)Hex(6)Fuc(0)NeuAc(0) | K.CDISNSTEAGQK.L                              | 546 | Undecorated |
| HexNAc(7)Hex(5)Fuc(0)NeuAc(0) | K.CDISNSTEAGQK.L                              | 546 | Undecorated |
| HexNAc(7)Hex(5)Fuc(4)NeuAc(0) | K.FNHEAEDLFYQSSLASWNYNTNITEE<br>NVQNMNNAGDK.W | 690 | Fucosylated |
| HexNAc(5)Hex(5)Fuc(4)NeuAc(0) | K.NVSDIIPR.T                                  | 690 | Fucosylated |
| HexNAc(4)Hex(5)Fuc(2)NeuAc(0) | K.NVSDIIPR.T                                  | 690 | Fucosylated |
| HexNAc(5)Hex(7)Fuc(2)NeuAc(0) | K.NVSDIIPR.T                                  | 690 | Fucosylated |
| HexNAc(3)Hex(4)Fuc(1)NeuAc(0) | K.NVSDIIPR.T                                  | 690 | Fucosylated |
| HexNAc(4)Hex(5)Fuc(1)NeuAc(0) | K.NVSDIIPR.T                                  | 690 | Fucosylated |
| HexNAc(4)Hex(3)Fuc(1)NeuAc(0) | K.NVSDIIPR.T                                  | 690 | Fucosylated |
| HexNAc(4)Hex(4)Fuc(1)NeuAc(0) | K.NVSDIIPR.T                                  | 690 | Fucosylated |
| HexNAc(3)Hex(3)Fuc(1)NeuAc(0) | K.NVSDIIPR.T                                  | 690 | Fucosylated |
| HexNAc(5)Hex(6)Fuc(1)NeuAc(0) | K.NVSDIIPR.T                                  | 690 | Fucosylated |
| HexNAc(5)Hex(5)Fuc(1)NeuAc(0) | K.NVSDIIPR.T                                  | 690 | Fucosylated |

|                               |              |     |                      |
|-------------------------------|--------------|-----|----------------------|
| HexNAc(5)Hex(4)Fuc(1)NeuAc(0) | K.NVSDIIPR.T | 690 | Fucosylated          |
| HexNAc(5)Hex(7)Fuc(1)NeuAc(0) | K.NVSDIIPR.T | 690 | Fucosylated          |
| HexNAc(6)Hex(7)Fuc(1)NeuAc(0) | K.NVSDIIPR.T | 690 | Fucosylated          |
| HexNAc(5)Hex(6)Fuc(3)NeuAc(1) | K.NVSDIIPR.T | 690 | Sialyfuco<br>sylated |
| HexNAc(4)Hex(5)Fuc(2)NeuAc(1) | K.NVSDIIPR.T | 690 | Sialyfuco<br>sylated |
| HexNAc(5)Hex(6)Fuc(2)NeuAc(1) | K.NVSDIIPR.T | 690 | Sialyfuco<br>sylated |
|                               |              |     |                      |
| HexNAc(5)Hex(7)Fuc(2)NeuAc(1) | K.NVSDIIPR.T | 690 | Sialyfuco<br>sylated |
| HexNAc(5)Hex(5)Fuc(2)NeuAc(1) | K.NVSDIIPR.T | 690 | Sialyfuco<br>sylated |
| HexNAc(4)Hex(5)Fuc(1)NeuAc(1) | K.NVSDIIPR.T | 690 | Sialyfuco<br>sylated |
| HexNAc(4)Hex(4)Fuc(1)NeuAc(1) | K.NVSDIIPR.T | 690 | Sialyfuco<br>sylated |
| HexNAc(5)Hex(6)Fuc(1)NeuAc(1) | K.NVSDIIPR.T | 690 | Sialyfuco<br>sylated |
| HexNAc(5)Hex(4)Fuc(1)NeuAc(1) | K.NVSDIIPR.T | 690 | Sialyfuco<br>sylated |
| HexNAc(4)Hex(5)Fuc(1)NeuAc(2) | K.NVSDIIPR.T | 690 | Sialyfuco<br>sylated |
| HexNAc(5)Hex(6)Fuc(1)NeuAc(2) | K.NVSDIIPR.T | 690 | Sialyfuco<br>sylated |
| HexNAc(5)Hex(5)Fuc(1)NeuAc(1) | K.NVSDIIPR.T | 690 | Sialyfuco<br>sylated |
| HexNAc(5)Hex(6)Fuc(1)NeuAc(3) | K.NVSDIIPR.T | 690 | Sialyfuco<br>sylated |

|                               |              |     |                      |
|-------------------------------|--------------|-----|----------------------|
| HexNAc(6)Hex(7)Fuc(1)NeuAc(1) | K.NVSDIIPR.T | 690 | Sialyfuco<br>sylated |
| HexNAc(6)Hex(7)Fuc(1)NeuAc(2) | K.NVSDIIPR.T | 690 | Sialyfuco<br>sylated |
| HexNAc(6)Hex(6)Fuc(1)NeuAc(1) | K.NVSDIIPR.T | 690 | Sialyfuco<br>sylated |
| HexNAc(6)Hex(6)Fuc(1)NeuAc(2) | K.NVSDIIPR.T | 690 | Sialyfuco<br>sylated |
| HexNAc(6)Hex(5)Fuc(1)NeuAc(1) | K.NVSDIIPR.T | 690 | Sialyfuco<br>sylated |
| HexNAc(6)Hex(7)Fuc(1)NeuAc(3) | K.NVSDIIPR.T | 690 | Sialyfuco<br>sylated |
| HexNAc(4)Hex(5)Fuc(0)NeuAc(1) | K.NVSDIIPR.T | 690 | Sialylated           |
| HexNAc(4)Hex(4)Fuc(0)NeuAc(1) | K.NVSDIIPR.T | 690 | Sialylated           |
| HexNAc(4)Hex(5)Fuc(0)NeuAc(2) | K.NVSDIIPR.T | 690 | Sialylated           |
| HexNAc(5)Hex(6)Fuc(0)NeuAc(1) | K.NVSDIIPR.T | 690 | Sialylated           |
| HexNAc(5)Hex(5)Fuc(0)NeuAc(1) | K.NVSDIIPR.T | 690 | Sialylated           |
| HexNAc(5)Hex(4)Fuc(0)NeuAc(1) | K.NVSDIIPR.T | 690 | Sialylated           |
| HexNAc(6)Hex(6)Fuc(0)NeuAc(2) | K.NVSDIIPR.T | 690 | Sialylated           |
| HexNAc(5)Hex(5)Fuc(0)NeuAc(2) | K.NVSDIIPR.T | 690 | Sialylated           |
| HexNAc(6)Hex(6)Fuc(0)NeuAc(1) | K.NVSDIIPR.T | 690 | Sialylated           |
| HexNAc(5)Hex(6)Fuc(0)NeuAc(2) | K.NVSDIIPR.T | 690 | Sialylated           |

|                               |              |     |             |
|-------------------------------|--------------|-----|-------------|
| HexNAc(6)Hex(7)Fuc(0)NeuAc(1) | K.NVSDIIPR.T | 690 | Sialylated  |
| HexNAc(6)Hex(5)Fuc(0)NeuAc(1) | K.NVSDIIPR.T | 690 | Sialylated  |
| HexNAc(6)Hex(4)Fuc(0)NeuAc(1) | K.NVSDIIPR.T | 690 | Sialylated  |
| HexNAc(6)Hex(5)Fuc(0)NeuAc(2) | K.NVSDIIPR.T | 690 | Sialylated  |
| HexNAc(3)Hex(4)Fuc(0)NeuAc(0) | K.NVSDIIPR.T | 690 | Undecorated |
| HexNAc(4)Hex(5)Fuc(0)NeuAc(0) | K.NVSDIIPR.T | 690 | Undecorated |
| HexNAc(4)Hex(4)Fuc(0)NeuAc(0) | K.NVSDIIPR.T | 690 | Undecorated |
| HexNAc(4)Hex(3)Fuc(0)NeuAc(0) | K.NVSDIIPR.T | 690 | Undecorated |
| HexNAc(5)Hex(5)Fuc(0)NeuAc(0) | K.NVSDIIPR.T | 690 | Undecorated |
| HexNAc(6)Hex(7)Fuc(0)NeuAc(0) | K.NVSDIIPR.T | 690 | Undecorated |
| HexNAc(3)Hex(3)Fuc(0)NeuAc(0) | K.NVSDIIPR.T | 690 | Undecorated |
| HexNAc(5)Hex(6)Fuc(0)NeuAc(0) | K.NVSDIIPR.T | 690 | Undecorated |
| HexNAc(5)Hex(4)Fuc(0)NeuAc(0) | K.NVSDIIPR.T | 690 | Undecorated |
| HexNAc(5)Hex(3)Fuc(0)NeuAc(0) | K.NVSDIIPR.T | 690 | Undecorated |
| HexNAc(6)Hex(6)Fuc(0)NeuAc(0) | K.NVSDIIPR.T | 690 | Undecorated |

**Table S4.3 HepG2 N-Glycome Profiles**

| <b>Treatment</b> | <b>Mass (exp.)</b> | <b>Glycan Subtype</b> | <b>Hex</b> | <b>HexN Ac</b> | <b>Fuc</b> | <b>Neu Ac</b> | <b>RT</b>  | <b>Relative Abundance</b> |
|------------------|--------------------|-----------------------|------------|----------------|------------|---------------|------------|---------------------------|
| Control          | 3171.1077          | Sialyfucoylated       | 6          | 5              | 2          | 3             | 33.79      | 17.09                     |
| Control          | 3025.0521<br>5     | Sialyfucoylated       | 6          | 5              | 1          | 3             | 33.43<br>5 | 11.45                     |
| Control          | 2368.8277<br>2     | Sialyfucoylated       | 5          | 4              | 1          | 2             | 27.27<br>2 | 9.59                      |
| Control          | 2880.0164<br>8     | Sialyfucoylated       | 6          | 5              | 2          | 2             | 28.09<br>9 | 6.53                      |
| Control          | 3536.2307<br>5     | Sialyfucoylated       | 7          | 6              | 2          | 3             | 32.88      | 4.60                      |
| Control          | 2733.9566<br>8     | Sialyfucoylated       | 6          | 5              | 1          | 2             | 26.79<br>2 | 4.43                      |
| Control          | 2222.7762<br>9     | Sialylated            | 5          | 4              | 0          | 2             | 26.40<br>6 | 3.73                      |
| Control          | 1720.5879<br>7     | High Mannose          | 8          | 2              | 0          | 0             | 16.52<br>7 | 2.81                      |
| Control          | 1558.5350<br>7     | High Mannose          | 7          | 2              | 0          | 0             | 16.53<br>5 | 2.30                      |
| Control          | 2878.9964<br>9     | Sialylated            | 6          | 5              | 0          | 3             | 30.24<br>9 | 2.25                      |
| Control          | 3099.0862<br>7     | Sialyfucoylated       | 7          | 6              | 1          | 2             | 28.92<br>8 | 2.25                      |
| Control          | 1882.6376<br>4     | High Mannose          | 9          | 2              | 0          | 0             | 14.87<br>6 | 2.06                      |
| Control          | 1396.4848<br>9     | High Mannose          | 6          | 2              | 0          | 0             | 16.53<br>4 | 1.90                      |
| Control          | 1234.4336<br>1     | High Mannose          | 5          | 2              | 0          | 0             | 15.05<br>5 | 1.73                      |
| Control          | 3245.1414<br>7     | Sialyfucoylated       | 7          | 6              | 2          | 2             | 28.27<br>6 | 1.68                      |

|         |                |                 |   |   |   |   |            |      |
|---------|----------------|-----------------|---|---|---|---|------------|------|
| Control | 2077.7441<br>1 | Sialyfucoylated | 5 | 4 | 1 | 1 | 25.03<br>4 | 1.53 |
| Control | 3901.3654<br>8 | Sialyfucoylated | 8 | 7 | 2 | 3 | 32.56<br>2 | 1.52 |
| Control | 4047.4210<br>8 | Sialyfucoylated | 8 | 7 | 3 | 3 | 32.67<br>4 | 1.26 |
| Control | 2807.9910<br>8 | Sialyfucoylated | 7 | 6 | 1 | 1 | 25.40<br>1 | 1.20 |
| Control | 4412.5444<br>2 | Sialyfucoylated | 9 | 8 | 3 | 3 | 31.83<br>2 | 1.11 |
| Control | 2587.9302      | Sialylated      | 6 | 5 | 0 | 2 | 26.24<br>6 | 1.11 |
| Control | 4558.6099<br>3 | Sialyfucoylated | 9 | 8 | 4 | 3 | 32.39      | 1.10 |
| Control | 4265.4787<br>3 | Sialylated      | 9 | 8 | 0 | 4 | 33.24<br>8 | 0.78 |
| Control | 2514.9040<br>7 | Sialyfucoylated | 5 | 4 | 2 | 2 | 28.52<br>3 | 0.75 |
| Control | 3026.0631<br>7 | Sialyfucoylated | 6 | 5 | 3 | 2 | 28.56<br>3 | 0.73 |
| Control | 3682.2928      | Sialyfucoylated | 7 | 6 | 3 | 3 | 33.00<br>2 | 0.73 |
| Control | 3683.3119<br>6 | Sialylated      | 9 | 8 | 0 | 2 | 33.29<br>6 | 0.64 |
| Control | 4048.4200<br>4 | Sialyfucoylated | 8 | 7 | 5 | 2 | 32.69<br>9 | 0.59 |
| Control | 3756.3283<br>8 | Sialyfucoylated | 8 | 7 | 3 | 2 | 28.07      | 0.57 |
| Control | 3391.2044<br>9 | Sialyfucoylated | 7 | 6 | 3 | 2 | 28.02<br>7 | 0.53 |
| Control | 3101.0926<br>5 | Undecorated     | 9 | 8 | 0 | 0 | 28.41<br>5 | 0.49 |

|         |                |                 |    |   |   |   |            |      |
|---------|----------------|-----------------|----|---|---|---|------------|------|
| Control | 2881.0048<br>8 | Sialyfucoylated | 6  | 5 | 4 | 1 | 27.69<br>2 | 0.42 |
| Control | 2571.9094<br>6 | Sialyfucoylated | 5  | 5 | 1 | 2 | 26.29<br>5 | 0.42 |
| Control | 2734.9685<br>1 | Sialyfucoylated | 6  | 5 | 3 | 1 | 33.65<br>1 | 0.39 |
| Control | 1931.6825<br>8 | Sialylated      | 5  | 4 | 0 | 1 | 23.75<br>3 | 0.39 |
| Control | 2954.0552<br>7 | Sialyfucoylated | 7  | 6 | 2 | 1 | 26.09<br>7 | 0.38 |
| Control | 2044.6830<br>8 | High Mannose    | 10 | 2 | 0 | 0 | 17.20<br>3 | 0.38 |
| Control | 1728.6037<br>8 | Sialylated      | 5  | 3 | 0 | 1 | 21.68<br>1 | 0.38 |
| Control | 3431.1340<br>6 | Sialyfucoylated | 6  | 7 | 1 | 3 | 31.98<br>2 | 0.36 |
| Control | 2223.8024<br>7 | Sialyfucoylated | 5  | 4 | 2 | 1 | 25.50<br>2 | 0.35 |
| Control | 1072.3786<br>2 | High Mannose    | 4  | 2 | 0 | 0 | 16.52<br>1 | 0.31 |
| Control | 1890.6534<br>5 | Sialylated      | 6  | 3 | 0 | 1 | 22.72<br>3 | 0.30 |
| Control | 2953.0510<br>5 | Sialylated      | 7  | 6 | 0 | 2 | 26.13<br>9 | 0.29 |
| Control | 3757.3054<br>7 | Sialyfucoylated | 8  | 7 | 5 | 1 | 32.82<br>2 | 0.27 |
| Control | 2589.9179<br>5 | Fucosylated     | 6  | 5 | 4 | 0 | 28.08<br>5 | 0.23 |
| Control | 2409.8688<br>1 | Sialyfucoylated | 4  | 5 | 1 | 2 | 27.00<br>5 | 0.23 |
| Control | 2661.9472<br>3 | Sialylated      | 7  | 6 | 0 | 1 | 25.69<br>6 | 0.23 |

|         |                |                 |    |   |   |   |            |      |
|---------|----------------|-----------------|----|---|---|---|------------|------|
| Control | 4339.5284<br>8 | Sialyfucoylated | 8  | 7 | 5 | 3 | 33.27<br>5 | 0.20 |
| Control | 2296.8019<br>3 | Sialylated      | 6  | 5 | 0 | 1 | 25.70<br>5 | 0.20 |
| Control | 3319.1353<br>4 | Sialyfucoylated | 8  | 7 | 2 | 1 | 28.78<br>1 | 0.19 |
| Control | 4119.4195<br>8 | Sialyfucoylated | 7  | 6 | 4 | 4 | 35.18<br>4 | 0.19 |
| Control | 4485.6726<br>8 | Sialyfucoylated | 8  | 7 | 6 | 3 | 38.82<br>8 | 0.19 |
| Control | 3828.3585<br>2 | Sialyfucoylated | 7  | 6 | 4 | 3 | 34.00<br>4 | 0.18 |
| Control | 1462.5422      | Fucosylated     | 3  | 4 | 1 | 0 | 20.95      | 0.18 |
| Control | 3100.1006<br>8 | Sialyfucoylated | 7  | 6 | 3 | 1 | 25.85<br>2 | 0.17 |
| Control | 4015.4480<br>4 | Sialyfucoylated | 6  | 7 | 5 | 3 | 31.98<br>3 | 0.17 |
| Control | 2206.7558<br>8 | High Mannose    | 11 | 2 | 0 | 0 | 18.81<br>3 | 0.16 |
| Control | 2692.9092      | Sialyfucoylated | 7  | 4 | 1 | 2 | 38.67<br>5 | 0.15 |
| Control | 2572.9664<br>4 | Sialyfucoylated | 5  | 5 | 3 | 1 | 29.54<br>8 | 0.15 |
| Control | 910.32508      | High Mannose    | 3  | 2 | 0 | 0 | 17.59<br>8 | 0.15 |
| Control | 3390.1677<br>3 | Sialyfucoylated | 7  | 6 | 1 | 3 | 33.25<br>9 | 0.14 |
| Control | 3448.2178<br>4 | Sialyfucoylated | 7  | 7 | 2 | 2 | 33.23<br>3 | 0.14 |
| Control | 3244.1124      | Sialylated      | 7  | 6 | 0 | 3 | 26.78      | 0.14 |
| Control | 2442.8558      | Sialyfucoylated | 6  | 5 | 1 | 1 | 25.67      | 0.13 |
| Control | 5067.7955      | Sialyfucoylated | 8  | 7 | 6 | 5 | 36.38<br>6 | 0.13 |

|         |                |                 |   |   |   |   |            |      |
|---------|----------------|-----------------|---|---|---|---|------------|------|
| Control | 3830.3221<br>7 | Sialyfucoylated | 9 | 8 | 3 | 1 | 30.32      | 0.12 |
| Control | 2458.8865      | Sialylated      | 7 | 5 | 0 | 1 | 37.85<br>7 | 0.12 |
| Control | 3522.2345<br>5 | Sialyfucoylated | 8 | 8 | 2 | 1 | 32.88<br>7 | 0.12 |
| Control | 2524.9034<br>1 | Sialyfucoylated | 4 | 7 | 1 | 1 | 32.42<br>8 | 0.12 |
| Control | 1712.6154<br>4 | Sialyfucoylated | 4 | 3 | 1 | 1 | 25.71<br>6 | 0.12 |
| Control | 2614.9231<br>5 | Fucosylated     | 4 | 6 | 5 | 0 | 33.29<br>8 | 0.11 |
| Control | 3611.2652<br>4 | Sialyfucoylated | 8 | 7 | 4 | 1 | 38.78<br>3 | 0.11 |
| Control | 2790.9773<br>9 | Sialylated      | 6 | 6 | 0 | 2 | 32.44<br>4 | 0.11 |
| Control | 2425.8288<br>3 | Sialylated      | 5 | 5 | 0 | 2 | 35.07<br>8 | 0.10 |
| Control | 2921.0787<br>9 | Sialyfucoylated | 5 | 6 | 2 | 2 | 35.26<br>8 | 0.10 |
| Control | 4046.4239<br>2 | Sialyfucoylated | 8 | 7 | 1 | 4 | 35.08<br>5 | 0.10 |
| Control | 3975.3901<br>9 | Sialyfucoylated | 9 | 8 | 2 | 2 | 31.28<br>1 | 0.10 |
| Control | 3318.1641<br>8 | Sialylated      | 8 | 7 | 0 | 2 | 30.16<br>4 | 0.09 |
| Control | 2882.1068<br>1 | Fucosylated     | 8 | 7 | 1 | 0 | 30.81<br>6 | 0.09 |
| Control | 3027.0510<br>3 | Sialylated      | 8 | 7 | 0 | 1 | 28.57<br>8 | 0.09 |
| Control | 2588.8987<br>7 | Sialyfucoylated | 6 | 5 | 2 | 1 | 36.52<br>7 | 0.09 |

|         |                |                 |    |   |   |   |            |      |
|---------|----------------|-----------------|----|---|---|---|------------|------|
| Control | 2384.8316<br>5 | Sialylated      | 6  | 4 | 0 | 2 | 27.74<br>4 | 0.08 |
| Control | 2906.0901<br>8 | Sialyfucoylated | 4  | 6 | 5 | 1 | 38.74<br>4 | 0.08 |
| Control | 1275.4453<br>3 | Undecorated     | 4  | 3 | 0 | 0 | 35.01      | 0.08 |
| Control | 3083.1021<br>8 | Sialyfucoylated | 6  | 6 | 2 | 2 | 26.23      | 0.07 |
| Control | 3593.2505<br>2 | Sialyfucoylated | 7  | 7 | 1 | 3 | 31.95<br>5 | 0.07 |
| Control | 3539.2375<br>5 | Fucosylated     | 9  | 8 | 3 | 0 | 27.74<br>7 | 0.06 |
| Control | 2939.0116<br>7 | Undecorated     | 8  | 8 | 0 | 0 | 36.39<br>3 | 0.06 |
| Control | 2645.9230<br>9 | Sialyfucoylated | 6  | 6 | 1 | 1 | 31.99<br>8 | 0.06 |
| Control | 2240.8538<br>7 | Fucosylated     | 6  | 4 | 3 | 0 | 37.91<br>2 | 0.06 |
| Control | 2305.7810<br>3 | Sialyfucoylated | 3  | 6 | 2 | 1 | 37.21<br>9 | 0.06 |
| Control | 2834.0391<br>6 | Fucosylated     | 5  | 7 | 4 | 0 | 38.01<br>8 | 0.06 |
| Control | 2838.9766<br>7 | Sialyfucoylated | 7  | 4 | 2 | 2 | 37.94<br>1 | 0.05 |
| Control | 2513.9067<br>7 | Sialylated      | 5  | 4 | 0 | 3 | 35.88      | 0.04 |
| Control | 2955.0629<br>6 | Fucosylated     | 7  | 6 | 4 | 0 | 28.23<br>1 | 0.04 |
| Control | 2368.8296<br>9 | High Mannose    | 12 | 2 | 0 | 0 | 29.21<br>3 | 0.04 |
| Control | 2809.0332<br>4 | Fucosylated     | 7  | 6 | 3 | 0 | 37.71<br>5 | 0.04 |

|               |                |                   |   |   |   |   |            |       |
|---------------|----------------|-------------------|---|---|---|---|------------|-------|
| Control       | 2297.8108<br>8 | Fucosylated       | 6 | 5 | 2 | 0 | 29.71<br>3 | 0.03  |
| 2F-<br>Fucose | 2222.7750<br>5 | Sialylated        | 5 | 4 | 0 | 2 | 25.67<br>6 | 19.62 |
| 2F-<br>Fucose | 2878.9965<br>8 | Sialylated        | 6 | 5 | 0 | 3 | 26.03<br>7 | 16.78 |
| 2F-<br>Fucose | 2953.0318<br>2 | Sialylated        | 7 | 6 | 0 | 2 | 27.70<br>5 | 6.79  |
| 2F-<br>Fucose | 2587.9047<br>6 | Sialylated        | 6 | 5 | 0 | 2 | 26.53<br>3 | 6.78  |
| 2F-<br>Fucose | 1720.5880<br>2 | High Mannose      | 8 | 2 | 0 | 0 | 16.56<br>6 | 3.77  |
| 2F-<br>Fucose | 2661.9430<br>2 | Sialylated        | 7 | 6 | 0 | 1 | 25.26<br>7 | 3.75  |
| 2F-<br>Fucose | 1931.6763<br>3 | Sialylated        | 5 | 4 | 0 | 1 | 23.07<br>9 | 3.42  |
| 2F-<br>Fucose | 3244.1125<br>3 | Sialylated        | 7 | 6 | 0 | 3 | 28.84<br>6 | 2.92  |
| 2F-<br>Fucose | 1558.5382<br>2 | High Mannose      | 7 | 2 | 0 | 0 | 15.04<br>1 | 2.90  |
| 2F-<br>Fucose | 2296.8079<br>2 | Sialylated        | 6 | 5 | 0 | 1 | 24.02<br>5 | 2.77  |
| 2F-<br>Fucose | 1882.647       | High Mannose      | 9 | 2 | 0 | 0 | 14.12<br>3 | 2.75  |
| 2F-<br>Fucose | 1234.4333<br>9 | High Mannose      | 5 | 2 | 0 | 0 | 15.19      | 2.45  |
| 2F-<br>Fucose | 1396.4889<br>8 | High Mannose      | 6 | 2 | 0 | 0 | 16.56<br>8 | 2.42  |
| 2F-<br>Fucose | 2368.8276<br>5 | Sialyufucosylated | 5 | 4 | 1 | 2 | 27.77<br>9 | 1.86  |
| 2F-<br>Fucose | 3318.1651<br>5 | Sialylated        | 8 | 7 | 0 | 2 | 29.09<br>8 | 1.74  |

|           |                |                 |    |   |   |   |            |      |
|-----------|----------------|-----------------|----|---|---|---|------------|------|
| 2F-Fucose | 3609.2539<br>6 | Sialylated      | 8  | 7 | 0 | 3 | 33.50<br>3 | 1.32 |
| 2F-Fucose | 3683.2951<br>8 | Sialylated      | 9  | 8 | 0 | 2 | 29.58<br>3 | 1.25 |
| 2F-Fucose | 3974.3831<br>5 | Sialylated      | 9  | 8 | 0 | 3 | 33.78<br>6 | 1.13 |
| 2F-Fucose | 2879.9945<br>3 | Sialyfucoylated | 6  | 5 | 2 | 2 | 30.61<br>7 | 0.89 |
| 2F-Fucose | 1728.6088<br>4 | Sialylated      | 5  | 3 | 0 | 1 | 21.69<br>4 | 0.88 |
| 2F-Fucose | 1890.6565<br>2 | Sialylated      | 6  | 3 | 0 | 1 | 22.72<br>9 | 0.78 |
| 2F-Fucose | 2588.9101<br>4 | Sialyfucoylated | 6  | 5 | 2 | 1 | 24.98      | 0.72 |
| 2F-Fucose | 3025.0444<br>2 | Sialyfucoylated | 6  | 5 | 1 | 3 | 36.65<br>7 | 0.71 |
| 2F-Fucose | 2733.9320<br>9 | Sialyfucoylated | 6  | 5 | 1 | 2 | 28.39<br>7 | 0.62 |
| 2F-Fucose | 2954.0254<br>3 | Sialyfucoylated | 7  | 6 | 2 | 1 | 28.18<br>9 | 0.60 |
| 2F-Fucose | 3099.0983<br>3 | Sialyfucoylated | 7  | 6 | 1 | 2 | 28.85<br>5 | 0.58 |
| 2F-Fucose | 2044.6801<br>4 | High Mannose    | 10 | 2 | 0 | 0 | 17.21<br>6 | 0.53 |
| 2F-Fucose | 3026.0646<br>9 | Sialyfucoylated | 6  | 5 | 3 | 2 | 26.21<br>9 | 0.52 |
| 2F-Fucose | 1072.3813<br>9 | High Mannose    | 4  | 2 | 0 | 0 | 16.57<br>7 | 0.50 |
| 2F-Fucose | 2589.9561<br>8 | Fucosylated     | 6  | 5 | 4 | 0 | 26.63<br>6 | 0.50 |
| 2F-Fucose | 2881.9906<br>3 | Fucosylated     | 8  | 7 | 1 | 0 | 25.48<br>6 | 0.46 |

|           |                |                 |    |   |   |   |            |      |
|-----------|----------------|-----------------|----|---|---|---|------------|------|
| 2F-Fucose | 3685.2804<br>6 | Fucosylated     | 9  | 8 | 4 | 0 | 29.58      | 0.46 |
| 2F-Fucose | 3027.0649<br>8 | Sialylated      | 8  | 7 | 0 | 1 | 26.75<br>5 | 0.44 |
| 2F-Fucose | 2425.8582<br>1 | Sialylated      | 5  | 5 | 0 | 2 | 25.17<br>1 | 0.43 |
| 2F-Fucose | 3245.1144<br>3 | Sialyfuosylated | 7  | 6 | 2 | 2 | 33.64<br>7 | 0.36 |
| 2F-Fucose | 3976.3661<br>4 | Sialyfuosylated | 9  | 8 | 4 | 1 | 34.04<br>7 | 0.32 |
| 2F-Fucose | 910.3236       | High Mannose    | 3  | 2 | 0 | 0 | 17.62<br>6 | 0.29 |
| 2F-Fucose | 2790.9762      | Sialylated      | 6  | 6 | 0 | 2 | 25.61      | 0.28 |
| 2F-Fucose | 1566.5659<br>1 | Sialylated      | 4  | 3 | 0 | 1 | 23.02<br>6 | 0.27 |
| 2F-Fucose | 2206.7494<br>5 | High Mannose    | 11 | 2 | 0 | 0 | 18.82<br>3 | 0.26 |
| 2F-Fucose | 2660.9738<br>8 | Sialyfuosylated | 5  | 4 | 3 | 2 | 21.89<br>8 | 0.24 |
| 2F-Fucose | 3682.2912      | Sialyfuosylated | 7  | 6 | 3 | 3 | 29.57<br>4 | 0.24 |
| 2F-Fucose | 2077.7307<br>8 | Sialyfuosylated | 5  | 4 | 1 | 1 | 25.72<br>8 | 0.24 |
| 2F-Fucose | 2368.8039<br>5 | High Mannose    | 12 | 2 | 0 | 0 | 27.19<br>2 | 0.21 |
| 2F-Fucose | 4048.4076<br>4 | Sialyfuosylated | 8  | 7 | 5 | 2 | 29.82<br>5 | 0.21 |
| 2F-Fucose | 2735.9262<br>4 | Undecorated     | 8  | 7 | 0 | 0 | 28.94<br>5 | 0.18 |
| 2F-Fucose | 3611.2500<br>6 | Sialyfuosylated | 8  | 7 | 4 | 1 | 35.84<br>4 | 0.18 |

|           |                |                 |   |   |   |   |            |      |
|-----------|----------------|-----------------|---|---|---|---|------------|------|
| 2F-Fucose | 4413.4887      | Sialyfucoylated | 9 | 8 | 5 | 2 | 31.14      | 0.18 |
| 2F-Fucose | 2264.8070<br>1 | Sialyfucoylated | 4 | 5 | 2 | 1 | 25.91<br>3 | 0.17 |
| 2F-Fucose | 2881.0068<br>5 | Sialyfucoylated | 6 | 5 | 4 | 1 | 33.12<br>4 | 0.17 |
| 2F-Fucose | 2734.9652<br>6 | Sialyfucoylated | 6 | 5 | 3 | 1 | 27.87<br>4 | 0.14 |
| 2F-Fucose | 2061.7216<br>1 | Sialyfucoylated | 4 | 4 | 2 | 1 | 37.57<br>3 | 0.14 |
| 2F-Fucose | 3684.2920<br>3 | Sialyfucoylated | 9 | 8 | 2 | 1 | 31.63<br>8 | 0.14 |
| 2F-Fucose | 3320.1147<br>2 | Fucosylated     | 8 | 7 | 4 | 0 | 35.41<br>9 | 0.12 |
| 2F-Fucose | 3101.1476<br>9 | Fucosylated     | 7 | 6 | 5 | 0 | 39.21<br>9 | 0.12 |
| 2F-Fucose | 4339.5007<br>8 | Sialyfucoylated | 8 | 7 | 5 | 3 | 33.90<br>4 | 0.10 |
| 2F-Fucose | 3246.1168<br>1 | Sialyfucoylated | 7 | 6 | 4 | 1 | 35.72<br>6 | 0.10 |
| 2F-Fucose | 2426.8951<br>3 | Sialyfucoylated | 5 | 5 | 2 | 1 | 35.33<br>3 | 0.10 |
| 2F-Fucose | 1802.6326      | Undecorated     | 6 | 4 | 0 | 0 | 33.99<br>9 | 0.10 |
| 2F-Fucose | 2808.0338<br>1 | Sialyfucoylated | 7 | 6 | 1 | 1 | 26.38<br>7 | 0.10 |
| 2F-Fucose | 2499.9437      | Sialylated      | 6 | 6 | 0 | 1 | 38.20<br>9 | 0.10 |
| 2F-Fucose | 3392.1751<br>6 | Sialylated      | 9 | 8 | 0 | 1 | 33.65<br>5 | 0.09 |
| 2F-Fucose | 2297.8321<br>7 | Fucosylated     | 6 | 5 | 2 | 0 | 35.68<br>2 | 0.08 |

|                 |                |                 |   |   |   |   |            |       |
|-----------------|----------------|-----------------|---|---|---|---|------------|-------|
| 2F-Fucose       | 1316.4865<br>9 | Undecorated     | 3 | 4 | 0 | 0 | 18.27      | 0.07  |
| 2F-Fucose       | 2719.9355<br>3 | Fucosylated     | 7 | 7 | 1 | 0 | 37.56<br>5 | 0.07  |
| 2F-Fucose       | 2662.9479<br>4 | Fucosylated     | 7 | 6 | 2 | 0 | 26.18<br>8 | 0.07  |
| 2F-Fucose       | 2304.8560<br>9 | Sialylated      | 3 | 6 | 0 | 2 | 26.47<br>5 | 0.07  |
| 2F-Fucose       | 2994.0059<br>8 | Sialylated      | 6 | 7 | 0 | 2 | 30.16<br>9 | 0.06  |
| 2F-Fucose       | 4705.6190<br>1 | Sialyfucoylated | 9 | 8 | 7 | 2 | 35.79      | 0.06  |
| 2F-Fucose       | 2078.7685<br>7 | Fucosylated     | 5 | 4 | 3 | 0 | 25.12<br>2 | 0.06  |
| 2F-Fucose       | 3319.1372<br>9 | Sialyfucoylated | 8 | 7 | 2 | 1 | 30.64<br>8 | 0.05  |
| 2F-Fucose       | 2546.8532      | Sialylated      | 7 | 4 | 0 | 2 | 26.24<br>8 | 0.05  |
| 2F-Fucose       | 3903.4742<br>1 | Sialyfucoylated | 8 | 7 | 6 | 1 | 37.47<br>9 | 0.05  |
| 2F-Fucose       | 2458.9124<br>9 | Sialylated      | 7 | 5 | 0 | 1 | 26.11<br>7 | 0.04  |
| 2F-Fucose       | 2385.8952<br>4 | Sialyfucoylated | 6 | 4 | 2 | 1 | 35.94<br>8 | 0.04  |
| 2F-Fucose       | 2571.8790<br>2 | Sialyfucoylated | 5 | 5 | 1 | 2 | 26.28<br>7 | 0.04  |
| Kifunensi<br>ne | 1882.6365<br>4 | High Mannose    | 9 | 2 | 0 | 0 | 18.42      | 30.04 |
| Kifunensi<br>ne | 1720.5896<br>1 | High Mannose    | 8 | 2 | 0 | 0 | 18.55<br>2 | 23.46 |
| Kifunensi<br>ne | 1558.5355<br>4 | High Mannose    | 7 | 2 | 0 | 0 | 18.57<br>1 | 15.68 |

|                 |                |                 |    |   |   |   |            |      |
|-----------------|----------------|-----------------|----|---|---|---|------------|------|
| Kifunensi<br>ne | 1396.4848<br>9 | High Mannose    | 6  | 2 | 0 | 0 | 18.57<br>1 | 8.29 |
| Kifunensi<br>ne | 1234.4334<br>1 | High Mannose    | 5  | 2 | 0 | 0 | 21.97<br>6 | 5.19 |
| Kifunensi<br>ne | 2044.6927<br>5 | High Mannose    | 10 | 2 | 0 | 0 | 18.42<br>2 | 2.46 |
| Kifunensi<br>ne | 2368.8277<br>5 | Sialyucosylated | 5  | 4 | 1 | 2 | 28.26<br>6 | 1.89 |
| Kifunensi<br>ne | 2036.7156<br>6 | Sialyucosylated | 6  | 3 | 1 | 1 | 25.08<br>4 | 1.64 |
| Kifunensi<br>ne | 1072.3719<br>7 | High Mannose    | 4  | 2 | 0 | 0 | 18.57<br>1 | 1.52 |
| Kifunensi<br>ne | 1890.6592<br>2 | Sialylated      | 6  | 3 | 0 | 1 | 25.07<br>3 | 0.98 |
| Kifunensi<br>ne | 3318.1966<br>4 | Sialylated      | 8  | 7 | 0 | 2 | 31.92<br>2 | 0.88 |
| Kifunensi<br>ne | 910.32426      | High Mannose    | 3  | 2 | 0 | 0 | 18.57<br>4 | 0.79 |
| Kifunensi<br>ne | 2206.7384<br>8 | High Mannose    | 11 | 2 | 0 | 0 | 20.12<br>6 | 0.70 |
| Kifunensi<br>ne | 1874.6619<br>3 | Sialyucosylated | 5  | 3 | 1 | 1 | 24.95<br>3 | 0.57 |
| Kifunensi<br>ne | 3521.2584<br>3 | Sialylated      | 8  | 8 | 0 | 2 | 37.86<br>9 | 0.48 |
| Kifunensi<br>ne | 2401.8344<br>6 | Sialyucosylated | 7  | 4 | 1 | 1 | 35.17<br>7 | 0.41 |
| Kifunensi<br>ne | 3084.1360<br>1 | Sialyucosylated | 6  | 6 | 4 | 1 | 35.58<br>2 | 0.40 |
| Kifunensi<br>ne | 1728.6068<br>1 | Sialylated      | 5  | 3 | 0 | 1 | 25.00<br>7 | 0.38 |
| Kifunensi<br>ne | 2368.7711<br>8 | High Mannose    | 12 | 2 | 0 | 0 | 33.84<br>6 | 0.36 |

|                 |                |                 |   |   |   |   |            |      |
|-----------------|----------------|-----------------|---|---|---|---|------------|------|
| Kifunensi<br>ne | 2662.9663<br>9 | Fucosylated     | 7 | 6 | 2 | 0 | 35.27      | 0.34 |
| Kifunensi<br>ne | 2906.1600<br>5 | Sialyucosylated | 4 | 6 | 5 | 1 | 28.74<br>8 | 0.31 |
| Kifunensi<br>ne | 2540.9326<br>2 | Sialylated      | 5 | 7 | 0 | 1 | 39.01<br>6 | 0.30 |
| Kifunensi<br>ne | 2255.7578<br>2 | Sialylated      | 7 | 4 | 0 | 1 | 31.50<br>5 | 0.29 |
| Kifunensi<br>ne | 2880.0053<br>9 | Sialyucosylated | 6 | 5 | 2 | 2 | 28.56<br>2 | 0.28 |
| Kifunensi<br>ne | 2222.7751<br>8 | Sialylated      | 5 | 4 | 0 | 2 | 27.39<br>7 | 0.27 |
| Kifunensi<br>ne | 2735.9979<br>2 | Undecorated     | 8 | 7 | 0 | 0 | 38.27<br>5 | 0.26 |
| Kifunensi<br>ne | 2217.8771<br>9 | Fucosylated     | 3 | 7 | 2 | 0 | 37.52<br>4 | 0.20 |
| Kifunensi<br>ne | 1915.7040<br>8 | Sialyucosylated | 4 | 4 | 1 | 1 | 36.11<br>8 | 0.18 |
| Kifunensi<br>ne | 2459.8941<br>9 | Fucosylated     | 7 | 5 | 2 | 0 | 36.87<br>2 | 0.17 |
| Kifunensi<br>ne | 2160.7648<br>8 | Fucosylated     | 3 | 6 | 3 | 0 | 34.83<br>8 | 0.16 |
| Kifunensi<br>ne | 2524.9870<br>9 | Sialyucosylated | 4 | 7 | 1 | 1 | 38.96<br>7 | 0.15 |
| Kifunensi<br>ne | 2450.8661<br>3 | Sialyucosylated | 3 | 6 | 1 | 2 | 25.09<br>3 | 0.13 |
| Kifunensi<br>ne | 4179.4455<br>1 | Sialyucosylated | 9 | 9 | 4 | 1 | 35.09<br>9 | 0.12 |
| Kifunensi<br>ne | 2134.7287<br>5 | Sialylated      | 5 | 5 | 0 | 1 | 33.37<br>8 | 0.11 |
| Kifunensi<br>ne | 2369.8400<br>4 | Sialyucosylated | 5 | 4 | 3 | 1 | 32.44<br>3 | 0.11 |

|                 |                |                  |   |   |   |   |            |      |
|-----------------|----------------|------------------|---|---|---|---|------------|------|
| Kifunensi<br>ne | 2379.8438<br>6 | Fucosylated      | 4 | 7 | 2 | 0 | 32.92<br>3 | 0.11 |
| Kifunensi<br>ne | 1891.6451<br>6 | Fucosylated      | 6 | 3 | 2 | 0 | 21.91<br>8 | 0.11 |
| Kifunensi<br>ne | 2734.0219<br>7 | Sialyfucosylated | 6 | 5 | 1 | 2 | 30.82<br>2 | 0.09 |
| Kifunensi<br>ne | 2547.8558      | Sialyfucosylated | 7 | 4 | 2 | 1 | 35.57<br>6 | 0.09 |
| Kifunensi<br>ne | 2530.8255<br>2 | Sialyfucosylated | 6 | 4 | 1 | 2 | 32.54<br>4 | 0.07 |
| Kifunensi<br>ne | 2573.9273<br>6 | Undecorated      | 7 | 7 | 0 | 0 | 30.66<br>6 | 0.05 |
| 3-F-Sia         | 1720.586       | High Mannose     | 8 | 2 | 0 | 0 | 17.35<br>3 | 6.88 |
| 3-F-Sia         | 2516.9077      | Fucosylated      | 7 | 6 | 1 | 0 | 25.94<br>1 | 5.50 |
| 3-F-Sia         | 1558.5353<br>8 | High Mannose     | 7 | 2 | 0 | 0 | 17.35<br>2 | 5.39 |
| 3-F-Sia         | 2077.7428<br>6 | Sialyfucosylated | 5 | 4 | 1 | 1 | 28.38<br>9 | 5.18 |
| 3-F-Sia         | 2368.8336<br>4 | Sialyfucosylated | 5 | 4 | 1 | 2 | 30.59<br>3 | 4.85 |
| 3-F-Sia         | 1882.6382<br>9 | High Mannose     | 9 | 2 | 0 | 0 | 17.21<br>9 | 4.26 |
| 3-F-Sia         | 1396.4847<br>6 | High Mannose     | 6 | 2 | 0 | 0 | 17.44<br>3 | 4.25 |
| 3-F-Sia         | 1234.4309      | High Mannose     | 5 | 2 | 0 | 0 | 21.10<br>6 | 3.94 |
| 3-F-Sia         | 1786.6409<br>7 | Fucosylated      | 5 | 4 | 1 | 0 | 25.25<br>8 | 3.48 |
| 3-F-Sia         | 2370.8360<br>5 | Undecorated      | 7 | 6 | 0 | 0 | 25.01<br>9 | 3.23 |

|         |                |                 |   |   |   |   |            |      |
|---------|----------------|-----------------|---|---|---|---|------------|------|
| 3-F-Sia | 2808.0046<br>2 | Sialyfucoylated | 7 | 6 | 1 | 1 | 27.07<br>4 | 2.99 |
| 3-F-Sia | 2954.0493<br>7 | Sialyfucoylated | 7 | 6 | 2 | 1 | 26.21<br>3 | 2.36 |
| 3-F-Sia | 2297.8132<br>6 | Fucosylated     | 6 | 5 | 2 | 0 | 25.43<br>1 | 2.09 |
| 3-F-Sia | 2882.0277<br>1 | Fucosylated     | 8 | 7 | 1 | 0 | 26.09<br>8 | 2.05 |
| 3-F-Sia | 2588.9252<br>5 | Sialyfucoylated | 6 | 5 | 2 | 1 | 26.39<br>6 | 1.94 |
| 3-F-Sia | 2223.7945<br>5 | Sialyfucoylated | 5 | 4 | 2 | 1 | 25.67<br>5 | 1.90 |
| 3-F-Sia | 1932.6790<br>7 | Fucosylated     | 5 | 4 | 2 | 0 | 24.97<br>6 | 1.87 |
| 3-F-Sia | 2442.8686<br>6 | Sialyfucoylated | 6 | 5 | 1 | 1 | 26.62      | 1.74 |
| 3-F-Sia | 3028.0965<br>9 | Fucosylated     | 8 | 7 | 2 | 0 | 28.43<br>7 | 1.71 |
| 3-F-Sia | 1640.5859<br>1 | Undecorated     | 5 | 4 | 0 | 0 | 35.01<br>3 | 1.71 |
| 3-F-Sia | 2880.0465<br>4 | Sialyfucoylated | 6 | 5 | 2 | 2 | 38.95<br>9 | 1.70 |
| 3-F-Sia | 2809.0077<br>8 | Fucosylated     | 7 | 6 | 3 | 0 | 23.87<br>5 | 1.63 |
| 3-F-Sia | 3099.0863<br>9 | Sialyfucoylated | 7 | 6 | 1 | 2 | 29.61<br>7 | 1.59 |
| 3-F-Sia | 2005.7176<br>7 | Undecorated     | 6 | 5 | 0 | 0 | 23.09<br>3 | 1.45 |
| 3-F-Sia | 3100.0999<br>3 | Sialyfucoylated | 7 | 6 | 3 | 1 | 29.53<br>7 | 1.43 |
| 3-F-Sia | 3245.1443<br>7 | Sialyfucoylated | 7 | 6 | 2 | 2 | 30.51<br>6 | 1.40 |

|         |                |                 |    |   |   |   |            |      |
|---------|----------------|-----------------|----|---|---|---|------------|------|
| 3-F-Sia | 2662.9493<br>3 | Fucosylated     | 7  | 6 | 2 | 0 | 25.46<br>6 | 1.38 |
| 3-F-Sia | 3247.15        | Fucosylated     | 9  | 8 | 1 | 0 | 26.71<br>3 | 1.32 |
| 3-F-Sia | 2222.7747      | Sialylated      | 5  | 4 | 0 | 2 | 29.57<br>8 | 1.08 |
| 3-F-Sia | 2044.6909<br>3 | High Mannose    | 10 | 2 | 0 | 0 | 20.01<br>6 | 0.92 |
| 3-F-Sia | 3319.1648<br>3 | Sialyfucoylated | 8  | 7 | 2 | 1 | 26.54<br>2 | 0.87 |
| 3-F-Sia | 1072.3775<br>2 | High Mannose    | 4  | 2 | 0 | 0 | 17.43<br>7 | 0.79 |
| 3-F-Sia | 1599.5590<br>7 | Undecorated     | 6  | 3 | 0 | 0 | 19.55<br>2 | 0.70 |
| 3-F-Sia | 3539.2630<br>7 | Fucosylated     | 9  | 8 | 3 | 0 | 25.30<br>5 | 0.65 |
| 3-F-Sia | 3465.2330<br>2 | Sialyfucoylated | 8  | 7 | 3 | 1 | 26.33<br>9 | 0.57 |
| 3-F-Sia | 1712.6203<br>5 | Sialyfucoylated | 4  | 3 | 1 | 1 | 28.38<br>3 | 0.51 |
| 3-F-Sia | 3537.2502<br>2 | Sialyfucoylated | 7  | 6 | 4 | 2 | 28.27<br>4 | 0.49 |
| 3-F-Sia | 2661.9432<br>8 | Sialylated      | 7  | 6 | 0 | 1 | 25.8       | 0.49 |
| 3-F-Sia | 3246.1553<br>6 | Sialyfucoylated | 7  | 6 | 4 | 1 | 25.68<br>9 | 0.49 |
| 3-F-Sia | 3976.4053<br>3 | Sialyfucoylated | 9  | 8 | 4 | 1 | 26.48<br>3 | 0.48 |
| 3-F-Sia | 2078.7563<br>3 | Fucosylated     | 5  | 4 | 3 | 0 | 21.16<br>3 | 0.48 |
| 3-F-Sia | 2206.7380<br>1 | High Mannose    | 11 | 2 | 0 | 0 | 20.11<br>2 | 0.48 |

|         |                |                 |   |   |   |   |            |      |
|---------|----------------|-----------------|---|---|---|---|------------|------|
| 3-F-Sia | 3391.1931<br>8 | Sialyfucoylated | 7 | 6 | 3 | 2 | 28.49<br>5 | 0.47 |
| 3-F-Sia | 3464.2053      | Sialyfucoylated | 8 | 7 | 1 | 2 | 30.58<br>5 | 0.47 |
| 3-F-Sia | 2587.9039<br>6 | Sialylated      | 6 | 5 | 0 | 2 | 29.64<br>6 | 0.45 |
| 3-F-Sia | 1275.4572      | Undecorated     | 4 | 3 | 0 | 0 | 22.80<br>9 | 0.45 |
| 3-F-Sia | 1421.5179<br>8 | Fucosylated     | 4 | 3 | 1 | 0 | 21.97<br>8 | 0.41 |
| 3-F-Sia | 2734.9740<br>7 | Sialyfucoylated | 6 | 5 | 3 | 1 | 26.18<br>2 | 0.41 |
| 3-F-Sia | 1462.5413<br>5 | Fucosylated     | 3 | 4 | 1 | 0 | 20.63<br>1 | 0.40 |
| 3-F-Sia | 1728.6024<br>1 | Sialylated      | 5 | 3 | 0 | 1 | 23.49<br>5 | 0.39 |
| 3-F-Sia | 1437.5089      | Undecorated     | 5 | 3 | 0 | 0 | 19.53<br>5 | 0.37 |
| 3-F-Sia | 2719.9821<br>8 | Fucosylated     | 7 | 7 | 1 | 0 | 20.62<br>2 | 0.35 |
| 3-F-Sia | 2384.8561<br>7 | Sialylated      | 6 | 4 | 0 | 2 | 28.26<br>7 | 0.35 |
| 3-F-Sia | 1890.6574<br>2 | Sialylated      | 6 | 3 | 0 | 1 | 24.28      | 0.33 |
| 3-F-Sia | 3393.2067<br>1 | Fucosylated     | 9 | 8 | 2 | 0 | 26.06      | 0.31 |
| 3-F-Sia | 2093.7343<br>1 | Sialylated      | 6 | 4 | 0 | 1 | 25.87<br>6 | 0.29 |
| 3-F-Sia | 3903.3785<br>8 | Sialyfucoylated | 8 | 7 | 6 | 1 | 28.42<br>1 | 0.29 |
| 3-F-Sia | 4123.4653<br>6 | Fucosylated     | 9 | 8 | 7 | 0 | 26.95<br>9 | 0.28 |

|         |                |                 |   |   |   |   |            |      |
|---------|----------------|-----------------|---|---|---|---|------------|------|
| 3-F-Sia | 2645.9350<br>3 | Sialyfucoylated | 6 | 6 | 1 | 1 | 32.33<br>6 | 0.27 |
| 3-F-Sia | 2953.0235<br>7 | Sialylated      | 7 | 6 | 0 | 2 | 28.45<br>3 | 0.25 |
| 3-F-Sia | 1259.4676<br>9 | Fucosylated     | 3 | 3 | 1 | 0 | 24.14<br>7 | 0.25 |
| 3-F-Sia | 3685.2877<br>7 | Fucosylated     | 9 | 8 | 4 | 0 | 37.54<br>1 | 0.24 |
| 3-F-Sia | 2589.9414      | Fucosylated     | 6 | 5 | 4 | 0 | 22.83<br>4 | 0.20 |
| 3-F-Sia | 910.32577      | High Mannose    | 3 | 2 | 0 | 0 | 21.01<br>3 | 0.20 |
| 3-F-Sia | 3174.1421<br>5 | Fucosylated     | 8 | 7 | 3 | 0 | 25.20<br>8 | 0.20 |
| 3-F-Sia | 3831.3537<br>9 | Fucosylated     | 9 | 8 | 5 | 0 | 26.68<br>3 | 0.19 |
| 3-F-Sia | 1915.6787<br>9 | Sialyfucoylated | 4 | 4 | 1 | 1 | 26.61<br>3 | 0.19 |
| 3-F-Sia | 1665.6196      | Fucosylated     | 3 | 5 | 1 | 0 | 21.99<br>3 | 0.19 |
| 3-F-Sia | 3026.0632<br>8 | Sialyfucoylated | 6 | 5 | 3 | 2 | 29.01<br>2 | 0.19 |
| 3-F-Sia | 1868.7007<br>2 | Fucosylated     | 3 | 6 | 1 | 0 | 21.44<br>6 | 0.18 |
| 3-F-Sia | 1583.5720<br>8 | Fucosylated     | 5 | 3 | 1 | 0 | 20.47<br>1 | 0.18 |
| 3-F-Sia | 3466.2415<br>3 | Fucosylated     | 8 | 7 | 5 | 0 | 26.41<br>4 | 0.18 |
| 3-F-Sia | 3536.2271<br>5 | Sialyfucoylated | 7 | 6 | 2 | 3 | 31.09      | 0.17 |
| 3-F-Sia | 2354.8569      | Fucosylated     | 6 | 6 | 1 | 0 | 19.95<br>8 | 0.17 |

|         |                |                 |    |   |   |   |            |      |
|---------|----------------|-----------------|----|---|---|---|------------|------|
| 3-F-Sia | 2630.9932<br>9 | Fucosylated     | 5  | 6 | 4 | 0 | 36.59<br>6 | 0.15 |
| 3-F-Sia | 2955.0288<br>6 | Fucosylated     | 7  | 6 | 4 | 0 | 28.72<br>4 | 0.15 |
| 3-F-Sia | 1989.7138<br>7 | Fucosylated     | 5  | 5 | 1 | 0 | 23.97<br>3 | 0.14 |
| 3-F-Sia | 3757.3187<br>9 | Sialyfuosylated | 8  | 7 | 5 | 1 | 25.67<br>7 | 0.14 |
| 3-F-Sia | 2368.8058<br>5 | High Mannose    | 12 | 2 | 0 | 0 | 21.66<br>9 | 0.14 |
| 3-F-Sia | 2134.7195<br>8 | Sialylated      | 5  | 5 | 0 | 1 | 37.62<br>8 | 0.13 |
| 3-F-Sia | 1931.6913<br>3 | Sialylated      | 5  | 4 | 0 | 1 | 29.62<br>4 | 0.13 |
| 3-F-Sia | 2264.8190<br>9 | Sialyfuosylated | 4  | 5 | 2 | 1 | 25.28<br>3 | 0.12 |
| 3-F-Sia | 3684.2584      | Sialyfuosylated | 9  | 8 | 2 | 1 | 33.30<br>1 | 0.10 |
| 3-F-Sia | 1745.6118<br>7 | Fucosylated     | 6  | 3 | 1 | 0 | 18.61<br>9 | 0.10 |
| 3-F-Sia | 3612.2598<br>7 | Fucosylated     | 8  | 7 | 6 | 0 | 28.50<br>4 | 0.09 |
| 3-F-Sia | 2897.0332<br>6 | Sialyfuosylated | 7  | 5 | 3 | 1 | 36.03<br>9 | 0.09 |
| 3-F-Sia | 2151.7790<br>1 | Fucosylated     | 6  | 5 | 1 | 0 | 26.53<br>4 | 0.09 |
| 3-F-Sia | 2094.7481<br>3 | Fucosylated     | 6  | 4 | 2 | 0 | 36.06<br>9 | 0.08 |
| 3-F-Sia | 2547.9025<br>5 | Sialyfuosylated | 7  | 4 | 2 | 1 | 35.66<br>8 | 0.08 |
| 3-F-Sia | 4414.5679<br>7 | Sialyfuosylated | 9  | 8 | 7 | 1 | 28.25<br>5 | 0.07 |

|         |                |                 |   |   |   |   |            |      |
|---------|----------------|-----------------|---|---|---|---|------------|------|
| 3-F-Sia | 2822.9378<br>5 | Sialyfucoylated | 6 | 4 | 3 | 2 | 37.12<br>2 | 0.07 |
| 3-F-Sia | 2087.8071<br>4 | Undecorated     | 4 | 7 | 0 | 0 | 32.63<br>9 | 0.06 |
| 3-F-Sia | 4996.7447<br>2 | Sialyfucoylated | 9 | 8 | 7 | 3 | 36.32<br>4 | 0.06 |
| 3-F-Sia | 2572.8839<br>5 | Sialyfucoylated | 5 | 5 | 3 | 1 | 26.79      | 0.06 |
| 3-F-Sia | 2280.8109      | Sialyfucoylated | 5 | 5 | 1 | 1 | 23.01<br>8 | 0.06 |
| 3-F-Sia | 2426.8671<br>9 | Sialyfucoylated | 5 | 5 | 2 | 1 | 26.83      | 0.06 |
| 3-F-Sia | 2978.0652<br>5 | Sialyfucoylated | 5 | 7 | 1 | 2 | 34.58<br>1 | 0.05 |
| 3-F-Sia | 2239.7915<br>3 | Sialyfucoylated | 6 | 4 | 1 | 1 | 25.62<br>9 | 0.05 |
| 3-F-Sia | 2646.9346<br>8 | Fucosylated     | 6 | 6 | 3 | 0 | 34.23<br>9 | 0.05 |
| 3-F-Sia | 2790.9665<br>7 | Sialylated      | 6 | 6 | 0 | 2 | 33.31<br>4 | 0.04 |
| 3-F-Sia | 3010.0538<br>3 | Sialyfucoylated | 5 | 5 | 4 | 2 | 37.02<br>6 | 0.04 |
| 3-F-Sia | 2369.8441<br>6 | Sialyfucoylated | 5 | 4 | 3 | 1 | 18.8       | 0.03 |
| 3-F-Sia | 2864.9736<br>4 | Sialylated      | 7 | 7 | 0 | 1 | 36.65<br>9 | 0.03 |
| 3-F-Sia | 2530.8740<br>3 | Sialyfucoylated | 6 | 4 | 1 | 2 | 37.90<br>9 | 0.02 |
| 3-F-Sia | 2499.8874<br>8 | Sialylated      | 6 | 6 | 0 | 1 | 28.37<br>7 | 0.02 |

**Table S4.4 Site-specific occupancy of recombinant Spike protein RBD derived from HEK293 cells**

| <b>Glycans</b>                    | <b>Peptide Sequence</b>    | <b>Glycosite</b> | <b>Glycan Subtype</b> |
|-----------------------------------|----------------------------|------------------|-----------------------|
| HexNAc(8)Hex(9)Fuc(3)Neu<br>Ac(0) | R.FPNITNLCPFGEVFNA<br>TR.F | 331              | Fucosylated           |
| HexNAc(9)Hex(9)Fuc(3)Neu<br>Ac(0) | R.FPNITNLCPFGEVFNA<br>TR.F | 331              | Fucosylated           |
| HexNAc(9)Hex(9)Fuc(6)Neu<br>Ac(0) | R.FPNITNLCPFGEVFNA<br>TR.F | 331              | Fucosylated           |
| HexNAc(9)Hex(9)Fuc(2)Neu<br>Ac(1) | R.FPNITNLCPFGEVFNA<br>TR.F | 331              | Sialyfucoylate<br>d   |
| HexNAc(7)Hex(6)Fuc(5)Neu<br>Ac(1) | R.FPNITNLCPFGEVFNA<br>TR.F | 331              | Sialyfucoylate<br>d   |
| HexNAc(9)Hex(9)Fuc(5)Neu<br>Ac(1) | R.FPNITNLCPFGEVFNA<br>TR.F | 331              | Sialyfucoylate<br>d   |
| HexNAc(9)Hex(9)Fuc(1)Neu<br>Ac(1) | R.FPNITNLCPFGEVFNA<br>TR.F | 331              | Sialyfucoylate<br>d   |
| HexNAc(9)Hex(9)Fuc(4)Neu<br>Ac(2) | R.FPNITNLCPFGEVFNA<br>TR.F | 331              | Sialyfucoylate<br>d   |
| HexNAc(7)Hex(7)Fuc(4)Neu<br>Ac(2) | R.FPNITNLCPFGEVFNA<br>TR.F | 331              | Sialyfucoylate<br>d   |
| HexNAc(7)Hex(6)Fuc(5)Neu<br>Ac(2) | R.FPNITNLCPFGEVFNA<br>TR.F | 331              | Sialyfucoylate<br>d   |
| HexNAc(8)Hex(8)Fuc(0)Neu<br>Ac(2) | R.FPNITNLCPFGEVFNA<br>TR.F | 331              | Sialylated            |
| HexNAc(8)Hex(9)Fuc(7)Neu<br>Ac(2) | R.FPNITNLCPFGEVFNA<br>TR.F | 331              | Sialyfucoylate<br>d   |
| HexNAc(7)Hex(6)Fuc(4)Neu<br>Ac(2) | R.FPNITNLCPFGEVFNA<br>TR.F | 331              | Sialyfucoylate<br>d   |
| HexNAc(7)Hex(8)Fuc(6)Neu<br>Ac(3) | R.FPNITNLCPFGEVFNA<br>TR.F | 331              | Sialyfucoylate<br>d   |

|                                   |                            |     |                     |
|-----------------------------------|----------------------------|-----|---------------------|
| HexNAc(7)Hex(7)Fuc(2)Neu<br>Ac(3) | R.FPNITNLCPFGEVFNA<br>TR.F | 331 | Sialyucosylate<br>d |
| HexNAc(8)Hex(9)Fuc(2)Neu<br>Ac(1) | R.FPNITNLCPFGEVFNA<br>TR.F | 343 | Sialyucosylate<br>d |
| HexNAc(9)Hex(9)Fuc(3)Neu<br>Ac(1) | R.FPNITNLCPFGEVFNA<br>TR.F | 343 | Sialyucosylate<br>d |
| HexNAc(6)Hex(7)Fuc(4)Neu<br>Ac(2) | R.FPNITNLCPFGEVFNA<br>TR.F | 343 | Sialyucosylate<br>d |
| HexNAc(9)Hex(9)Fuc(2)Neu<br>Ac(1) | R.FPNITNLCPFGEVFNA<br>TR.F | 343 | Sialyucosylate<br>d |
| HexNAc(9)Hex(9)Fuc(6)Neu<br>Ac(0) | R.FPNITNLCPFGEVFNA<br>TR.F | 343 | Fucosylated         |
| HexNAc(8)Hex(9)Fuc(3)Neu<br>Ac(0) | R.FPNITNLCPFGEVFNA<br>TR.F | 343 | Fucosylated         |
| HexNAc(9)Hex(9)Fuc(4)Neu<br>Ac(1) | R.FPNITNLCPFGEVFNA<br>TR.F | 343 | Sialyucosylate<br>d |
| HexNAc(9)Hex(9)Fuc(3)Neu<br>Ac(0) | R.FPNITNLCPFGEVFNA<br>TR.F | 343 | Fucosylated         |
| HexNAc(7)Hex(7)Fuc(2)Neu<br>Ac(2) | R.FPNITNLCPFGEVFNA<br>TR.F | 343 | Sialyucosylate<br>d |
| HexNAc(8)Hex(8)Fuc(6)Neu<br>Ac(2) | R.FPNITNLCPFGEVFNA<br>TR.F | 343 | Sialyucosylate<br>d |
| HexNAc(9)Hex(9)Fuc(2)Neu<br>Ac(0) | R.FPNITNLCPFGEVFNA<br>TR.F | 343 | Fucosylated         |
| HexNAc(8)Hex(8)Fuc(6)Neu<br>Ac(3) | R.FPNITNLCPFGEVFNA<br>TR.F | 343 | Sialyucosylate<br>d |
| HexNAc(7)Hex(6)Fuc(2)Neu<br>Ac(2) | R.FPNITNLCPFGEVFNA<br>TR.F | 343 | Sialyucosylate<br>d |
| HexNAc(7)Hex(8)Fuc(6)Neu<br>Ac(2) | R.FPNITNLCPFGEVFNA<br>TR.F | 343 | Sialyucosylate<br>d |
| HexNAc(9)Hex(9)Fuc(4)Neu<br>Ac(0) | R.FPNITNLCPFGEVFNA<br>TR.F | 343 | Fucosylated         |

|                                   |                            |     |                     |
|-----------------------------------|----------------------------|-----|---------------------|
| HexNAc(9)Hex(9)Fuc(1)Neu<br>Ac(2) | R.FPNITNLCPFGEVFNA<br>TR.F | 343 | Sialyfucoylate<br>d |
| HexNAc(8)Hex(9)Fuc(5)Neu<br>Ac(1) | R.FPNITNLCPFGEVFNA<br>TR.F | 343 | Sialyfucoylate<br>d |
| HexNAc(8)Hex(8)Fuc(3)Neu<br>Ac(0) | R.FPNITNLCPFGEVFNA<br>TR.F | 343 | Fucosylated         |
| HexNAc(9)Hex(9)Fuc(2)Neu<br>Ac(2) | R.FPNITNLCPFGEVFNA<br>TR.F | 343 | Sialyfucoylate<br>d |
| HexNAc(8)Hex(9)Fuc(2)Neu<br>Ac(0) | R.FPNITNLCPFGEVFNA<br>TR.F | 343 | Fucosylated         |
| HexNAc(8)Hex(8)Fuc(5)Neu<br>Ac(2) | R.FPNITNLCPFGEVFNA<br>TR.F | 343 | Sialyfucoylate<br>d |
| HexNAc(7)Hex(8)Fuc(5)Neu<br>Ac(3) | R.FPNITNLCPFGEVFNA<br>TR.F | 343 | Sialyfucoylate<br>d |
| HexNAc(8)Hex(9)Fuc(6)Neu<br>Ac(0) | R.FPNITNLCPFGEVFNA<br>TR.F | 343 | Fucosylated         |
| HexNAc(7)Hex(6)Fuc(4)Neu<br>Ac(2) | R.FPNITNLCPFGEVFNA<br>TR.F | 343 | Sialyfucoylate<br>d |
| HexNAc(8)Hex(8)Fuc(2)Neu<br>Ac(0) | R.FPNITNLCPFGEVFNA<br>TR.F | 343 | Fucosylated         |
| HexNAc(9)Hex(9)Fuc(5)Neu<br>Ac(0) | R.FPNITNLCPFGEVFNA<br>TR.F | 343 | Fucosylated         |
| HexNAc(8)Hex(9)Fuc(3)Neu<br>Ac(1) | R.FPNITNLCPFGEVFNA<br>TR.F | 343 | Sialyfucoylate<br>d |
| HexNAc(9)Hex(9)Fuc(2)Neu<br>Ac(3) | R.FPNITNLCPFGEVFNA<br>TR.F | 343 | Sialyfucoylate<br>d |
| HexNAc(8)Hex(8)Fuc(5)Neu<br>Ac(3) | R.FPNITNLCPFGEVFNA<br>TR.F | 343 | Sialyfucoylate<br>d |
| HexNAc(9)Hex(9)Fuc(6)Neu<br>Ac(2) | R.FPNITNLCPFGEVFNA<br>TR.F | 343 | Sialyfucoylate<br>d |
| HexNAc(7)Hex(6)Fuc(3)Neu<br>Ac(2) | R.FPNITNLCPFGEVFNA<br>TR.F | 343 | Sialyfucoylate<br>d |

|                                   |                            |     |                     |
|-----------------------------------|----------------------------|-----|---------------------|
| HexNAc(8)Hex(9)Fuc(3)Neu<br>Ac(2) | R.FPNITNLCPFGEVFNA<br>TR.F | 343 | Sialyucosylate<br>d |
| HexNAc(7)Hex(8)Fuc(6)Neu<br>Ac(3) | R.FPNITNLCPFGEVFNA<br>TR.F | 343 | Sialyucosylate<br>d |
| HexNAc(8)Hex(8)Fuc(2)Neu<br>Ac(1) | R.FPNITNLCPFGEVFNA<br>TR.F | 343 | Sialyucosylate<br>d |
| HexNAc(8)Hex(9)Fuc(7)Neu<br>Ac(2) | R.FPNITNLCPFGEVFNA<br>TR.F | 343 | Sialyucosylate<br>d |
| HexNAc(9)Hex(9)Fuc(3)Neu<br>Ac(2) | R.FPNITNLCPFGEVFNA<br>TR.F | 343 | Sialyucosylate<br>d |
| HexNAc(8)Hex(8)Fuc(6)Neu<br>Ac(1) | R.FPNITNLCPFGEVFNA<br>TR.F | 343 | Sialyucosylate<br>d |

## **ACKNOWLEDGMENT**

The molecular dynamics calculations were carried out using the High-Performance Computing Cluster, COARE Facility of the Department of Science and Technology – Advance Science and Technology Institute, Philippines.

**Funding:** This work was supported by grants from the NIH (R01GM049077 to C.L.)

## REFERENCE

1. Zhu, N.; Zhang, D.; Wang, W.; Li, X.; Yang, B.; Song, J.; Zhao, X.; Huang, B.; Shi, W.; Lu, R.; Niu, P.; Zhan, F.; Ma, X.; Wang, D.; Xu, W.; Wu, G.; Gao, G. F.; Tan, W.; Team, C. N. C. I. a. R., A Novel Coronavirus from Patients with Pneumonia in China, 2019. *N Engl J Med* **2020**, *382* (8), 727-733.
2. Walls, A. C.; Park, Y. J.; Tortorici, M. A.; Wall, A.; McGuire, A. T.; Velesler, D., Structure, Function, and Antigenicity of the SARS-CoV-2 Spike Glycoprotein. *Cell* **2020**, *183* (6), 1735.
3. Wan, Y.; Shang, J.; Graham, R.; Baric, R. S.; Li, F., Receptor Recognition by the Novel Coronavirus from Wuhan: an Analysis Based on Decade-Long Structural Studies of SARS Coronavirus. *J Virol* **2020**, *94* (7).
4. Wrapp, D.; Wang, N.; Corbett, K. S.; Goldsmith, J. A.; Hsieh, C. L.; Abiona, O.; Graham, B. S.; McLellan, J. S., Cryo-EM structure of the 2019-nCoV spike in the prefusion conformation. *Science* **2020**, *367* (6483), 1260-1263.
5. Hoffmann, M.; Kleine-Weber, H.; Schroeder, S.; Krüger, N.; Herrler, T.; Erichsen, S.; Schiergens, T. S.; Herrler, G.; Wu, N. H.; Nitsche, A.; Müller, M. A.; Drosten, C.; Pöhlmann, S., SARS-CoV-2 Cell Entry Depends on ACE2 and TMPRSS2 and Is Blocked by a Clinically Proven Protease Inhibitor. *Cell* **2020**, *181* (2), 271-280.e8.
6. Gstöttner, C.; Zhang, T.; Resemann, A.; Ruben, S.; Pengelley, S.; Suckau, D.; Welsink, T.; Wührer, M.; Domínguez-Vega, E., Structural and Functional Characterization of SARS-CoV-2 RBD Domains Produced in Mammalian Cells. *Anal Chem* **2021**, *93* (17), 6839-6847.
7. Peiris, J. S.; Lai, S. T.; Poon, L. L.; Guan, Y.; Yam, L. Y.; Lim, W.; Nicholls, J.; Yee, W. K.; Yan, W. W.; Cheung, M. T.; Cheng, V. C.; Chan, K. H.; Tsang, D. N.; Yung, R. W.; Ng, T. K.; Yuen, K. Y.; group, S. s., Coronavirus as a possible cause of severe acute respiratory syndrome. *Lancet* **2003**, *361* (9366), 1319-25.
8. Viruses, C. S. G. o. t. I. C. o. T. o., The species Severe acute respiratory syndrome-related coronavirus: classifying 2019-nCoV and naming it SARS-CoV-2. *Nat Microbiol* **2020**, *5* (4), 536-544.
9. Li, W.; Moore, M. J.; Vasilieva, N.; Sui, J.; Wong, S. K.; Berne, M. A.; Somasundaran, M.; Sullivan, J. L.; Luzuriaga, K.; Greenough, T. C.; Choe, H.; Farzan, M., Angiotensin-converting enzyme 2 is a functional receptor for the SARS coronavirus. *Nature* **2003**, *426* (6965), 450-4.
10. Letko, M.; Marzi, A.; Munster, V., Functional assessment of cell entry and receptor usage for SARS-CoV-2 and other lineage B betacoronaviruses. *Nat Microbiol* **2020**, *5* (4), 562-569.
11. Tai, W.; He, L.; Zhang, X.; Pu, J.; Voronin, D.; Jiang, S.; Zhou, Y.; Du, L., Characterization of the receptor-binding domain (RBD) of 2019 novel coronavirus: implication for development of RBD protein as a viral attachment inhibitor and vaccine. *Cell Mol Immunol* **2020**, *17* (6), 613-620.
12. Lan, J.; Ge, J.; Yu, J.; Shan, S.; Zhou, H.; Fan, S.; Zhang, Q.; Shi, X.; Wang, Q.; Zhang, L.; Wang, X., Structure of the SARS-CoV-2 spike receptor-binding domain bound to the ACE2 receptor. *Nature* **2020**, *581* (7807), 215-220.

13. Tian, X.; Li, C.; Huang, A.; Xia, S.; Lu, S.; Shi, Z.; Lu, L.; Jiang, S.; Yang, Z.; Wu, Y.; Ying, T., Potent binding of 2019 novel coronavirus spike protein by a SARS coronavirus-specific human monoclonal antibody. *Emerg Microbes Infect* **2020**, *9* (1), 382-385.
14. Hamming, I.; Timens, W.; Bulthuis, M. L.; Lely, A. T.; Navis, G.; van Goor, H., Tissue distribution of ACE2 protein, the functional receptor for SARS coronavirus. A first step in understanding SARS pathogenesis. *J Pathol* **2004**, *203* (2), 631-7.
15. Park, D.; Xu, G.; Barboza, M.; Shah, I. M.; Wong, M.; Raybould, H.; Mills, D. A.; Lebrilla, C. B., Enterocyte glycosylation is responsive to changes in extracellular conditions: implications for membrane functions. *Glycobiology* **2017**, *27* (9), 847-860.
16. Park, D.; Brune, K. A.; Mitra, A.; Marusina, A. I.; Maverakis, E.; Lebrilla, C. B., Characteristic Changes in Cell Surface Glycosylation Accompany Intestinal Epithelial Cell (IEC) Differentiation: High Mannose Structures Dominate the Cell Surface Glycome of Undifferentiated Enterocytes. *Mol Cell Proteomics* **2015**, *14* (11), 2910-21.
17. Shajahan, A.; Archer-Hartmann, S.; Supekar, N. T.; Gleinich, A. S.; Heiss, C.; Azadi, P., Comprehensive characterization of N- and O- glycosylation of SARS-CoV-2 human receptor angiotensin converting enzyme 2. *Glycobiology* **2021**, *31* (4), 410-424.
18. Watanabe, Y.; Allen, J. D.; Wrapp, D.; McLellan, J. S.; Crispin, M., Site-specific glycan analysis of the SARS-CoV-2 spike. *Science* **2020**, *369* (6501), 330-333.
19. Shajahan, A.; Supekar, N. T.; Gleinich, A. S.; Azadi, P., Deducing the N- and O-glycosylation profile of the spike protein of novel coronavirus SARS-CoV-2. *Glycobiology* **2020**, *30* (12), 981-988.
20. Mehdipour, A. R.; Hummer, G., Dual nature of human ACE2 glycosylation in binding to SARS-CoV-2 spike. *Proc Natl Acad Sci U S A* **2021**, *118* (19).
21. Zhao, P.; Praissman, J. L.; Grant, O. C.; Cai, Y.; Xiao, T.; Rosenbalm, K. E.; Aoki, K.; Kellman, B. P.; Bridger, R.; Barouch, D. H.; Brindley, M. A.; Lewis, N. E.; Tiemeyer, M.; Chen, B.; Woods, R. J.; Wells, L., Virus-Receptor Interactions of Glycosylated SARS-CoV-2 Spike and Human ACE2 Receptor. *Cell Host Microbe* **2020**, *28* (4), 586-601.e6.
22. Eric W. Stawiski , D. D., Kushal Suryamohan , Ravi Gupta , Frederic A. Fellouse , J. Fah Sathirapongsasuti , Jiang Liu , Ying-Ping Jiang , Aakrosh Ratan , Monika Mis , Devi Santhosh , Sneha Somasekar , Sangeetha Mohan , Sameer Phalke , Boney Kuriakose , Aju Antony , Jagath R. Junutula , Stephan C. Schuster , Natalia Jura , Somasekar Seshagiri, Human ACE2 receptor polymorphisms predict SARS-CoV-2 susceptibility. <https://www.biorxiv.org/>, 2021.
23. Chan, K. K.; Dorosky, D.; Sharma, P.; Abbasi, S. A.; Dye, J. M.; Kranz, D. M.; Herbert, A. S.; Procko, E., Engineering human ACE2 to optimize binding to the spike protein of SARS coronavirus 2. *Science* **2020**, *369* (6508), 1261-1265.
24. Kim, S. Y.; Jin, W.; Sood, A.; Montgomery, D. W.; Grant, O. C.; Fuster, M. M.; Fu, L.; Dordick, J. S.; Woods, R. J.; Zhang, F.; Linhardt, R. J., Characterization of heparin and severe acute respiratory syndrome-related coronavirus 2 (SARS-CoV-2) spike glycoprotein binding interactions. *Antiviral Res* **2020**, *181*, 104873.
25. Clausen, T. M.; Sandoval, D. R.; Spliid, C. B.; Pihl, J.; Perrett, H. R.; Painter, C. D.; Narayanan, A.; Majowicz, S. A.; Kwong, E. M.; McVicar, R. N.; Thacker, B. E.; Glass, C. A.; Yang, Z.; Torres, J. L.; Golden, G. J.; Bartels, P. L.; Porell, R. N.; Garretson, A. F.; Laubach, L.; Feldman, J.; Yin, X.; Pu, Y.; Hauser, B. M.; Caradonna, T. M.; Kellman, B. P.; Martino, C.; Gordts, P. L. S. M.; Chanda, S. K.; Schmidt, A. G.; Godula, K.; Leibel, S. L.;

- Jose, J.; Corbett, K. D.; Ward, A. B.; Carlin, A. F.; Esko, J. D., SARS-CoV-2 Infection Depends on Cellular Heparan Sulfate and ACE2. *Cell* **2020**, *183* (4), 1043-1057.e15.
26. Moore, R. E.; Xu, L. L.; Townsend, S. D., Prospecting Human Milk Oligosaccharides as a Defense Against Viral Infections. *ACS Infect Dis* **2021**.
27. Wu, S.; Grimm, R.; German, J. B.; Lebrilla, C. B., Annotation and structural analysis of sialylated human milk oligosaccharides. *J Proteome Res* **2011**, *10* (2), 856-68.
28. Wu, S.; Tao, N.; German, J. B.; Grimm, R.; Lebrilla, C. B., Development of an annotated library of neutral human milk oligosaccharides. *J Proteome Res* **2010**, *9* (8), 4138-51.
29. Li, Q.; Xie, Y.; Xu, G.; Lebrilla, C. B., Identification of potential sialic acid binding proteins on cell membranes by proximity chemical labeling. *Chem Sci* **2019**, *10* (24), 6199-6209.
30. Li, Q.; Xie, Y.; Wong, M.; Barboza, M.; Lebrilla, C. B., Comprehensive structural glycomic characterization of the glycocalyxes of cells and tissues. *Nat Protoc* **2020**, *15* (8), 2668-2704.
31. Xu, C.; Wang, Y.; Liu, C.; Zhang, C.; Han, W.; Hong, X.; Hong, Q.; Wang, S.; Zhao, Q.; Yang, Y.; Chen, K.; Zheng, W.; Kong, L.; Wang, F.; Zuo, Q.; Huang, Z.; Cong, Y., Conformational dynamics of SARS-CoV-2 trimeric spike glycoprotein in complex with receptor ACE2 revealed by cryo-EM. *Sci Adv* **2021**, *7* (1).
32. Park, S. J.; Lee, J.; Qi, Y.; Kern, N. R.; Lee, H. S.; Jo, S.; Joung, I.; Joo, K.; Im, W., CHARMM-GUI Glycan Modeler for modeling and simulation of carbohydrates and glycoconjugates. *Glycobiology* **2019**, *29* (4), 320-331.
33. Guvench, O.; Mallajosyula, S. S.; Raman, E. P.; Hatcher, E.; Vanommeslaeghe, K.; Foster, T. J.; Jamison, F. W.; Mackerell, A. D., CHARMM additive all-atom force field for carbohydrate derivatives and its utility in polysaccharide and carbohydrate-protein modeling. *J Chem Theory Comput* **2011**, *7* (10), 3162-3180.
34. Huang, J.; Rauscher, S.; Nawrocki, G.; Ran, T.; Feig, M.; de Groot, B. L.; Grubmüller, H.; MacKerell, A. D., CHARMM36m: an improved force field for folded and intrinsically disordered proteins. *Nat Methods* **2017**, *14* (1), 71-73.
35. Acun, B.; Hardy, D. J.; Kale, L. V.; Li, K.; Phillips, J. C.; Stone, J. E., Scalable Molecular Dynamics with NAMD on the Summit System. *IBM J Res Dev* **2018**, *62* (6), 1-9.
36. Mallajosyula, S. S.; Jo, S.; Im, W.; MacKerell, A. D., Molecular dynamics simulations of glycoproteins using CHARMM. *Methods Mol Biol* **2015**, *1273*, 407-29.
37. Jo, S.; Cheng, X.; Lee, J.; Kim, S.; Park, S. J.; Patel, D. S.; Beaven, A. H.; Lee, K. I.; Rui, H.; Park, S.; Lee, H. S.; Roux, B.; MacKerell, A. D.; Klauda, J. B.; Qi, Y.; Im, W., CHARMM-GUI 10 years for biomolecular modeling and simulation. *J Comput Chem* **2017**, *38* (15), 1114-1124.
38. Humphrey, W.; Dalke, A.; Schulten, K., VMD: visual molecular dynamics. *J Mol Graph* **1996**, *14* (1), 33-8, 27-8.
39. Castanys-Muñoz, E.; Martin, M. J.; Prieto, P. A., 2'-fucosyllactose: an abundant, genetically determined soluble glycan present in human milk. *Nutr Rev* **2013**, *71* (12), 773-89.
40. Digre, A.; Lindskog, C., The Human Protein Atlas-Spatial localization of the human proteome in health and disease. *Protein Sci* **2021**, *30* (1), 218-233.
41. Thul, P. J.; Lindskog, C., The human protein atlas: A spatial map of the human proteome. *Protein Sci* **2018**, *27* (1), 233-244.
42. Zhou, Q.; Xie, Y.; Lam, M.; Lebrilla, C. B., -Glycomic Analysis of the Cell Shows Specific Effects of Glycosyl Transferase Inhibitors. *Cells* **2021**, *10* (9).

43. Villalobos, J. A.; Yi, B. R.; Wallace, I. S., 2-Fluoro-L-Fucose Is a Metabolically Incorporated Inhibitor of Plant Cell Wall Polysaccharide Fucosylation. *PLoS One* **2015**, *10* (9), e0139091.
44. Zhou, Y.; Fukuda, T.; Hang, Q.; Hou, S.; Isaji, T.; Kameyama, A.; Gu, J., Inhibition of fucosylation by 2-fluorofucose suppresses human liver cancer HepG2 cell proliferation and migration as well as tumor formation. *Sci Rep* **2017**, *7* (1), 11563.
45. Suzuki, K.; Daikoku, S.; Son, S. H.; Ito, Y.; Kanie, O., Synthetic study of 3-fluorinated sialic acid derivatives. *Carbohydr Res* **2015**, *406*, 1-9.
46. Varki A, C. R., Esko JD, et al., editors., *Essentials of Glycobiology*, 3rd edition.
47. Shinya, K.; Ebina, M.; Yamada, S.; Ono, M.; Kasai, N.; Kawaoka, Y., Avian flu: influenza virus receptors in the human airway. *Nature* **2006**, *440* (7083), 435-6.
48. Nicholls, J. M.; Bourne, A. J.; Chen, H.; Guan, Y.; Peiris, J. S., Sialic acid receptor detection in the human respiratory tract: evidence for widespread distribution of potential binding sites for human and avian influenza viruses. *Respir Res* **2007**, *8*, 73.
49. Schneider, M.; Al-Shareffi, E.; Haltiwanger, R. S., Biological functions of fucose in mammals. *Glycobiology* **2017**, *27* (7), 601-618.
50. Ma, B.; Simala-Grant, J. L.; Taylor, D. E., Fucosylation in prokaryotes and eukaryotes. *Glycobiology* **2006**, *16* (12), 158R-184R.
51. Hulswit, R. J. G.; Lang, Y.; Bakkers, M. J. G.; Li, W.; Li, Z.; Schouten, A.; Ophorst, B.; van Kuppeveld, F. J. M.; Boons, G. J.; Bosch, B. J.; Huizinga, E. G.; de Groot, R. J., Human coronaviruses OC43 and HKU1 bind to 9-. *Proc Natl Acad Sci U S A* **2019**, *116* (7), 2681-2690.
52. Han, D. P.; Lohani, M.; Cho, M. W., Specific asparagine-linked glycosylation sites are critical for DC-SIGN- and L-SIGN-mediated severe acute respiratory syndrome coronavirus entry. *J Virol* **2007**, *81* (21), 12029-39.
53. Kommineni, V.; Markert, M.; Ren, Z.; Palle, S.; Carrillo, B.; Deng, J.; Tejeda, A.; Nandi, S.; McDonald, K. A.; Marcel, S.; Holtz, B., In Vivo Glycan Engineering via the Mannosidase I Inhibitor (Kifunensine) Improves Efficacy of Rituximab Manufactured in. *Int J Mol Sci* **2019**, *20* (1).
54. Choi, H. Y.; Park, H.; Hong, J. K.; Kim, S. D.; Kwon, J. Y.; You, S.; Do, J.; Lee, D. Y.; Kim, H. H.; Kim, D. I., N-glycan Remodeling Using Mannosidase Inhibitors to Increase High-mannose Glycans on Acid  $\alpha$ -Glucosidase in Transgenic Rice Cell Cultures. *Sci Rep* **2018**, *8* (1), 16130.
55. Nguyen, L.; McCord, K. A.; Bui, D. T.; Bouwman, K. M.; Kitova, E. N.; Kumawat, D.; Daskhan, G. C.; Tomris, I.; Han, L.; Chopra, P.; Yang, T.-J.; Willows, S. D.; Mason, A. L.; Lowary, T. L.; West, L. J.; Hsu, S.-T. D.; Tompkins, S. M.; Boons, G.-J.; de Vries, R. P.; Macauley, M. S.; Klassen, J. S., Sialic acid-Dependent Binding and Viral Entry of SARS-CoV-2. *bioRxiv* **2021**, 2021.03.08.434228.
56. Wong, S. K.; Li, W.; Moore, M. J.; Choe, H.; Farzan, M., A 193-amino acid fragment of the SARS coronavirus S protein efficiently binds angiotensin-converting enzyme 2. *J Biol Chem* **2004**, *279* (5), 3197-201.
57. Trebbien, R.; Larsen, L. E.; Viuff, B. M., Distribution of sialic acid receptors and influenza A virus of avian and swine origin in experimentally infected pigs. *Virol J* **2011**, *8*, 434.
58. Wu, N. H.; Meng, F.; Seitz, M.; Valentin-Weigand, P.; Herrler, G., Sialic acid-dependent interactions between influenza viruses and *Streptococcus suis* affect the infection of porcine tracheal cells. *J Gen Virol* **2015**, *96* (9), 2557-2568.

59. Sieben, C.; Sezgin, E.; Eggeling, C.; Manley, S., Influenza A viruses use multivalent sialic acid clusters for cell binding and receptor activation. *PLoS Pathog* **2020**, *16* (7), e1008656.
60. Almond, R. J.; Flanagan, B. F.; Antonopoulos, A.; Haslam, S. M.; Dell, A.; Kimber, I.; Dearman, R. J., Differential immunogenicity and allergenicity of native and recombinant human lactoferrins: role of glycosylation. *Eur J Immunol* **2013**, *43* (1), 170-81.
61. Morniroli, D.; Consales, A.; Crippa, B. L.; Vizzari, G.; Ceroni, F.; Cerasani, J.; Colombo, L.; Mosca, F.; Gianni, M. L., The Antiviral Properties of Human Milk: A Multitude of Defence Tools from Mother Nature. *Nutrients* **2021**, *13* (2).
62. Smilowitz, J. T.; Totten, S. M.; Huang, J.; Grapov, D.; Durham, H. A.; Lammi-Keefe, C. J.; Lebrilla, C.; German, J. B., Human milk secretory immunoglobulin a and lactoferrin N-glycans are altered in women with gestational diabetes mellitus. *J Nutr* **2013**, *143* (12), 1906-12.
63. Jorgensen, J. M.; Arnold, C.; Ashorn, P.; Ashorn, U.; Chaima, D.; Cheung, Y. B.; Davis, J. C.; Fan, Y. M.; Goonatilleke, E.; Kortekangas, E.; Kumwenda, C.; Lebrilla, C. B.; Maleta, K.; Totten, S. M.; Wu, L. D.; Dewey, K. G., Lipid-Based Nutrient Supplements During Pregnancy and Lactation Did Not Affect Human Milk Oligosaccharides and Bioactive Proteins in a Randomized Trial. *J Nutr* **2017**, *147* (10), 1867-1874.
64. Wang, X.; Zhou, Y.; Jiang, N.; Zhou, Q.; Ma, W. L., Persistence of intestinal SARS-CoV-2 infection in patients with COVID-19 leads to re-admission after pneumonia resolved. *Int J Infect Dis* **2020**, *95*, 433-435.
65. Hansson, G. C., Mucus and mucins in diseases of the intestinal and respiratory tracts. *J Intern Med* **2019**, *285* (5), 479-490.
66. Tran, D. T.; Ten Hagen, K. G., Mucin-type O-glycosylation during development. *J Biol Chem* **2013**, *288* (10), 6921-9.
67. Tailford, L. E.; Crost, E. H.; Kavanaugh, D.; Juge, N., Mucin glycan foraging in the human gut microbiome. *Front Genet* **2015**, *6*, 81.
68. Radcliffe, C. M.; Arnold, J. N.; Suter, D. M.; Wormald, M. R.; Harvey, D. J.; Royle, L.; Mimura, Y.; Kimura, Y.; Sim, R. B.; Inogès, S.; Rodriguez-Calvillo, M.; Zabalegui, N.; de Cerio, A. L.; Potter, K. N.; Mockridge, C. I.; Dwek, R. A.; Bendandi, M.; Rudd, P. M.; Stevenson, F. K., Human follicular lymphoma cells contain oligomannose glycans in the antigen-binding site of the B-cell receptor. *J Biol Chem* **2007**, *282* (10), 7405-15.
69. Möglinger, U.; Grunewald, S.; Hennig, R.; Kuo, C. W.; Schirmeister, F.; Voth, H.; Rapp, E.; Khoo, K. H.; Seeberger, P. H.; Simon, J. C.; Kolarich, D., Alterations of the Human Skin. *Front Oncol* **2018**, *8*, 70.
70. An, H. J.; Gip, P.; Kim, J.; Wu, S.; Park, K. W.; McVaugh, C. T.; Schaffer, D. V.; Bertozzi, C. R.; Lebrilla, C. B., Extensive determination of glycan heterogeneity reveals an unusual abundance of high mannose glycans in enriched plasma membranes of human embryonic stem cells. *Mol Cell Proteomics* **2012**, *11* (4), M111.010660.
71. Balog, C. I.; Stavenhagen, K.; Fung, W. L.; Koeleman, C. A.; McDonnell, L. A.; Verhoeven, A.; Mesker, W. E.; Tollenaar, R. A.; Deelder, A. M.; Wuhrer, M., N-glycosylation of colorectal cancer tissues: a liquid chromatography and mass spectrometry-based investigation. *Mol Cell Proteomics* **2012**, *11* (9), 571-85.
72. Ruhaak, L. R.; Taylor, S. L.; Stroble, C.; Nguyen, U. T.; Parker, E. A.; Song, T.; Lebrilla, C. B.; Rom, W. N.; Pass, H.; Kim, K.; Kelly, K.; Miyamoto, S., Differential N-Glycosylation Patterns in Lung Adenocarcinoma Tissue. *J Proteome Res* **2015**, *14* (11), 4538-49.
73. Park, D.; Arabyan, N.; Williams, C. C.; Song, T.; Mitra, A.; Weimer, B. C.; Maverakis, E.; Lebrilla, C. B., Salmonella Typhimurium Enzymatically Landscapes the Host

Intestinal Epithelial Cell (IEC) Surface Glycome to Increase Invasion. *Mol Cell Proteomics* **2016**, *15* (12), 3653-3664.

74. Reading, P. C.; Miller, J. L.; Anders, E. M., Involvement of the mannose receptor in infection of macrophages by influenza virus. *J Virol* **2000**, *74* (11), 5190-7.

75. Upham, J. P.; Pickett, D.; Irimura, T.; Anders, E. M.; Reading, P. C., Macrophage receptors for influenza A virus: role of the macrophage galactose-type lectin and mannose receptor in viral entry. *J Virol* **2010**, *84* (8), 3730-7.

76. Miller, J. L.; de Wet, B. J.; deWet, B. J.; Martinez-Pomares, L.; Radcliffe, C. M.; Dwek, R. A.; Rudd, P. M.; Gordon, S., The mannose receptor mediates dengue virus infection of macrophages. *PLoS Pathog* **2008**, *4* (2), e17.

77. Nguyen, D. G.; Hildreth, J. E., Involvement of macrophage mannose receptor in the binding and transmission of HIV by macrophages. *Eur J Immunol* **2003**, *33* (2), 483-93.

78. Routhu, N. K.; Lehoux, S. D.; Rouse, E. A.; Bidokhti, M. R. M.; Giron, L. B.; Anzurez, A.; Reid, S. P.; Abdel-Mohsen, M.; Cummings, R. D.; Byrareddy, S. N., Glycosylation of Zika Virus is Important in Host-Virus Interaction and Pathogenic Potential. *Int J Mol Sci* **2019**, *20* (20).

79. Varki, A.; Cummings, R. D.; Esko, J. D.; Stanley, P.; Hart, G. W.; Aebi, M.; Darvill, A. G.; Kinoshita, T.; Packer, N. H.; Prestegard, J. H.; Schnaar, R. L.; Seeberger, P. H., *Essentials of Glycobiology*. 2015.

80. Roberts, G.; Tarelli, E.; Homer, K. A.; Philpott-Howard, J.; Beighton, D., Production of an endo-beta-N-acetylglucosaminidase activity mediates growth of *Enterococcus faecalis* on a high-mannose-type glycoprotein. *J Bacteriol* **2000**, *182* (4), 882-90.

81. Wong, M.; Xu, G.; Barboza, M.; Maezawa, I.; Jin, L. W.; Zivkovic, A.; Lebrilla, C. B., Metabolic flux analysis of the neural cell glycocalyx reveals differential utilization of monosaccharides. *Glycobiology* **2020**, *30* (11), 859-871.